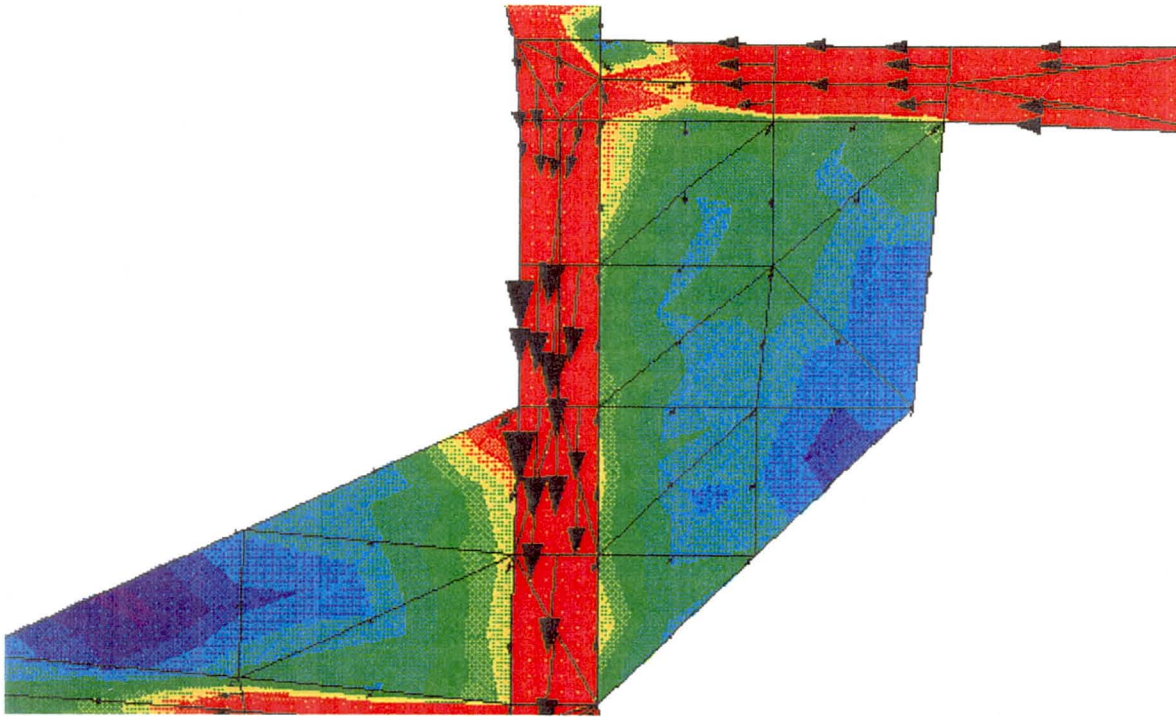


Final Report

CHRISTOWN MALL AREA FLOODPLAIN STUDY



FLOOD CONTROL DISTRICT

OF MARICOPA COUNTY

Submitted by:

July 21, 1995

Simons, Li & Associates, Inc.
Water Resources & Civil Engineering Consultants

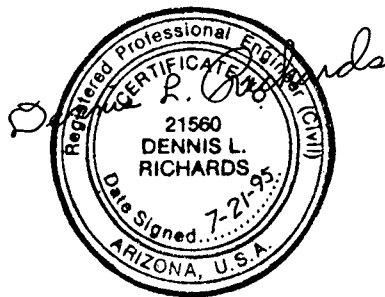
Final Report

**CHRISTOWN MALL AREA
FLOODPLAIN STUDY**

FLOOD CONTROL DISTRICT

OF MARICOPA COUNTY

July 21, 1995

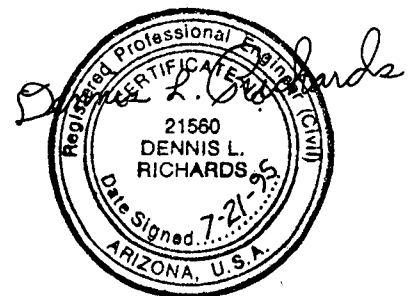


Submitted by:

Simons, Li & Associates, Inc.
Water Resources & Civil Engineering Consultants

TABLE OF CONTENTS

	Page
LIST OF TABLES	ii
LIST OF FIGURES	iii
Introduction	1
Concise Description of Study	1
Study Area	1
General Procedure Applied	2
Computational Mesh used for 2-Dimensional Flow Analysis	2
Boundary and Interior Flows	4
Characteristics of the TABS 2-Dimensional Flow Model	5
2-Dimensional Flood Simulation	8
The 1-Dimensional (HEC-2) Model	10
HEC-2 Modeling Results	11
Comparison of Analyses	11
Differences with Previous Studies	12
Discussion	12
 TABLES	
 FIGURES	



LIST OF TABLES

- Table 1** **Flow Hydrographs Used in the Current Study**
- Table 2** **Hydrographs Adjusted for Storm Drain Flow and Artificial Base Flow**

LIST OF FIGURES

- Figure 1 Aerial Photo of Study Area
- Figure 2 Glendale Avenue Profile between 17th Avenue and 7th Avenue
- Figure 3 Maryland Avenue Profile between 17th Avenue and 7th Avenue
- Figure 4 Bethany Home Road Profile between 17th Avenue and 7th Avenue
- Figure 5 Missouri Avenue Profile between 17th Avenue and 7th Avenue
- Figure 6 Camelback Road Profile between 17th Avenue and 7th Avenue
- Figure 7 Final Computational Mesh Configuration
- Figure 8 Street and Non-Street Areas within the Computational Mesh
- Figure 9 Flow Schematic for the Study Area
- Figure 10 Boundary Flow Hydrographs along Glendale Avenue
- Figure 11 Boundary Flow Hydrographs along Bethany Home Road
- Figure 12 Boundary Flow Hydrographs along Camelback Road
- Figure 13 Boundary Flow Hydrographs along the Grand Canal
- Figure 14 Maximum Computed Flow Depths -- 100-Year Flood
Condition 1 Analysis (minimum initial wet condition)
- Figure 15 Maximum Computed Flow Depths -- 100-Year Flood
Condition 2 Analysis (increased initial wet condition)
- Figure 16 Maximum Computed Flow Depths -- 100-year Flood
Condition 3 Analysis (altered initial geometry condition)
- Figure 17 Areas with 100-Year Flow Depth Exceeding 0.5 feet
Condition 1 Analysis (minimum initial wet condition)
- Figure 18 Areas with 100-Year Flow Depth Exceeding 0.4 feet
Condition 2 Analysis (increased initial wet condition)
- Figure 19 Areas with 100-Year Flow Depth Exceeding 0.4 feet
Condition 3 Analysis (altered initial geometry condition)
- Figure 20 Maximum Unit Discharge Variation -- 100-Year Flood
Condition 1 Analysis (minimum initial wet condition)

LIST OF FIGURES (Continued . . .)

- Figure 21 Dynamic Simulation of the 100-Year Flood through the Study Area
Computed Flow Depth at Time Step 1
- Figure 22 Dynamic Simulation of the 100-Year Flood through the Study Area
Computed Flow Depth at Time Step 3
- Figure 23 Dynamic Simulation of the 100-Year Flood through the Study Area
Computed Flow Depth at Time Step 5
- Figure 24 Dynamic Simulation of the 100-Year Flood through the Study Area
Computed Flow Depth at Time Step 7
- Figure 25 Dynamic Simulation of the 100-Year Flood through the Study Area
Computed Flow Depth at Time Step 9
- Figure 26 Dynamic Simulation of the 100-Year Flood through the Study Area
Computed Flow Depth at Time Step 11
- Figure 27 Dynamic Simulation of the 100-Year Flood through the Study Area
Computed Flow Depth at Time Step 13
- Figure 28 Dynamic Simulation of the 100-Year Flood through the Study Area
Computed Flow Depth at Time Step 15
- Figure 29 Dynamic Simulation of the 100-Year Flood through the Study Area
Computed Flow Depth at Time Step 17
- Figure 30 Dynamic Simulation of the 100-Year Flood through the Study Area
Computed Flow Depth at Time Step 19
- Figure 31 Dynamic Simulation of the 100-Year Flood through the Study Area
Computed Flow Depth at Time Step 21
- Figure 32 Dynamic Simulation of the 100-Year Flood through the Study Area
Computed Flow Depth at Time Step 23
- Figure 33 Dynamic Simulation of the 100-Year Flood through the Study Area
Computed Flow Depth at Time Step 25
- Figure 34 Dynamic Simulation of the 100-Year Flood through the Study Area
Computed Flow Depth at Time Step 27
- Figure 35 Dynamic Simulation of the 100-Year Flood through the Study Area
Computed Flow Depth at Time Step 29

LIST OF FIGURES (Continued . . .)

- Figure 36 Dynamic Simulation of the 100-Year Flood through the Study Area
Computed Flow Depth at Time Step 31
- Figure 37 Dynamic Simulation of the 100-Year Flood through the Study Area
Computed Flow Depth at Time Step 33
- Figure 38 Dynamic Simulation of the 100-Year Flood through the Study Area
Computed Flow Depth at Time Step 35
- Figure 39 Dynamic Simulation of the 100-Year Flood through the Study Area
Computed Flow Depth at Time Step 37
- Figure 40 Dynamic Simulation of the 100-Year Flood through the Study Area
Computed Flow Depth at Time Step 39
- Figure 41 Dynamic Simulation of the 100-Year Flood through the Study Area
Computed Unit Discharge at Time Step 1
- Figure 42 Dynamic Simulation of the 100-Year Flood through the Study Area
Computed Unit Discharge at Time Step 3
- Figure 43 Dynamic Simulation of the 100-Year Flood through the Study Area
Computed Unit Discharge at Time Step 5
- Figure 44 Dynamic Simulation of the 100-Year Flood through the Study Area
Computed Unit Discharge at Time Step 7
- Figure 45 Dynamic Simulation of the 100-Year Flood through the Study Area
Computed Unit Discharge at Time Step 9
- Figure 46 Dynamic Simulation of the 100-Year Flood through the Study Area
Computed Unit Discharge at Time Step 11
- Figure 47 Dynamic Simulation of the 100-Year Flood through the Study Area
Computed Unit Discharge at Time Step 13
- Figure 48 Dynamic Simulation of the 100-Year Flood through the Study Area
Computed Unit Discharge at Time Step 15
- Figure 49 Dynamic Simulation of the 100-Year Flood through the Study Area
Computed Unit Discharge at Time Step 17
- Figure 50 Dynamic Simulation of the 100-Year Flood through the Study Area
Computed Unit Discharge at Time Step 19

LIST OF FIGURES (Continued . . .)

- Figure 51** **Dynamic Simulation of the 100-Year Flood through the Study Area
Computed Unit Discharge at Time Step 21**
- Figure 52** **Dynamic Simulation of the 100-Year Flood through the Study Area
Computed Unit Discharge at Time Step 23**
- Figure 53** **Dynamic Simulation of the 100-Year Flood through the Study Area
Computed Unit Discharge at Time Step 25**
- Figure 54** **Dynamic Simulation of the 100-Year Flood through the Study Area
Computed Unit Discharge at Time Step 27**
- Figure 55** **Dynamic Simulation of the 100-Year Flood through the Study Area
Computed Unit Discharge at Time Step 29**
- Figure 56** **Dynamic Simulation of the 100-Year Flood through the Study Area
Computed Unit Discharge at Time Step 31**
- Figure 57** **Dynamic Simulation of the 100-Year Flood through the Study Area
Computed Unit Discharge at Time Step 33**
- Figure 58** **Dynamic Simulation of the 100-Year Flood through the Study Area
Computed Unit Discharge at Time Step 35**
- Figure 59** **Dynamic Simulation of the 100-Year Flood through the Study Area
Computed Unit Discharge at Time Step 37**
- Figure 60** **Dynamic Simulation of the 100-Year Flood through the Study Area
Computed Unit Discharge at Time Step 39**
- Figure 61** **Inner-Mesh Flood Hydrograph Computation Sections
(TABS-2 GC Strings)**
- Figure 62** **Computed Inner-Mesh Flood Hydrographs
17th Avenue within the Northern Portion of the Study Area**
- Figure 63** **Computed Inner-Mesh Flood Hydrographs
15th Avenue within the Northern Portion of the Study Area**
- Figure 64** **Computed Inner-Mesh Flood Hydrographs
15th Avenue within the Middle Portion of the Study Area**
- Figure 65** **Computed Inner-Mesh Flood Hydrographs
11th Avenue within the Southern Portion of the Study Area**

LIST OF FIGURES (Continued . . .)

- Figure 66** **Computed Inner-Mesh Flood Hydrographs**
11th Avenue within the Northern Portion of the Study Area
- Figure 67** **Computed Inner-Mesh Flood Hydrographs**
11th Avenue within the Middle Portion of the Study Area
- Figure 68** **Computed Inner-Mesh Flood Hydrographs**
15th Avenue within the Southern Portion of the Study Area
- Figure 69** **Computed Inner-Mesh Flood Hydrographs**
7th Avenue within the Northern Portion of the Study Area
- Figure 70** **Computed Inner-Mesh Flood Hydrographs**
7th Avenue within the Middle Portion of the Study Area
- Figure 71** **Computed Inner-Mesh Flood Hydrographs**
7th Avenue within the Southern Portion of the Study Area
- Figure 72** **Computed Inner-Mesh Flood Hydrographs**
3rd Avenue within the Southern Portion of the Study Area
- Figure 73** **Computed Inner-Mesh Flood Hydrographs**
Along the Grand Canal
- Figure 74** **Main Channel HEC-2 Run**
Cross-Section 0.0
- Figure 75** **Main Channel HEC-2 Run**
Cross-Section 0.1
- Figure 76** **Main Channel HEC-2 Run**
Cross-Section 0.4
- Figure 76** **Main Channel HEC-2 Run**
Cross-Section 0.7
- Figure 78** **Main Channel HEC-2 Run**
Cross-Section 1
- Figure 79** **Main Channel HEC-2 Run**
Cross-Section 2
- Figure 80** **Main Channel HEC-2 Run**
Cross-Section 3

LIST OF FIGURES (Continued . . .)

- Figure 81 Main Channel HEC-2 Run
Cross-Section 4
- Figure 82 Main Channel HEC-2 Run
Cross-Section 5
- Figure 83 Main Channel HEC-2 Run
Cross-Section 6
- Figure 84 Main Channel HEC-2 Run
Cross-Section 7
- Figure 85 Main Channel HEC-2 Run
Cross-Section 8
- Figure 86 Main Channel HEC-2 Run
Cross-Section 9
- Figure 87 Main Channel HEC-2 Run
Cross-Section 10
- Figure 88 Main Channel HEC-2 Run

Final Report

Christown Mall Area Floodplain Study

Introduction

This report summarizes the results of a floodplain analysis of the Christown Mall area of Phoenix, Arizona. Following this introduction, a concise description of the major study tasks is presented. The boundaries and the physical characteristics of the study area are then described, followed by a general study procedure outline. More detailed discussion of each of the study tasks then is provided, including identification of the assumptions and procedures applied throughout the course of the study. The results of the analysis are presented and are contrasted to the currently adopted FEMA floodplain mapping for the study area. A general discussion of the modeling techniques employed is included in the final section of this report.

Concise Description of Study

Apply the U.S. Army Corps of Engineers' TABS 2-dimensional hydrodynamic flow model to an urban area subject to shallow flooding, to aid in determination of floodplain depths and boundaries. Use the flow distributions and splits resulting from application of the 2-D model to develop a HEC-2 model of the study area. Apply the HEC-2 model to delineate the 100-year floodplain throughout the study area.

Study Area

The area modeled for this study is located within the city of Phoenix, and is bounded by Glendale Avenue on the north, the Grand Canal on the south, 17th Avenue on the west, and 3rd Avenue on the east. Figure 1 is an aerial photo of the study area, with the major streets identified.

The study area lies within the historical flood path of the Cave Creek Wash. The study area has been cut off from a large portion of the upstream watershed by the Arizona Canal Diversion Channel (the ACDC), which is located about 2 miles north of the northern boundary of the study area. The predominant slope of the study area is from north to south, with a general trend toward the southeast corner of the study area. Figures 2 through 6 illustrate the profiles of the major east-west streets within the study area. The southeasterly trend of the historical Cave Creek Wash may be seen through comparison of these figures.

A major feature located within the study area is the Christown Mall. Located at the intersection of 17th Avenue and Bethany Home Road, this large structure stands in the way of flows proceeding southward down 17th Avenue. The 17th Avenue flow path is cut off, and the runoff is forced eastward, to mix with those flows carried southward by 15th Avenue.

The Grand Canal is an additional major feature located within the study area. This canal is banked on its north side by a slight berm, which forces flow reaching it from the upstream watershed to parallel its path. Two street crossings of the Grand Canal are located within the study area -- at 7th Avenue and 15th Avenue.

General Procedure Applied

The general procedure applied in this re-evaluation of the Christown Mall area floodplain may be summarized as follows:

- (1) Develop a two-dimensional mesh of the study area, distinguishing between street and non-street elements. Adjust and massage the mesh to enable computation of a stable steady state solution under minimal flow conditions.
- (2) Use the previously reviewed HEC-1 model for definition of flows in and out of the study region. (The 2-D analysis will be used for determination of the flow paths and flow distributions within the study region).
- (3) Compute the time-varying flow conditions within the study area throughout passage of a 100-year flood event. Track the flow hydrographs at numerous interior locations.
- (4) Refine the computation results to eliminate the incremental depths and unit discharges associated with the initial steady state flow condition.
- (5) Screen the refined results to determine the maximum flow depth and maximum unit discharge at each location throughout passage of the 100-year flood event.
- (6) Plot the maximum depth and maximum unit discharge results to enable visualization of the areas of expected flow accumulation and general flow paths.
- (7) Using the results of the 2-D analysis as a guide, develop a HEC-2 model for each of the major flow paths through the study area.
- (8) Compute the steady state, 100-year floodplain for the area, assuming coincident peaking of the computed flood hydrographs at all locations.
- (9) Plot the floodplain, and distinguish between various flooding depths within the computed floodplain boundaries.
- (10) Compare the results of the HEC-2 analysis with those computed using the 2-D model, and explain any discrepancies.
- (11) Contrast the results of this study with the current FEMA map for the study area.

Details and results associated with each of these general procedure steps are discussed in the following paragraphs.

Computational Mesh used for 2-Dimensional Flow Analysis

An elemental mesh of interconnected nodes was developed to model the flow characteristics of the study area using the U.S. Army Corps of Engineers' TABS model. FastTABS, a PC software package developed by Brigham Young University and Boss Corporation, was used for mesh construction and

manipulation. Figure 7 illustrates the final mesh configuration, which was created after many trial meshes were attempted and determined to be unstable. Figure 8 identifies the street and non-street areas within the computational mesh. The mesh development process is described in the following paragraphs.

In general application, the density and configuration of the computational mesh to be used for the TABS analysis are dictated by the geometric variation evident within the study area, the dimensioning of the computer program, and the capacity of the computer employed for analysis. For the current study, a minimum element size of approximately 40-feet on a side was used to model areas of narrow street width and areas where rapid change in flow direction or basin elevation was evident. Surrounding mesh elements were configured to minimize abrupt change in adjacent element size. Larger elements were used in wide open, flat areas of solid or minimal development.

Knowing the total area of the region to be modeled and the maximum number of elements allowed in the version of the model employed, an initial estimate of the area of an average mesh element can be determined. The area of the study region is approximately 2.5 square miles, and the maximum number of elements allowed in the TABS model used was 3000 elements -- thus, an initial estimate of the average element size (assuming the maximum number of elements were used) would be 23,232 square feet. The square root of this area gives the average length of one side of a typical square element (152 feet), and double this value (304 feet) gives the average length of one side of a typical enclosing square element if triangular elements were to predominate.

For the current study, a moderately loose grid based on the underlying street layout and an average corner node spacing of approximately 300 feet was initially developed, using square-shaped elements. This mesh was then refined to smooth the transition between adjacent elements, with triangle elements typically used in off-street areas, and squares and rectangles typically used to represent the street elements. Additional refinement (removal of elements, addition of elements, re-orientation of elements) was then performed on a trial and error basis as the model was run and computation stability errors were encountered.

Node points for the mesh were developed manually using the topographic maps prepared for this study. An x-y reference grid for the map was developed based on the coordinate information provided on the mapping (with the N 909000, E 444000 point on the mapping used for the 0,0 point in the x-y grid). Node points were selected using, as a general guide, the average spacing (300 feet) determined as detailed above, with emphasis placed on attempting to accurately represent the street network. Thus, the mesh lines followed the street boundaries to the extent possible, with finer density used in areas of rapid elevation and/or planform change, and looser density used in areas of uniformity.

Elevations were determined for each node point through use of the underlying contour lines. The contour interval used in the mapping prepared for this study was 1.0 foot, which is the maximum contour interval that should be considered in situations similar to the project area (where the flooding is basically sheet flow, with flow depths under design flow conditions predominantly less than 1.0 foot).

The characteristics of the study application (relatively steep grade in an urbanized area with gradual east-west relief and very shallow flooding depths), stretched to the limit the capabilities of TABS routines, and required the development of a fairly intricate arrangement of computational elements. The final mesh consists of a total of 6,614 nodes and 2554 elements. Each node was defined in three dimensions (x,y,z), with the z value representing the local ground elevation at the given point, and with east/west and north/south coordinates of x and y, respectively.

Each element, composed of three or four nodes, was assigned a Manning roughness value and an eddy viscosity value. In initial mesh development, high values of both Manning n and eddy viscosity were used to develop the initial steady state condition. As the mesh was further developed and a stable steady state solution was achieved, these values were incrementally adjusted to represent more realistic conditions. Final computations were performed using Manning n values of 0.020 for the streets within the mesh (identical to the value used in the previous floodplain analysis for the study area), and 0.200 for the areas surrounding the street network. The order of magnitude higher Manning roughness assigned to the non-street areas was applied to model the extra resistance of the buildings, vegetation, etc., located in these areas, and to encourage the flow to concentrate in the streets as much as deemed appropriate. The size of the area being modeled did not allow elemental definition down to the level of the curb and gutter, and the large contrast in flow resistance between street and non-street areas was used to compensate for this lack of topographic refinement. Final eddy viscosity values were reduced to 25.0 (all directions), which is of appropriate magnitude for the given flow conditions (as indicated by the FastTABS manual) and provided Peclet numbers of 50 or less, which ensured numerical stability.

Boundary and Interior Inflows

Boundary and interior inflows to the study area were determined from the previous HEC-1 modeling of the Cave Creek Wash performed by Cella Barr Associates. Flows of concern to the study area include inflows from concentration points upstream, split flows into the study area from concentration points adjacent to the study area, split flows and storm drain flows out of the study area, and watershed runoff from sub-basins enclosed within the study area. In the previous hydrologic analysis, rating curves were used to determine the characteristics of the flow splits that are expected to occur at all major street intersections. For the current analysis, the previously computed sub-basin runoff quantities, storm drain losses and split flow quantities were used to define flows which enter and split out of the study area, but interior flow splits, flow distributions within the study area, and the outflow hydrograph at the major downstream outlet location (Grand Canal and 15th Avenue) were computed using the 2-dimensional TABS flow model.

The following table summarizes the flow items considered at each of the major concentration points within the study area (see also Figure 9):

Intersection	Flows Considered
Glendale and 17th Ave.	Inflow from Glendale and 19th Ave. flow split Sub-basin runoff
Glendale and 15th Ave.	Inflow from upstream watershed Outflow to storm drain
Glendale and 12th Ave.	Sub-basin runoff
Glendale and 7th Ave.	Inflow from Glendale and Central flow split Inflow from Northern and 7th Ave. flow split Sub-basin runoff
Bethany and 17th Ave.	Inflow from Bethany and 19th Ave. flow split

Bethany and 15th Ave.	Sub-basin runoff Outflow to storm drain
Bethany and 11th Ave.	Sub-basin runoff
Bethany and 7th Ave.	Inflow from Bethany and Central flow split Sub-basin runoff Outflow to storm drain
Camelback and 15th Ave.	Inflow from Camelback and 19th Ave. flow split Sub-basin runoff Outflow to storm drain
Camelback and 11th Ave.	Sub-basin runoff
Camelback and 7th Ave.	Sub-basin runoff
Camelback and 3rd Ave.	Inflow from Camelback and Central flow split Sub-basin runoff
Grand Canal and 15th Ave.	Sub-basin runoff Outflow to storm drain Outflow to downstream system
Grand Canal and 7th Ave.	Flow split over canal
Grand Canal and 3rd Ave.	Inflow from Grand Canal and Central flow split

The boundary inflows, sub-basin runoff values, and losses from the study area are actually hydrographs rather than steady-state discharges. **Figures 10 through 13** illustrate the boundary inflow and interior runoff hydrographs computed using the HEC-1 model for the study area. (Note that the acronyms used in the previous HEC-1 modeling for the concentration point locations have been used for the legend in the figure -- i.e. GLEN12 is the intersection of Glendale and 12th Ave., etc.). These boundary and interior runoff hydrographs, as well as those previously computed for storm drain loss and split flows out of the system, were used to compute the time-varying floodplain for the study area. **Table 1** summarizes the boundary, interior runoff, and storm drain flow hydrographs considered in the current analysis. Local runoff flows were adjusted to account for the local storm drain losses, resulting in a single input hydrograph for each of the concentration points indicated in **Figure 9**.

Characteristics of the TABS 2-Dimensional Flow Model

The TABS model requires development of two files: a geometry description file and a boundary condition file. The geometry description file includes a listing of the x, y and z values of each nodal point, describes how the nodal points are connected into elements, and assigns a material type to each element formed. The run control file allows various input/output options, assigns strings of nodes to be used for boundary conditions and flow continuity checks (GC strings), identifies time steps and run duration,

assigns resistance and eddy viscosity values for the various material types, and defines boundary conditions and how they change with time. Both of these files are generated by the FastTABS software, but to run complex time series or to break up a simulation into intervals with restart capability, the run control file must be edited outside of FastTABS.

The run control file is composed of lines of instructions referred to as "cards" (title cards, DE cards, GC cards, etc.) Many cards are optional, or contain fields with optional items. The top several cards from one run control file used for the current study is presented below:

```

T1
T2          SECOND 10 TIME STEPS
T3
DE  0.10  0.50  1
SI  0
$L          61 62 60 64 0 3
$M          1
TR          0 -1 1 0 0
G1          0.0 1.0 1.0 0
GC  2  2355 2358
GC  2  2262 2387
GC  2  2811 2809
GC  2  3548 3546
|          ) several more GC cards
GC  4  6338 6335 6438 6528
TZ          .167 3.34 20 11
TI          0 16 .1 .1
FT          17.0
IC 1122.00
EV  1          25.00      25.00      25.00      25.00      0.0200
EV  2          25.00      25.00      25.00      25.00      0.2000
EV  3          0.00       0.00       0.00       0.00       0.0000
|          ) several more EV cards
EV 12          0.00       0.00       0.00       0.00       0.0000
BQL 1 100.00  4.71
BQL 2 100.00  4.71
|          ) several more BQL cards
BQL 22 50.00  4.71
BHL 12 1123.00
END TIME STEP 0.0
BQL  1      125 4.71
BQL  2      100 4.71
|          ) several more BQL cards
BQL  22     72 4.71
END TIME STEP .167
|
|
STOP

```

The top three cards in this file (T1, T2, and T3) are the title cards which can be used to document the run being analyzed. The DE card controls elemental elimination -- if the depth in an element falls below a specified level it is removed from the computational grid. In this case, elements are eliminated if the depth falls below 0.1 foot, and becomes active again if the depth increases to 0.5 feet. The SI card controls the units used in the analysis (0 for English units, 1 for metric units). The \$L card controls the input/output logical unit numbers, which must be modified if the analysis is to be started mid-iteration or mid-flood simulation. The file presented above was used to model the second 10 time steps of the analysis, and was restarted using a HOTSTART file, which was created during analysis of the first 10 time steps. A number greater than zero in the first field indicates that a HOTSTART file will be used (the name of this file will be prompted for when the program is started). Another number greater than zero in the second field will indicate that a HOTSTART file is to be written after termination of the current simulation (again, a prompt is provided by the program for the desired file name). Default values for the remaining fields are filled in by the FastTABS software, and do not need to be changed by the user in normal applications. The \$M card is also filled in by FastTABS, and need not be modified. The TR card controls printout options, and may be used to suppress or elaborate on output -- in this case, the -1 in the second field is used to limit output to the last iteration of every computational time step. The G1 card can be used to add in Coriolis forces and adjust scale factors -- defaults are supplied by FastTABS and need not be modified by the user.

The GC cards identify strings of nodes -- lines across the mesh -- for identifying boundary lines (if boundary conditions are to be supplied) and continuity check lines. One GC card is used for each line, and the lines are addressed by the order in which they are listed (the first GC card specifies line 1, the second GC card specifies line 2, etc.). The GC cards are created with the FastTABS software at locations specified by the user. The boundary and continuity check lines can extend across small portions or the entire width of the computational mesh, at the user's discretion. The FastTABS software displays GC line location, and allows addition or deletion of lines. In the current analysis, 99 GC strings were used, with the first 22 strings used for boundary flow and water surface elevation specification, and the remaining 77 lines used to identify flow variation along the major streets within the mesh (see Figure 61 and the discussion presented in the following section of this report). (Note: in the program output, the flow passing each continuity check line is compared on a percentage basis to the amount of flow passing the initial GS string. In a more typical river or estuary analysis, boundary condition lines and interior continuity check lines extend perpendicularly across the study channel, and, at least under steady state conditions, the string to string comparison of flow continuity is useful for determination of the validity of the computations. In the current study, however, GC strings are used which cover only a small portion of the mesh, either along the boundary at a street inflow point, or within the mesh across a major street and its overbanks. In addition, the analysis performed is dynamic, similar to a routing analysis, and the flow which comes into the mesh at a given time step may require several computational time steps to pass all the way through the mesh. Thus, in this case, string by string comparison of the flows passing at a given time step do not provide the continuity check that is available under more normal analysis conditions.)

The TZ card specifies the computation time step, total run time, total number of time steps and how far to skip in the subsequent listing of boundary conditions before starting. In the file shown, the computational time step was 0.167 hours (10 minutes), the total simulation was 3.34 hours, involving 20 time steps, and the first time step to be considered at startup was number 11 (a HOTSTART was used, and the last time step of the prior run was number 10). The TI card controls the number of iterations and convergence criteria to be applied. In the case shown, 0 iterations were required for the initial solution (due to use of a HOTSTART), 16 maximum iterations were used in computation of each dynamic time

step, and 0.1 foot depth convergence was specified for both steady state and dynamic simulation. The FT card specifies the water temperature in degrees Celsius (default supplied by FastTABS), and the IC card specifies the average initial water surface elevation (of most significance in computation of the initial solution, where the IC value must be greater than the highest elevation within the computational mesh). The EV cards specify the eddy viscosity values for the various directions, and the Manning n value to be applied for the given material number. One EV card is required for each material type within the mesh. In the current case, two material types were used (1 = street and 2 = non-street, see Computational Mesh Development section for discussion of eddy viscosity and Manning n values). The FastTABS software includes a data entry routine which allows this information to be supplied without having to edit the run control file.

The final sets of cards identify the conditions to be applied at various boundary locations at each time step. Flows are specified in BQL cards, and water surface elevations are specified in BHL cards. An END card separates the information supplied for each time step, and a STOP card terminates the simulation. Data which does not change between time steps need not be re-specified in subsequent steps.

2-Dimensional Flood Simulation

Application of the TABS model requires an initial flowing or "wet" condition through the mesh at time step 0 (the steady state solution). Artificial boundary and interior runoff flow values for this initial state condition were minimized to the extent possible by trial and error (too small flow at a given location would cause the model to become unstable). For computation of the dynamic solution, each ordinate of the 100-year hydrograph for each of the boundary and interior inflow points was adjusted by the local artificial base flow amount required for the initial steady state condition (in effect, simulating the passage of a flood over an already "wet" condition). Table 2 presents the adjusted hydrographs used in simulation of the modified 100-year flood event through the study area.

Forty time steps, each 10 minutes apart, were computed in the simulation of the modified 100-year flood event. After simulation, the flow depths and unit discharges computed at each node under each time step of the modified event were corrected to account for the distortion associated with the artificial initial condition, and the results were plotted.

Three conditions were analyzed to investigate the sensitivity of the solution to the condition applied to generate the "wet" initial conditions. The first condition was that described above: initial flows at each boundary and interior inflow point that were the minimum required for a stable steady state condition. The second condition used flows at each inflow point that were double those used in the first condition. For the third condition, the z values of each of the nodal points were reduced by an amount equal to the flow depth computed in condition 2, and condition 2 was recomputed, resulting in "wet" topography which approximated (but still slightly distorted) that of the original, non-wet topography. Each of these procedures produced comparable results, but the effect of the distortion is identifiable -- the larger the flows used at the initial condition, the larger the spreading that will occur as the flood hydrographs pass over this initial condition, and the smaller the local flood depths tend to be. Thus, the areas with flow depths of 0.4 feet or greater is larger under condition 1 than under condition 2, and condition 3 results appear to be between those of 1 and 2. The absolute magnitude of the depth differences under each condition are actually very small, however.

Figures 14 through 19 illustrate these points. Figures 14 through 16 illustrate the maximum flow depths computed for each node throughout passage of the simulated 100-year flood event, for conditions 1, 2, and 3, respectively. Figure 17 highlights the areas with flooding depths exceeding 0.5 feet under condition 1, and Figures 18 and 19 highlight the areas with flooding depths exceeding 0.4 feet under conditions 2 and 3, respectively. Comparison of Figures 17 through 18 indicates that, although different results are obtained under the differing "wet" conditions applied at startup, the magnitude of the difference is on the order of 0.1 foot. The condition 1 startup is judged to provide the most accurate results, as this condition minimizes the wetting depth used as a baseline.

Figure 20 complements Figure 14, with areas of varying flow concentration (maximum unit discharge throughout passage of the simulated 100-year flood event) shown rather than flow depth. The unit discharge is the product of the flow depth and the flow velocity at each node. This parameter gives a better indication of flow paths and flow intensity than flow depth alone, and more clearly demonstrates the tendency for the flow to concentrate along the streets within the modeled mesh.

Figures 14 and 20 indicate that areas of maximum flow depth and unit discharge are concentrated in seven major areas: (1) 17th Avenue between Glendale Avenue and Bethany Home Road; (2) 15th Avenue between Maryland Avenue and Missouri Avenue; (3) the extension of 11th Avenue between Glendale Avenue and Maryland Avenue; (4) 7th Avenue between Glendale Avenue and Camelback Road; (5) the area north of Camelback Road between 7th Avenue and 15th Avenue; (6) 3rd Avenue between Camelback Road and the Grand Canal; and, (7) the area paralleling the Grand Canal between 3rd Avenue and 15th Avenue.

The above-described figures were developed through screening the results of the 40 computational time steps (with a delta time of 10 minutes) used for simulation of the 100-year flood event. The massive amounts of data generated in the simulation required the development of computer programs, outside of the FastTABS software, for screening and summarization of the data. One computer routine was developed to adjust the time-varying solution to account for the underlying base flow, another routine was used to find the maximum flow depth and unit discharge condition for each node over the 40 simulation steps, a third routine was developed to find locations with depth values that exceeded a given input value, and a fourth routine was used to create the depth and discharge variation displays. The figures were developed on a nodal basis, with a spot of appropriate color applied at the x,y location associated with each node.

Figures 14 through 20 display the results of various screenings, and summarize conditions that occurred at varying points within the flood simulation. Figures 21 through 40 and Figures 41 through 60, illustrate the time varying depth and unit discharge conditions, respectively, for the odd-numbered time steps used in simulation.

Flood hydrographs within the computational mesh were tracked at numerous locations, identified by string number in Figure 61. The inter-mesh hydrographs associated with these strings are plotted by street and location in Figures 62 through 73. The variations in peak discharge for the 100-year flood as it passes through each of the major streets are summarized below, and are compared to the values determined in the previous HEC-1 analysis.

Street	Location	HEC-1 Peak cfs	TABS-2 Peak Discharge Variation (north to south), cfs
17th Ave.	Glendale-Bethany	419	464 312 171 62 68 61 101
15th Ave.	Glendale-Bethany	15	34 151 426 461 485 520 489
	Bethany-Camelback	470	511 536 452 436 300 292 294 214
	Camelback-Grand Canal	358	285 294 460
11th Ave.	Glendale-Bethany	519	433 324 373 399 335 356 390
	Bethany-Camelback	490	348 397 415 403 386 359 373 330
	Camelback-Grand Canal	352	438 328
7th Ave.	Glendale-Bethany	254	395 233 179 170 191 138 133
	Bethany-Camelback	495	462 501 389 388 470 401 472 440
	Camelback-Grand Canal	386	376 456 330
3rd Ave.	Camelback-Grand Canal	602	452 388 241
Grand Canal	3rd Ave.-7th Ave.	203	475
	7th Ave.-11th Ave.	515	319
	11th Ave.-15th Ave.	771	552
	15th Ave. (outflow)	765	785

The 1-Dimensional (HEC-2) Model

HEC-2 models of the study area were initially developed following each of the major north-south streets, and the discharge variations noted above. However, it was soon noted that the streets and their overbanks do not, for the most part, provide adequate topographic relief to contain the flows indicated, and that sheet flow would be the predominant condition throughout the study area. New cross sections were developed, which were taken perpendicular to the major north-south streets but which crossed the entire study area from east to west (except near the Grand Canal, where the cross sections were bent to become perpendicular to the canal's north bank). Flows were distributed across these cross-sections as indicated by the results of the 2-D analysis, and encroachments were used to force flows along sheet flow paths.

Five different runs were used to compute the flow conditions likely throughout the study area during passage of the 100-year flood event. The main flow path flow along a south-south-easterly line from the intersection of Glendale Avenue and 15th Avenue to the intersection of 3rd Avenue and the Grand Canal. The flow then is forced to bend to the southwest, paralleling the canal and outletting over the canal near the 15th Street overcrossing. Smaller HEC-2 decks were used to model the split/sheet flow paths which follow the southern portions of 11th Avenue and 15th Avenue, and the northern portions of 17th Avenue and 7th Avenue. For each deck, NH cards were employed to vary the Manning n roughness values across each of the sections. For the HEC-2 analysis, a Manning n value of 0.020 was used for each of the major north-south streets, and a value of 0.130 was used for the areas between the streets (consistent with the HEC-1 analysis of the study area).

HEC-2 Modeling Results

Figures 74 through 136 illustrate the cross-sections and computed water surface elevations associated with each of the five HEC-2 runs used to model the 100-year flood over the study area. (Station 5000 in cross section 1 through 25 is located at the eastern boundary of 15th Avenue, and the cross-sections were taken looking downstream. For cross-sections 0 through 0.7, Station 0 is at the Grand Canal berm.) Figure 137 is a plan view of the computed floodplain, with the magnitude of the flow depths indicated. As indicated in these figures, the flooding depths throughout the study area under 100-year flood conditions are predominantly shallow, with only local areas generating flow depths exceeding 1.0 foot. The only area of significant, extensive flow accumulation is that adjacent to the Grand Canal, where the northern berm acts to dam the flow and re-direct it along a cross-slope path.

The areas bordered with a dashed line in Figure 137 are the "forced" floodplain areas -- floodplains which were generated through use of the X3 cards to create artificial walls for the flow (see Figures 106 and 121 for examples). Typically, the topographic relief existing in these areas is not sufficient to contain the flow, and the artificial walls were added to simulate the potential sheet flow condition. As indicated in Figure 137, even with these artificial walls employed, the depths generated were typically less than 1.0 foot in magnitude.

An area of uncertainty exists along the southeastern corner of the study area. Although the eastern boundary of the study area ends at 7th Avenue, the analysis boundaries were extended to 3rd Avenue to provide better evaluation of the conditions near the 7th Avenue/Grand Canal intersection. The new topography indicates that an east-west low point within the analysis boundaries occurs along 3rd Avenue (see Figure 78 -- 3rd Avenue is at Station 0.0). The previous hydrologic study (which used USGS quadrangle maps as a base) indicates that the slope east of 3rd Avenue is uphill to Central Avenue, and that flows that do not pass over the Grand Canal at Central Avenue pass westward to 3rd Avenue. Thus, one would assume that flows contributed from the north and west toward 3rd Avenue would pass no further westward and that an artificial wall at 3rd Avenue would be a reasonable way to model this area without additional topo to the east. At any rate, this is a conservative assumption, and any spreading of the flows further to the east would result in even shallower flow depths along this portion of the study area.

Comparison of Analyses

The 2-D analysis results indicate that the flow will tend to follow the trend of the underlying topography, which follows a general north-to-south path, with a slight trend toward the east. The flow will follow the major north-south streets to a large extent, but will use the side streets to a greater degree than previously assumed, to merge toward the underlying historic Cave Creek thalweg.

The 2-D analysis results indicate that unit discharges will be largest along the major north-south streets, particularly in the portion of the study area north of Missouri Avenue. Other areas of maximum unit discharge include 3rd Avenue between Camelback Road and the Grand Canal, 7th Avenue near the Grand Canal overcrossing, and 15th Avenue near the Grand Canal overcrossing. The 2-D analysis also indicates that only a fraction of the study area is expected to have flow depths exceeding 0.5 feet during the passage of the 100-year flood event, and locations with flow depths of 1.0 feet and larger are expected to encompass only a small portion of the study area.

The results of the 1-D (HEC-2) analysis generally confirm those of the 2-D analysis. The areas with flow depths exceeding 0.5 feet and 1.0 feet are larger using the HEC-2 model, but cover comparable areas. The area of most significant flooding potential parallels the Grand Canal along the southern boundary of the study area.

The 2-D and 1-D analyses yield results which differ somewhat near the locations of the flow inflow points (i.e. near the intersection of Glendale and 17th Avenue, and near the intersection Glendale and the extension of 11th Avenue). These discrepancies are due to the way that inflows are passed into the 2-D model -- in concentration rather than with gradual accumulation as would be demonstrated at these same locations if the model encompassed the entire watershed. The high flow concentration noted at these location are artificial and not realistic. In general, the results computed using the 2-D model are most reliable in areas away from the mesh boundaries, due to the concentration distortion typically demonstrated at the mesh inflow points.

Differences with Previous Studies

The floodplain limits identified in this latest analysis are quite different in many areas from those shown on the current FEMA map (Figure 138). The major differences are indicated in the area along and east of 15th Avenue, north of Bethany Home Road. This area was developed over the historical flow line of the Cave Creek Wash, and is indicated in the latest analysis as an area of flow accumulation. The previous study did not include this area as being within the 100-year floodplain.

The previous study assumed that the 100-year flood flows would tend to follow channels consisting of the major streets and their immediately adjacent overbanks. The results of the current study indicate that, with the exception of the area along 17th Avenue north of Bethany Home Road, little topographic relief is available to confine the flows to the degree suggested by the previous study. The current study indicates that the majority of the study region is subject to sheet flow conditions, with small pockets of depths exceeding 1.0 feet. According to the current analysis of the study area, the only well defined region of true floodplain (defined as an area with 100-year flow depths of 1.0 feet or greater) is that area along the northern boundary of the Grand Canal between 3rd Avenue and 15th Avenue.

Discussion

Use of the TABS-2 model to analyze the 100-year flooding conditions in the study area presented several challenges which had not originally been anticipated, and which will not necessarily be present in other future applications. The relatively steep topography, and the shallow flooding condition that occurs within the majority of the study area under the 100-year event are not conditions for which the TABS-2 model is ideally suited. A better situation for this model would be an estuary or river channel, braided or single channel, that contains a relatively mild slope and continuous, wet flow paths under pre-flood conditions.

The 100-year event under consideration produces time-varying flows entering the study area at a non-concurrent times (see Table 1). The flood event is not of long enough duration to create a steady state condition within the study area. As demonstrated in the dynamic simulation displays (Figures 21 through 60), conditions rapidly change from time step to time step throughout the simulation.

An artificial base flow condition had to be imposed on the study area to enable an active computational mesh (steady state condition) at startup. Care was taken to minimize the distortion associated with use of this artificial base flow, and the alternative startup conditions analyzed (Conditions 2 and 3) indicated

that the sensitivity of the initial state condition was not excessive. It should be noted that the startup conditions used in the original simulation, as well as the two simulations applied for sensitivity analysis, are artificial, and the subsequent dynamic solution output had to be adjusted to remove the effect of the imposed base flow. The third scenario analyzed (Condition 3), where the actual geometry of the flow paths were adjusted (lowered) to allow time step 0 flow elevations to approximate the true no-flow topography, is the most artificial condition analyzed, but demonstrates one logical (albeit cumbersome) means of minimizing the distortion associated with the imposed base flow.

An additional complication encountered with the current application involved the treatment of within-mesh watershed runoff that occurs during the flood simulation (see Figure 9). The TABS-2 model does not contain a module for generation of subbasin runoff (since it is a hydraulic model rather than a hydrology model). Mid-channel flow generation would not be a consideration in more typical river or estuary analysis. For this study, the mid-mesh subbasin runoff was treated as an inflow source at the concentration point used in the original HEC-1 model of the basin -- a small rectangular hole was created in the mesh and the inflow was passed through, along one side of this flow entry area.

In summary, the study area and the event to be analyzed presented some real challenges for use of the TABS-2 model -- less steep, more riverine conditions would definitely make application of the model more straight forward. However, the model is judged to provide an accurate means of determining the flow distributions throughout a street network being affected by time-varying inflows. The model is able to use the supplied topographic information to independently determine the routes that flows will take within a complex street system -- contrast this with the HEC-1 application, where rating curves must be supplied at user-designated points of flow split, and where the flow paths must be pre-determined.

Although the FastTABS software definitely simplifies the original mesh generation process, model refinement and solution generation is still a very time-consuming process. In addition, the user is forced to glean through reams of output to obtain maximum depth conditions at points of interest, and the user may be forced to write programs for summarization and display of features of concern (as was the case in this study). Future versions of the FastTABS software may provide more flexibility in solution display, and computer evolution will shorten the solution generation time.

The TABS-2 model, linked to a rainfall-runoff simulation model, will provide more accurate definition of the flooding conditions within an area such as the Christown Mall area of Phoenix than the more typical HEC-1, HEC-2 application, due to the ability of the 2-D model to consider interactions within the entire mesh throughout the entire simulated event. However, the flood hazard zones created through application of a tool such as TABS-2 within regions similar to the study area, will probably be less defined (more spotty) than floodplain regulators deal with normally (compare Figure 14 to Figure 138).

TABLE 1
FLOW HYDROGRAPHS USED IN THE CURRENT STUDY

Time hours	UNADJUSTED HYDROGRAPHS AT INFLOW POINTS																				STORM DRAIN LOSSES			
	1 BETH11	2 BETH15	3 B19E	4 BECW	5 BETHA7	6 G19E	7 GLEN17	8 GLEN12	9 GLEN7T	10 GLCW	11 GLEN15	13 C19E	14 CACW	15 GCCENW	17 SFGC7A	18 GRCA15	19 CAME15	20 CAME11	21 CAMEL7	22 CAME3A	2 SDFB15	19 SDFCA15	5 SDFB7	18 SDFGC15
0.17	25	27	0	13	17	0	17	21	21	20	0	0	0	4	0	37	40	24	41	22	27	40	30	42
0.33	72	83	0	53	42	0	56	74	55	37	0	0	24	21	0	122	114	74	115	65	55	114	65	75
0.50	144	175	0	105	83	0	122	160	136	68	0	0	95	63	0	240	234	136	192	111	55	135	74	75
0.67	222	279	0	112	127	0	199	254	188	109	0	0	109	107	0	351	367	186	244	145	55	135	74	75
0.84	296	371	0	156	165	40	268	336	213	152	0	0	165	114	0	438	482	224	278	167	55	135	74	75
1.00	334	444	0	192	191	105	325	403	229	179	0	0	218	114	0	505	571	252	299	183	55	135	74	75
1.17	350	472	0	218	201	105	347	421	229	192	0	0	267	114	84	502	604	239	277	171	55	135	74	75
1.34	306	418	3	225	184	105	305	351	193	184	3	0	304	114	194	381	537	165	190	117	55	135	74	75
1.50	229	313	20	218	145	105	226	245	111	162	20	0	322	114	310	241	407	96	110	68	55	135	74	75
1.67	155	213	64	201	104	114	152	157	69	126	21	0	328	114	388	150	280	60	69	42	55	135	74	75
1.84	105	144	105	177	71	127	103	107	46	90	8	0	322	114	423	101	190	40	45	28	55	135	74	75
2.00	75	103	105	150	51	137	74	76	32	59	0	0	308	114	439	72	135	29	32	20	55	135	74	75
2.17	55	76	105	122	37	143	54	56	24	40	0	0	286	114	447	55	99	23	25	16	55	135	74	75
2.34	42	58	105	105	28	147	42	44	18	30	0	0	257	114	452	43	75	18	20	12	55	135	74	75
2.51	32	45	105	105	22	149	33	35	14	24	0	12	224	114	452	34	59	15	16	10	55	135	74	75
2.67	26	37	105	86	17	152	27	29	11	20	0	49	190	114	446	30	48	13	15	9	55	135	74	75
2.84	23	32	105	53	15	153	24	26	10	20	0	86	157	114	432	28	41	13	14	9	55	135	74	75
3.01	21	29	105	29	13	153	22	25	9	20	0	100	123	114	410	27	37	13	14	9	55	135	74	75
3.17	20	28	108	17	12	150	21	24	9	19	0	100	105	114	381	27	35	13	14	9	55	135	74	75
3.34	19	27	110	11	11	145	20	23	8	17	0	100	105	114	350	26	33	12	14	9	55	135	74	75
3.51	18	26	111	8	10	137	19	23	8	16	0	100	79	114	317	26	32	12	13	8	55	135	74	75
3.67	17	24	111	6	10	127	18	22	8	15	0	100	45	114	282	24	31	11	12	8	55	135	61	75
3.84	15	21	110	2	9	115	16	18	7	13	0	100	25	114	254	19	27	8	9	6	55	135	52	75
4.01	12	17	108	1	7	105	13	14	5	11	0	100	12	114	226	14	22	6	7	4	55	135	45	75
4.18	9	13	105	0	6	105	10	11	4	9	0	100	4	114	192	11	17	5	5	3	55	135	38	75
4.34	8	11	105	0	5	105	8	9	3	7	0	100	0	114	155	10	14	4	5	3	55	135	32	75
4.51	7	10	105	0	4	105	7	8	3	6	0	100	0	114	119	9	12	4	4	3	55	135	28	75
4.68	6	9	105	0	4	105	7	8	3	6	0	100	0	114	87	8	11	4	4	3	55	135	24	75
4.84	6	9	105	0	4	105	7	8	3	6	0	100	0	114	61	9	11	4	5	3	55	135	21	75
5.01	6	9	105	0	4	102	7	8	3	5	0	100	0	114	43	9	11	4	5	3	55	135	20	75
5.18	6	9	105	0	4	83	7	8	3	5	0	100	0	114	31	9	11	4	5	3	55	135	19	75
5.34	6	9	75	0	4	68	7	8	3	5	0	100	0	114	24	9	11	4	5	3	55	135	18	75
5.51	6	8	38	0	3	54	6	8	3	5	0	78	0	114	20	8	11	4	4	3	55	135	17	75
5.68	6	8	18	0	3	42	6	7	3	4	0	40	0	114	19	8	10	4	4	3	55	135	16	75
5.85	6	8	12	0	3	32	6	8	3	4	0	11	0	114	18	9	10	4	4	3	55	135	15	75
6.01	6	9	9	0	3	24	7	8	3	4	0	0	0	114	18	9	11	4	5	3	55	135	14	75
6.18	6	9	7	0	4	18	7	8	3	4	0	0	0	114	18	9	11	5	5	3	55	135	14	75
6.35	7	9	5	0	4	12	7	8	3	4	0	0	0	114	18	10	11	5	5	3	55	135	13	75
6.51	7	9	3	0	4	6	7	8	3	4	0	0	0	114	18	10	12	5	5	3	55	135	13	75
6.68	7	9	2	0	4	7	8	8	3	4	0	0	0	107	18	10	12	5	5	3	55	135	13	75

TABLE 2
HYDROGRAPHS ADJUSTED FOR STORM DRAIN FLOW AND ARTIFICIAL BASE FLOW

Time hours	1 BETH11	2 BETH15	3 B19E	4 BECW	5 BETHA7	6 G19E	7 GLEN17	8 GLEN12	9 GLEN7T	10 GLCW	11 GLEN15	13 C19E	14 CACW	15 TOTL-S	17 SPGC7A	18 GRCA15	19 CAME15	20 CAME11	21 CAME17	22 CAME3A
0.00	100	100	100	170	150	170	250	350	170	170	210	250	50	50	1	100	200	100	100	50
0.17	125	100	100	183	137	170	267	371	191	190	210	250	50	54	1	95	200	124	141	72
0.33	172	128	100	223	127	170	306	424	225	207	210	250	74	71	1	147	200	174	215	115
0.50	244	220	100	275	159	170	372	510	306	238	210	250	145	113	1	265	299	236	292	161
0.67	322	324	100	282	203	170	449	604	358	279	210	250	159	157	1	376	432	286	344	195
0.84	386	416	100	326	241	210	518	686	383	322	210	250	215	164	1	463	547	324	378	217
1.00	434	489	100	362	267	275	575	753	399	349	210	250	268	164	1	530	636	352	399	233
1.17	450	517	100	388	277	275	597	771	399	362	210	250	317	164	85	527	669	339	377	221
1.34	406	463	103	395	260	275	555	701	363	354	213	250	354	164	195	406	602	265	290	167
1.50	329	358	120	388	221	275	476	595	281	332	230	250	372	164	311	266	472	196	210	118
1.67	255	258	164	371	180	284	402	507	239	296	231	250	378	164	389	175	345	160	169	92
1.84	205	189	205	347	147	297	353	457	216	260	218	250	372	164	424	126	255	140	145	78
2.00	175	148	205	320	127	307	324	426	202	229	210	250	358	164	440	97	200	129	132	70
2.17	155	121	205	292	113	313	304	406	194	210	210	250	336	164	448	80	164	123	125	66
2.34	142	103	205	275	104	317	292	394	188	200	210	250	307	164	453	68	140	118	120	62
2.51	132	90	205	275	98	319	283	385	184	194	210	262	274	164	453	59	124	115	116	60
2.67	126	82	205	256	93	322	277	379	181	190	210	299	240	164	447	55	113	113	115	59
2.84	123	77	205	223	91	323	274	376	180	190	210	336	207	164	433	53	106	113	114	59
3.01	121	74	205	199	89	323	272	375	179	190	210	350	173	164	411	52	102	113	114	59
3.17	120	73	208	187	88	320	271	374	179	189	210	350	155	164	382	52	100	113	114	59
3.34	119	72	210	181	87	315	270	373	178	187	210	350	155	164	351	51	98	112	114	59
3.51	118	71	211	178	87	307	269	373	178	186	210	350	129	164	318	51	97	112	113	58
3.67	117	69	211	176	99	297	268	372	178	185	210	350	95	164	283	49	96	111	112	58
3.84	115	66	210	172	107	285	266	369	183	183	210	350	75	164	255	44	92	108	109	56
4.01	112	62	208	171	112	275	263	364	175	181	210	350	62	164	227	39	87	106	107	54
4.18	109	58	205	170	118	275	260	361	174	179	210	350	54	164	193	36	82	105	105	53
4.34	108	56	205	170	123	275	258	359	173	177	210	350	50	164	156	35	79	104	105	53
4.51	107	55	205	170	126	275	257	358	173	176	210	350	50	164	120	34	77	104	104	53
4.68	106	54	205	170	130	275	257	358	173	176	210	350	50	164	98	33	76	104	104	53
4.84	106	54	205	170	133	275	257	358	173	176	210	350	50	164	62	34	76	104	105	53
5.01	106	54	205	170	134	272	257	358	173	175	210	350	50	164	44	34	76	104	105	53
5.18	106	54	205	170	135	253	257	358	173	175	210	350	50	164	32	34	76	104	105	53
5.34	106	54	175	170	136	238	257	358	173	175	210	350	50	164	25	34	76	104	105	53
5.51	106	53	138	170	136	224	256	358	173	175	210	328	50	164	21	33	76	104	104	53
5.68	106	53	118	170	137	212	256	357	173	174	210	290	50	164	20	33	75	104	104	53
5.85	106	53	112	170	138	202	256	358	173	174	210	261	50	164	19	34	75	104	105	53
6.01	106	54	109	170	139	194	257	358	173	174	210	250	50	164	19	34	76	104	105	53
6.18	106	54	107	170	140	188	257	358	173	174	210	250	50	164	19	34	76	105	105	53
6.35	107	54	105	170	141	182	257	358	173	174	210	250	50	164	19	35	76	105	105	53
6.51	107	54	103	170	141	176	257	358	173	174	210	250	50	164	19	35	77	105	105	53
6.68	107	54	102	170	141	172	257	358	173	174	210	250	50	157	19	35	77	104	105	53

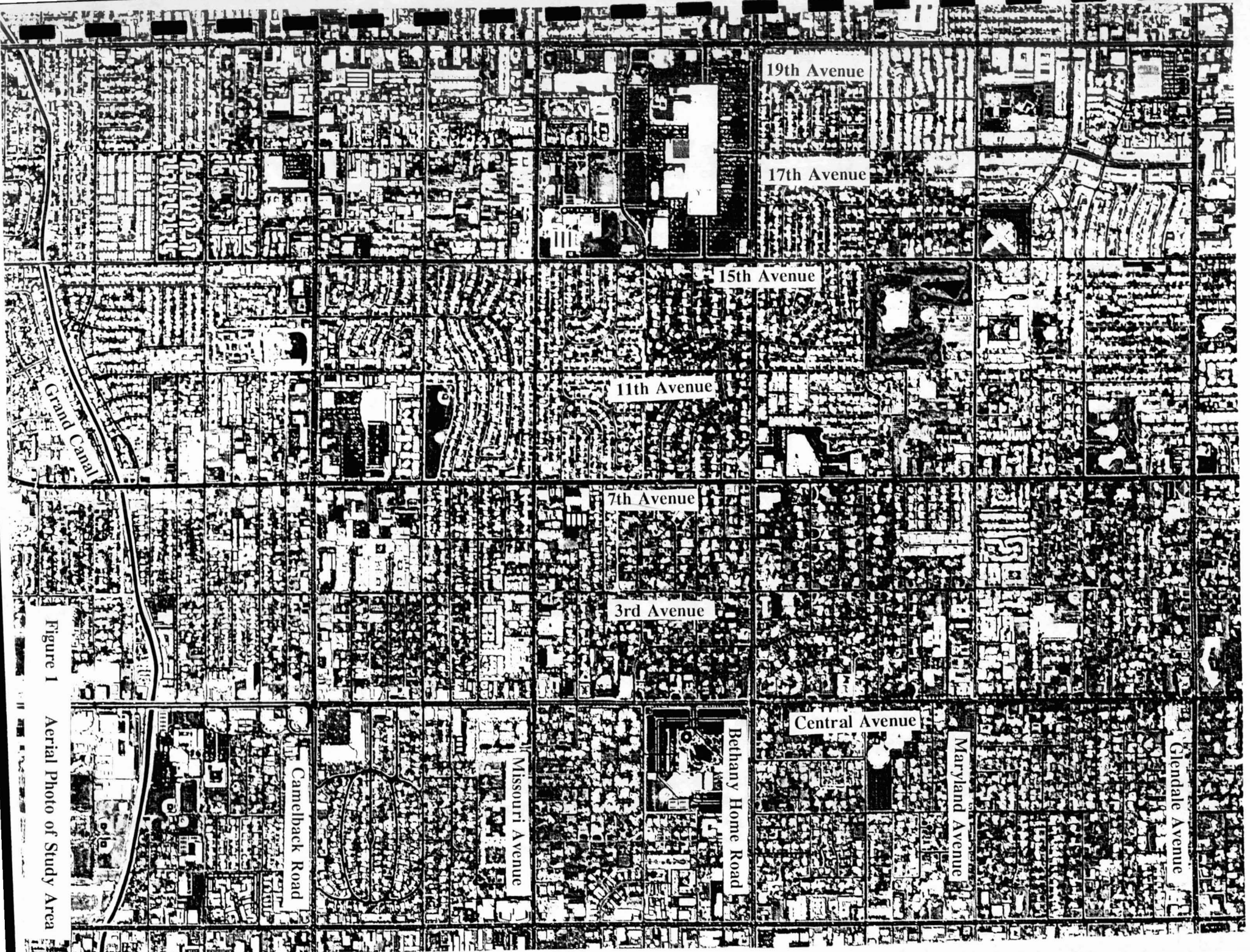


Figure 1 Aerial Photo of Study Area

GLENDALE ROAD PROFILE

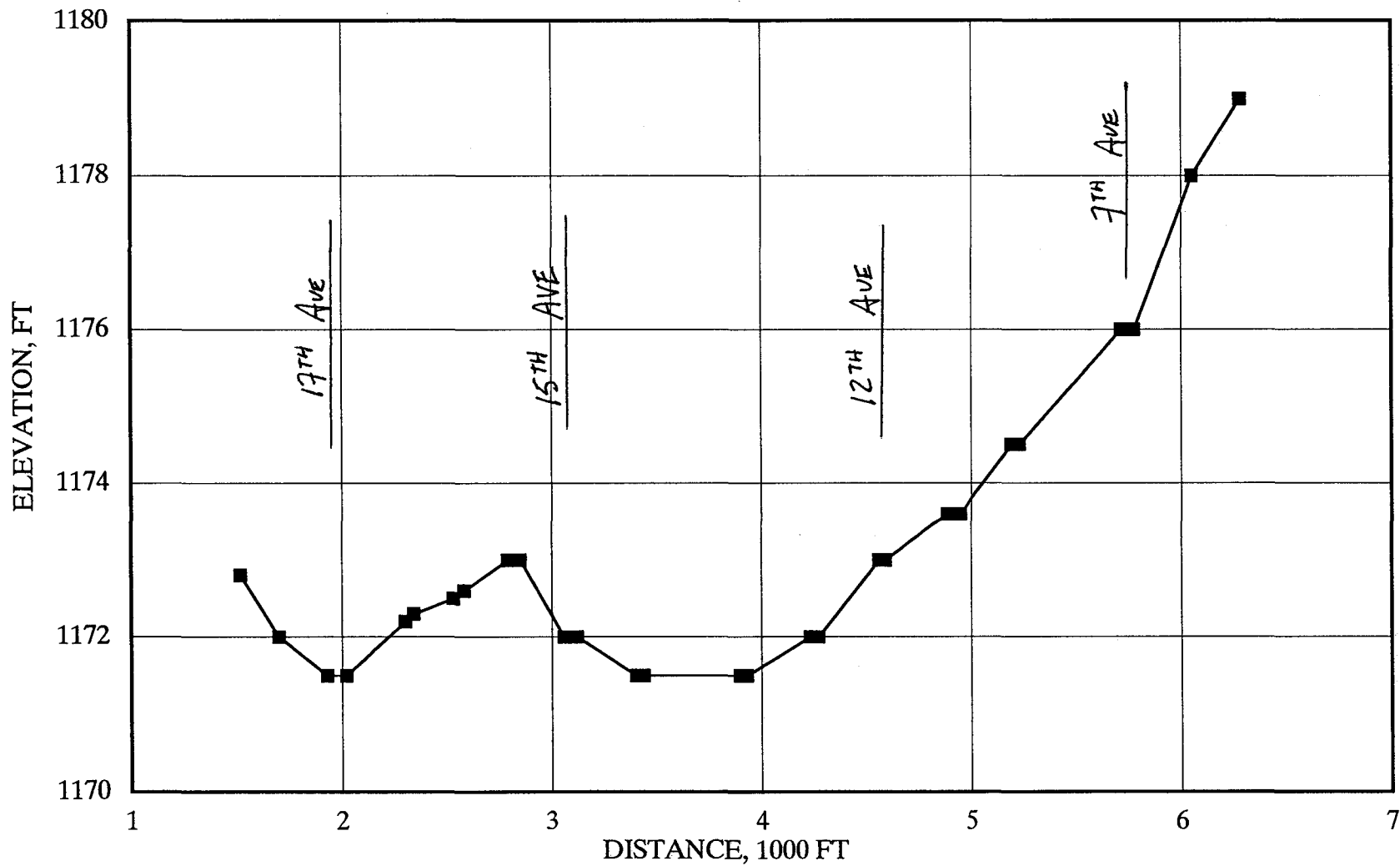


Figure 2 Glendale Avenue Profile between 17th Avenue and 7th Avenue

MARYLAND AVENUE PROFILE

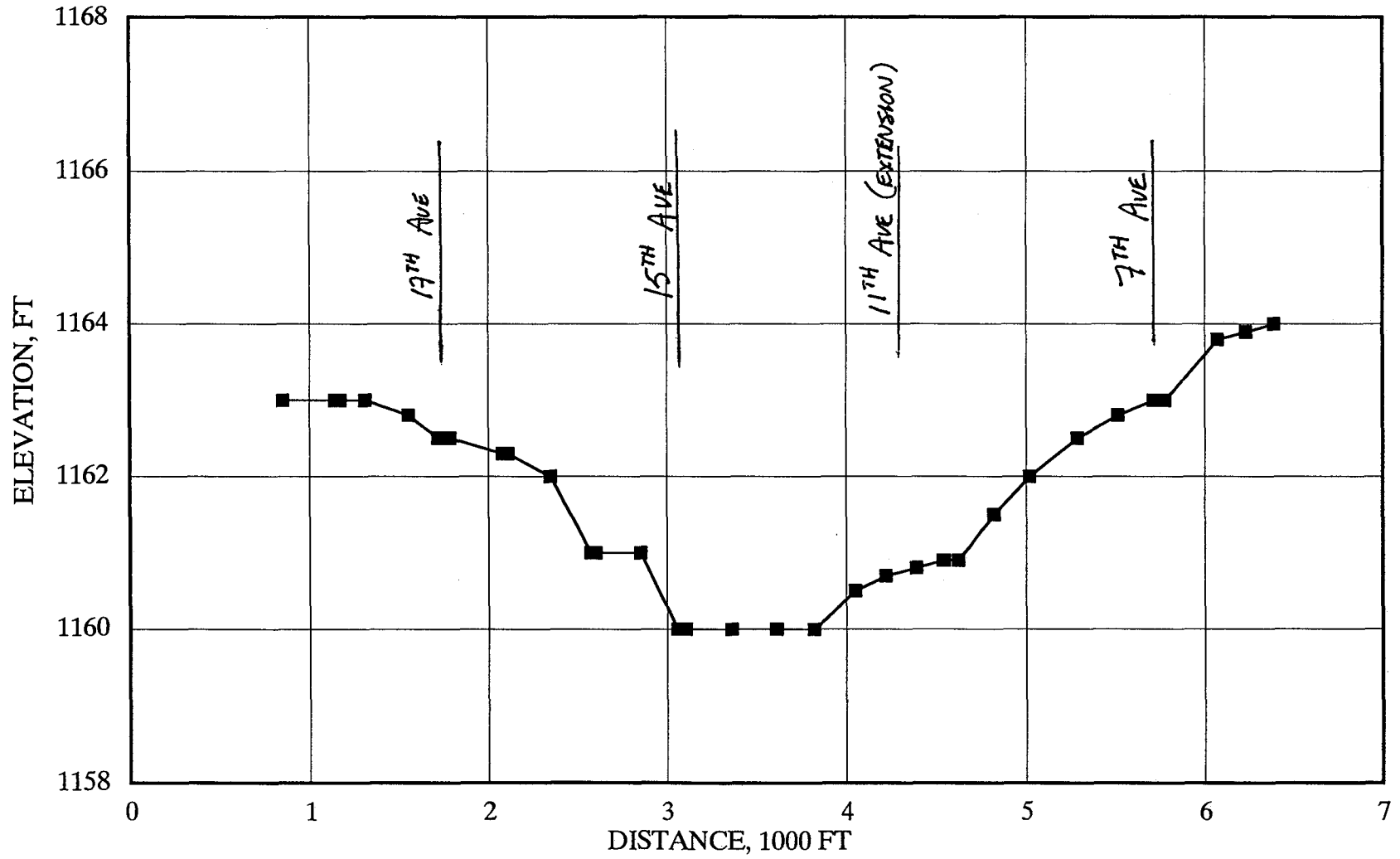


Figure 3 Maryland Avenue Profile between 17th Avenue and 7th Avenue

BETHANY HOME ROAD PROFILE

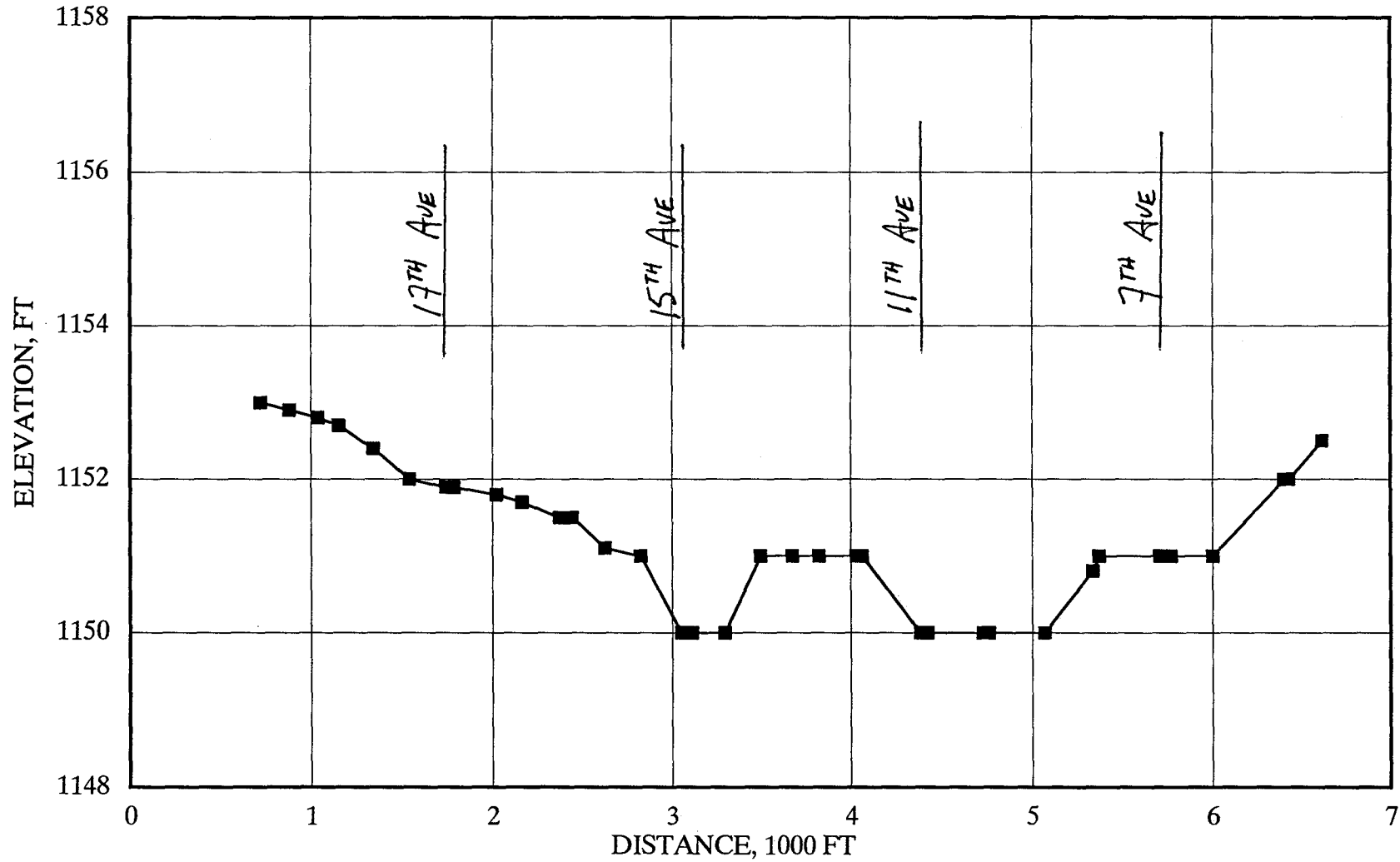


Figure 4 Bethany Home Road Profile between 17th Avenue and 7th Avenue

MISSOURI AVENUE PROFILE

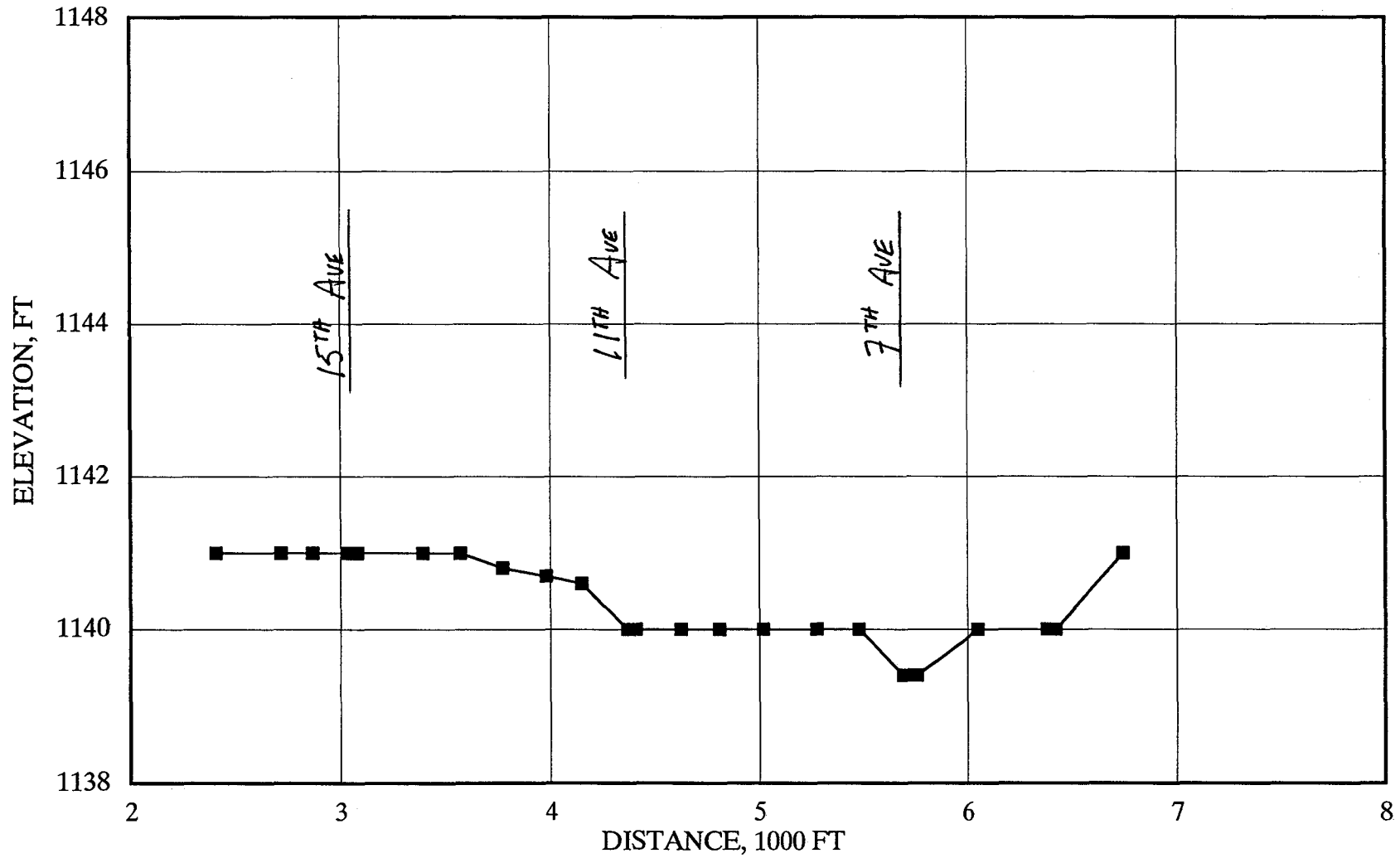


Figure 5 Missouri Avenue Profile between 17th Avenue and 7th Avenue

CAMELBACK ROAD PROFILE

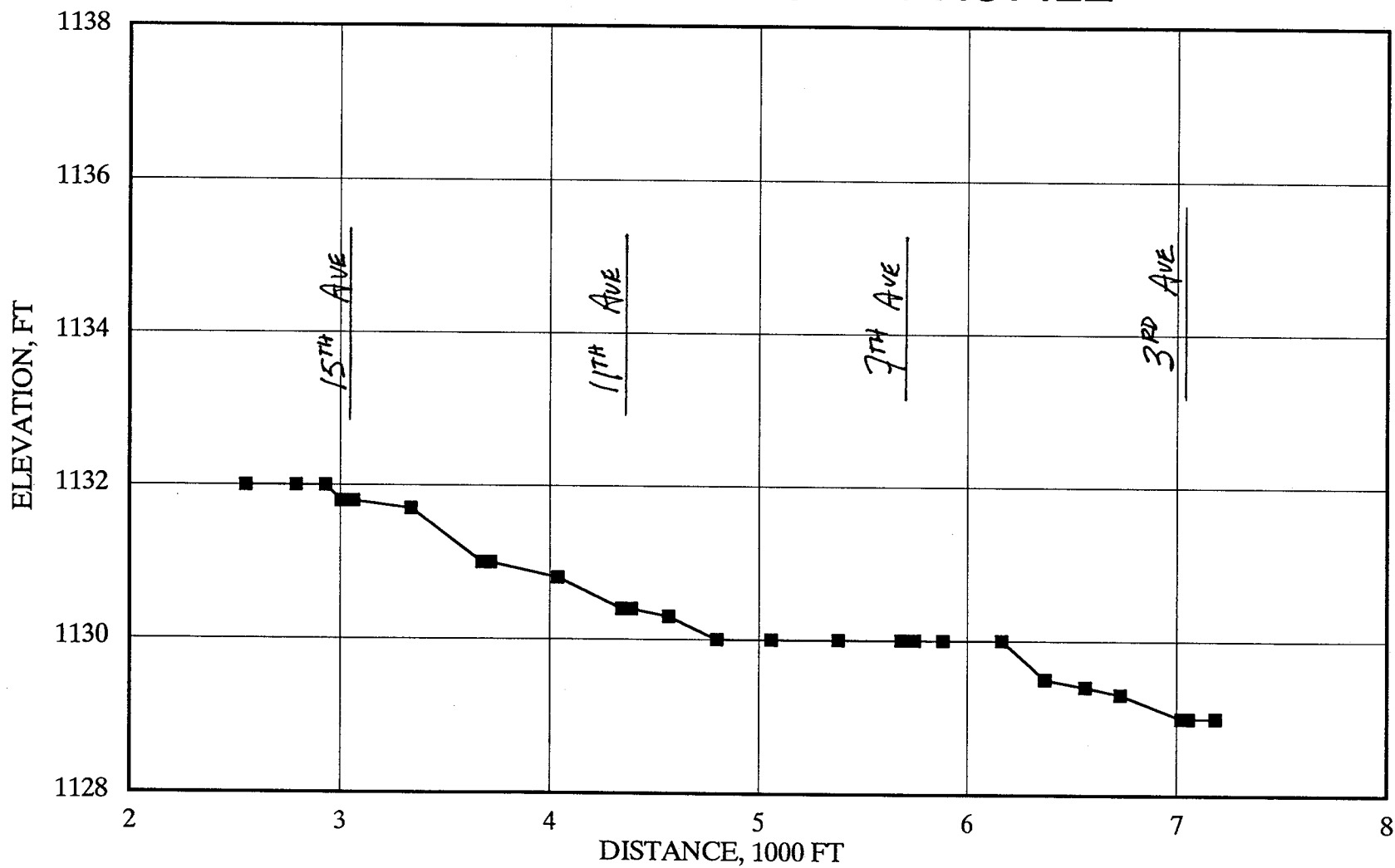


Figure 6 Camelback Road Profile between 17th Avenue and 7th Avenue

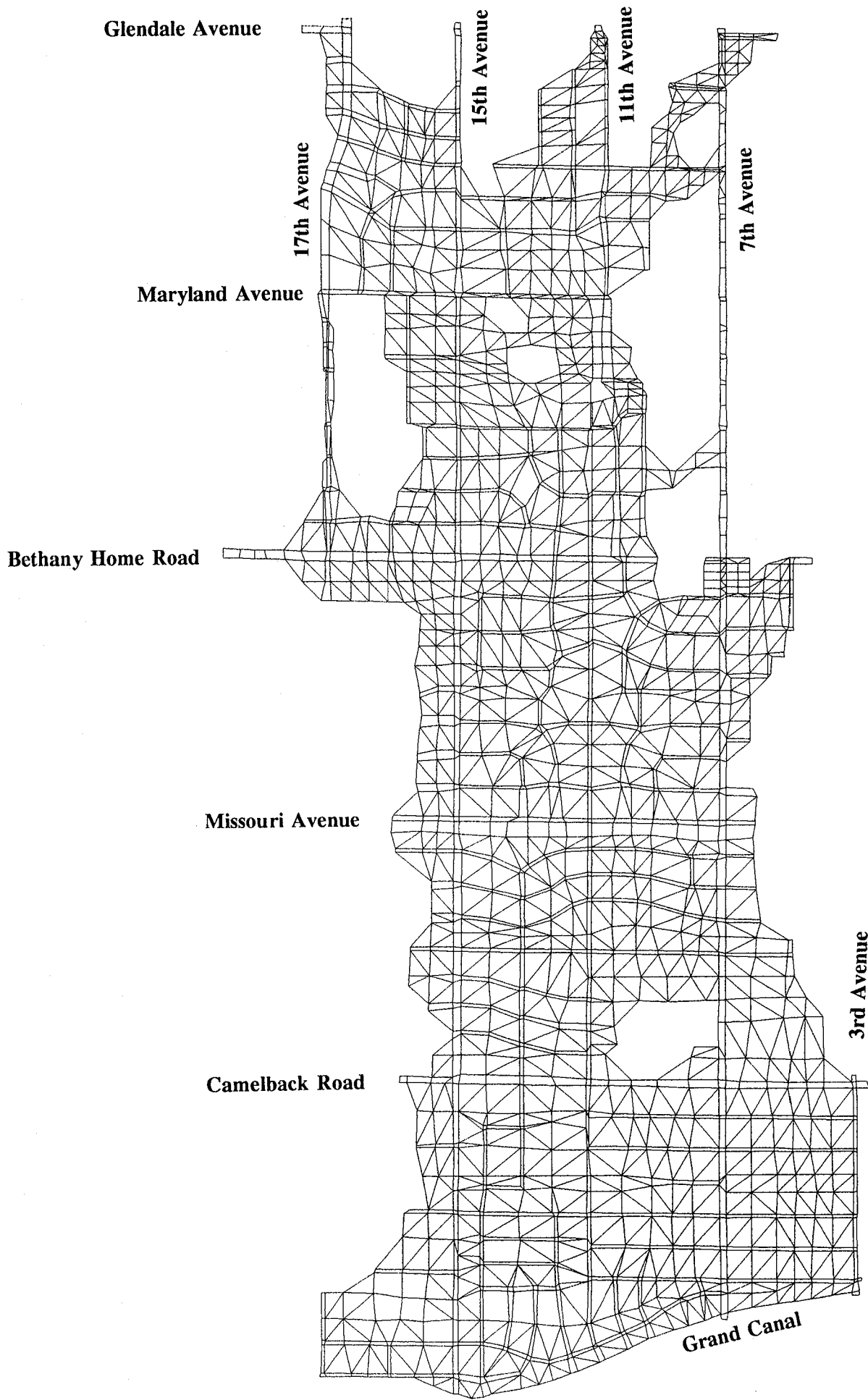


Figure 7 Final Computational Mesh Configurati

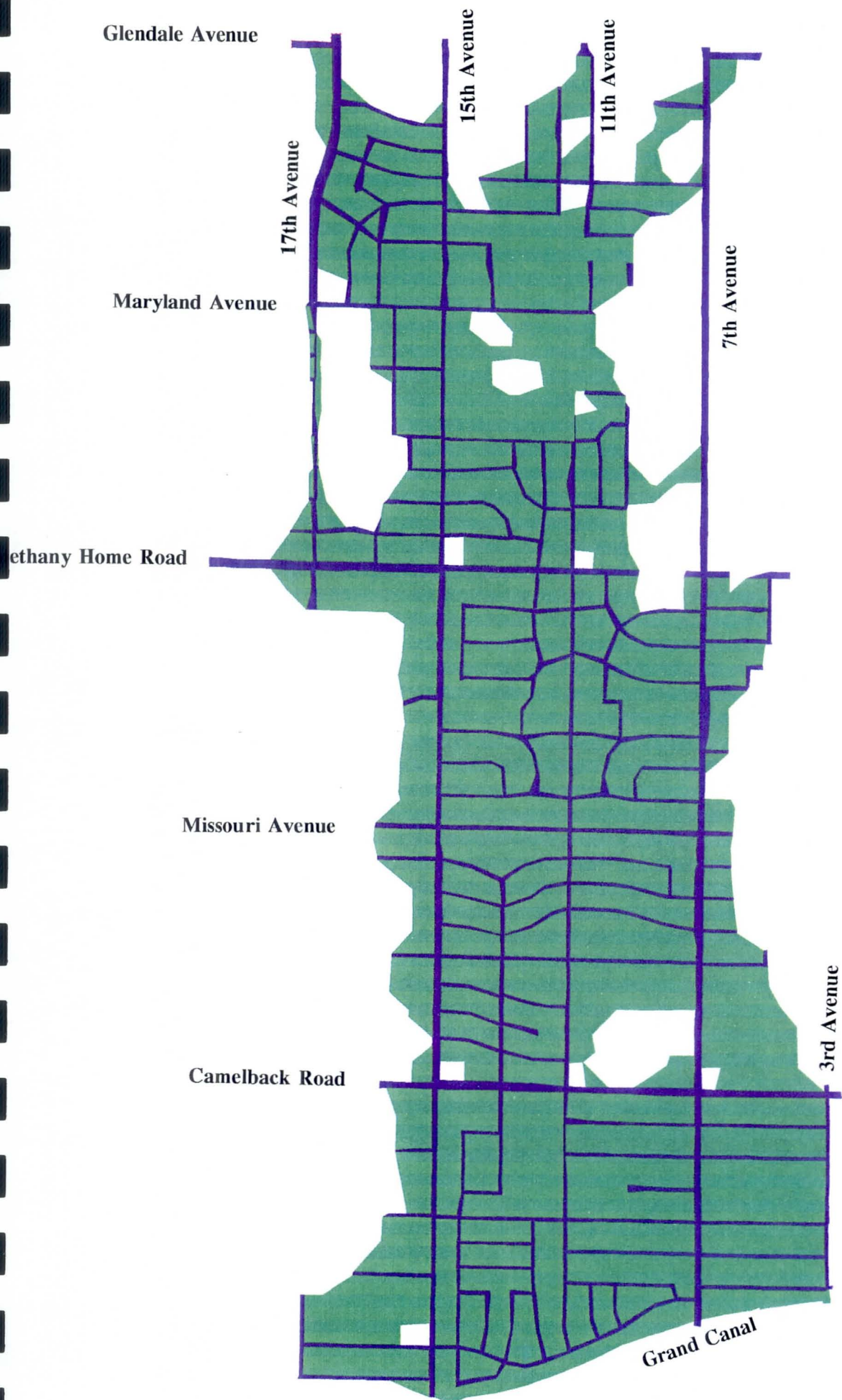
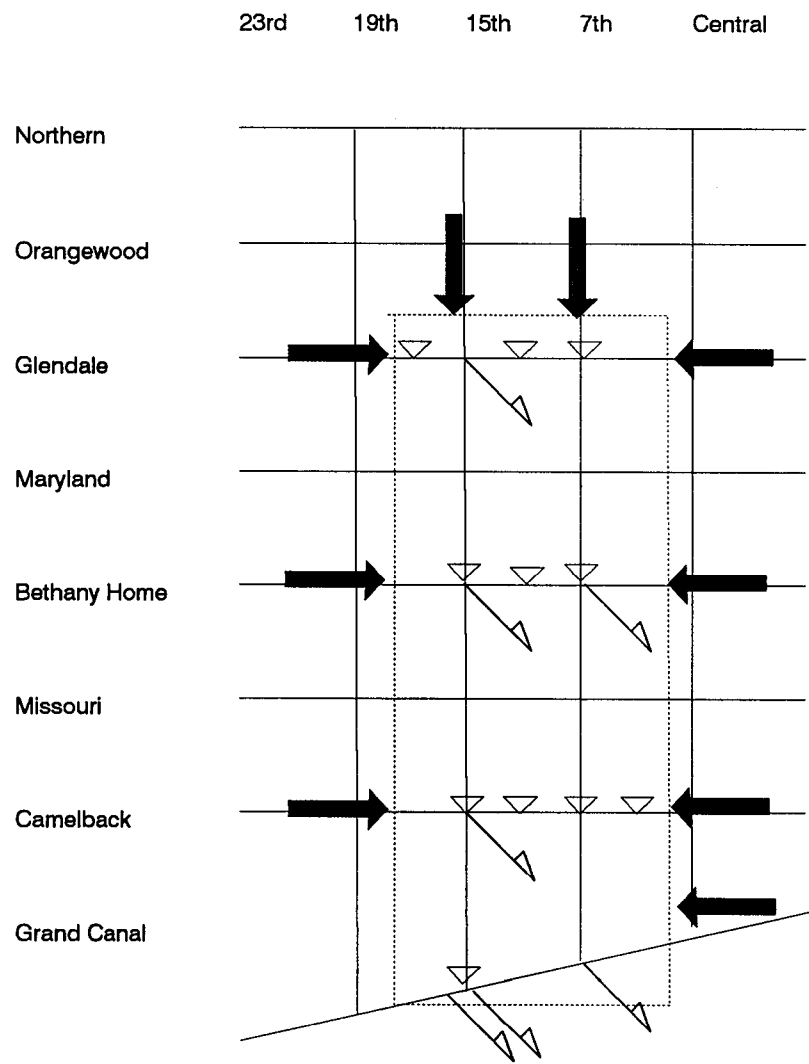


Figure 8 Street and Non-Street Areas within the Computational Mesh



LEGEND

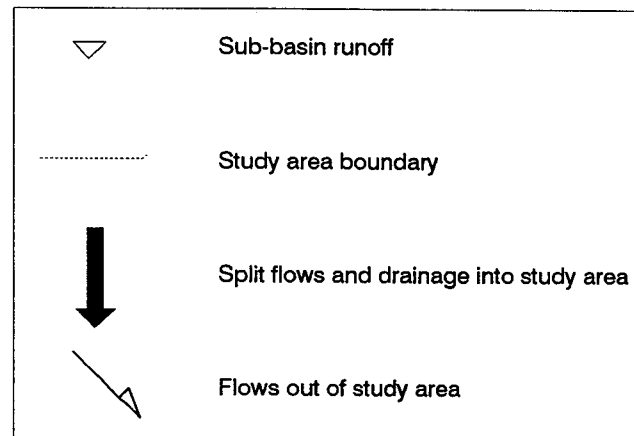


Figure 9 Flow Schematic for the Study Area

BOUNDARY FLOWS AT GLENDALE

100-YEAR FLOOD

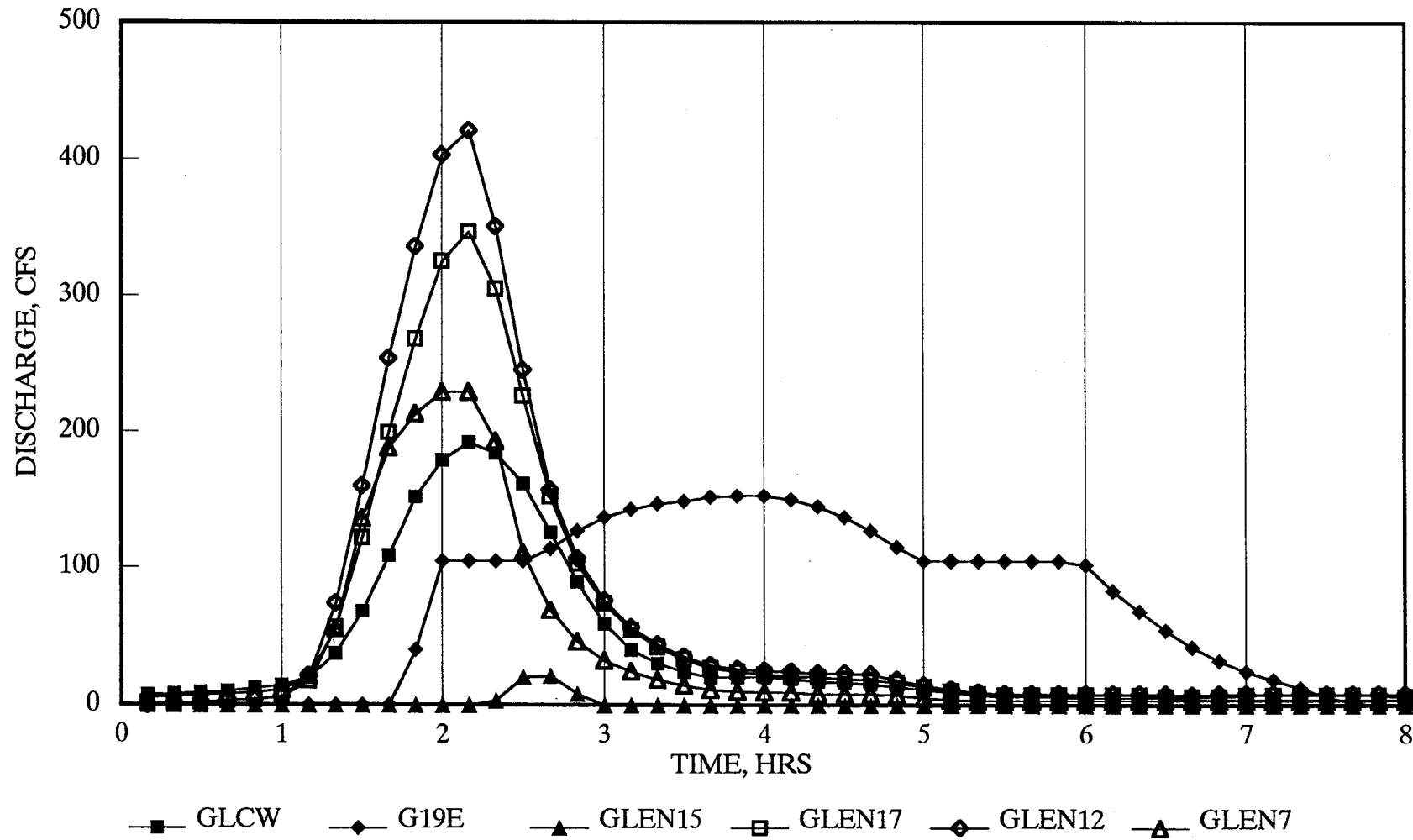


Figure 10 Boundary Flow Hydrographs along Glendale Avenue

BOUNDARY FLOWS AT BETHANY HOME

100-YEAR FLOOD

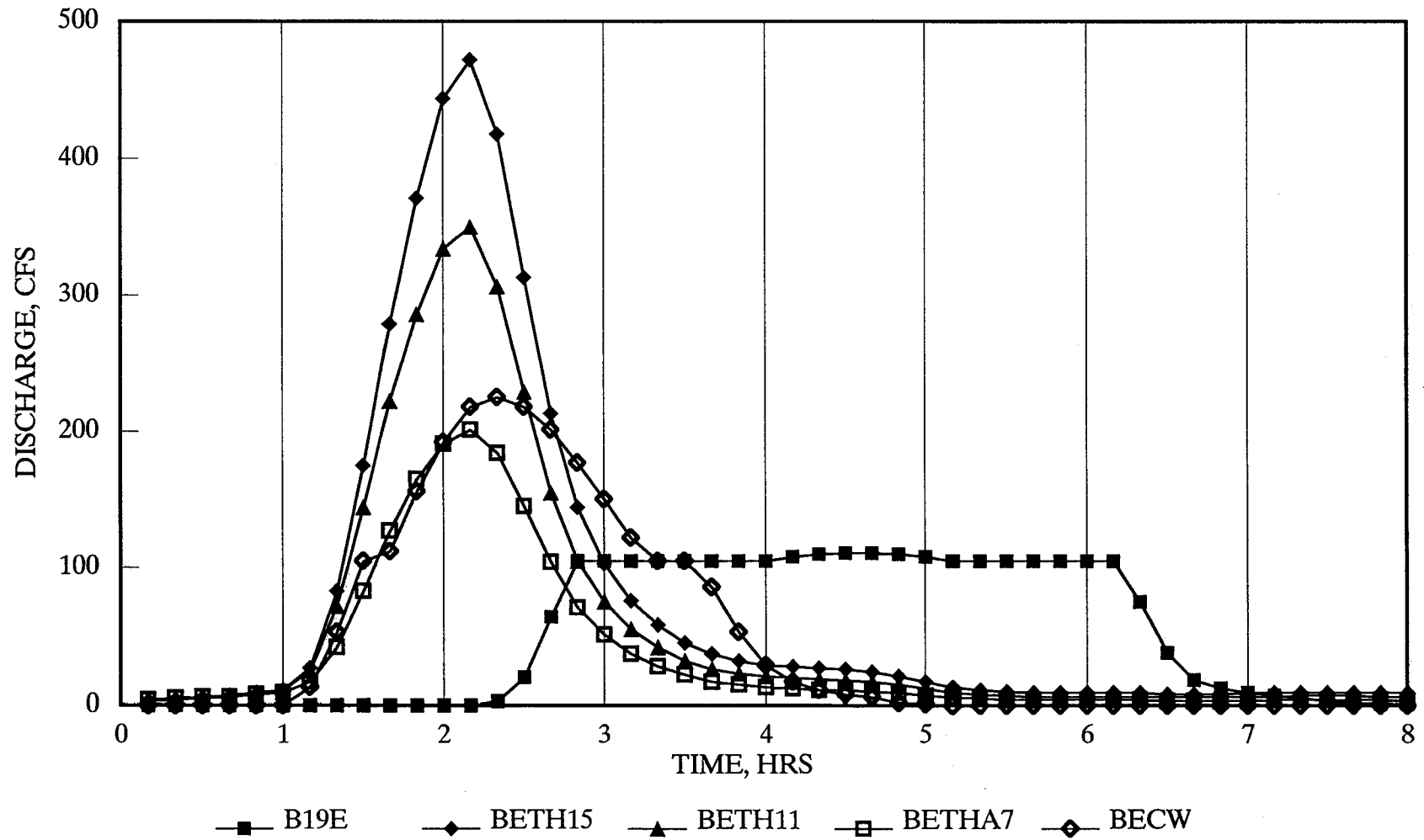


Figure 11 Boundary Flow Hydrographs along Bethany Home Road

BOUNDARY FLOWS AT CAMELBACK

100-YEAR FLOOD

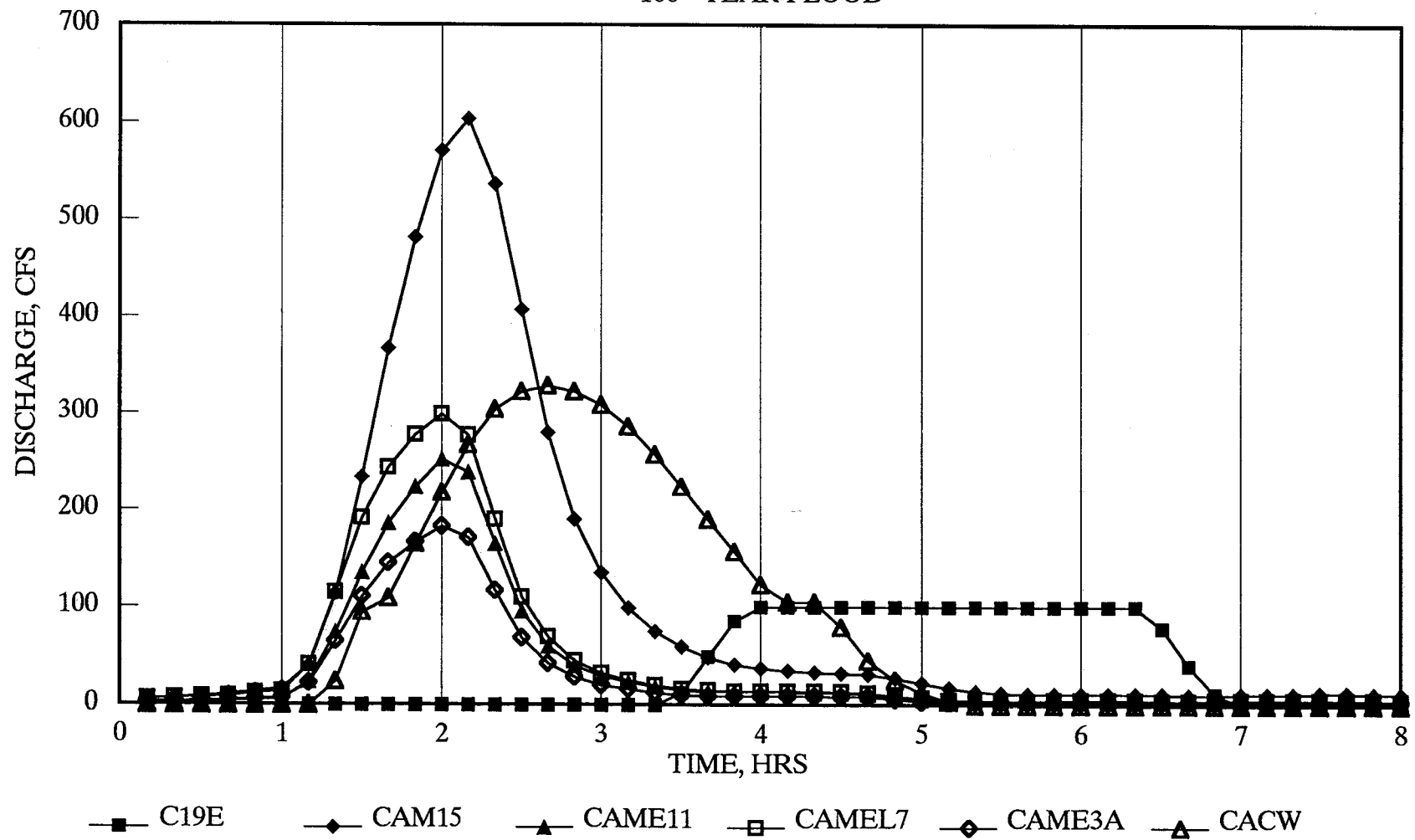


Figure 12 Boundary Flow Hydrographs along Camelback Road

BOUNDARY FLOWS AT GRAND CANAL

100-YEAR FLOOD

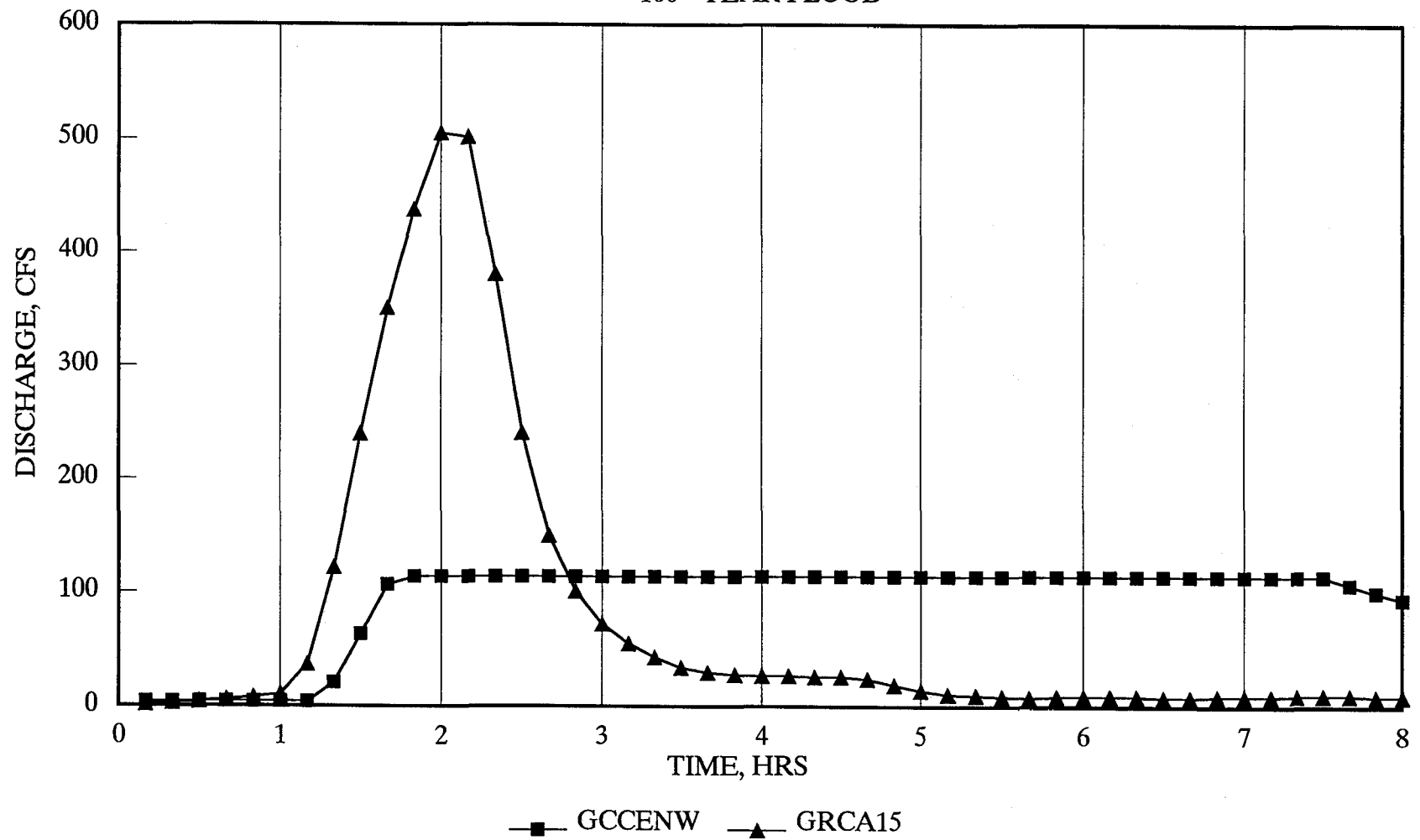


Figure 13 Boundary Flow Hydrographs along the Grand Canal

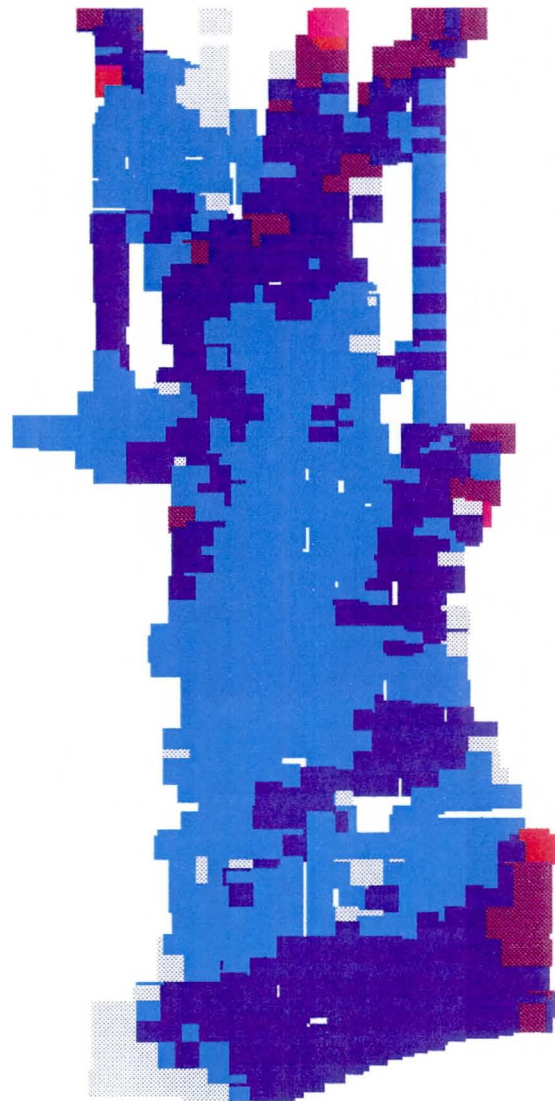


Figure 14 Maximum Computed Flow Depths -- 100-Year Flood Condition 1 Analysis (minimum initial wet condition)

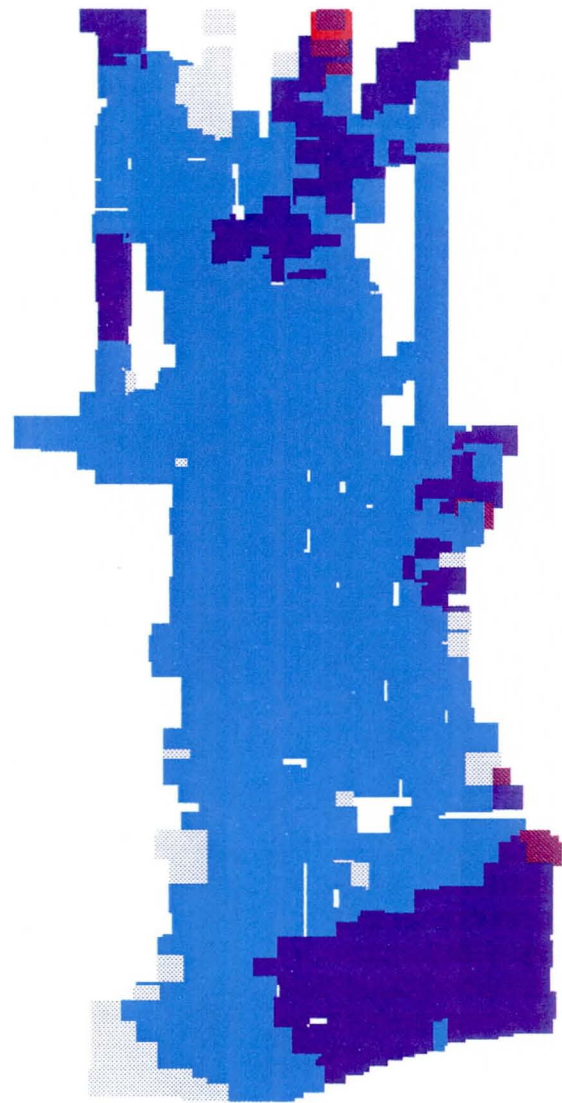


Figure 15 Maximum Computed Flow Depths -- 100-Year Flood Condition 2 Analysis (increased initial wet condition)

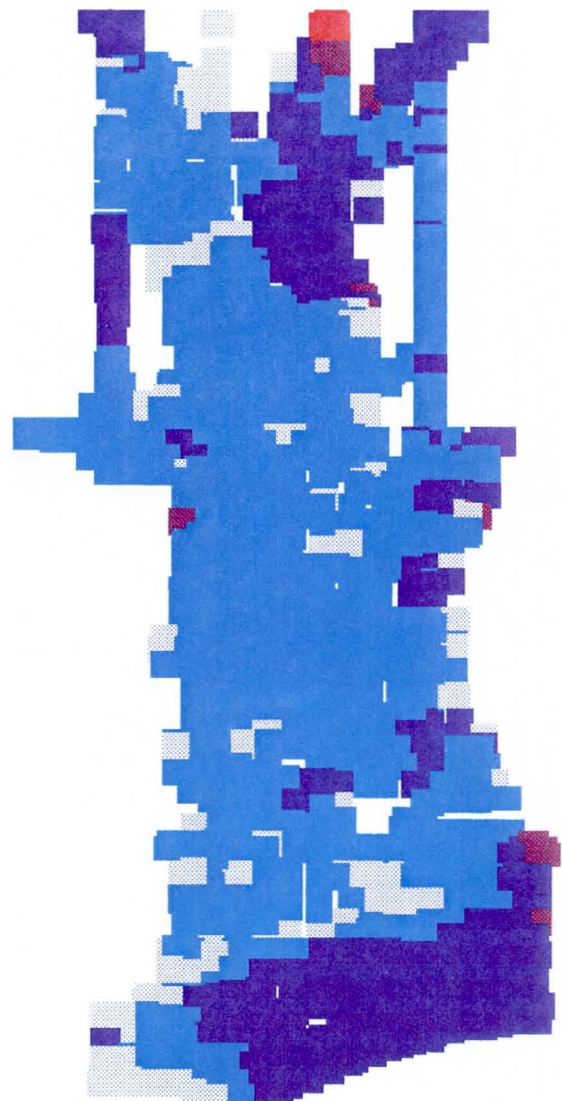


Figure 16 Maximum Computed Flow Depths -- 100-year Flood
 Condition 3 Analysis (altered initial geometry condition)



Figure 17 Areas with 100-Year Flow Depth Exceeding 0.5 feet
Condition 1 Analysis (minimum initial wet condition)

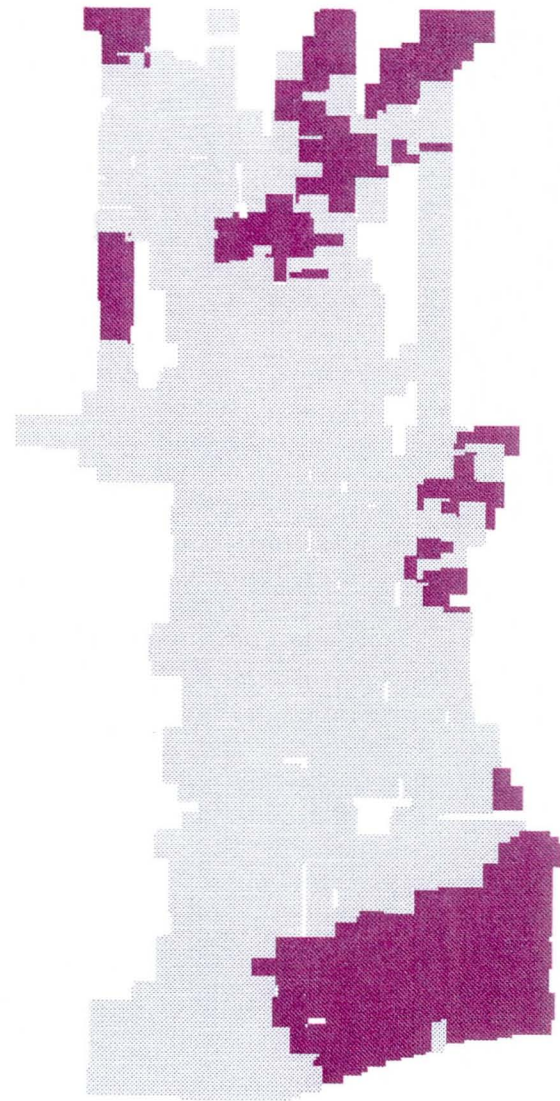


Figure 18 Areas with 100-Year Flow Depth Exceeding 0.4 feet
Condition 2 Analysis (increased initial wet condition)

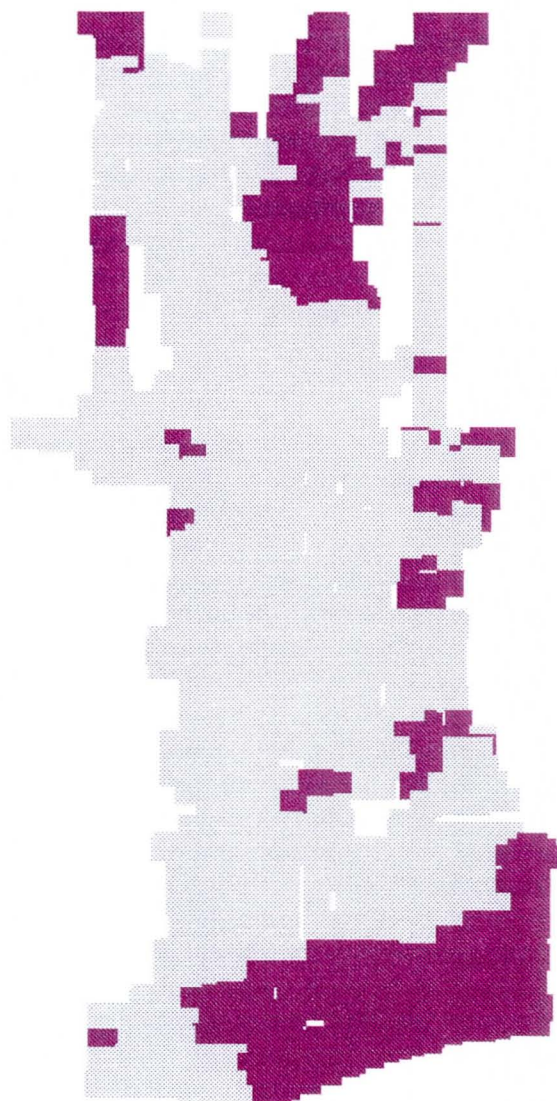


Figure 19 Areas with 100-Year Flow Depth Exceeding 0.4 feet
Condition 3 Analysis (altered initial geometry condition)

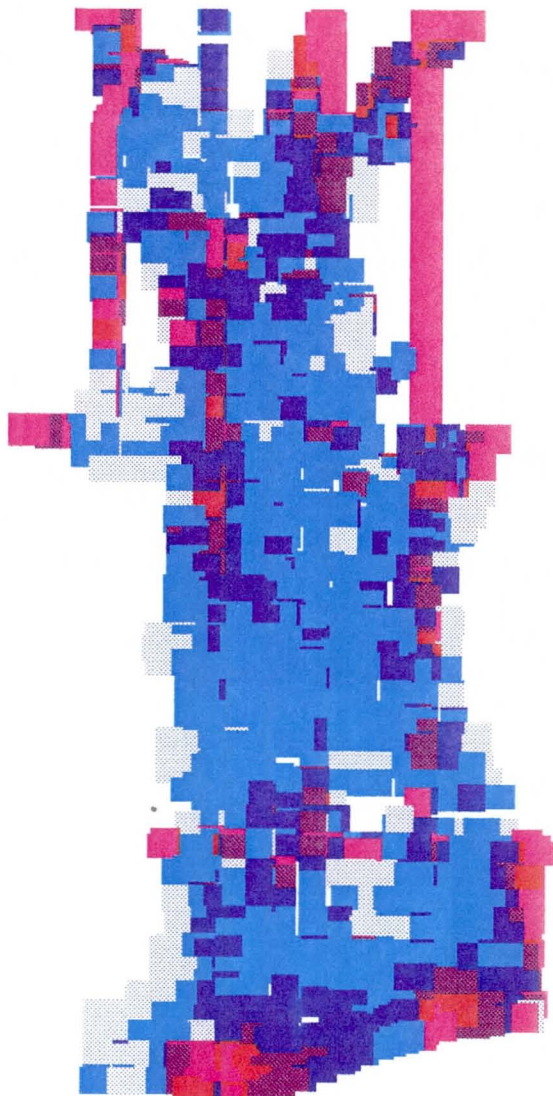
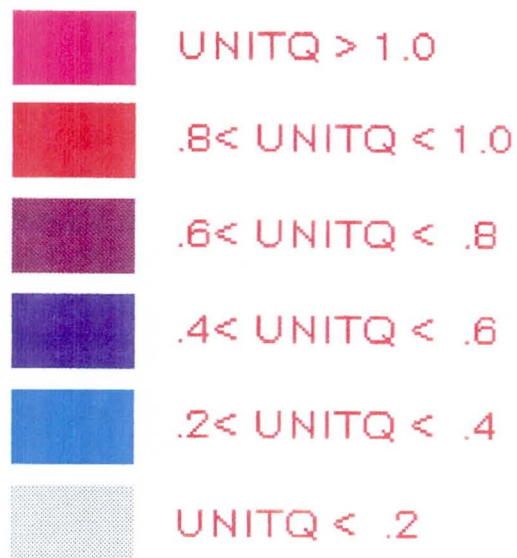


Figure 20 Maximum Unit Discharge Variation -- 100-Year Flood Condition 1 Analysis (minimum initial wet condition)

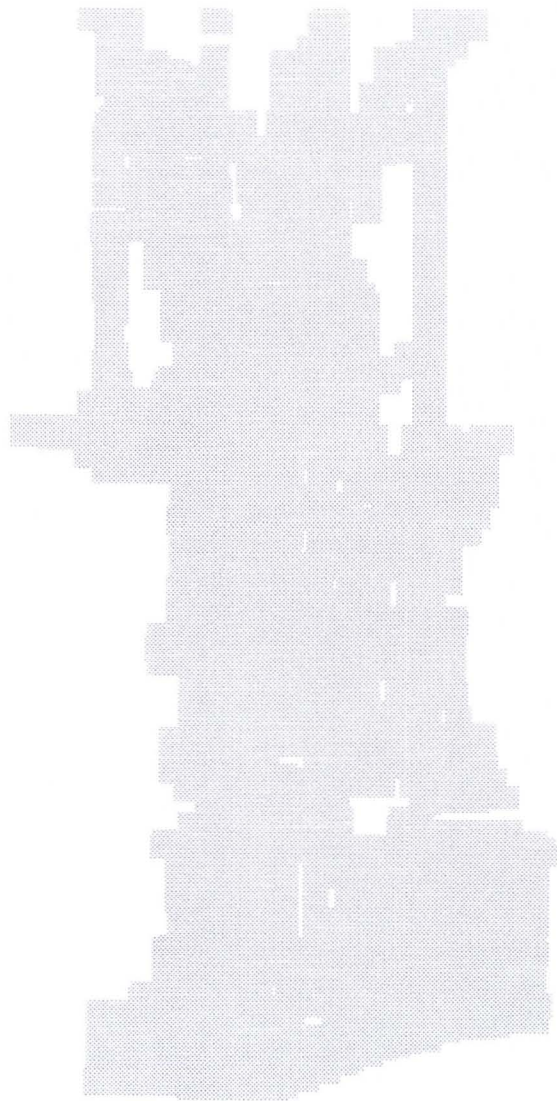


Figure 21 Dynamic Simulation of the 100-Year Flood through the Study Area
 Computed Flow Depth at Time Step 1

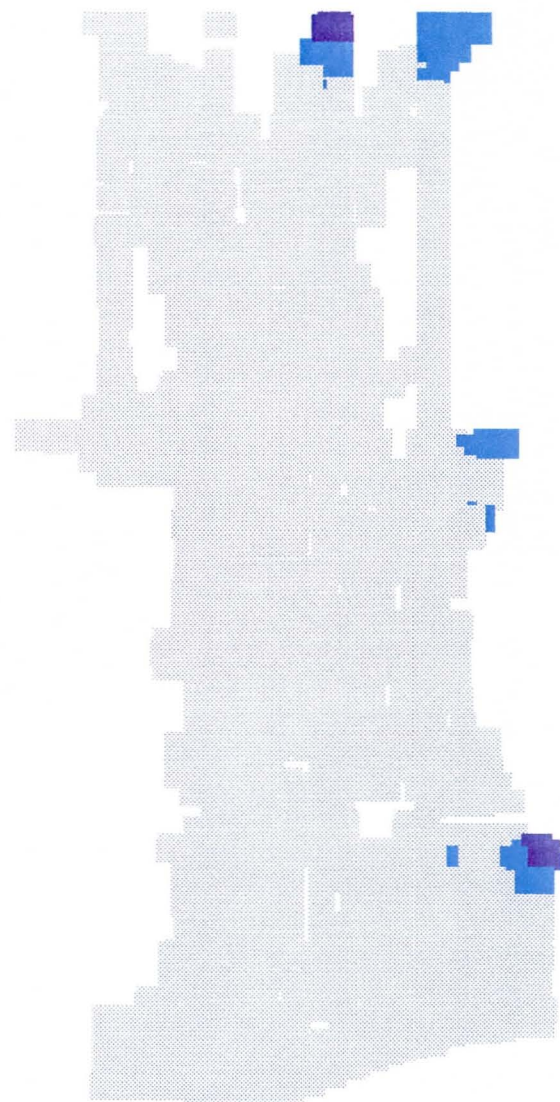


Figure 22 Dynamic Simulation of the 100-Year Flood through the Study Area
 Computed Flow Depth at Time Step 3

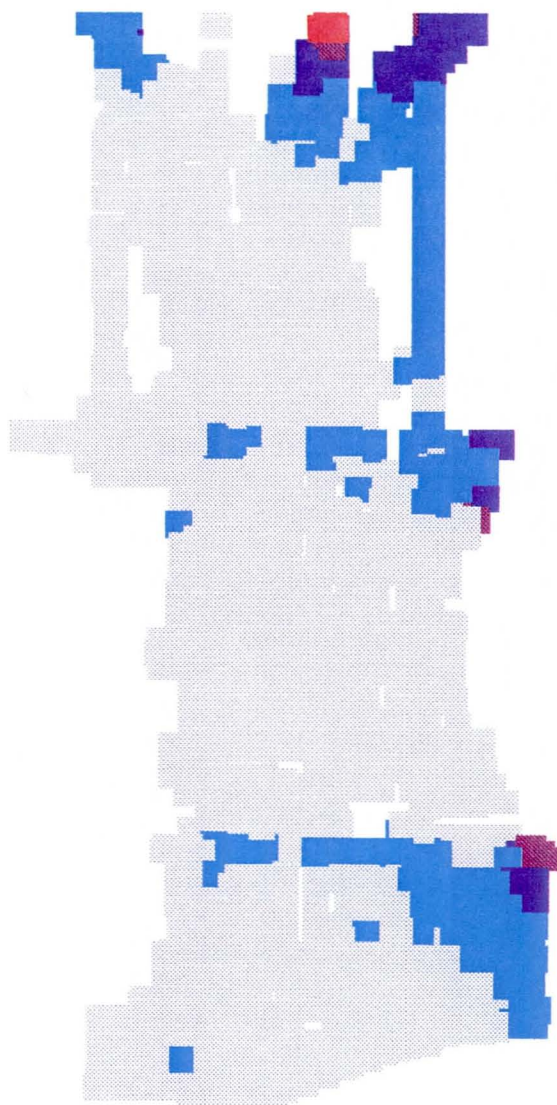


Figure 23 Dynamic Simulation of the 100-Year Flood through the Study Area
 Computed Flow Depth at Time Step 5

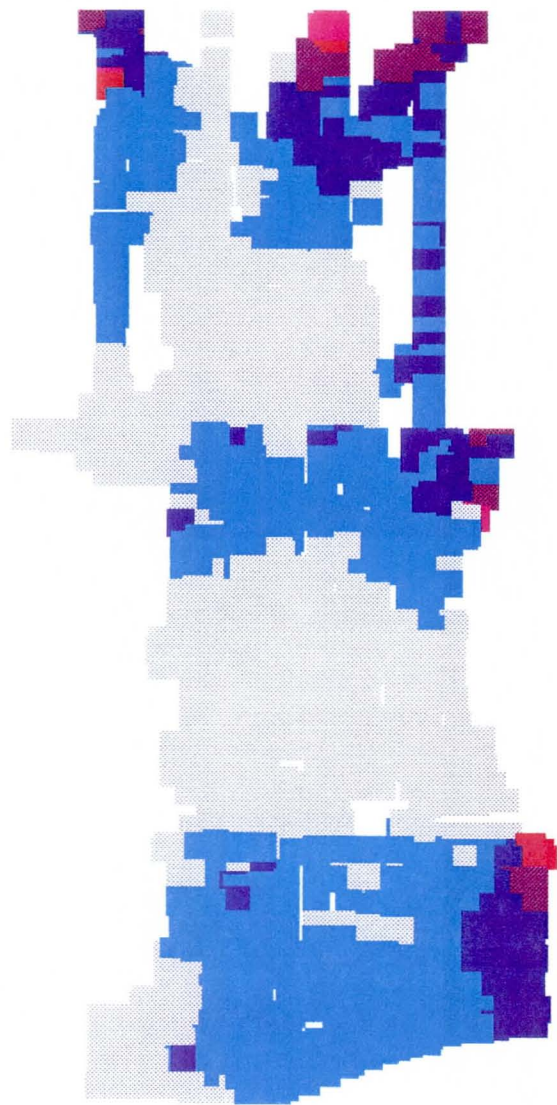


Figure 24 Dynamic Simulation of the 100-Year Flood through the Study Area
Computed Flow Depth at Time Step 7

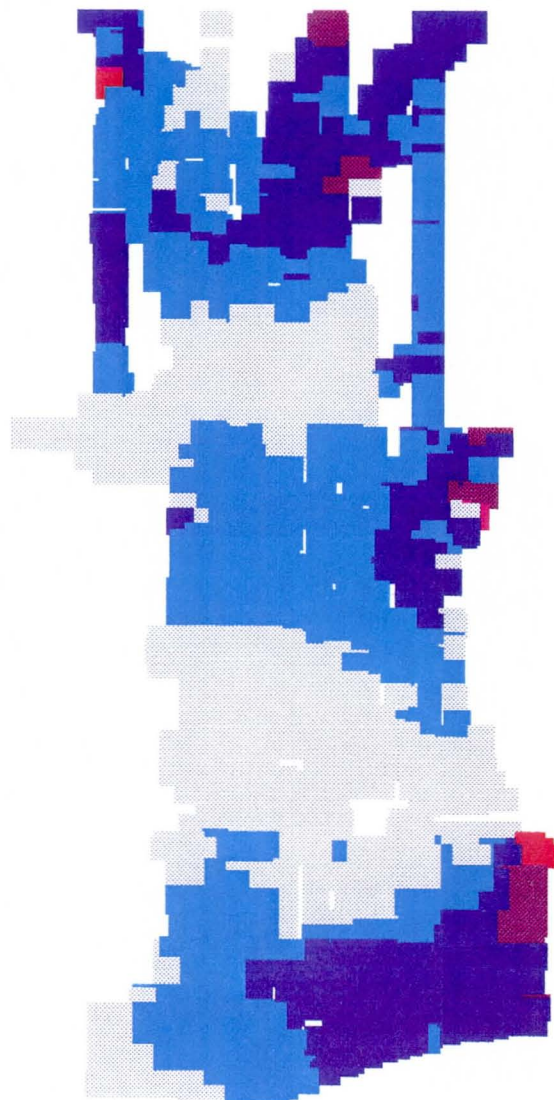


Figure 25 Dynamic Simulation of the 100-Year Flood through the Study Area
Computed Flow Depth at Time Step 9

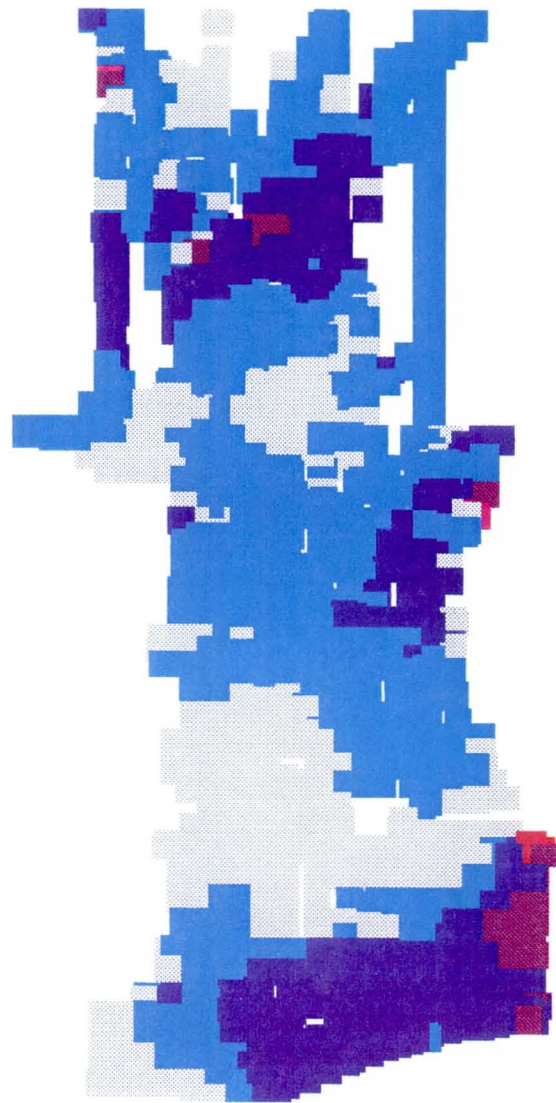


Figure 26 Dynamic Simulation of the 100-Year Flood through the Study Area
 Computed Flow Depth at Time Step 11

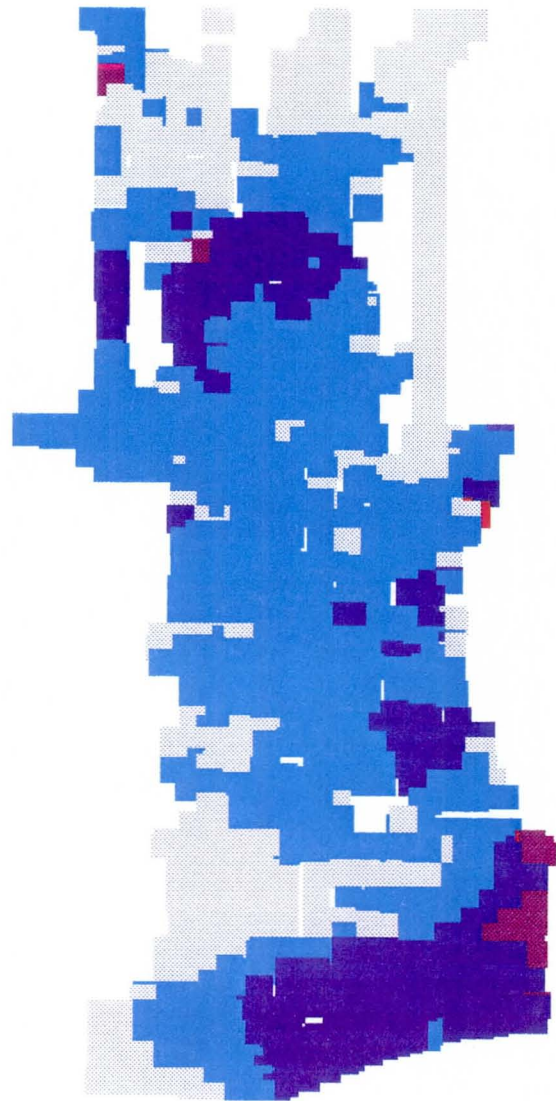


Figure 27 Dynamic Simulation of the 100-Year Flood through the Study Area
Computed Flow Depth at Time Step 13

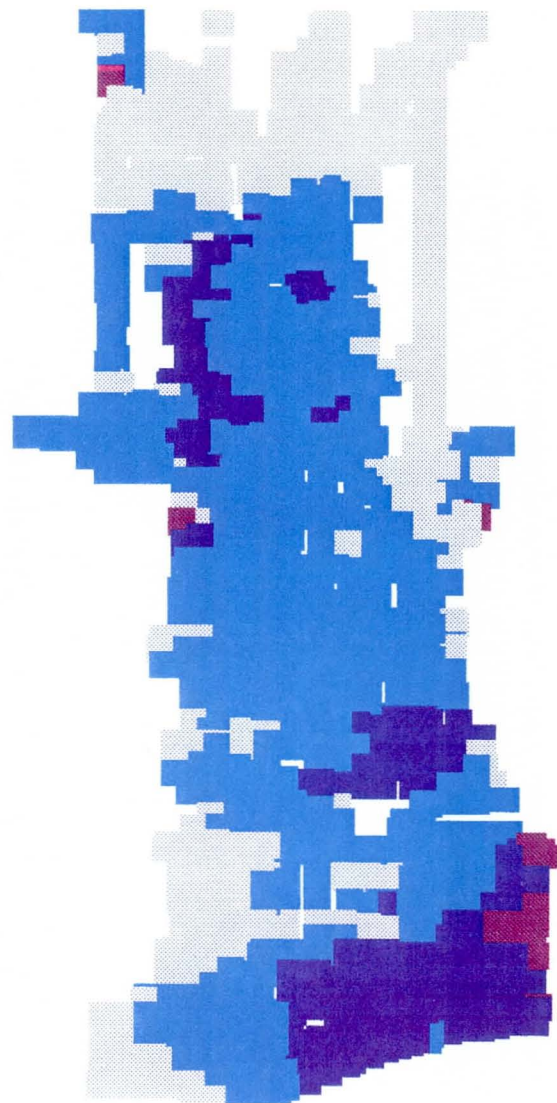


Figure 28 Dynamic Simulation of the 100-Year Flood through the Study Area
Computed Flow Depth at Time Step 15

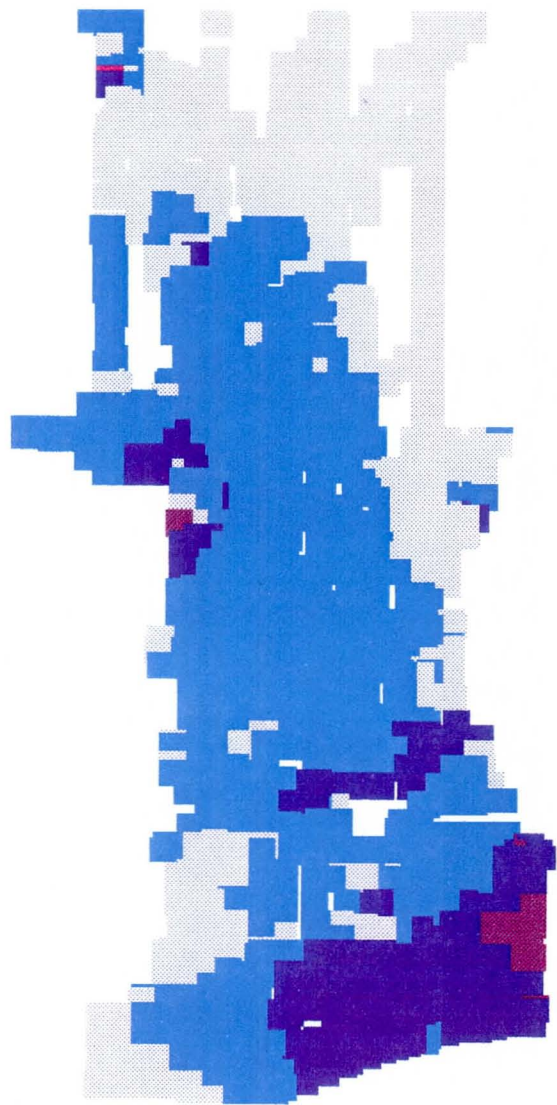


Figure 29 Dynamic Simulation of the 100-Year Flood through the Study Area
 Computed Flow Depth at Time Step 17



Figure 30 Dynamic Simulation of the 100-Year Flood through the Study Area
Computed Flow Depth at Time Step 19

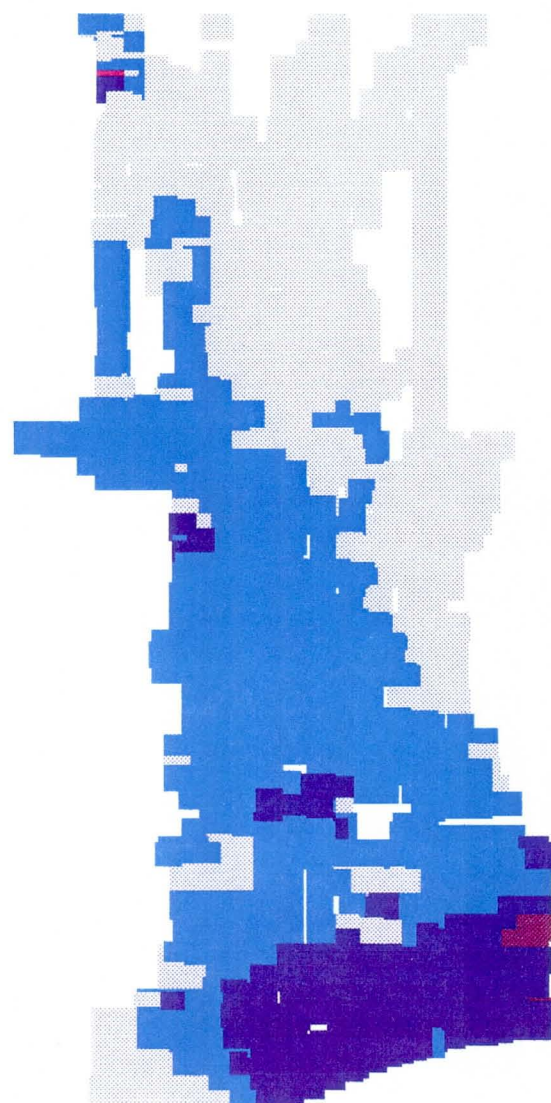


Figure 31 Dynamic Simulation of the 100-Year Flood through the Study Area
 Computed Flow Depth at Time Step 21

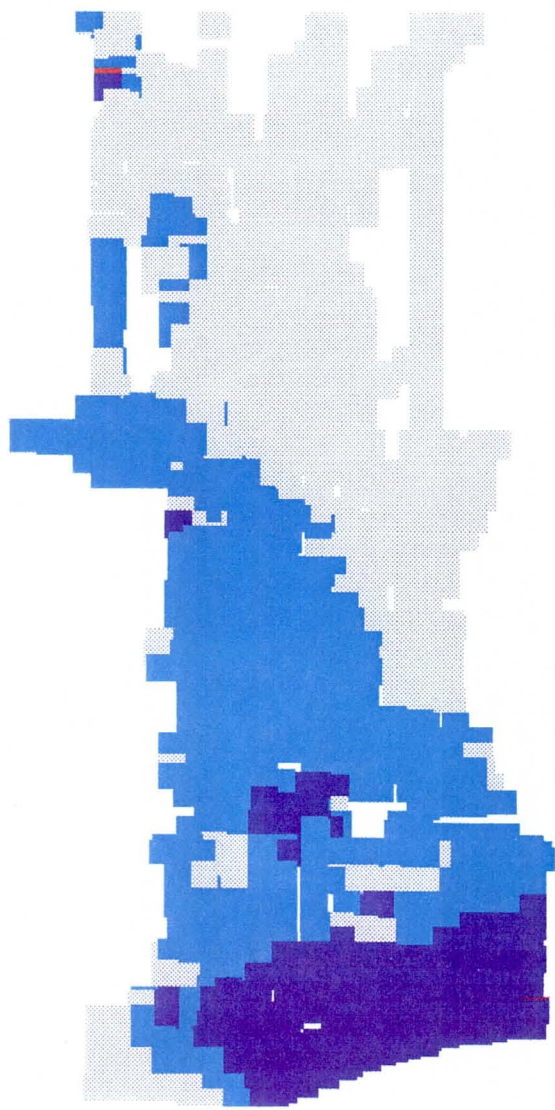


Figure 32 Dynamic Simulation of the 100-Year Flood through the Study Area
 Computed Flow Depth at Time Step 23

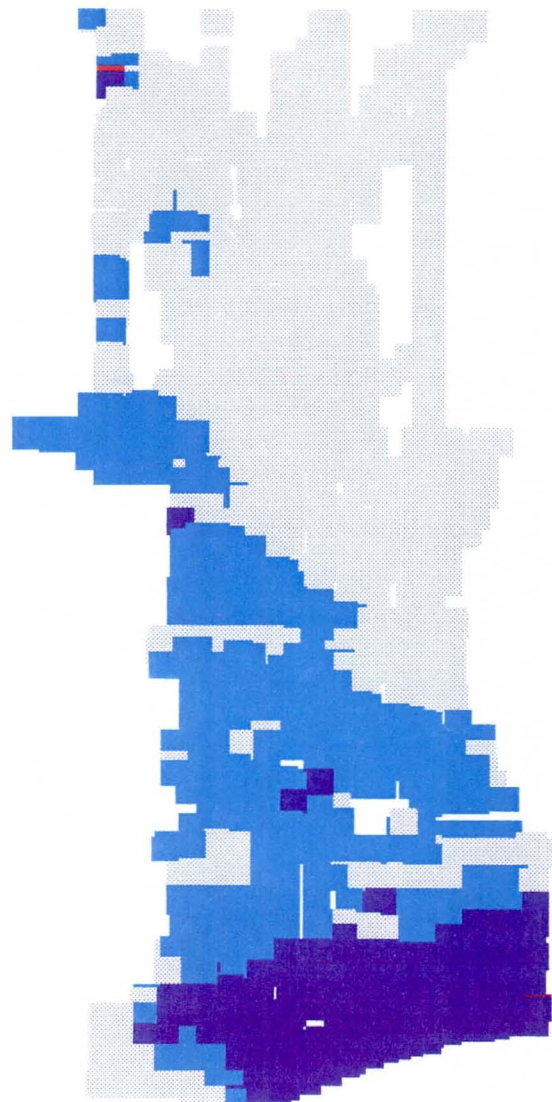


Figure 33 Dynamic Simulation of the 100-Year Flood through the Study Area
Computed Flow Depth at Time Step 25

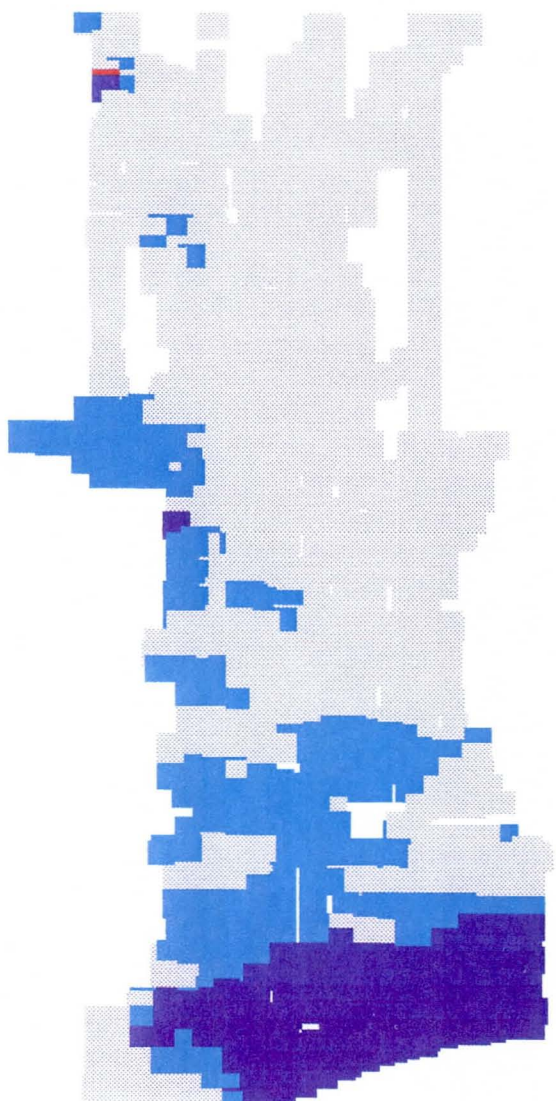


Figure 34 Dynamic Simulation of the 100-Year Flood through the Study Area
 Computed Flow Depth at Time Step 27

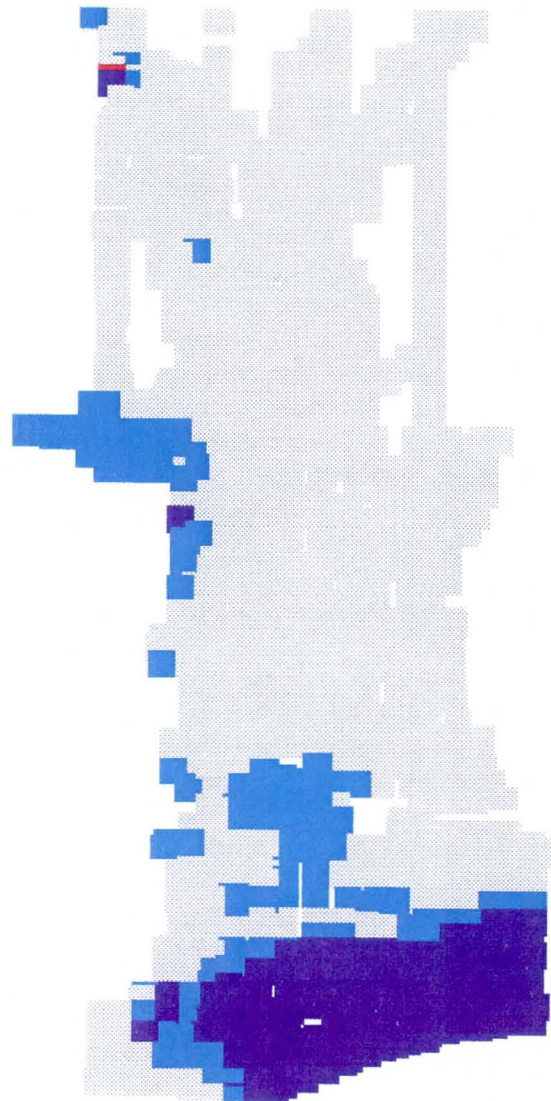


Figure 35 Dynamic Simulation of the 100-Year Flood through the Study Area
 Computed Flow Depth at Time Step 29

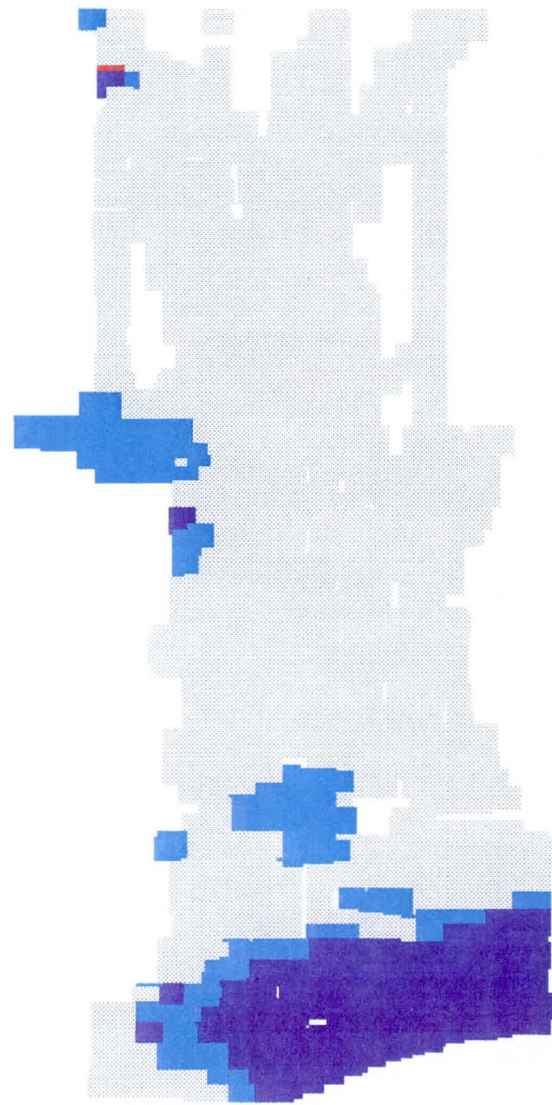


Figure 36 Dynamic Simulation of the 100-Year Flood through the Study Area
 Computed Flow Depth at Time Step 31

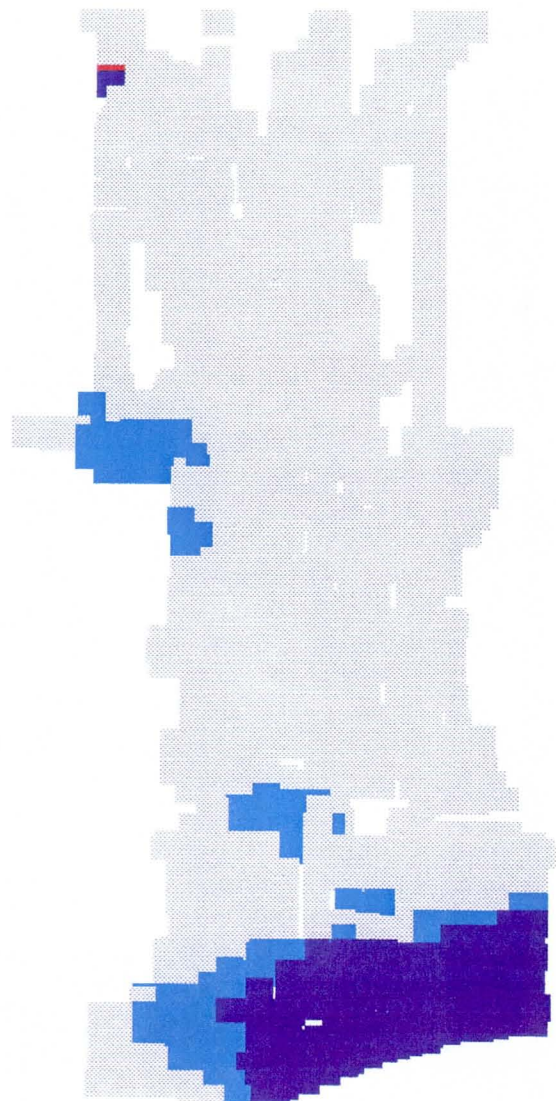


Figure 37 Dynamic Simulation of the 100-Year Flood through the Study Area
Computed Flow Depth at Time Step 33

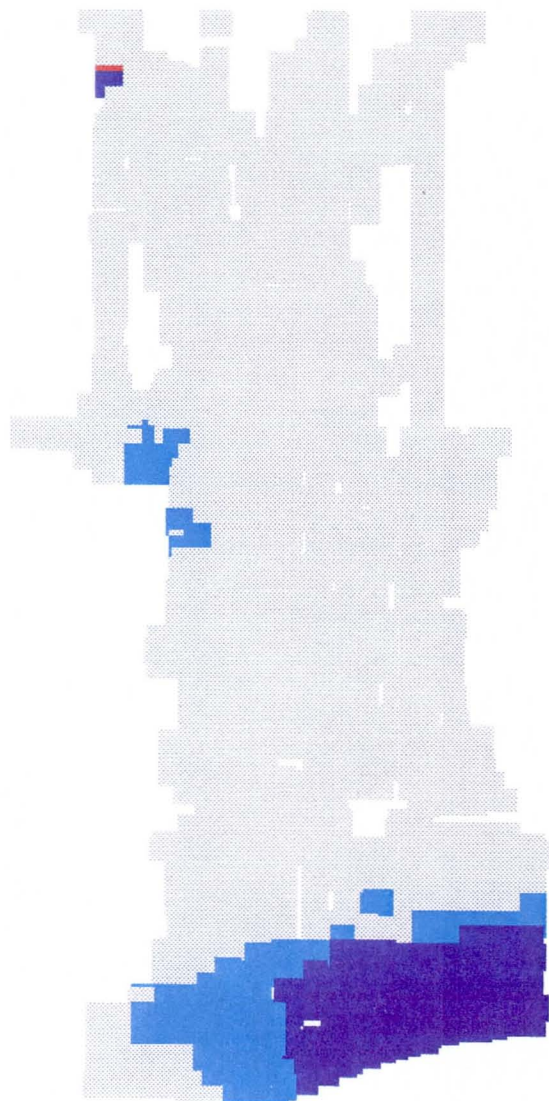


Figure 38 Dynamic Simulation of the 100-Year Flood through the Study Area
 Computed Flow Depth at Time Step 35

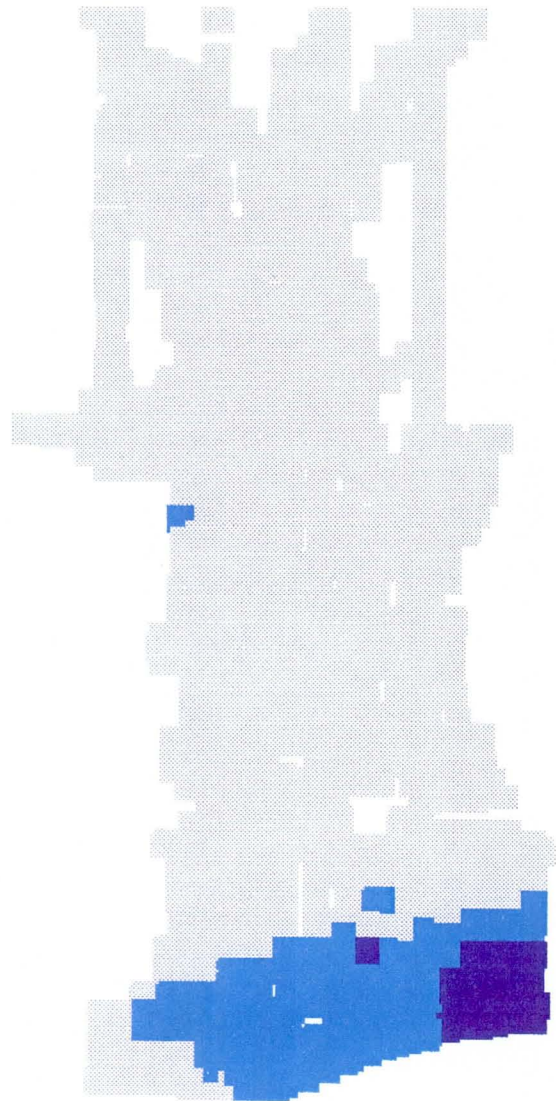


Figure 39 Dynamic Simulation of the 100-Year Flood through the Study Area
Computed Flow Depth at Time Step 37

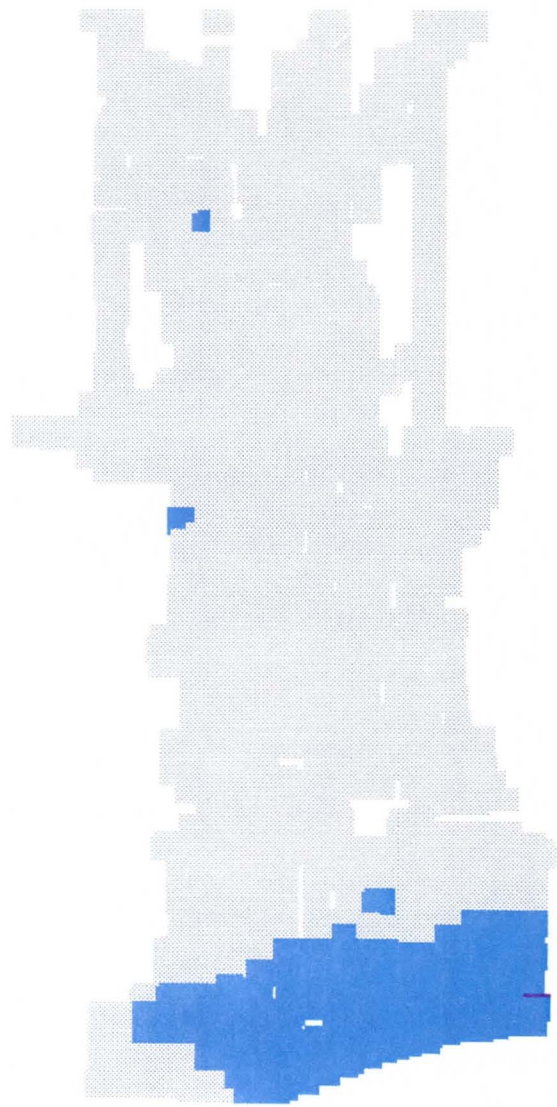


Figure 40 Dynamic Simulation of the 100-Year Flood through the Study Area
 Computed Flow Depth at Time Step 39

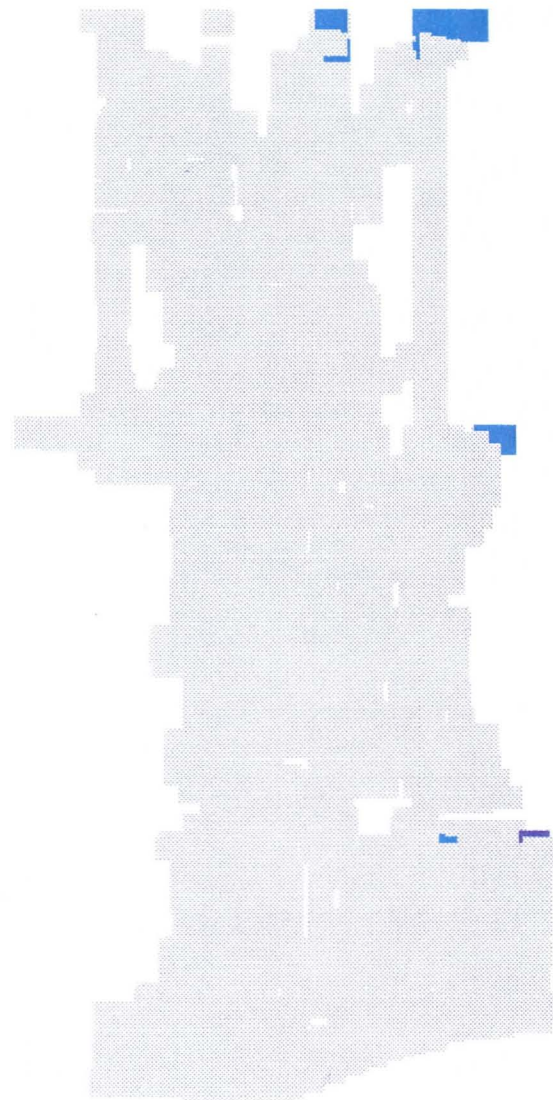


Figure 41 Dynamic Simulation of the 100-Year Flood through the Study Area
Computed Unit Discharge at Time Step 1

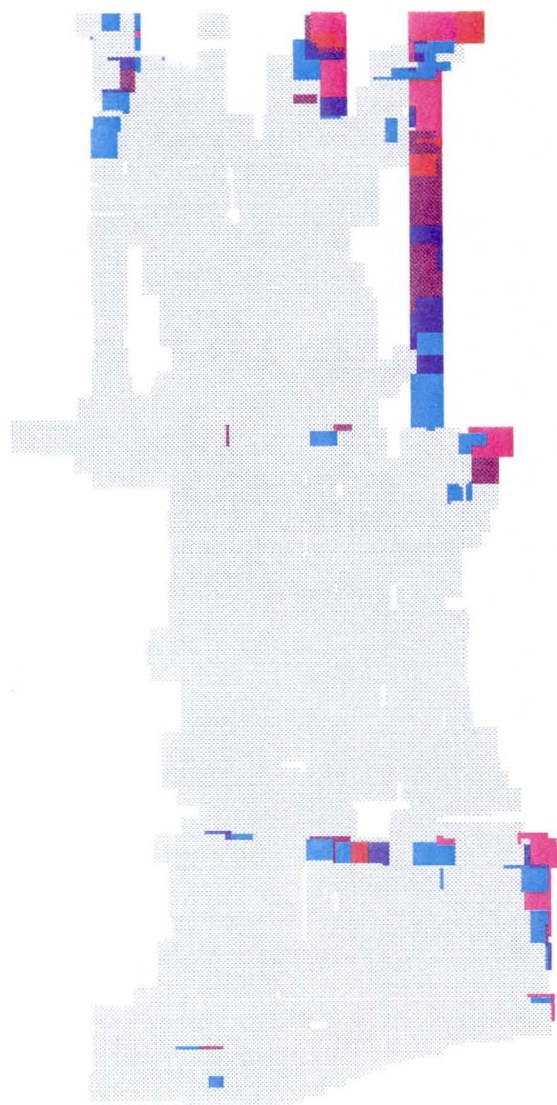


Figure 42 Dynamic Simulation of the 100-Year Flood through the Study Area
 Computed Unit Discharge at Time Step 3

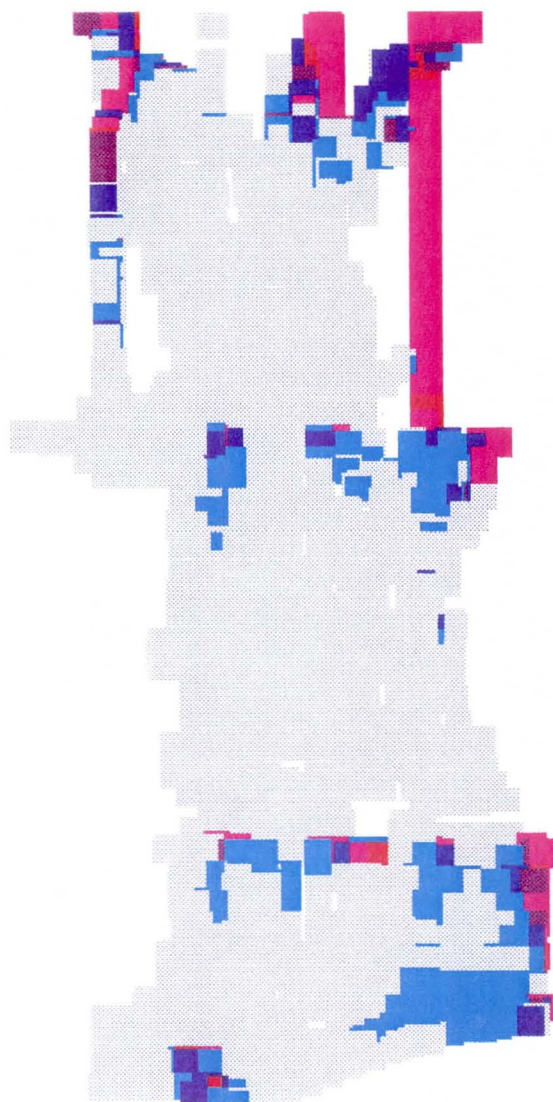


Figure 43 Dynamic Simulation of the 100-Year Flood through the Study Area
 Computed Unit Discharge at Time Step 5

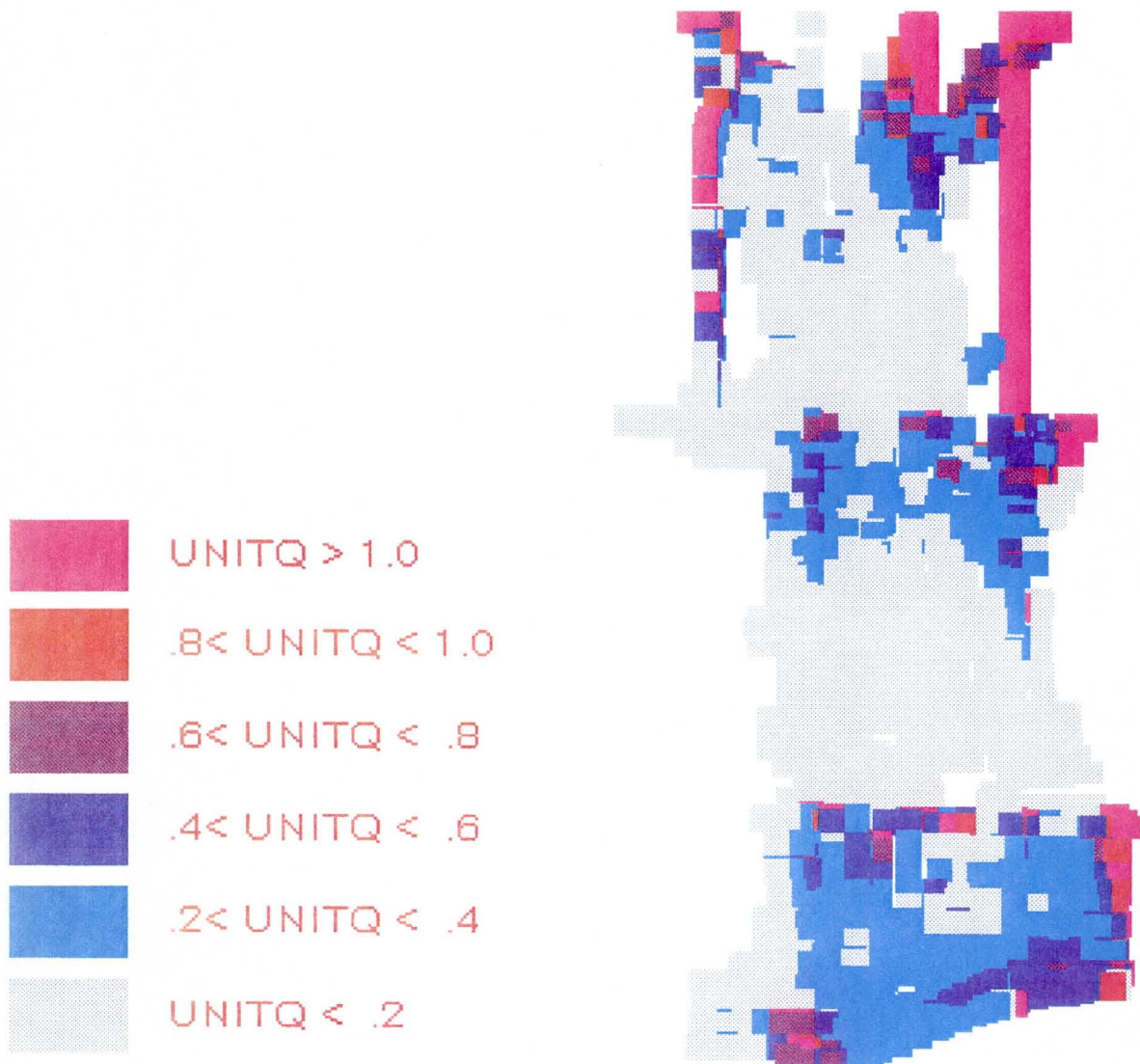


Figure 44 Dynamic Simulation of the 100-Year Flood through the Study Area
 Computed Unit Discharge at Time Step 7

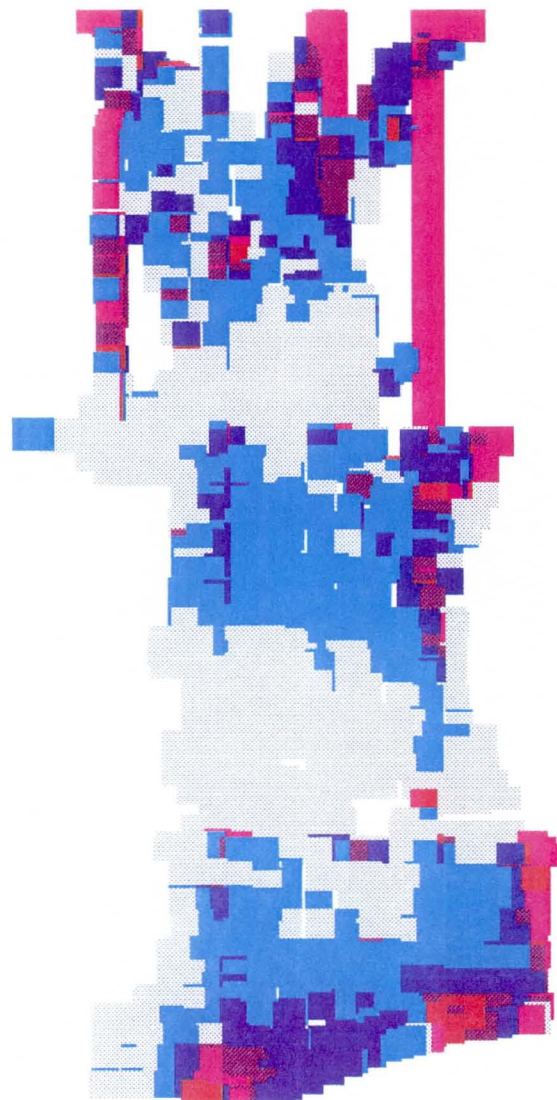


Figure 45 Dynamic Simulation of the 100-Year Flood through the Study Area
Computed Unit Discharge at Time Step 9

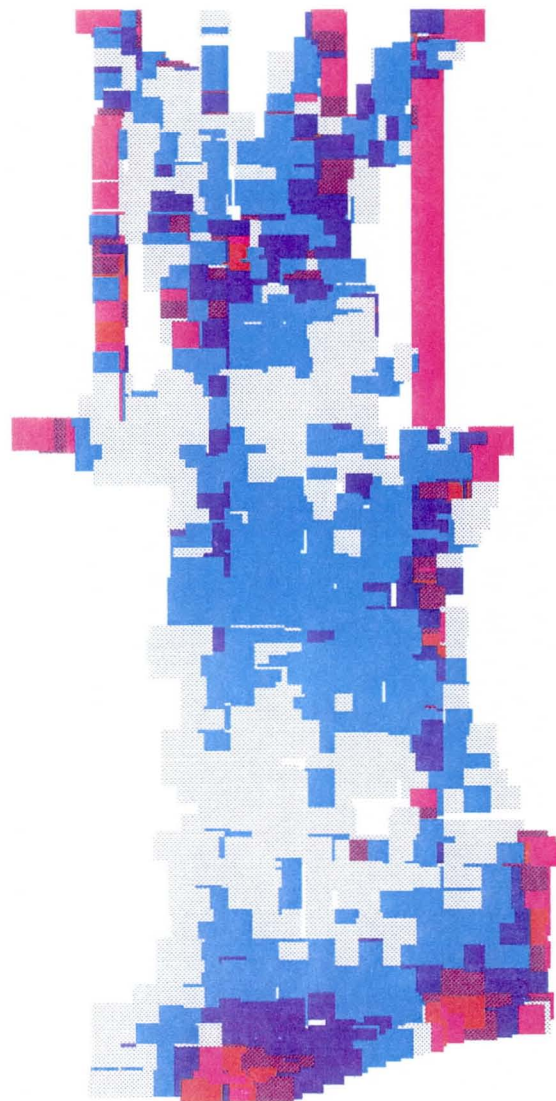


Figure 46 Dynamic Simulation of the 100-Year Flood through the Study Area
 Computed Unit Discharge at Time Step 11

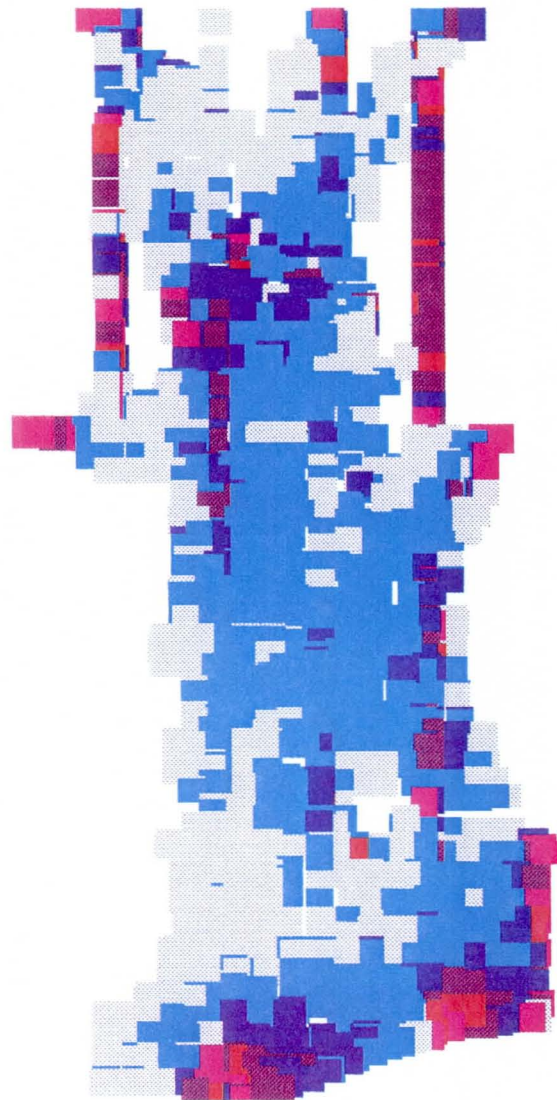


Figure 47 Dynamic Simulation of the 100-Year Flood through the Study Area
 Computed Unit Discharge at Time Step 13

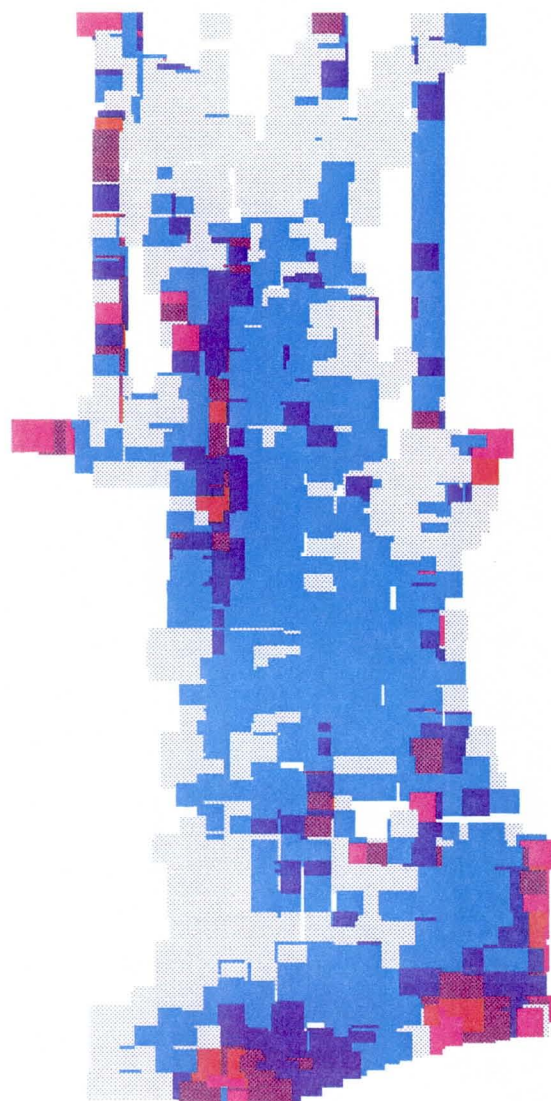


Figure 48 Dynamic Simulation of the 100-Year Flood through the Study Area
Computed Unit Discharge at Time Step 15

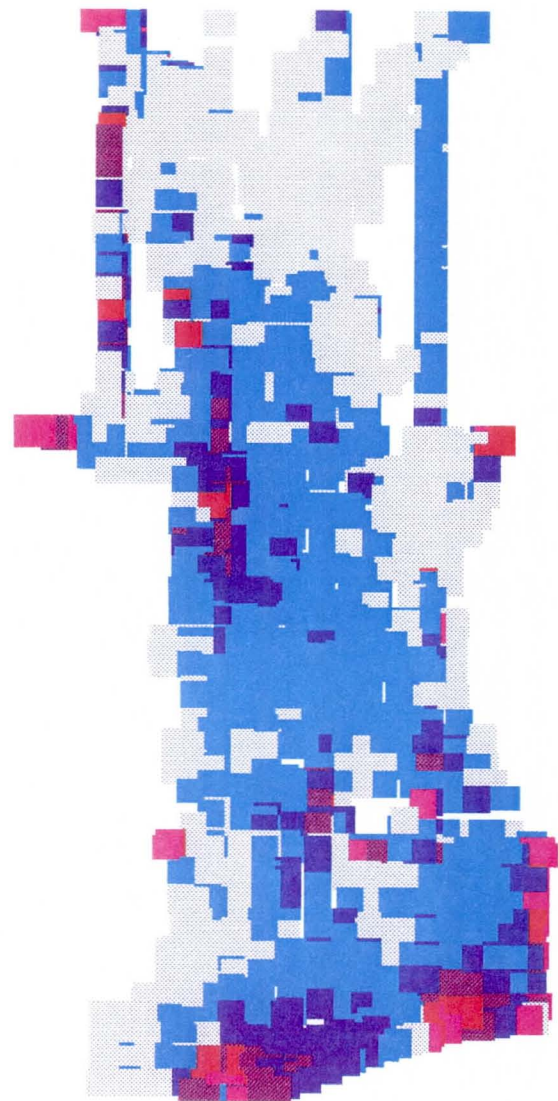


Figure 49 Dynamic Simulation of the 100-Year Flood through the Study Area
Computed Unit Discharge at Time Step 17

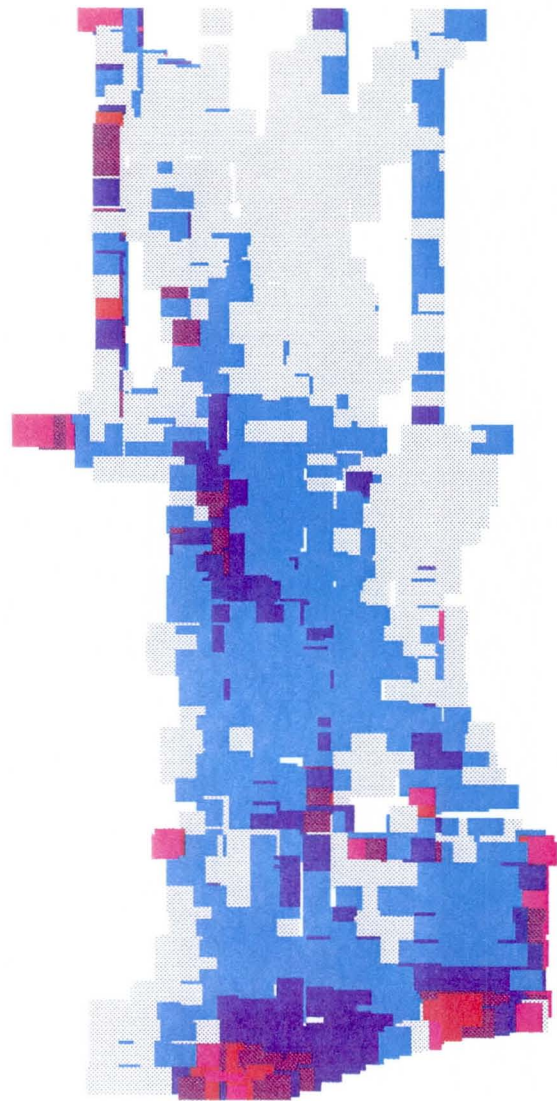


Figure 50 Dynamic Simulation of the 100-Year Flood through the Study Area
 Computed Unit Discharge at Time Step 19

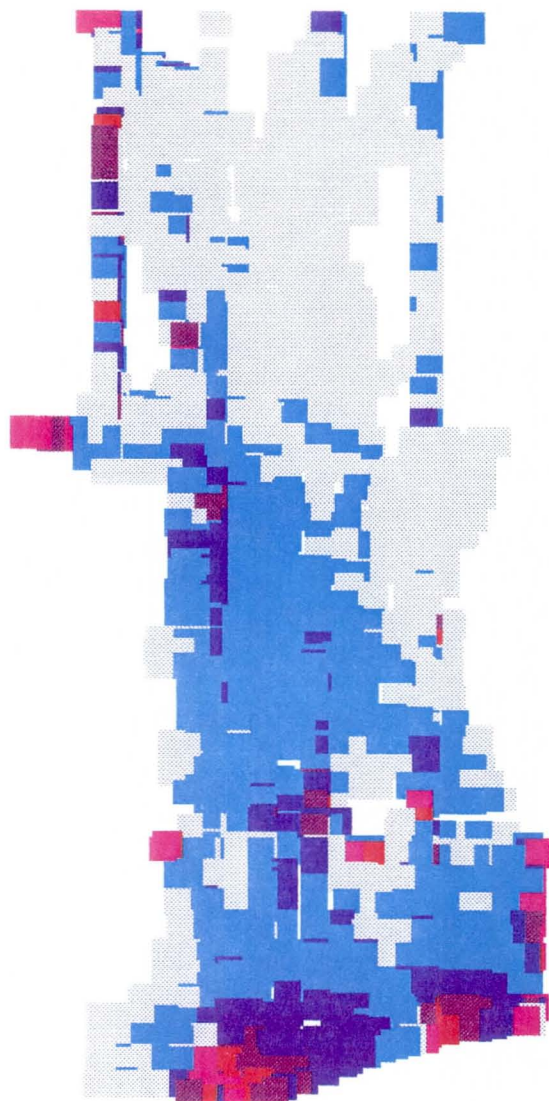


Figure 51 Dynamic Simulation of the 100-Year Flood through the Study Area
Computed Unit Discharge at Time Step 21

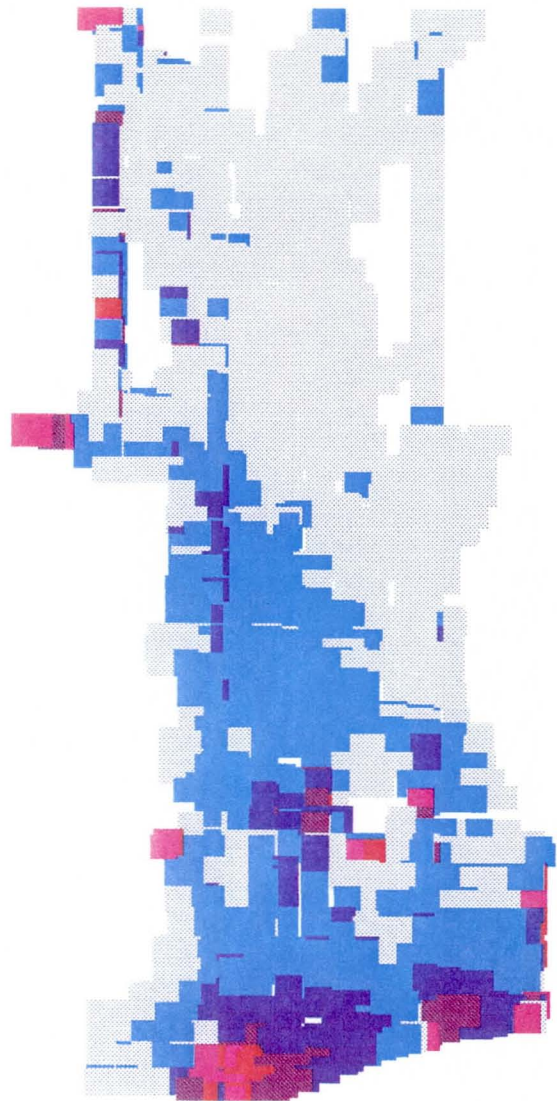


Figure 52 Dynamic Simulation of the 100-Year Flood through the Study Area
Computed Unit Discharge at Time Step 23

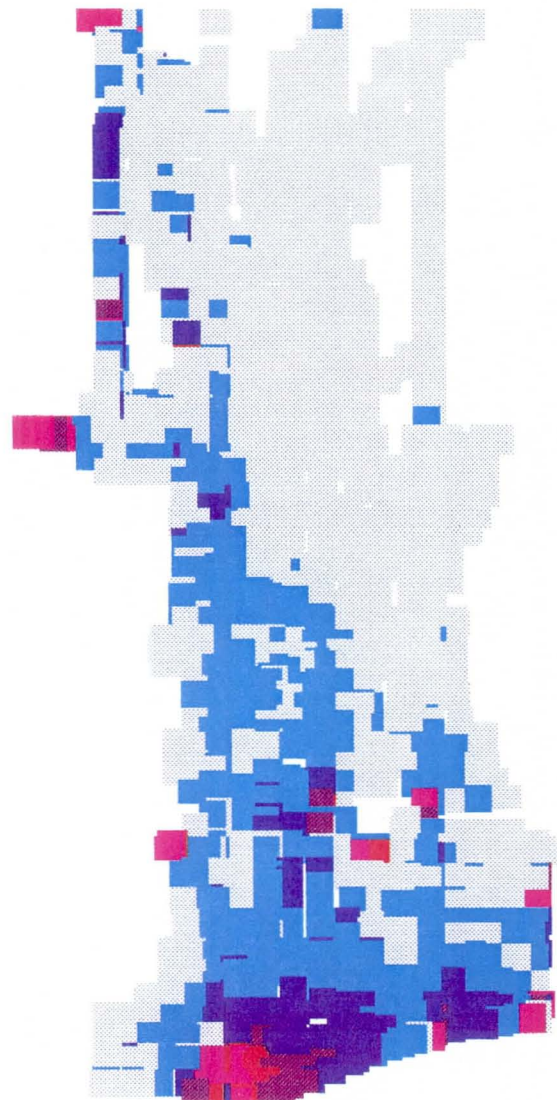


Figure 53 Dynamic Simulation of the 100-Year Flood through the Study Area
Computed Unit Discharge at Time Step 25

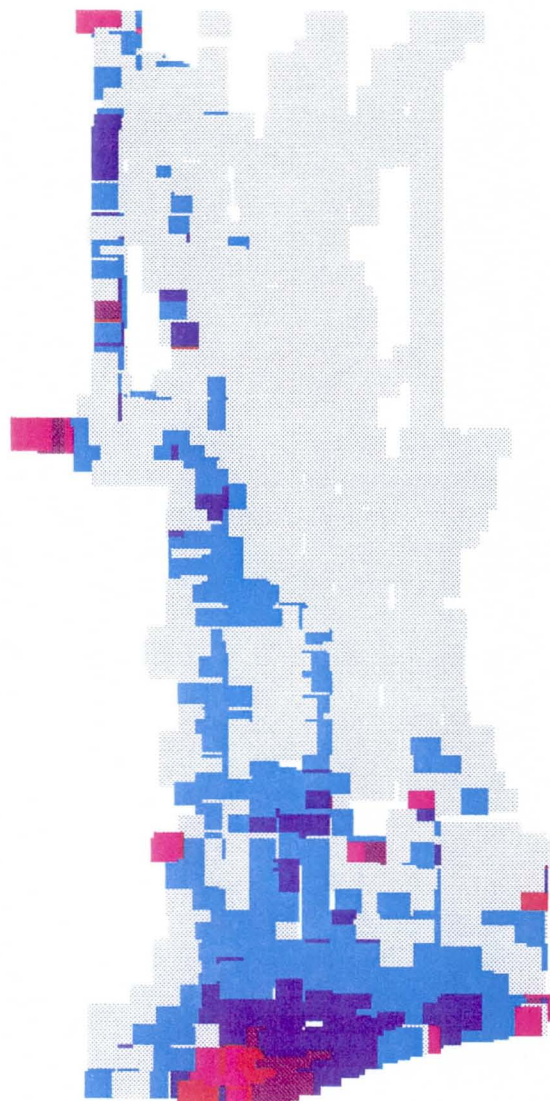


Figure 54 Dynamic Simulation of the 100-Year Flood through the Study Area
Computed Unit Discharge at Time Step 27

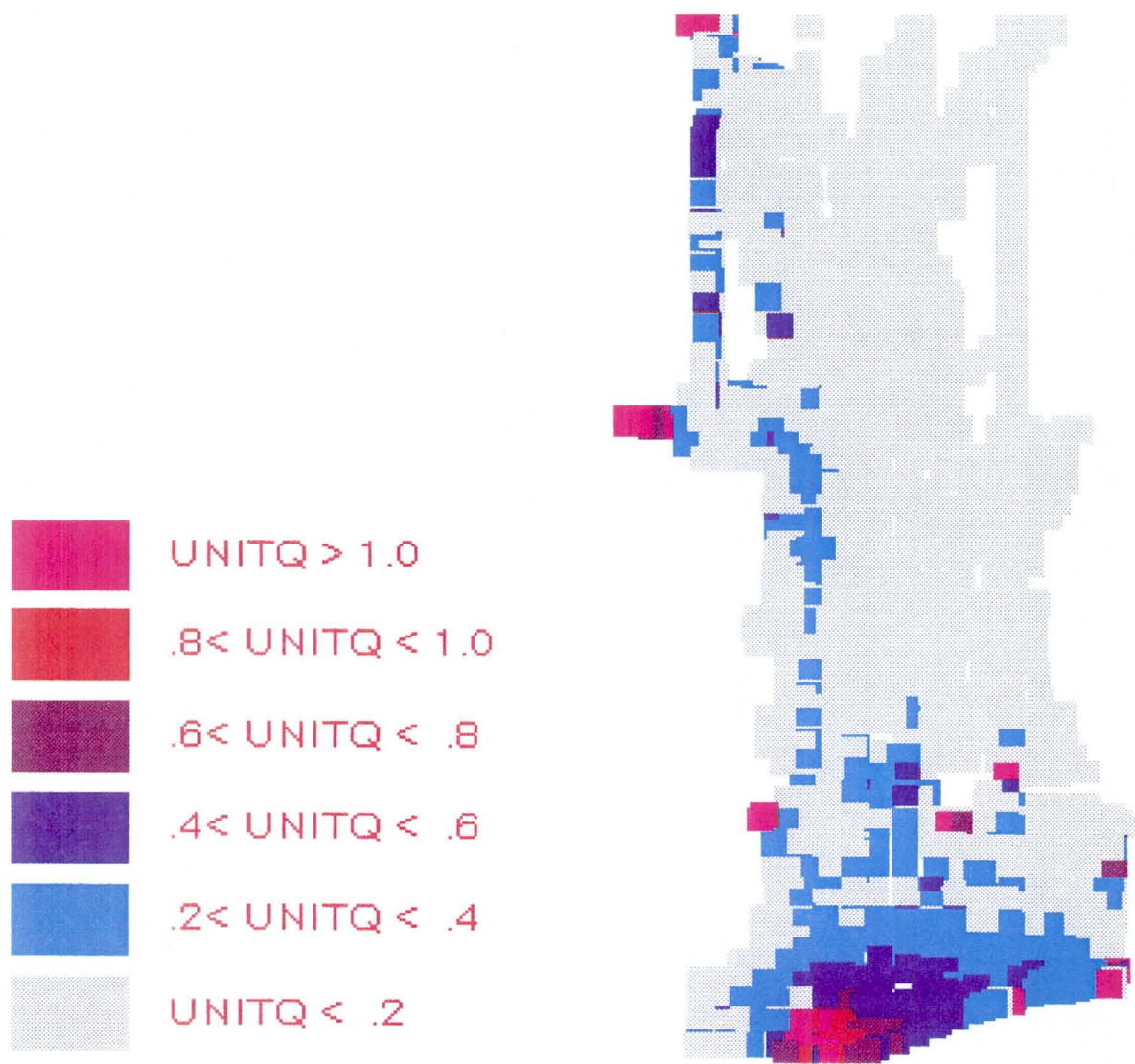


Figure 55 Dynamic Simulation of the 100-Year Flood through the Study Area
Computed Unit Discharge at Time Step 29

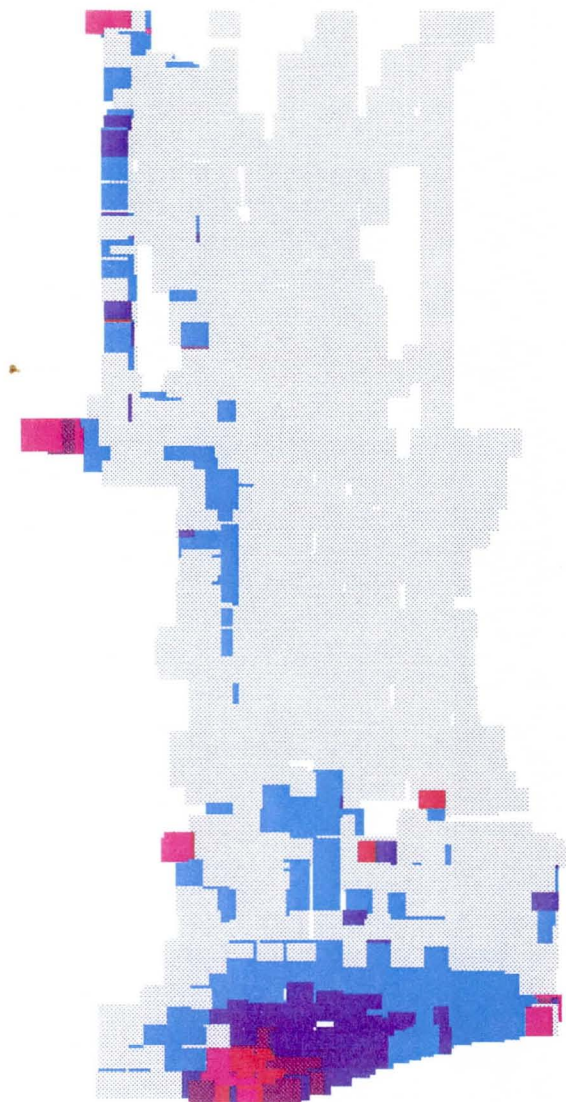


Figure 56 Dynamic Simulation of the 100-Year Flood through the Study Area
Computed Unit Discharge at Time Step 31

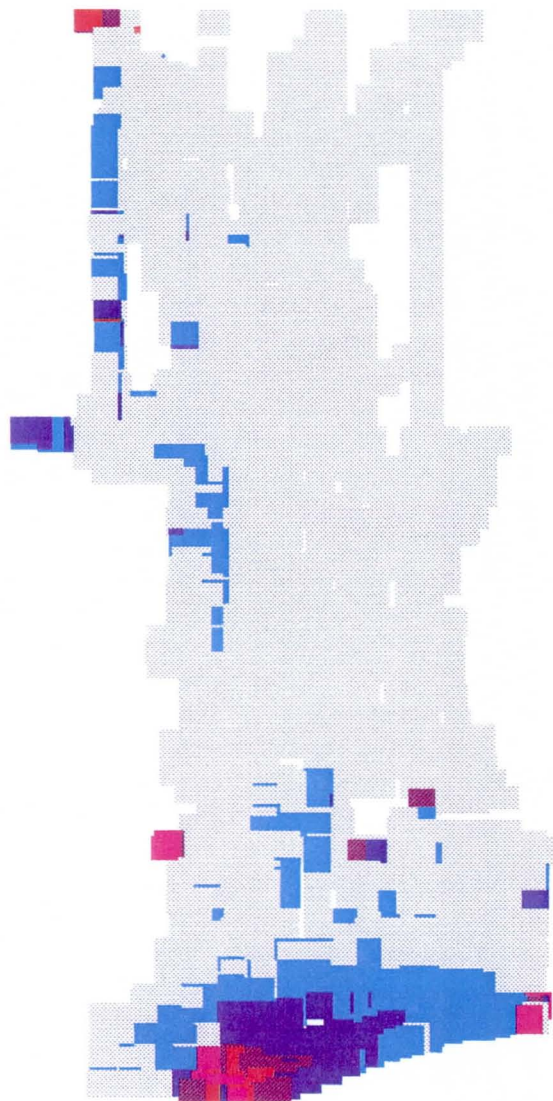


Figure 57 Dynamic Simulation of the 100-Year Flood through the Study Area
 Computed Unit Discharge at Time Step 33

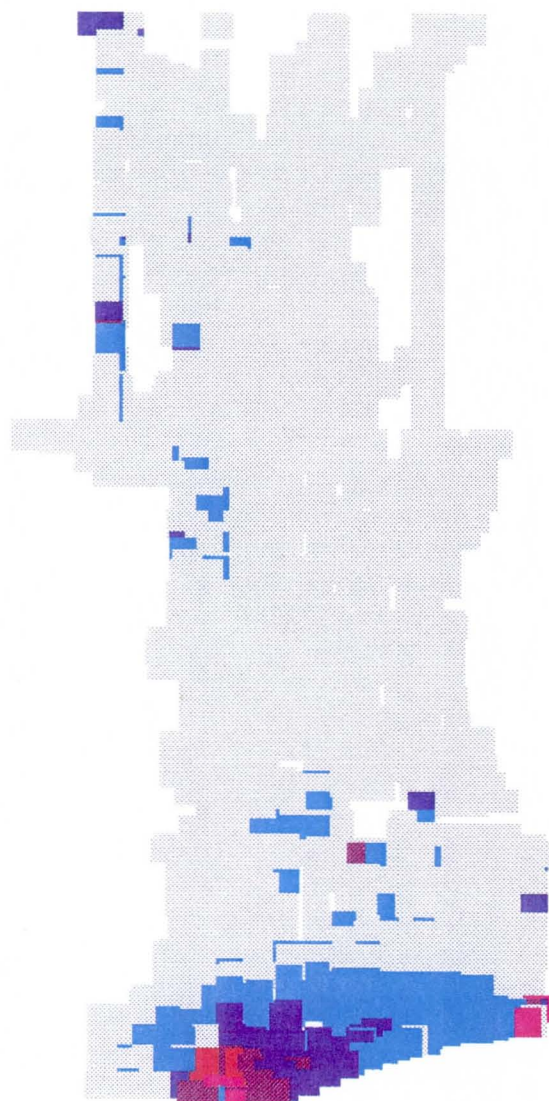


Figure 58 Dynamic Simulation of the 100-Year Flood through the Study Area
 Computed Unit Discharge at Time Step 35

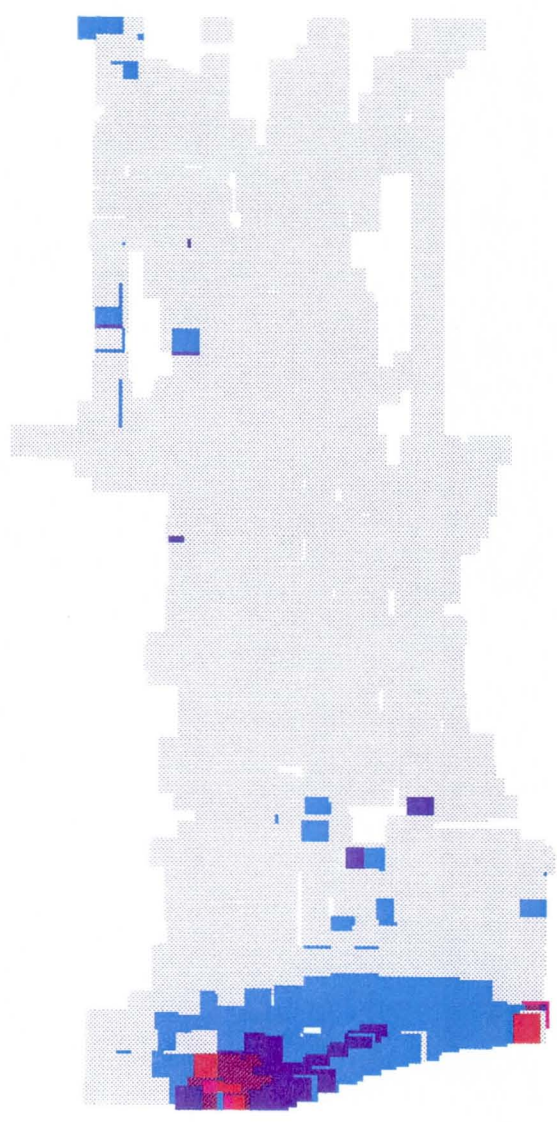


Figure 59 Dynamic Simulation of the 100-Year Flood through the Study Area
 Computed Unit Discharge at Time Step 37

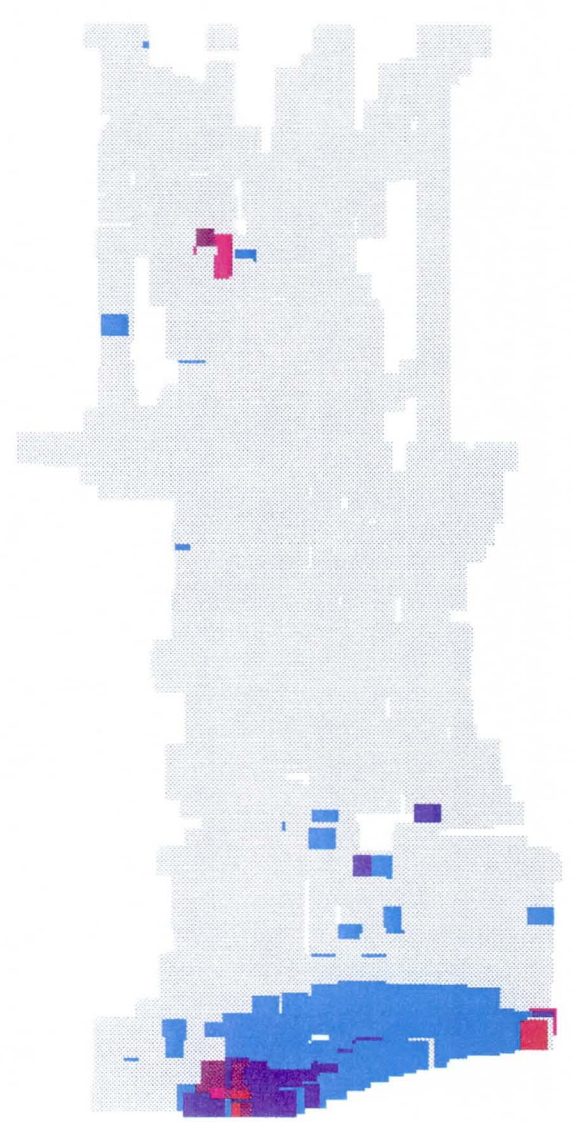


Figure 60 Dynamic Simulation of the 100-Year Flood through the Study Area Computed Unit Discharge at Time Step 39

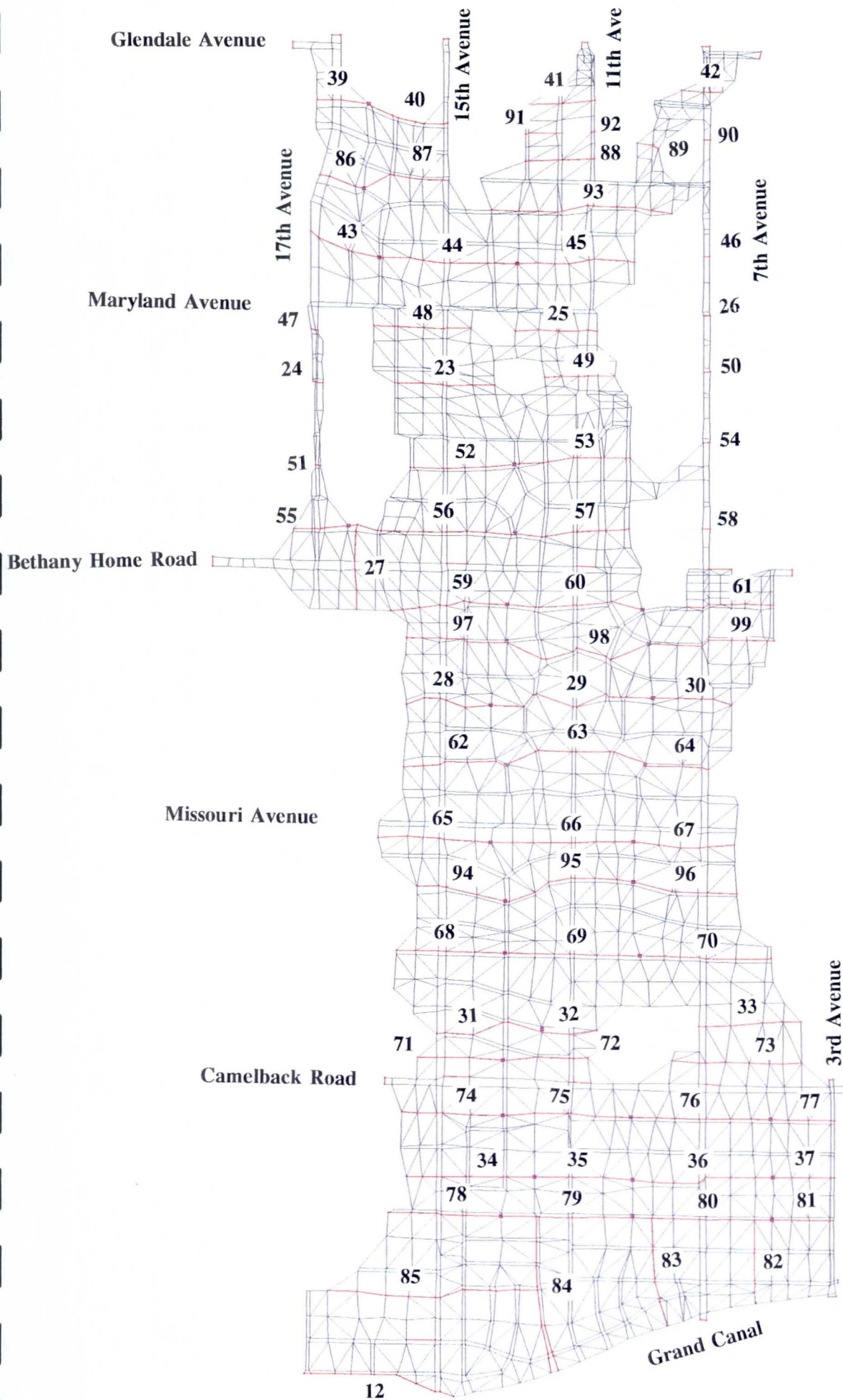


Figure 61 Inner-Mesh Flood Hydrograph Computation Sections (TABS-2 GC Strings)

DISCHARGE VARIATION ALONG 17TH AVE

BETWEEN GLENDALE AND BETHANY HOME ROAD

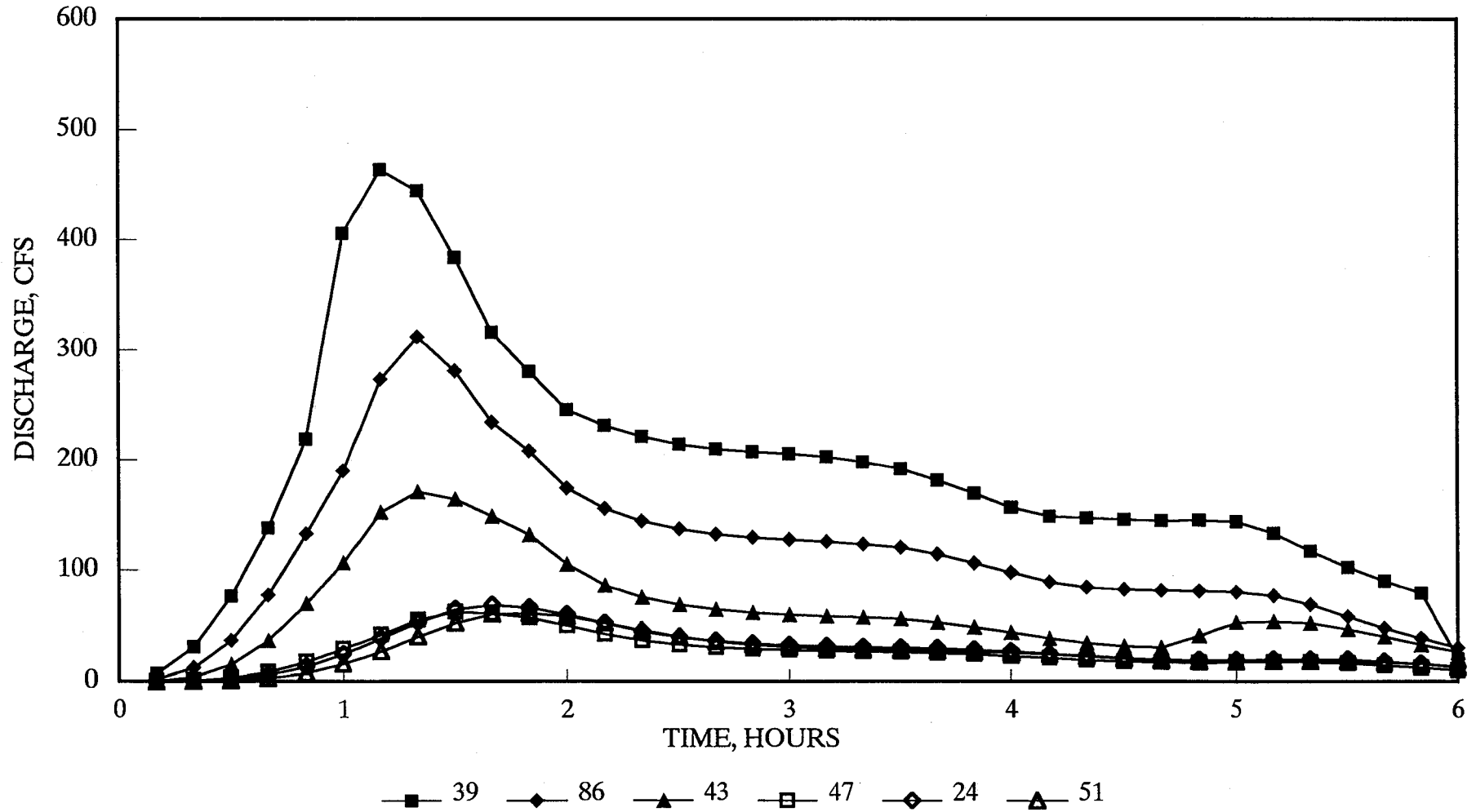


Figure 62 Computed Inner-Mesh Flood Hydrographs
17th Avenue within the Northern Portion of the Study Area

DISCHARGE VARIATION ALONG 15TH AVE

BETWEEN GLENDALE AND BETHANY HOME ROAD

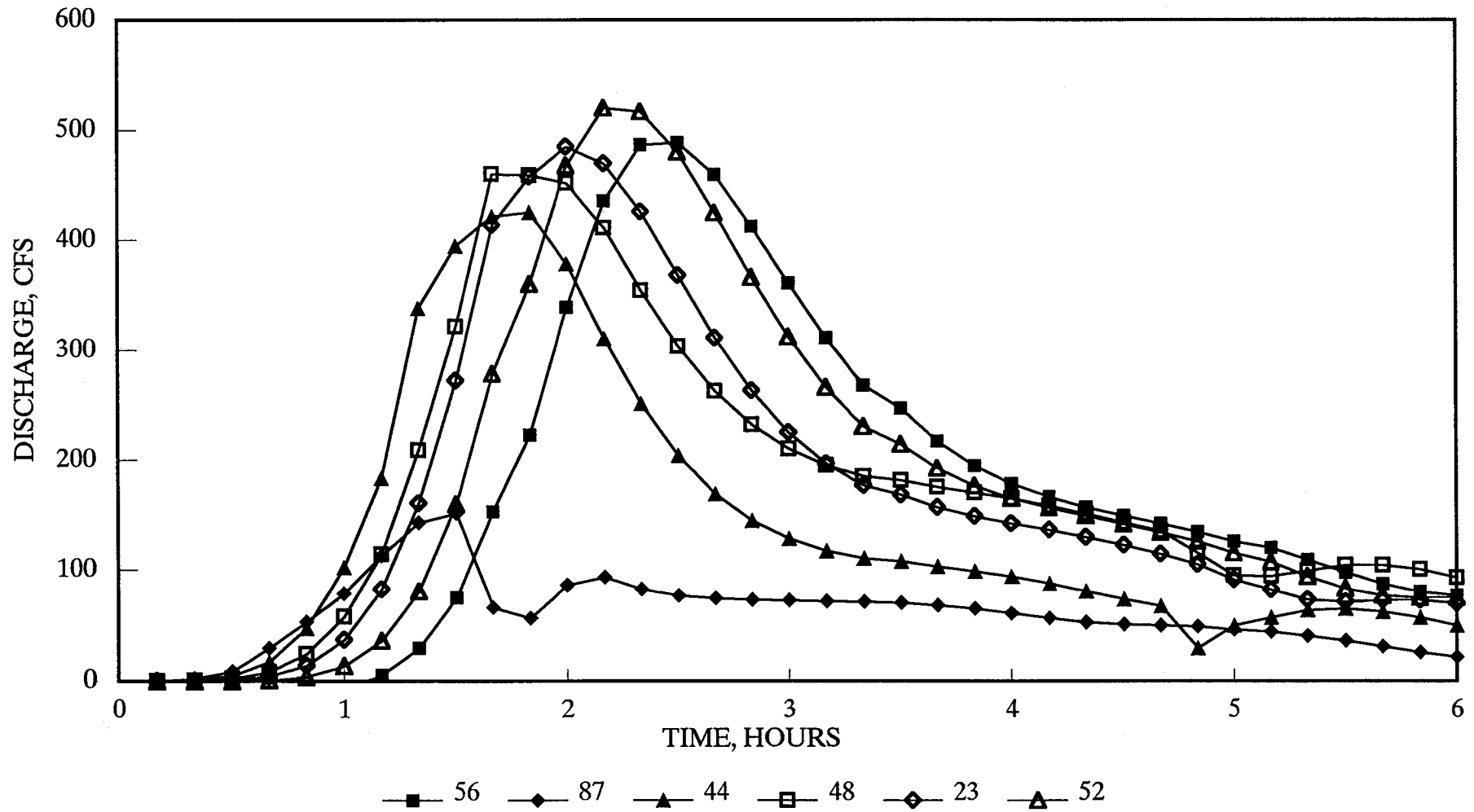


Figure 63 Computed Inner-Mesh Flood Hydrographs
15th Avenue within the Northern Portion of the Study Area

DISCHARGE VARIATION ALONG 15TH AVE BETWEEN BETHANY HOME ROAD AND CAMELBACK ROAD

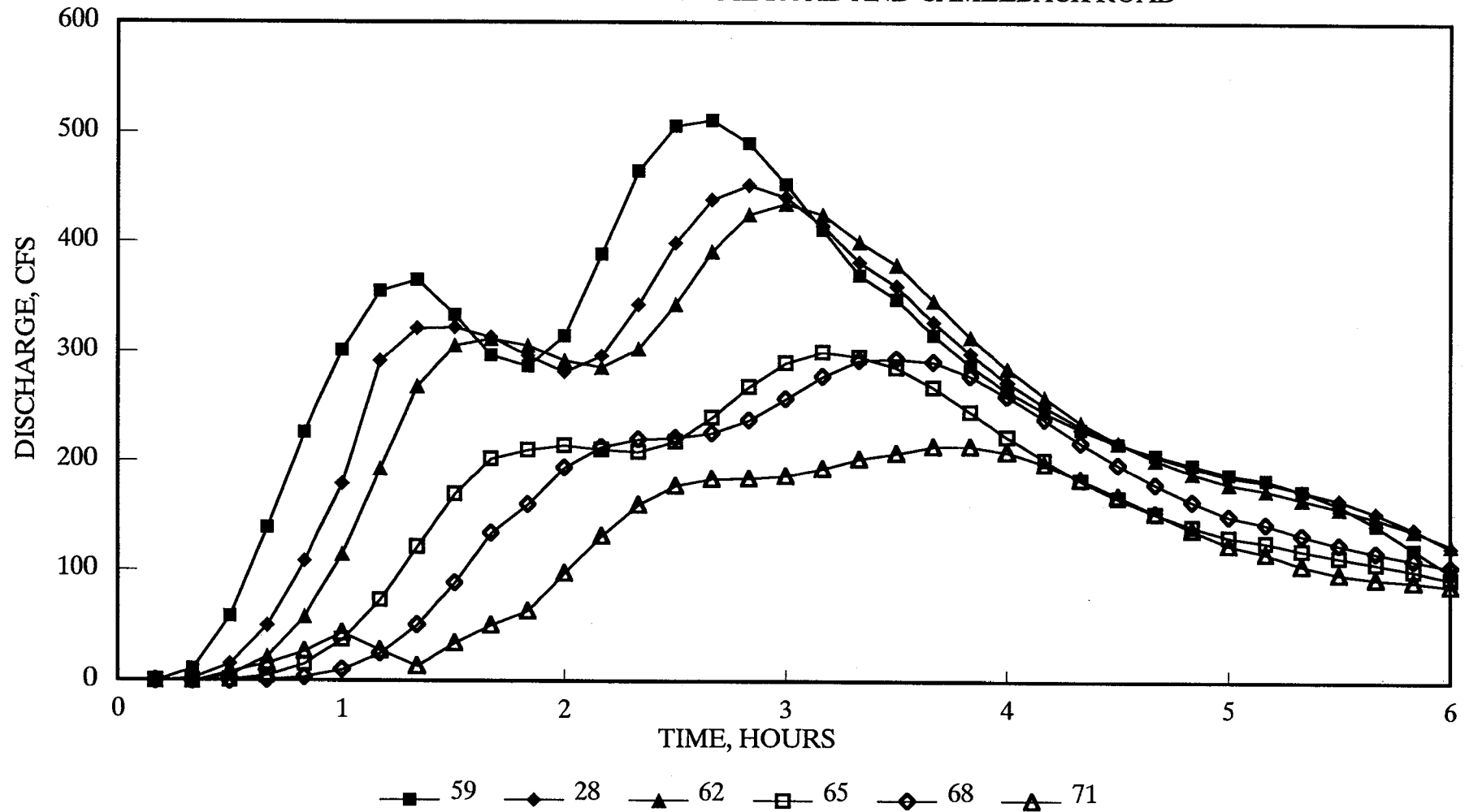


Figure 64 Computed Inner-Mesh Flood Hydrographs
15th Avenue within the Middle Portion of the Study Area

DISCHARGE VARIATION ALONG 11TH AVE BETWEEN CAMELBACK ROAD AND GRAND CANAL

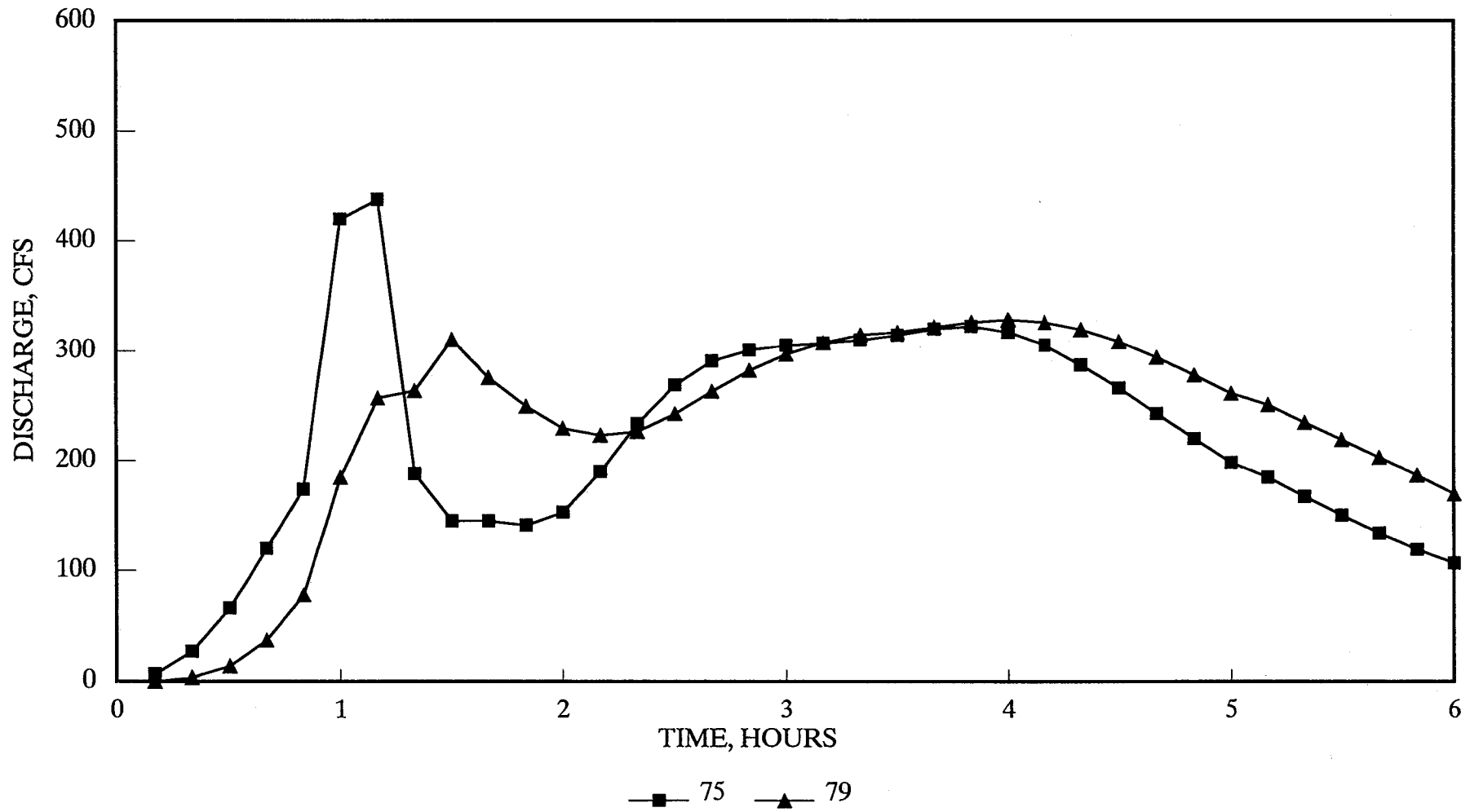


Figure 65 Computed Inner-Mesh Flood Hydrographs
11th Avenue within the Southern Portion of the Study Area

DISCHARGE VARIATION ALONG 11TH AVE BETWEEN GLENDALE AND BETHANY HOME ROAD

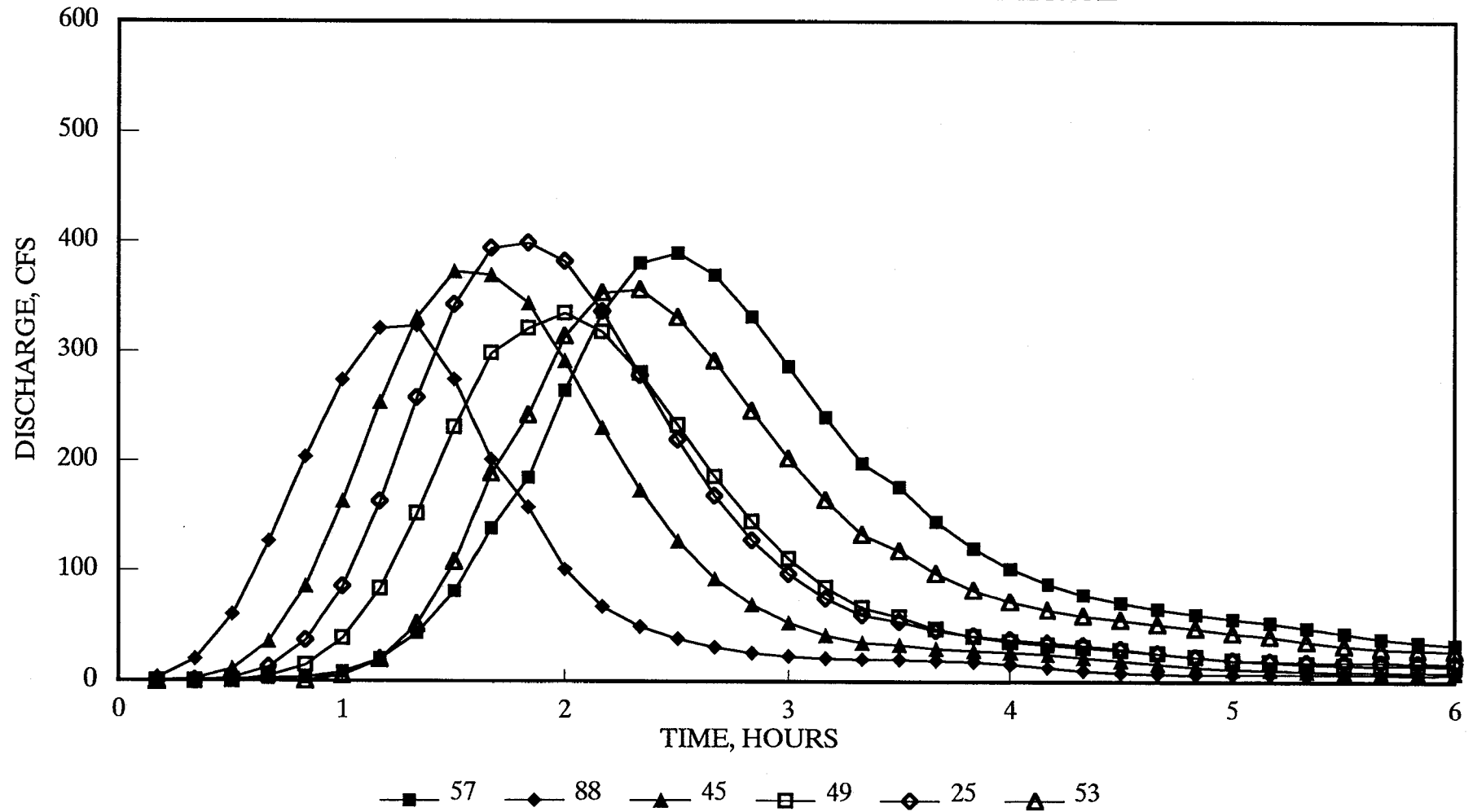


Figure 66 Computed Inner-Mesh Flood Hydrographs
11th Avenue within the Northern Portion of the Study Area

DISCHARGE VARIATION ALONG 11TH AVE

BETWEEN BETHANY HOME ROAD AND CAMELBACK ROAD

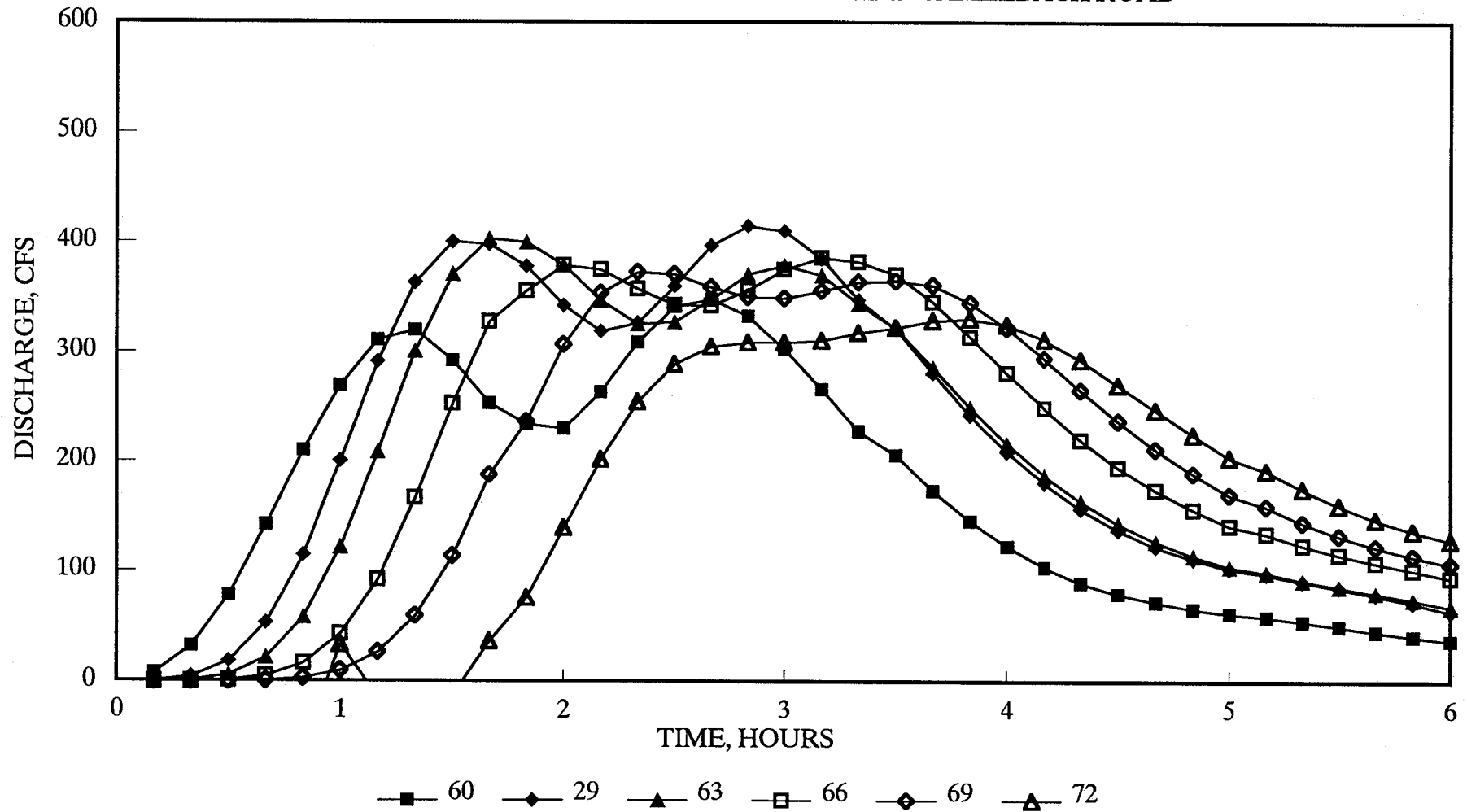


Figure 67 Computed Inner-Mesh Flood Hydrographs
11th Avenue within the Middle Portion of the Study Area

DISCHARGE VARIATION ALONG 15TH AVE

BETWEEN CAMELBACK ROAD AND GRAND CANAL

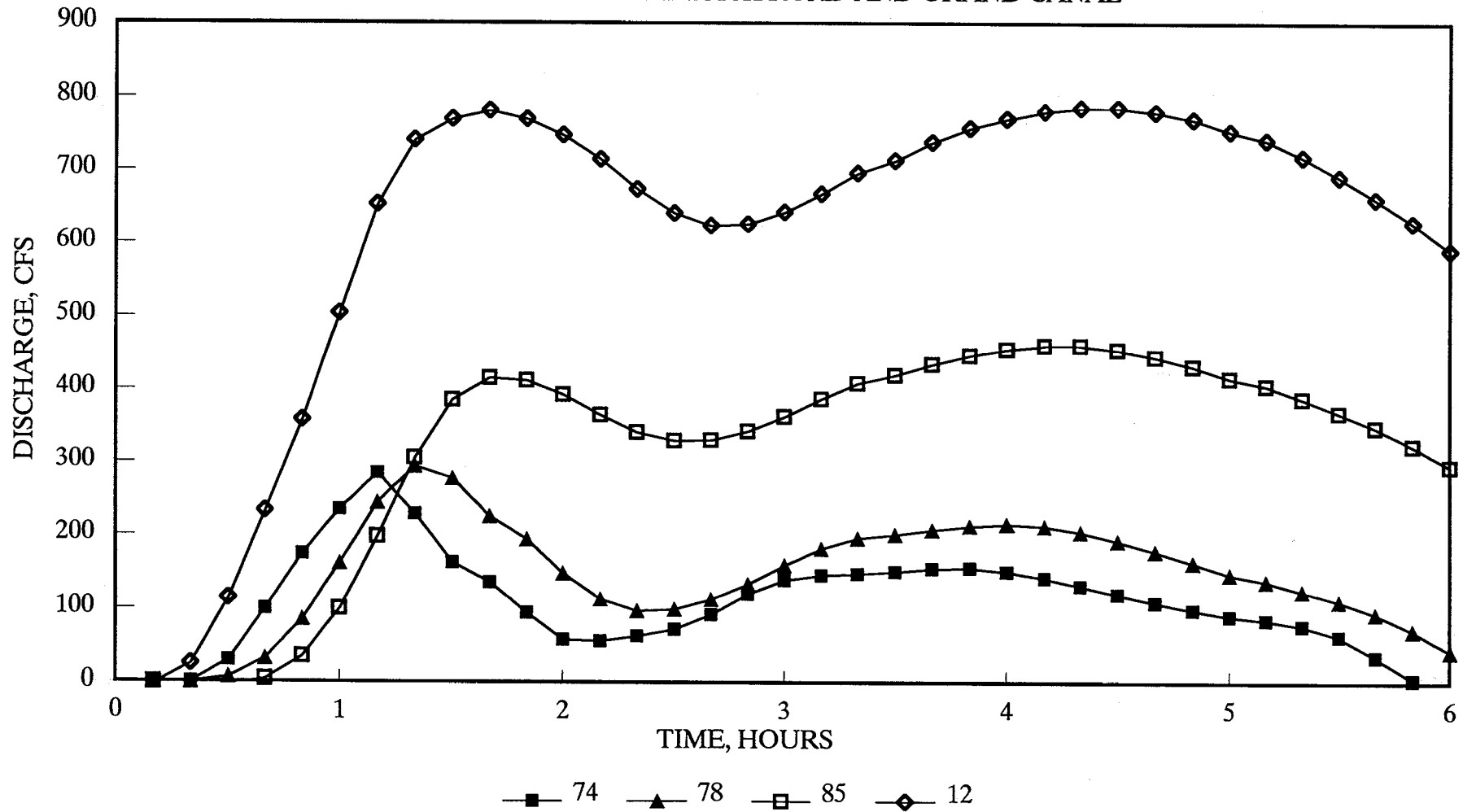


Figure 68 Computed Inner-Mesh Flood Hydrographs
15th Avenue within the Southern Portion of the Study Area

DISCHARGE VARIATION ALONG 7TH AVE BETWEEN GLENDALE AND BETHANY HOME ROAD

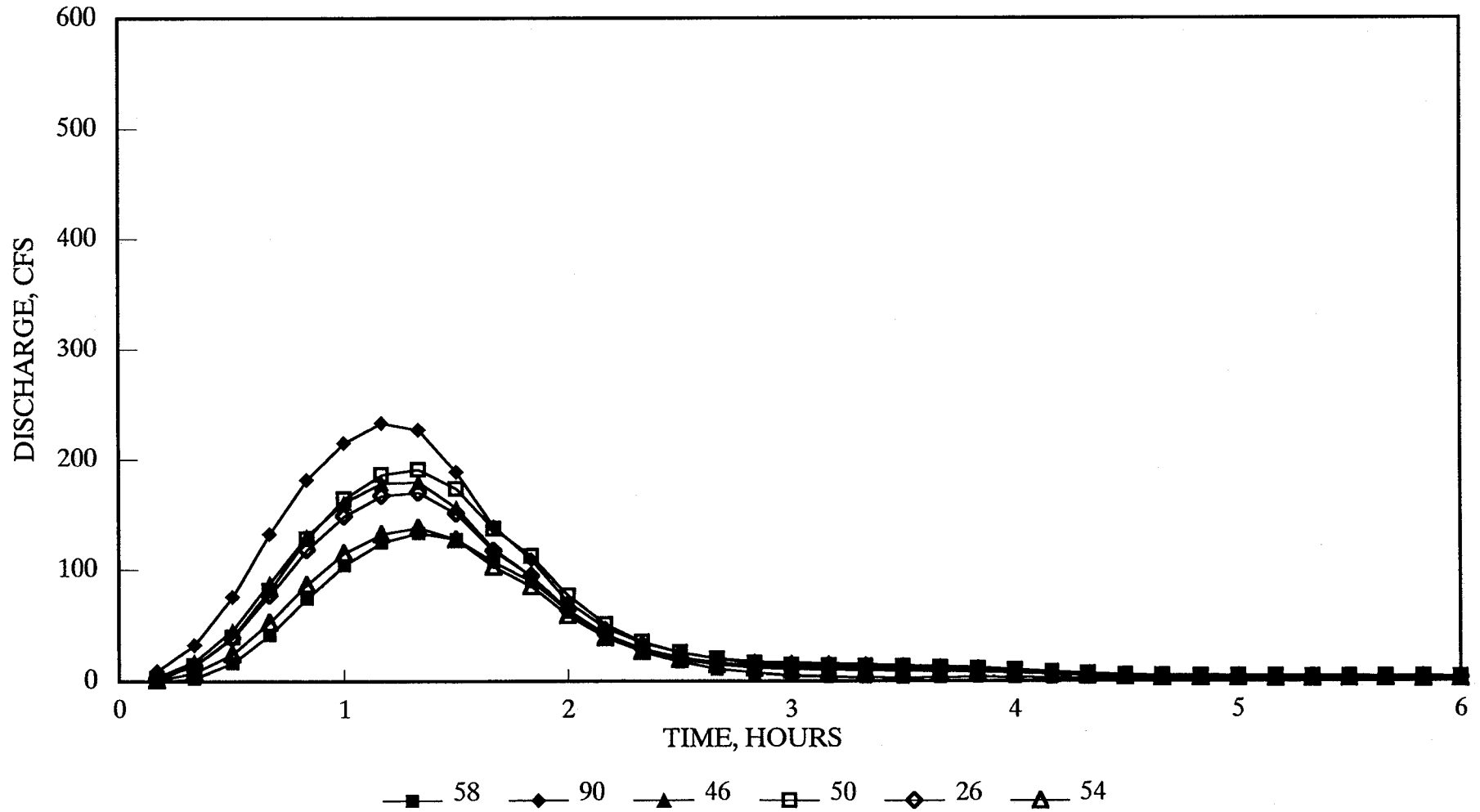


Figure 69 Computed Inner-Mesh Flood Hydrographs
7th Avenue within the Northern Portion of the Study Area

DISCHARGE VARIATION ALONG 7TH AVE

BETWEEN BETHANY HOME ROAD AND CAMELBACK ROAD

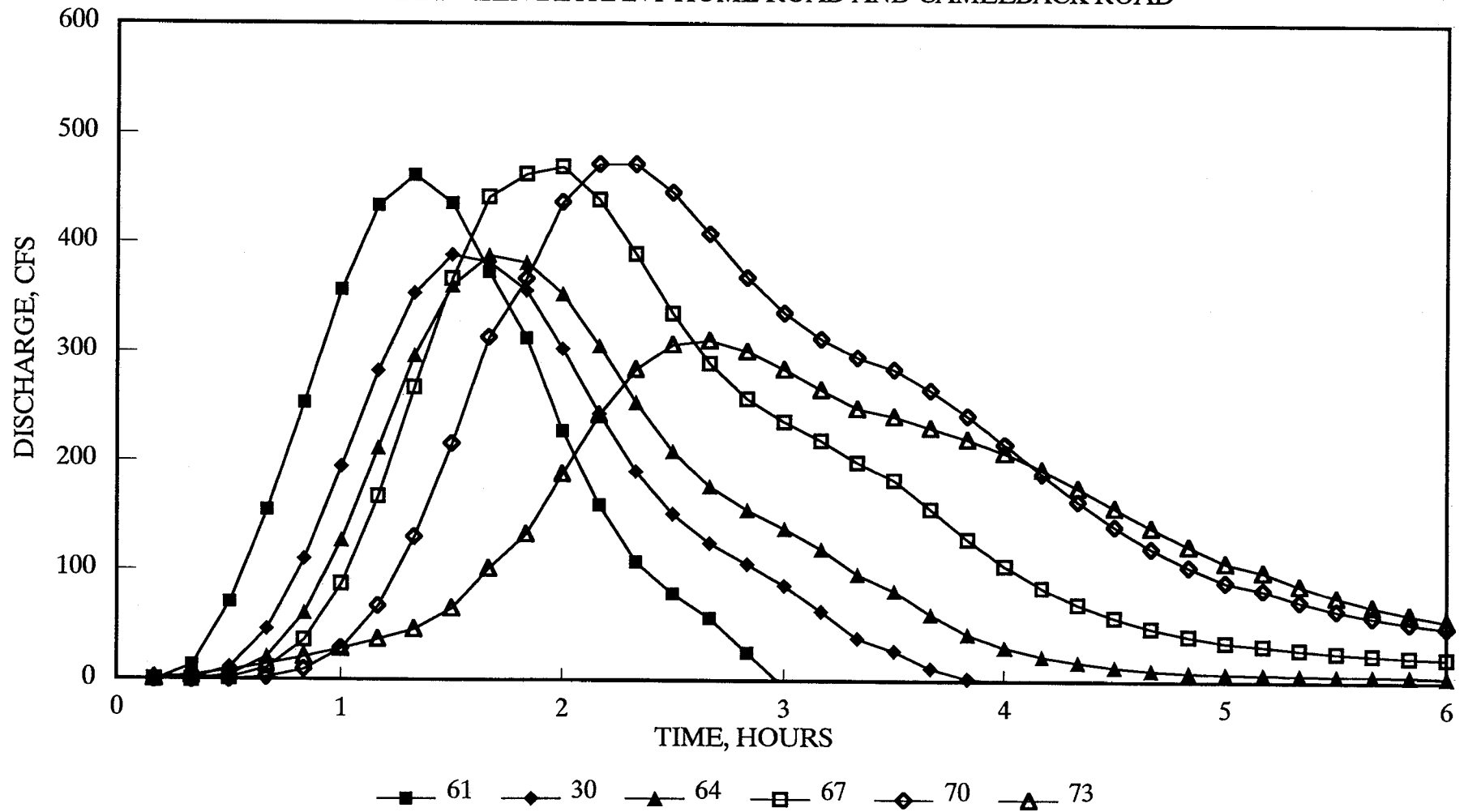


Figure 70 Computed Inner-Mesh Flood Hydrographs
7th Avenue within the Middle Portion of the Study Area

DISCHARGE VARIATION ALONG 7TH AVE BETWEEN CAMELBACK ROAD AND GRAND CANAL

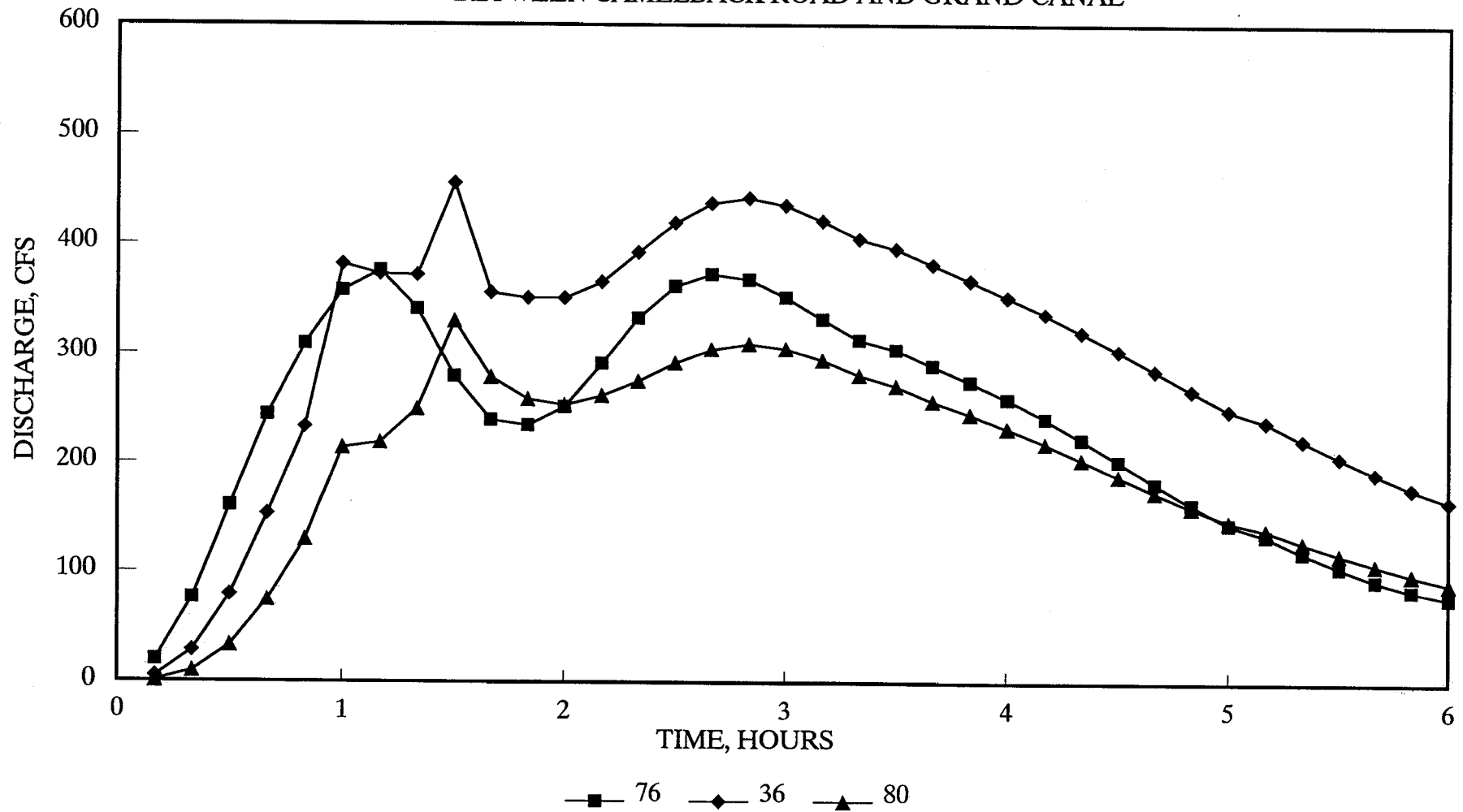


Figure 71 Computed Inner-Mesh Flood Hydrographs
7th Avenue within the Southern Portion of the Study Area

DISCHARGE VARIATION ALONG 3RD AVE BETWEEN CAMELBACK ROAD AND GRAND CANAL

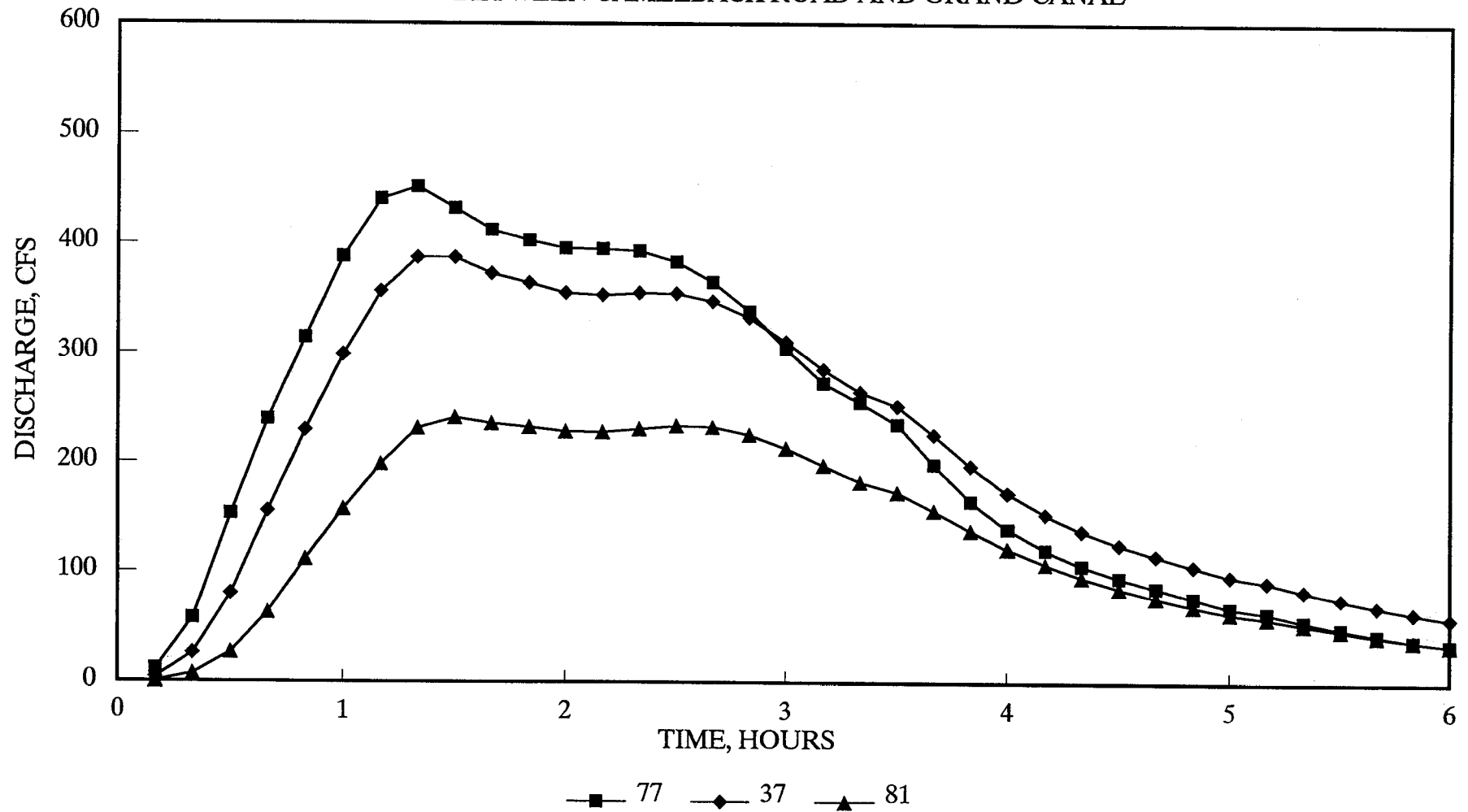


Figure 72 Computed Inner-Mesh Flood Hydrographs
3rd Avenue within the Southern Portion of the Study Area

DISCHARGE VARIATION ALONG GRAND CANAL

BETWEEN 15TH AVENUE AND 3RD AVENUE

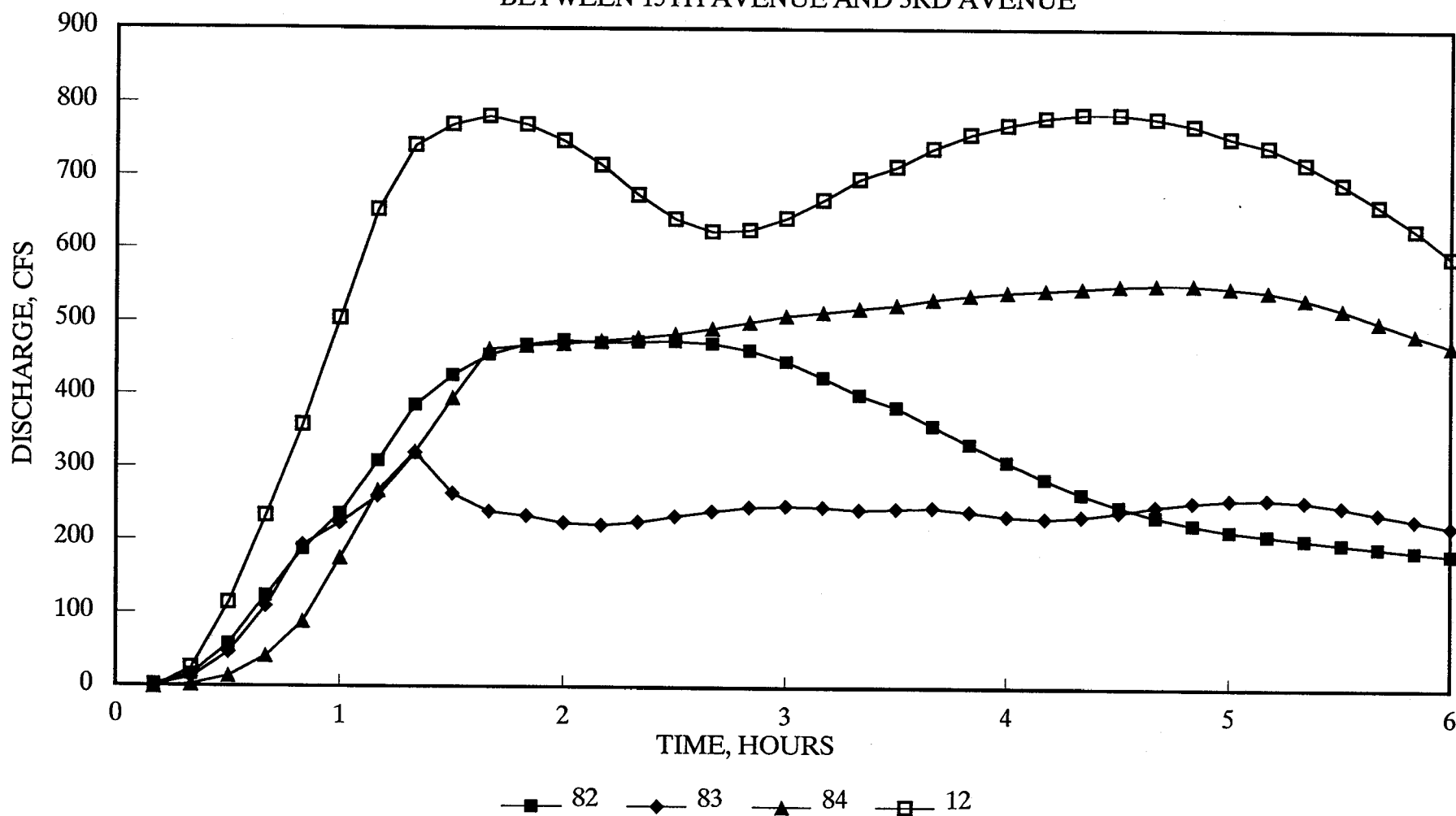


Figure 73 Computed Inner-Mesh Flood Hydrographs Along the Grand Canal

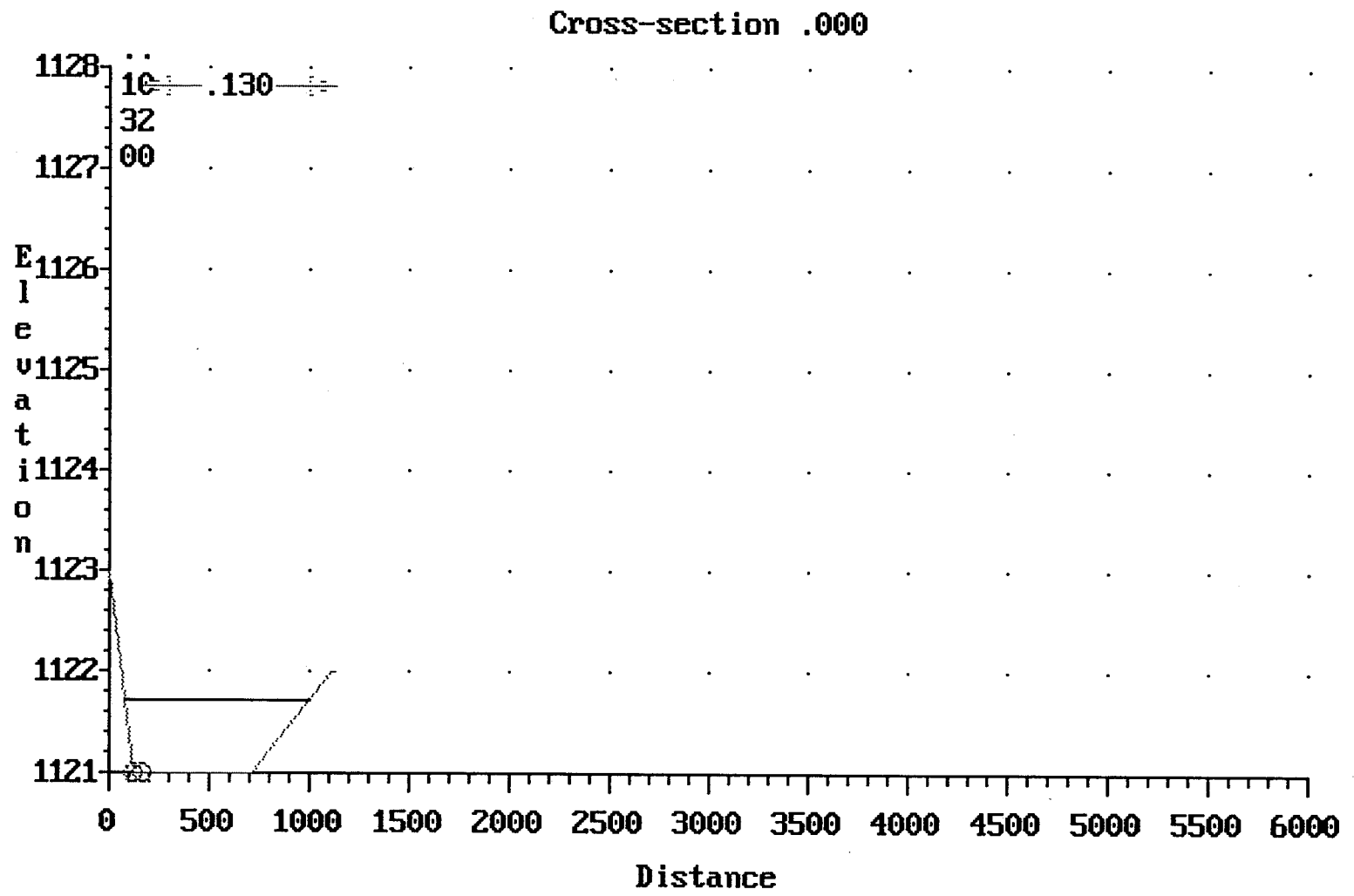


Figure 74 Main Channel HEC-2 Run
Cross-Section 0.0

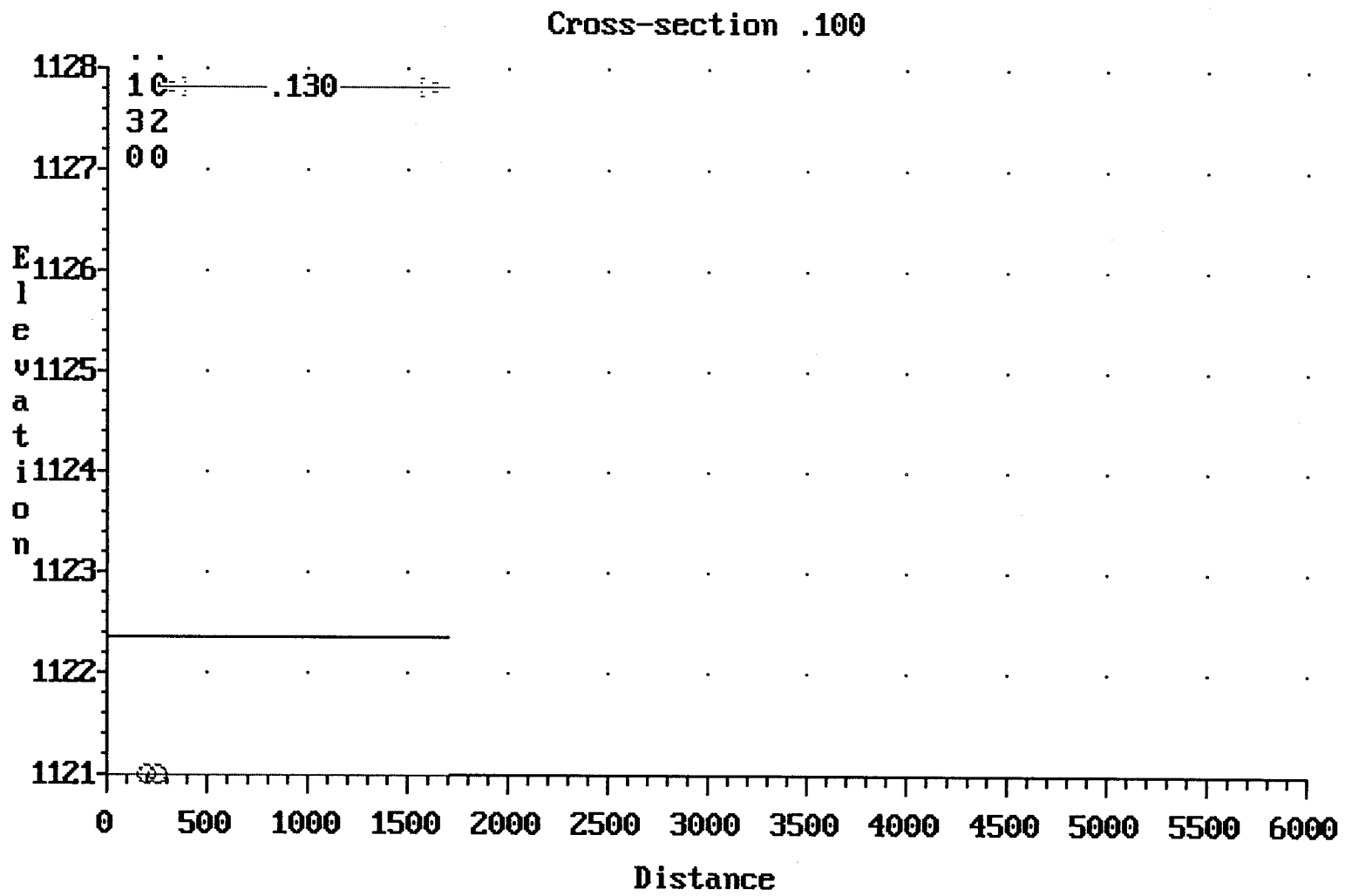


Figure 75 Main Channel HEC-2 Run
Cross-Section 0.1

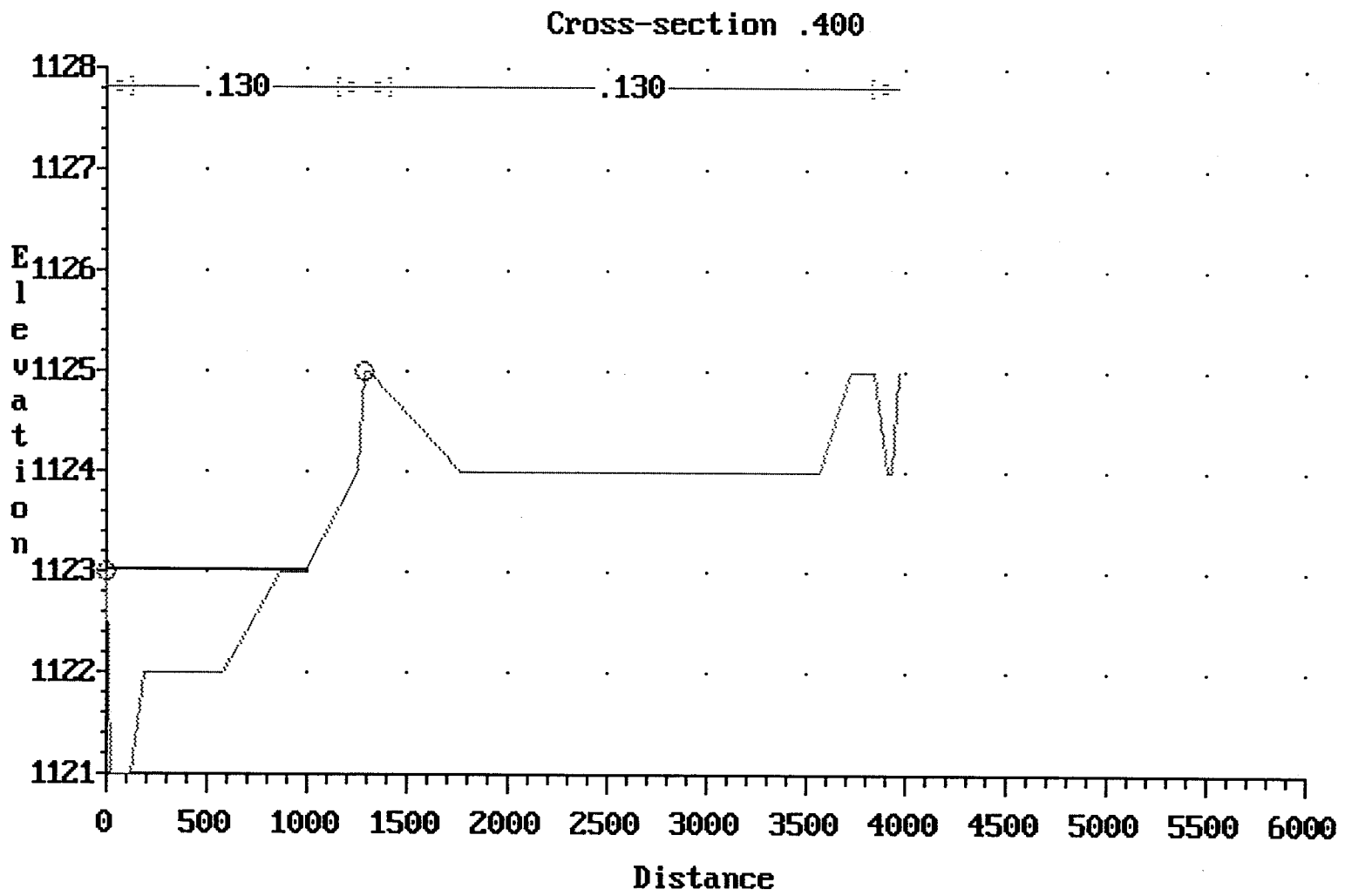


Figure 76 Main Channel HEC-2 Run
Cross-Section 0.4

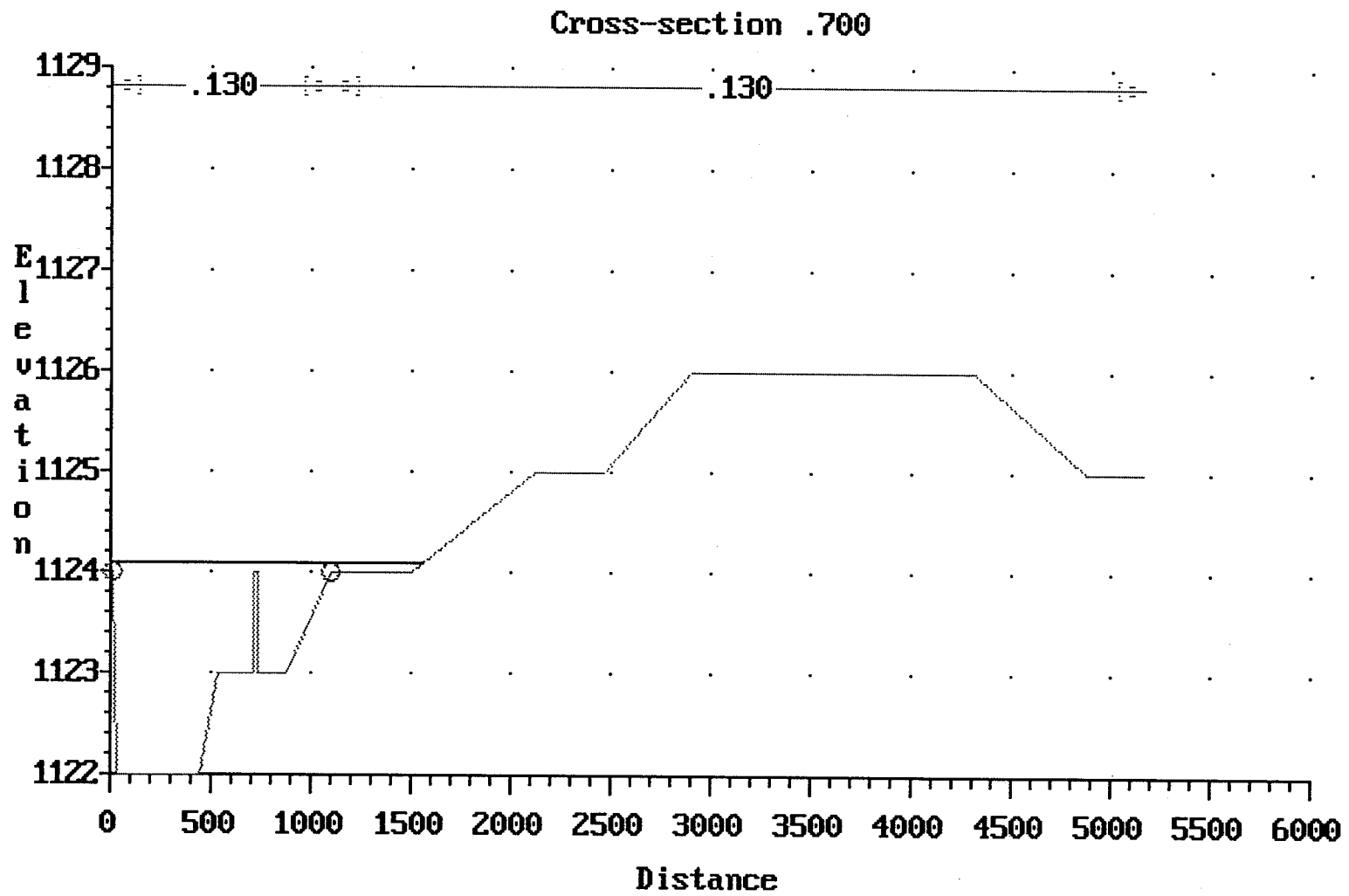


Figure 76 Main Channel HEC-2 Run
Cross-Section 0.7

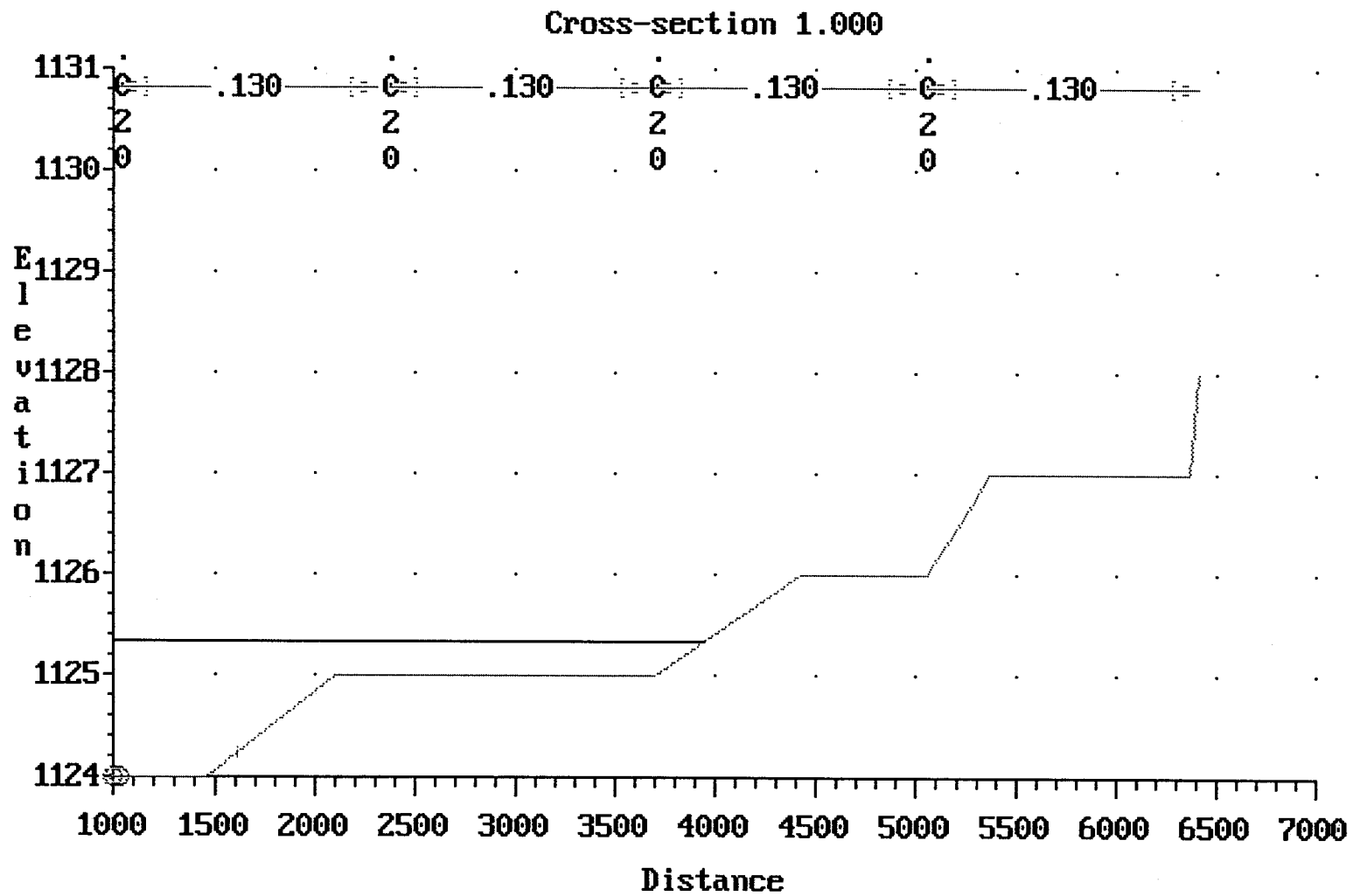


Figure 78 Main Channel HEC-2 Run
Cross-Section 1

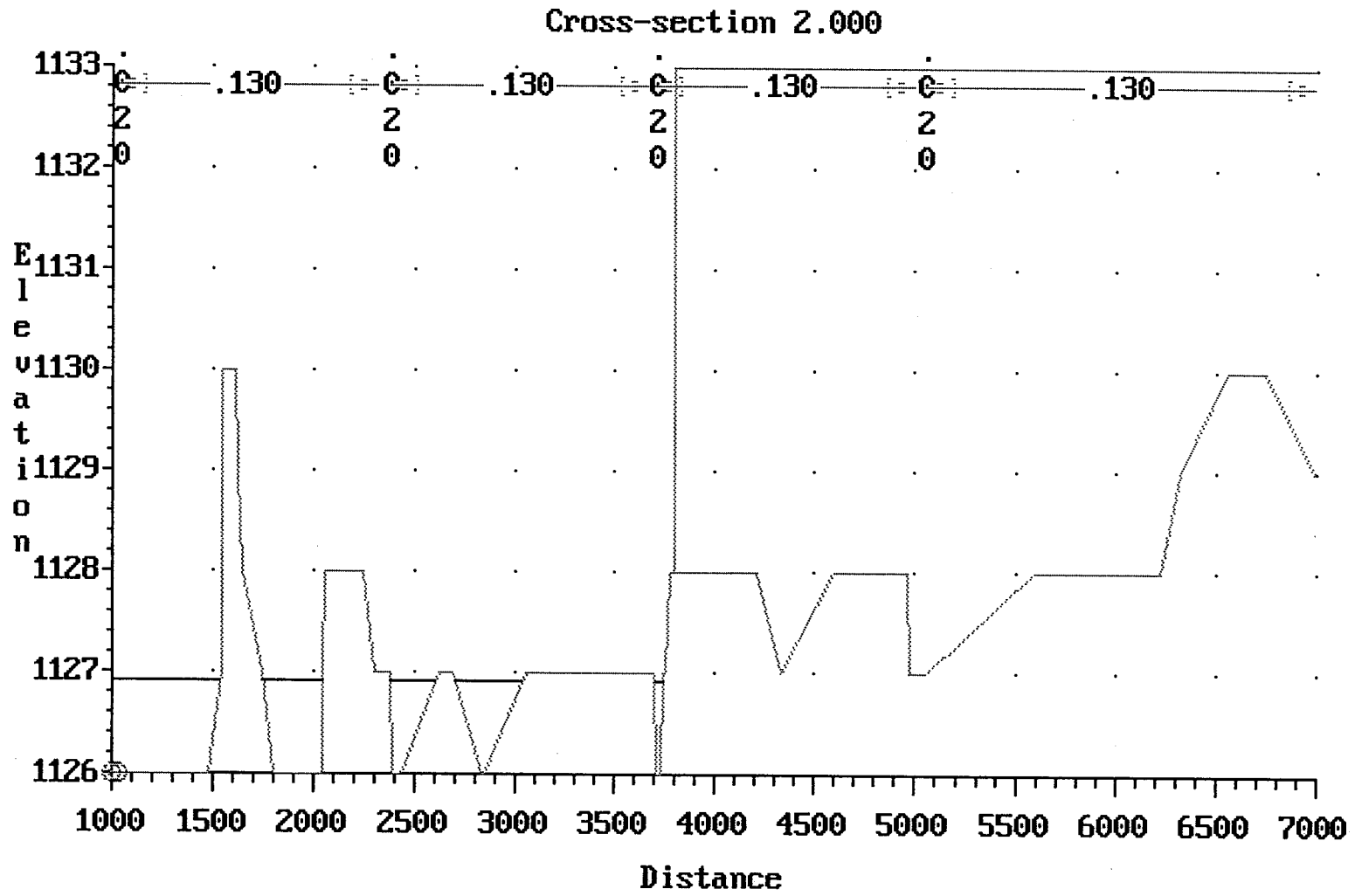


Figure 79 Main Channel HEC-2 Run
Cross-Section 2

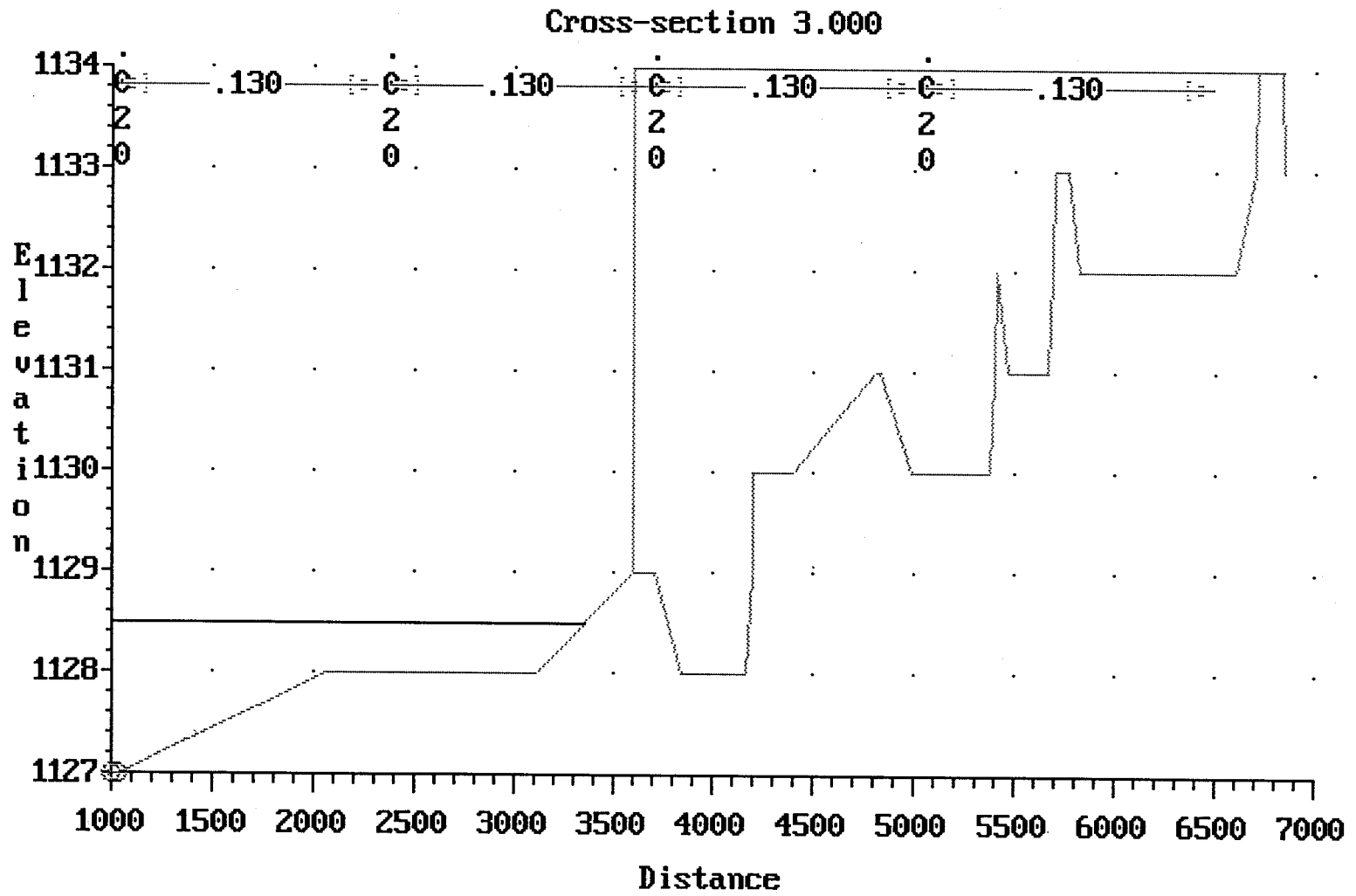


Figure 80 Main Channel HEC-2 Run
Cross-Section 3

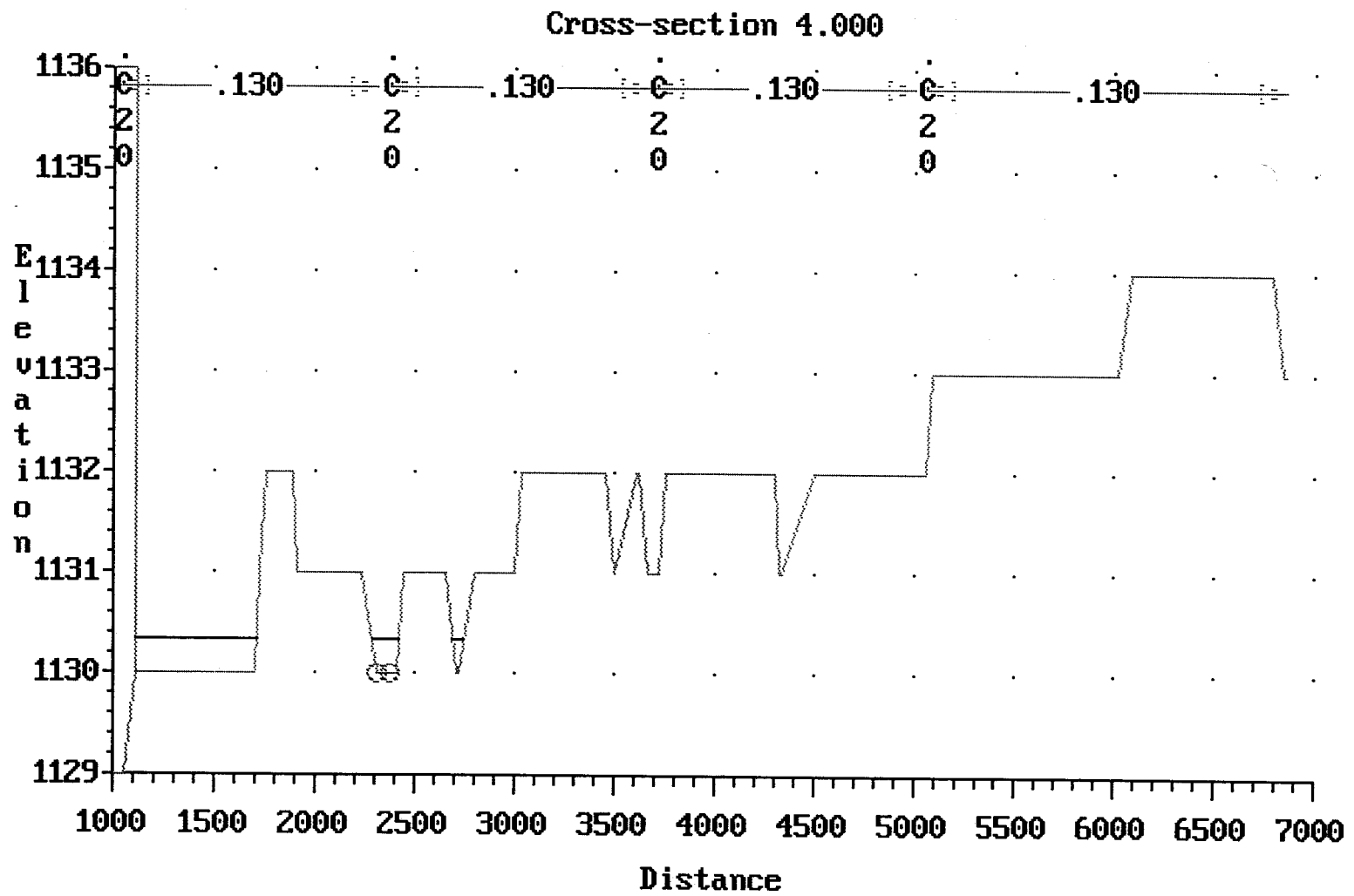


Figure 81 Main Channel HEC-2 Run Cross-Section 4

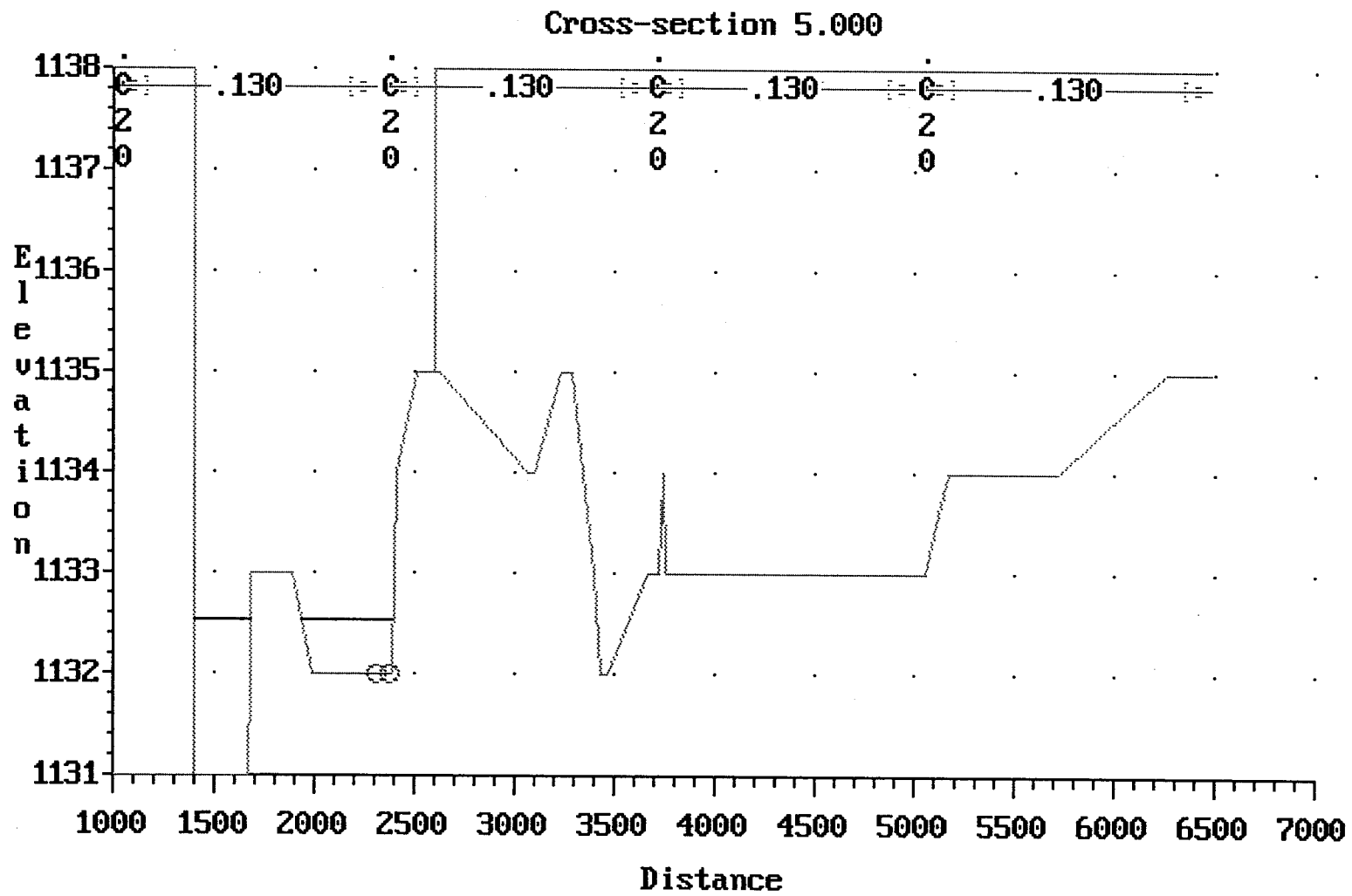


Figure 82 Main Channel HEC-2 Run
Cross-Section 5

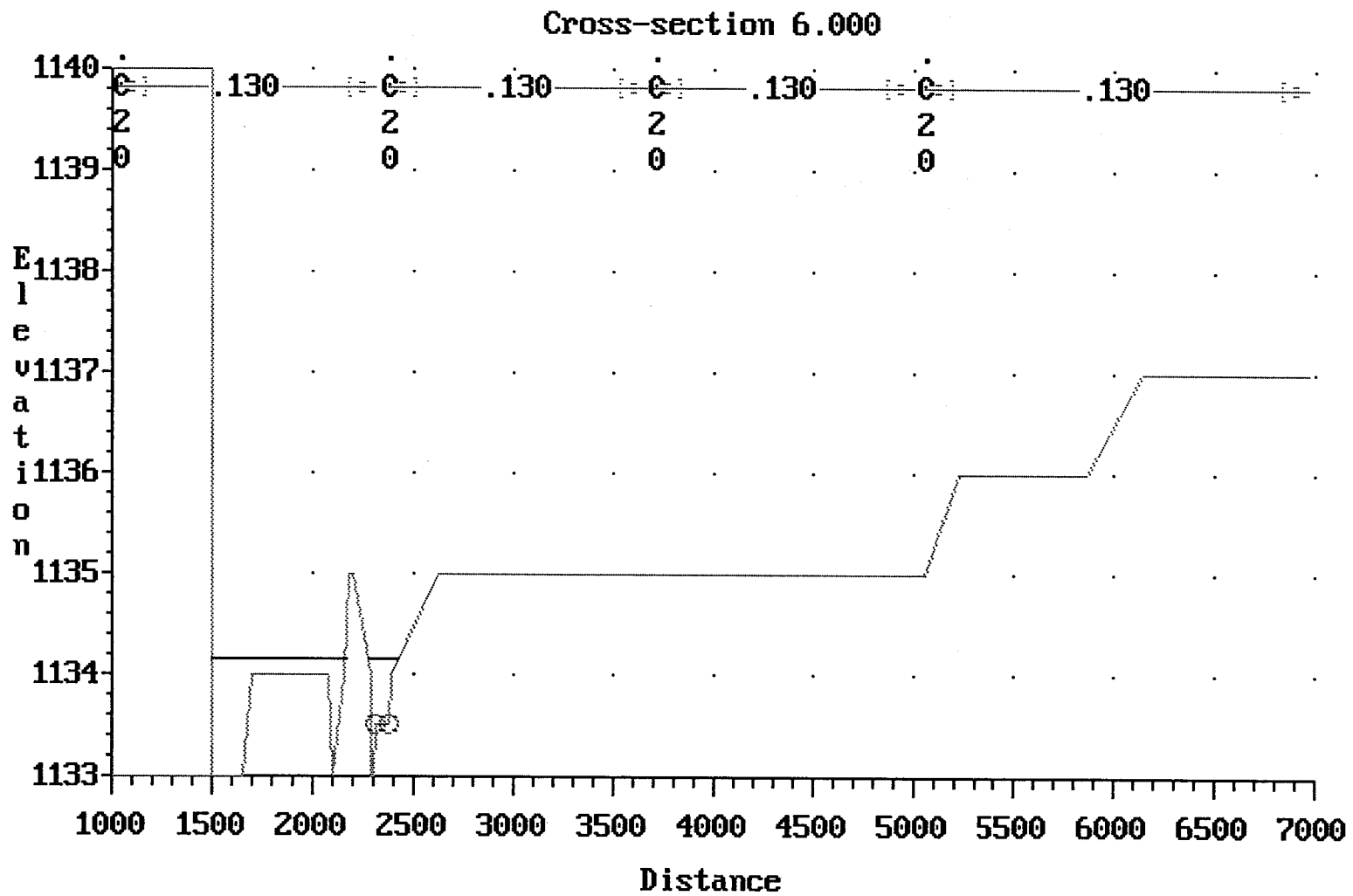


Figure 83 Main Channel HEC-2 Run
Cross-Section 6

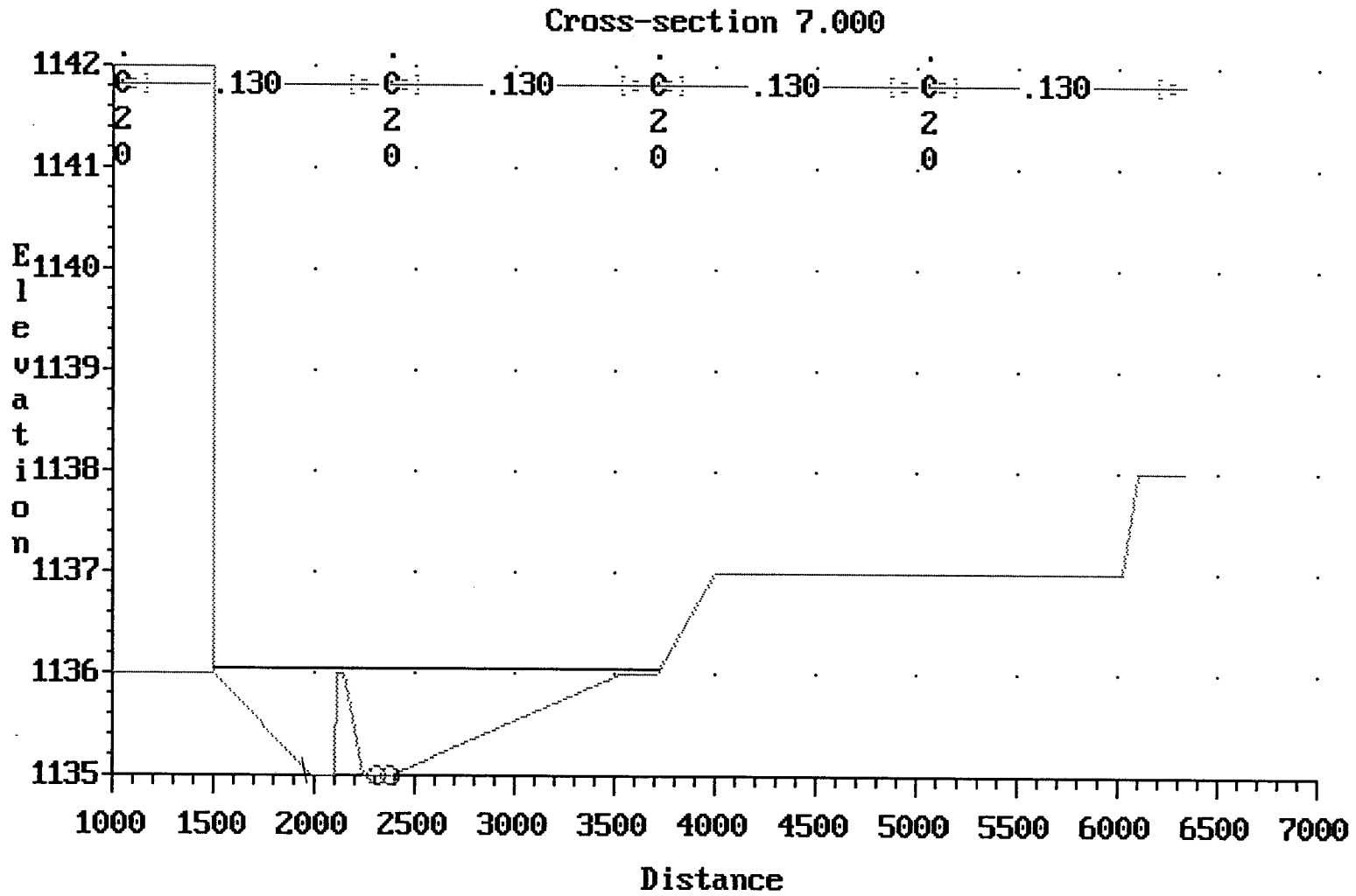


Figure 84 Main Channel HEC-2 Run
Cross-Section 7

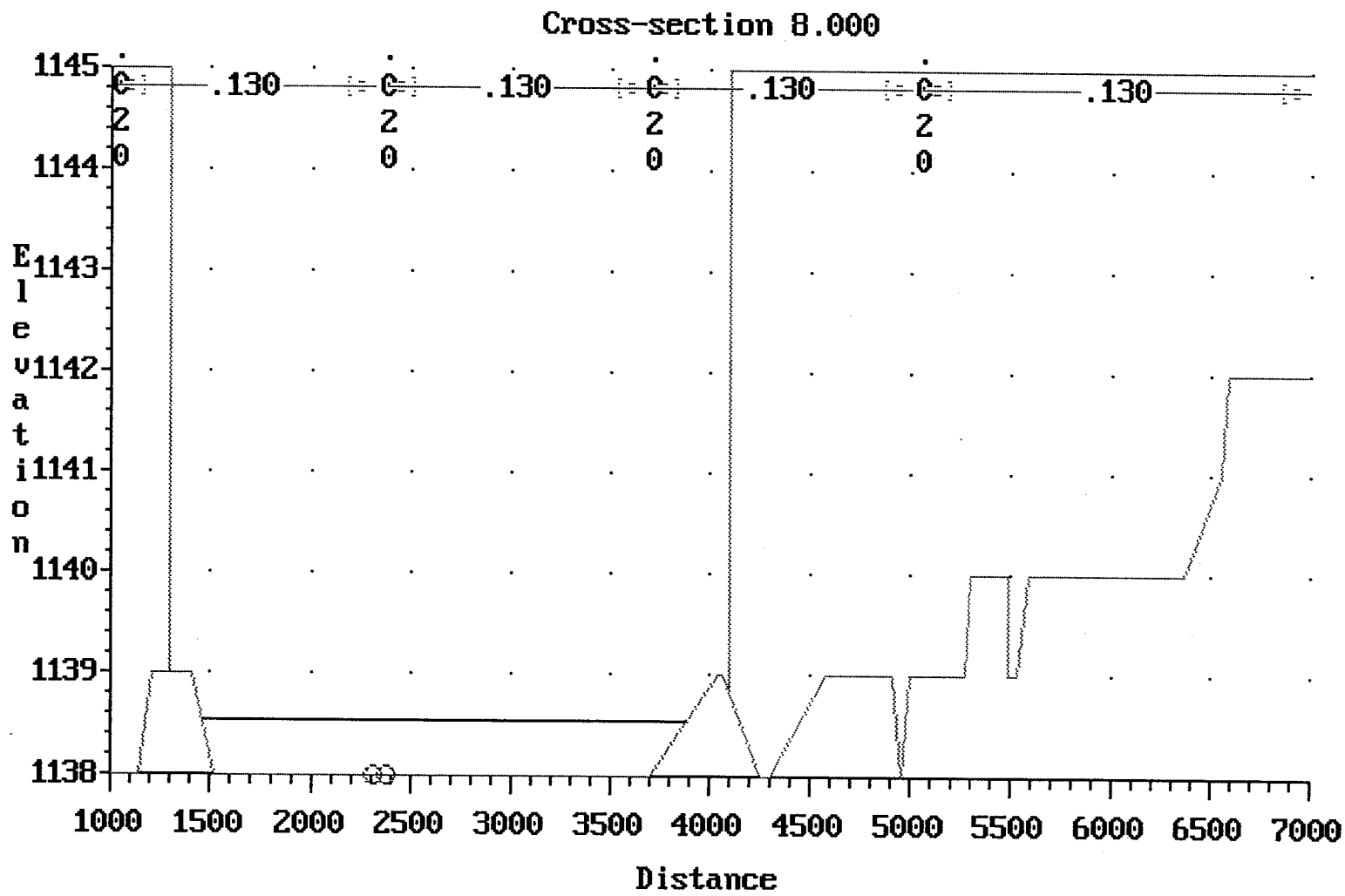


Figure 85 Main Channel HEC-2 Run
Cross-Section 8

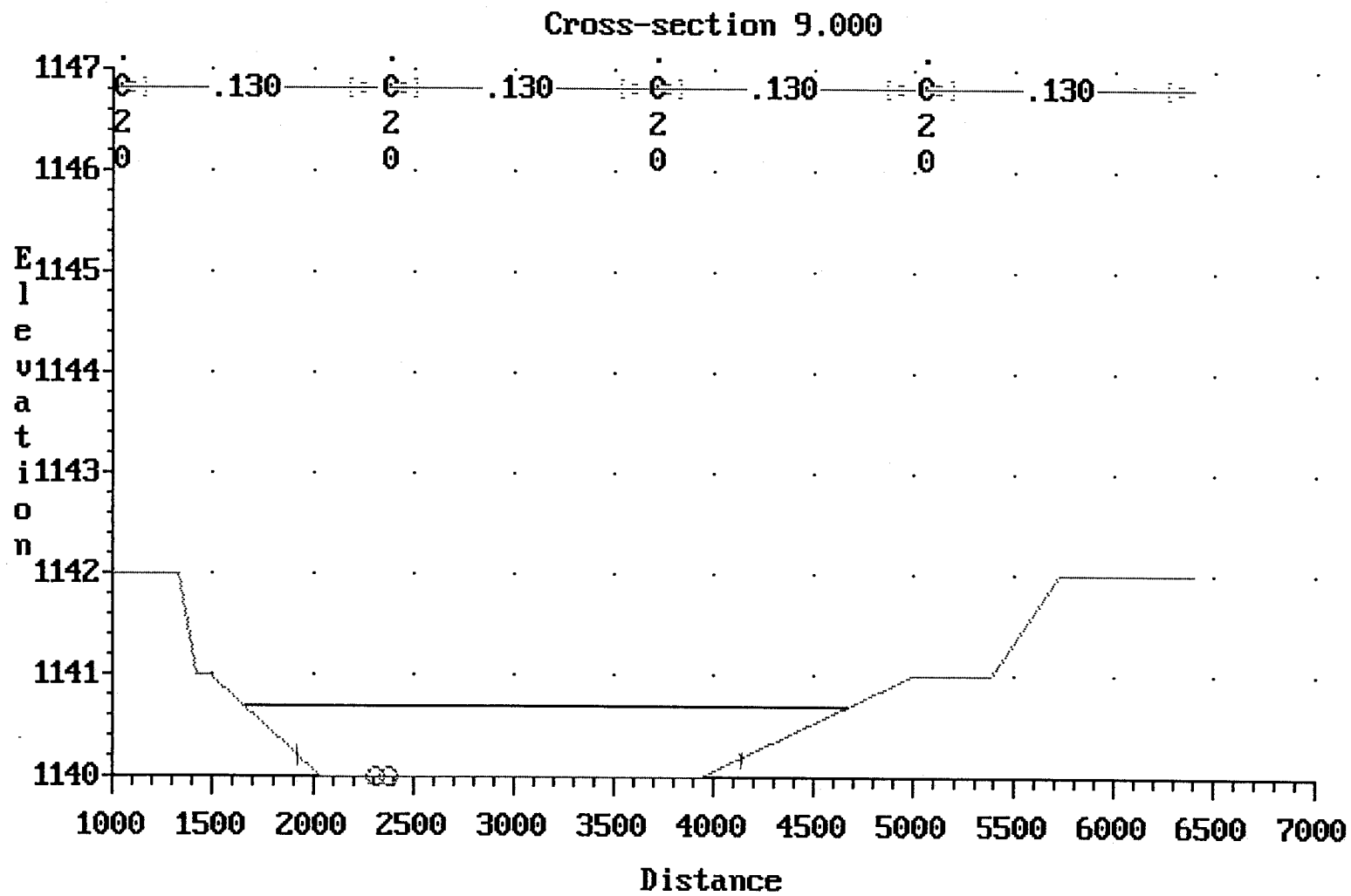


Figure 86 Main Channel HEC-2 Run
Cross-Section 9

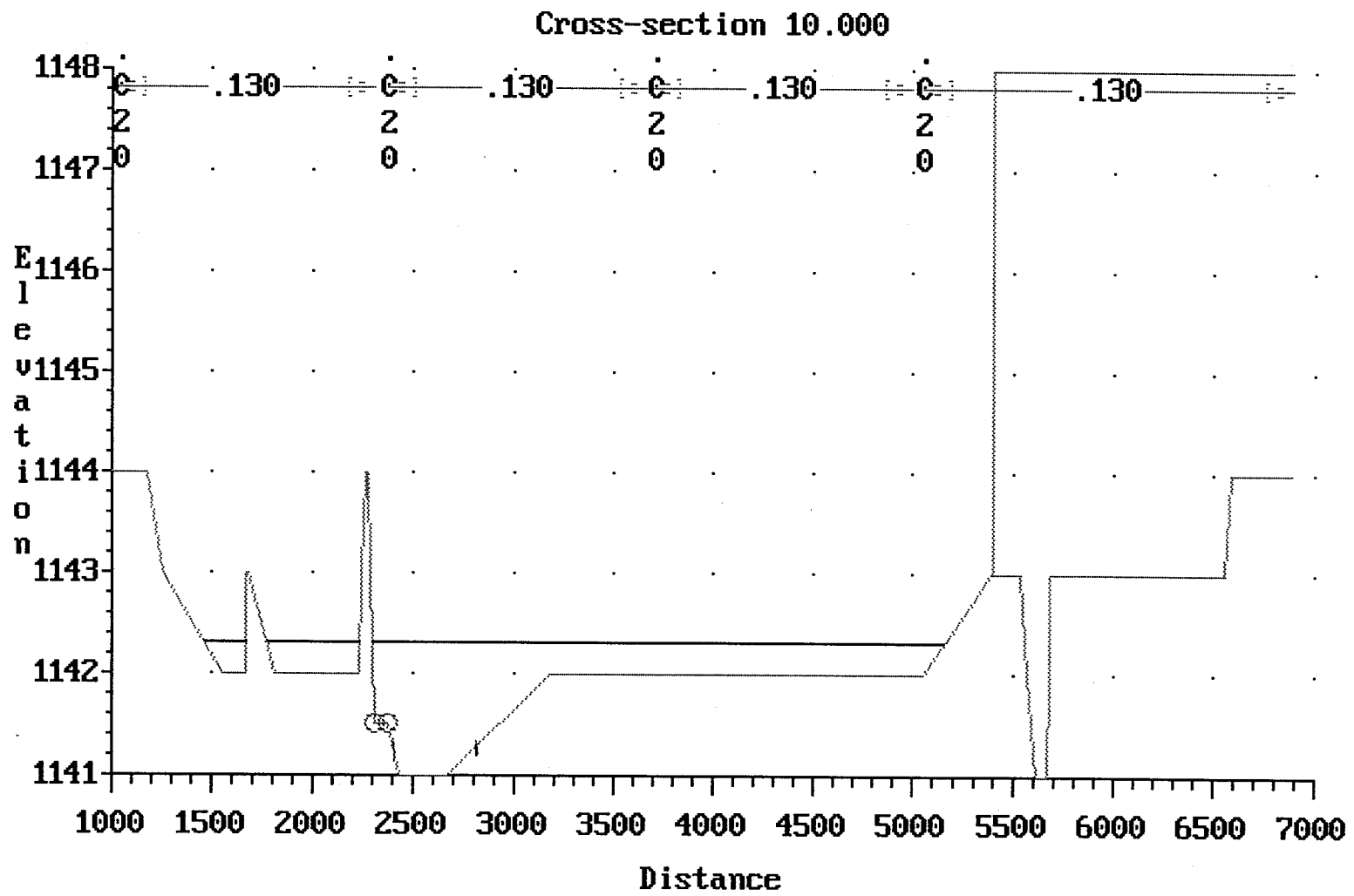


Figure 87 Main Channel HEC-2 Run
Cross-Section 10

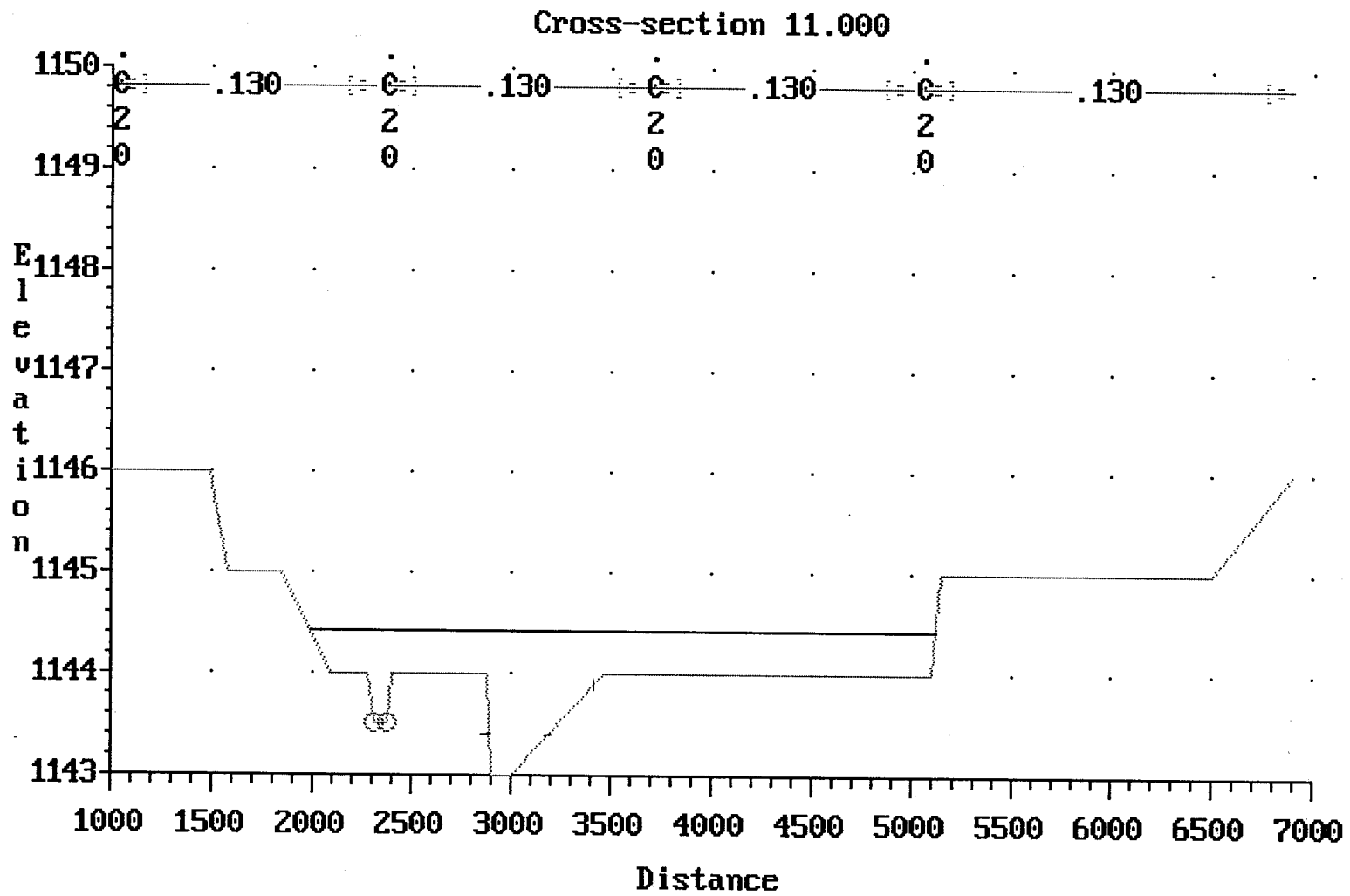


Figure 88 Main Channel HEC-2 Run
Cross-Section 11

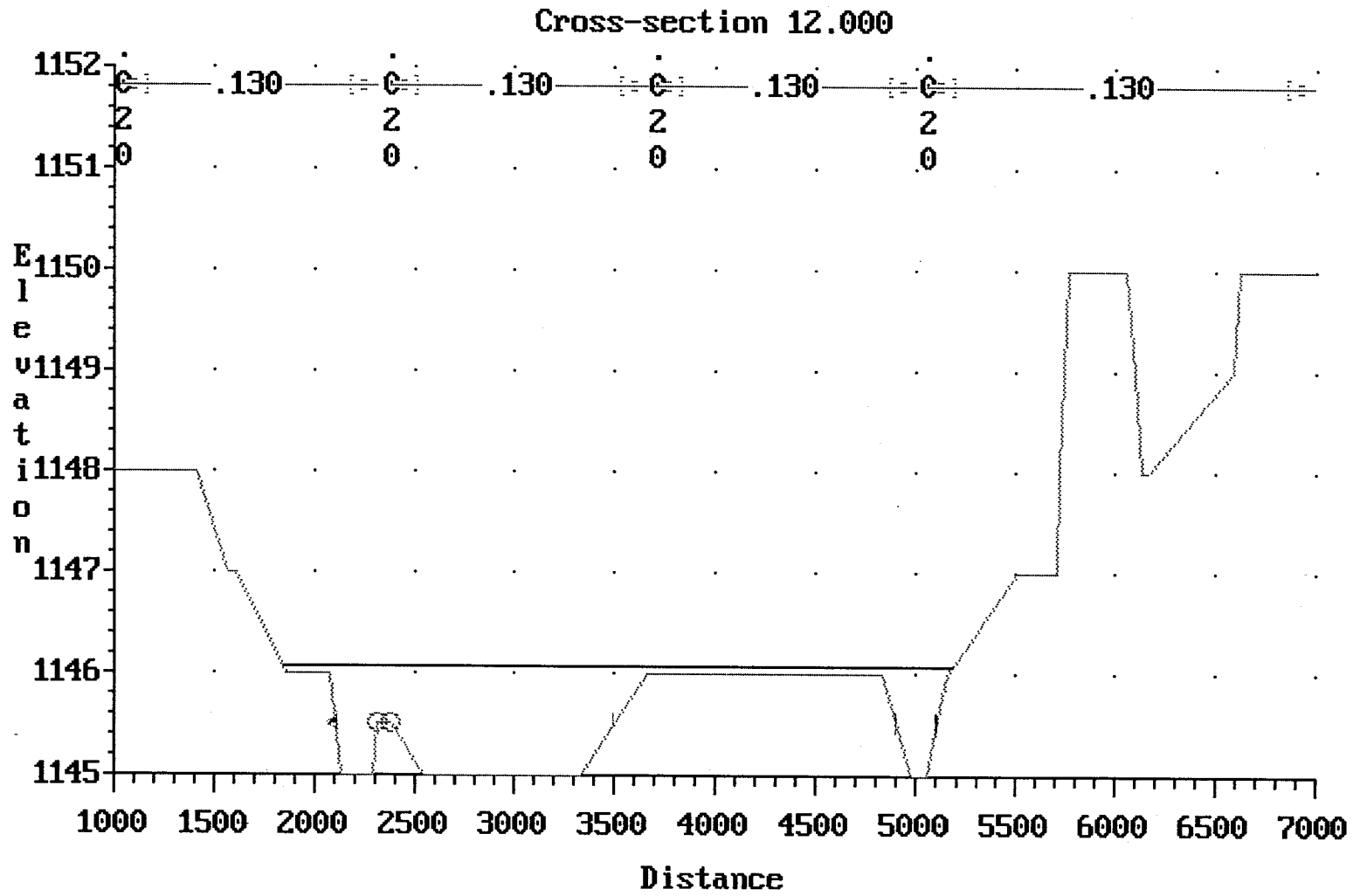


Figure 89 Main Channel HEC-2 Run
Cross-Section 12

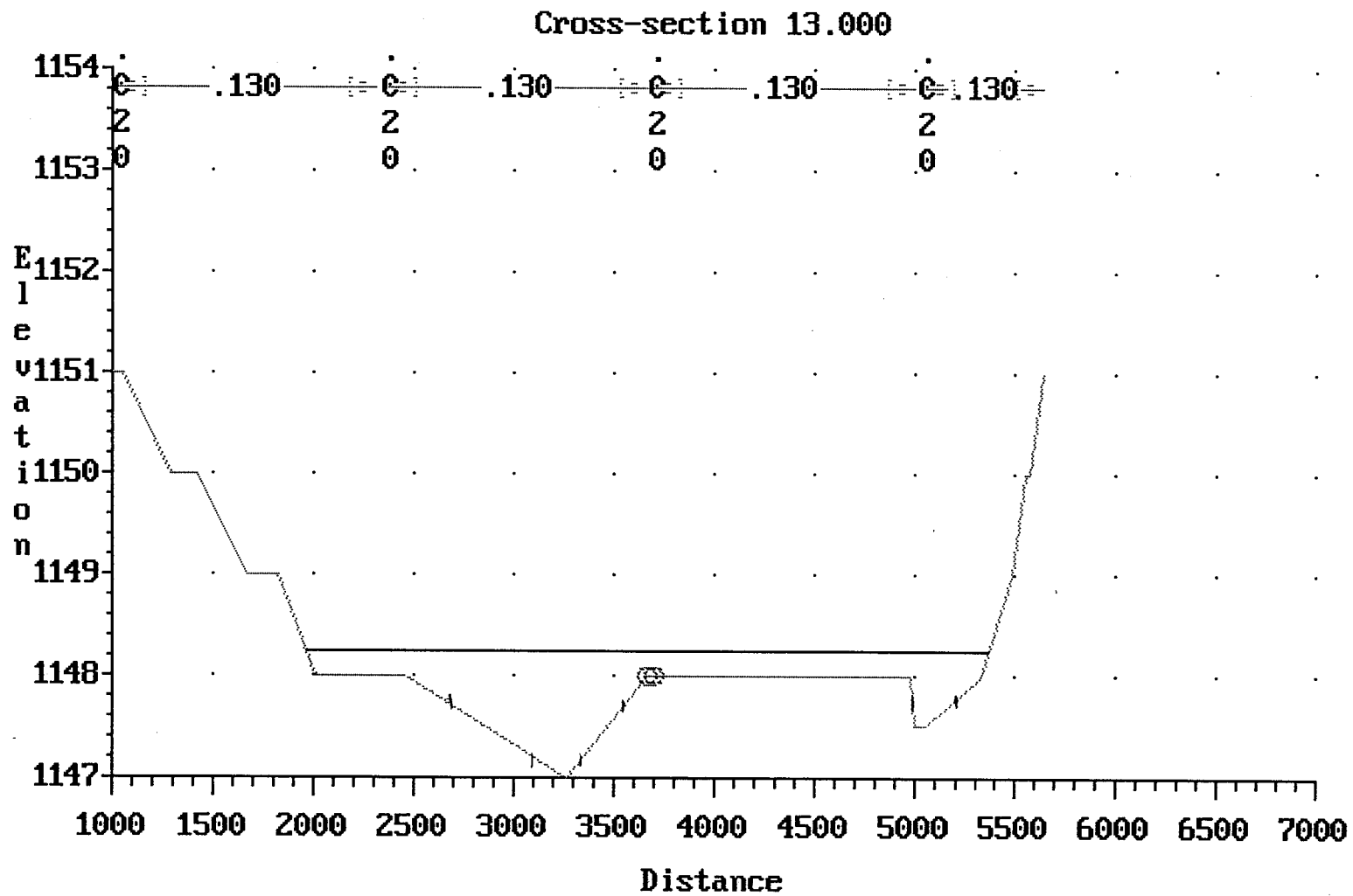


Figure 90 Main Channel HEC-2 Run
Cross-Section 13

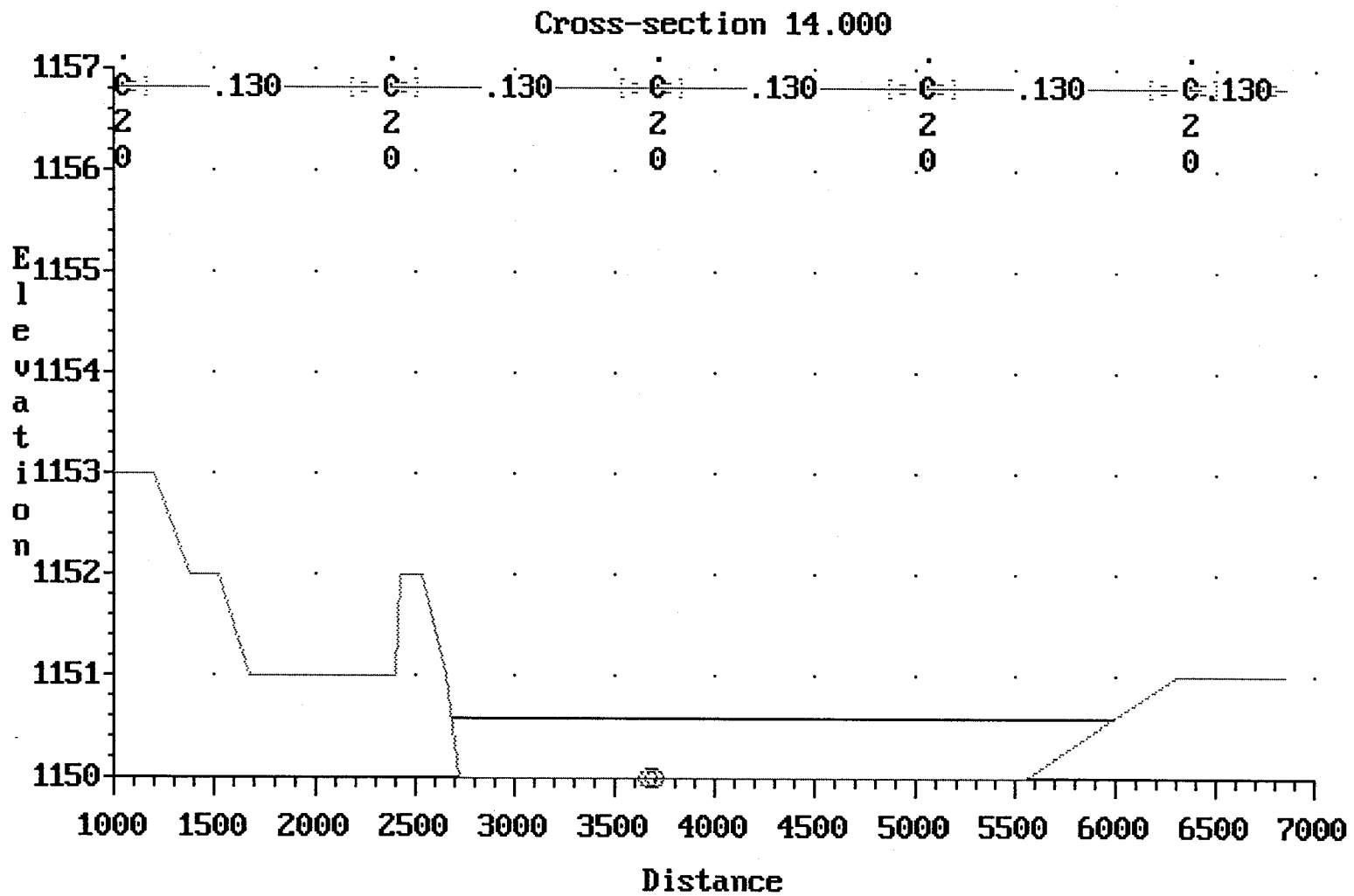


Figure 91 Main Channel HEC-2 Run
Cross-Section 14

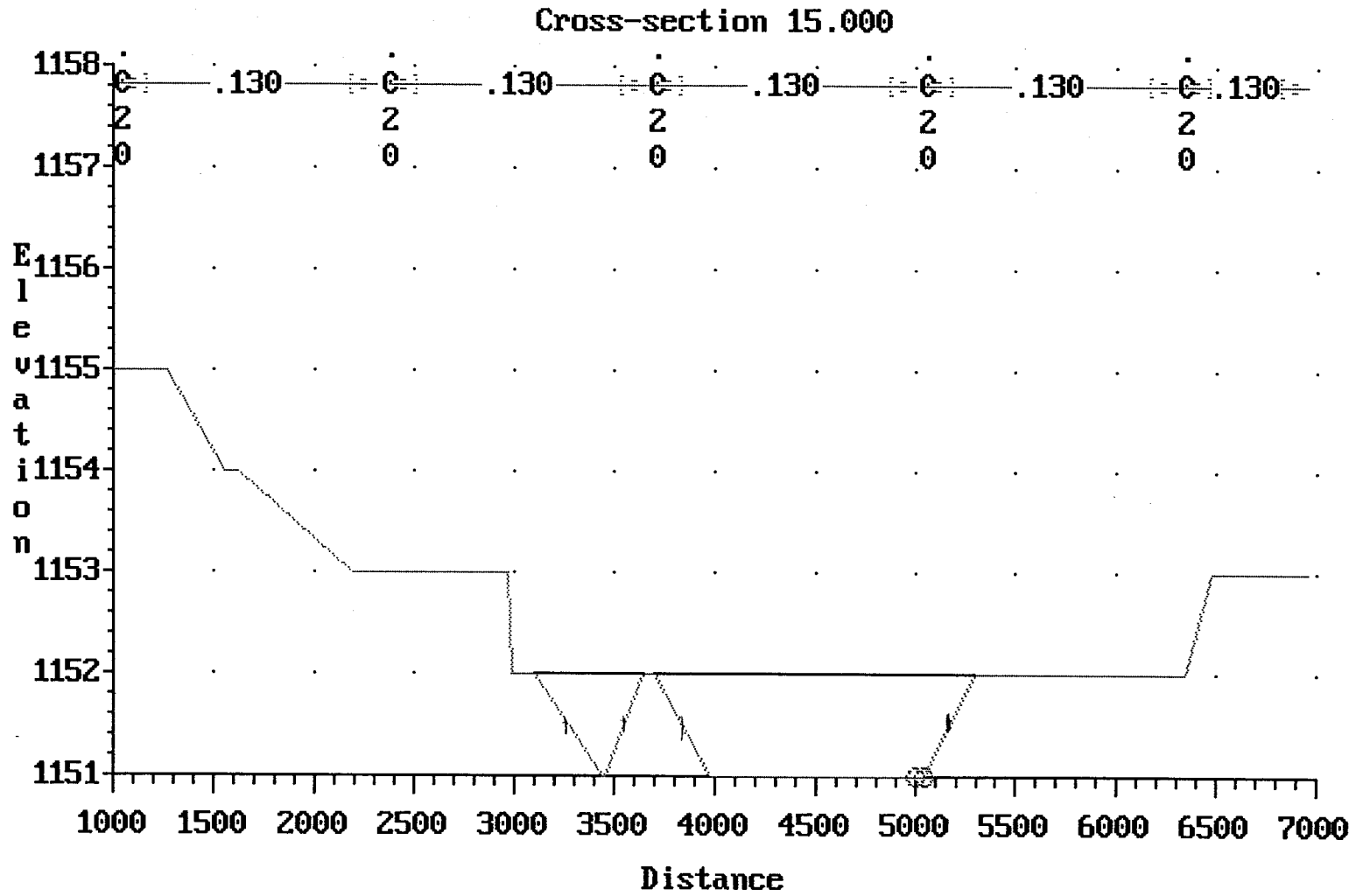


Figure 92 Main Channel HEC-2 Run
Cross-Section 15

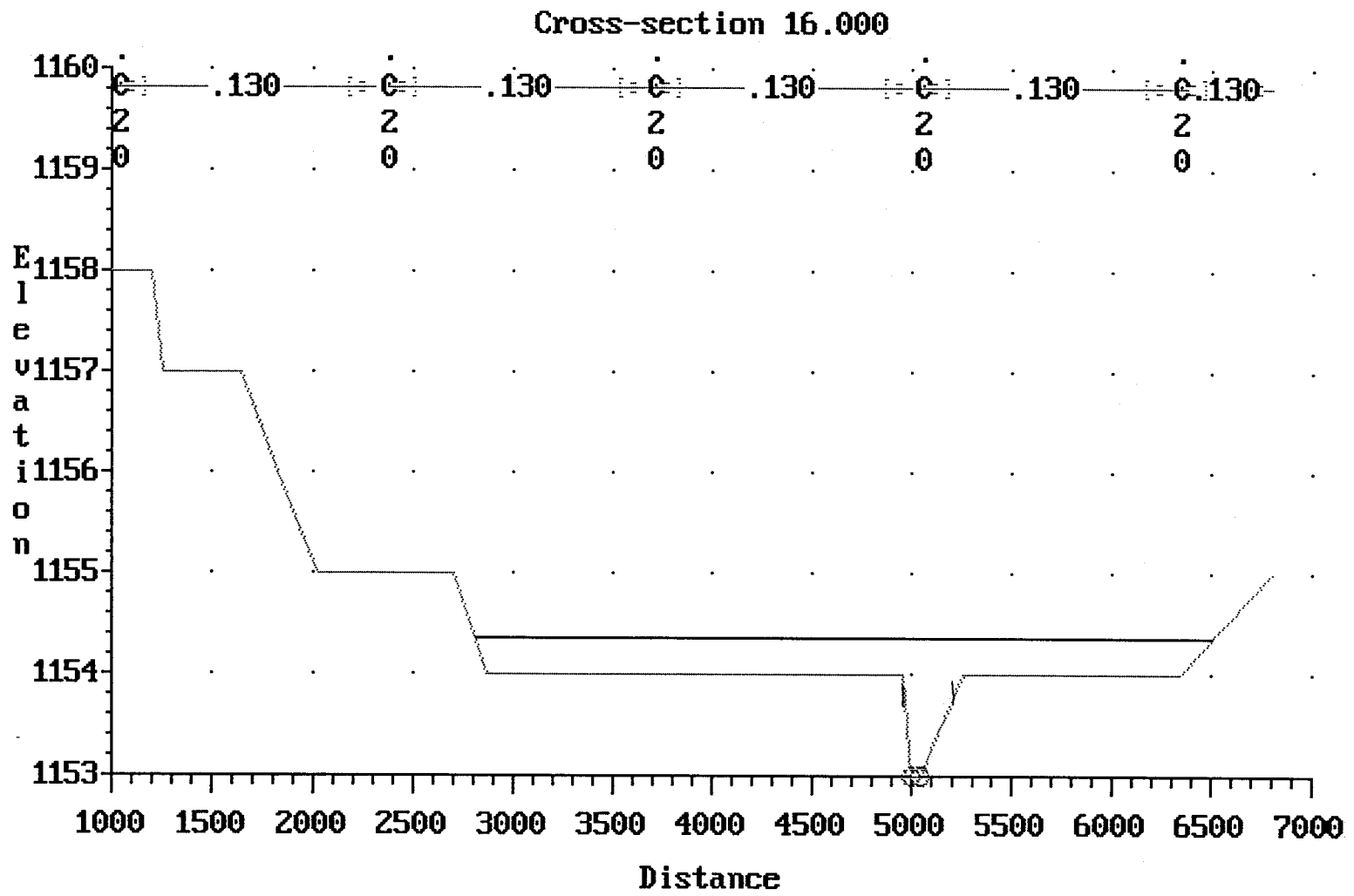


Figure 93 Main Channel HEC-2 Run Cross-Section 16

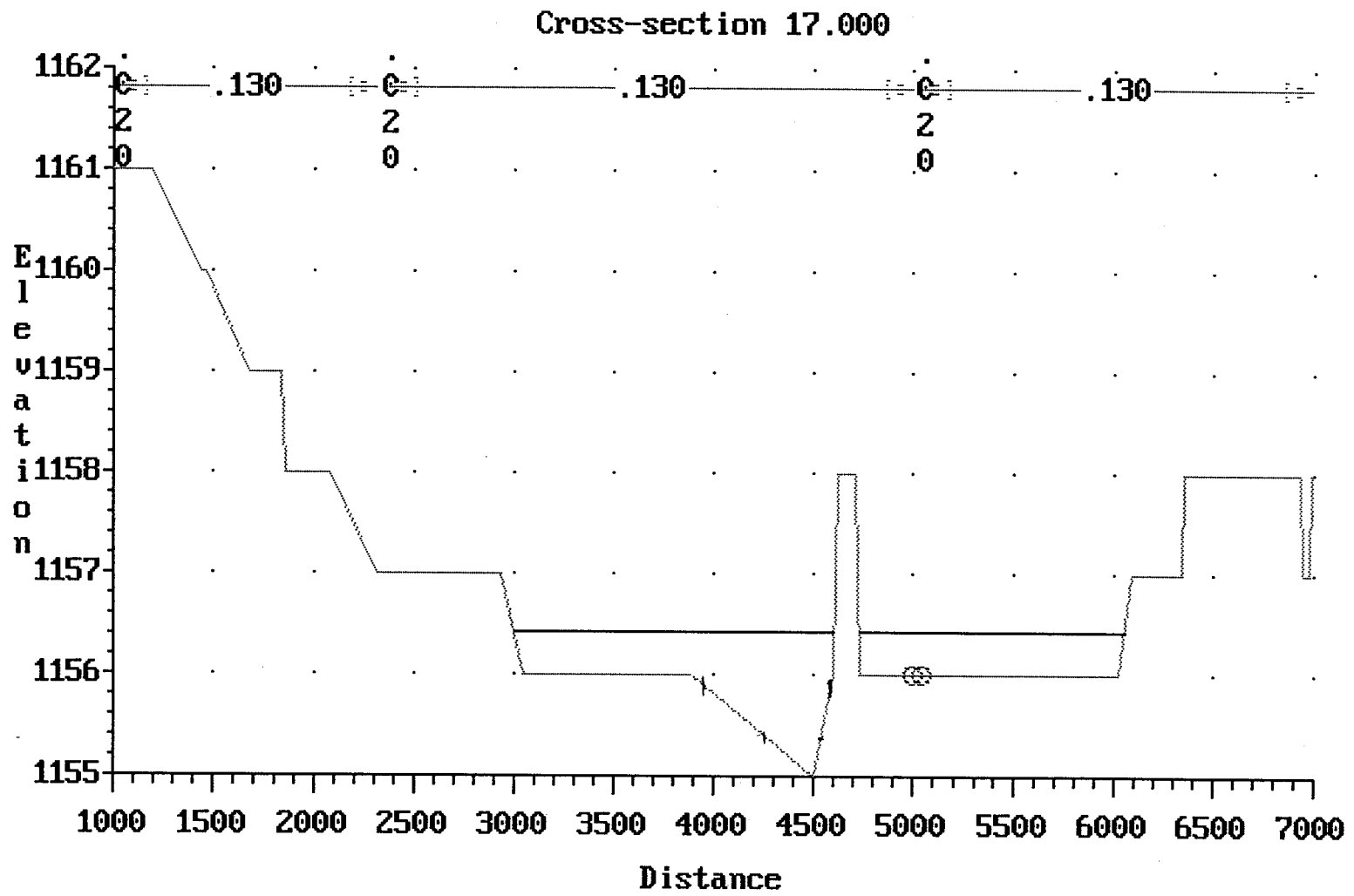


Figure 94 Main Channel HEC-2 Run Cross-Section 17

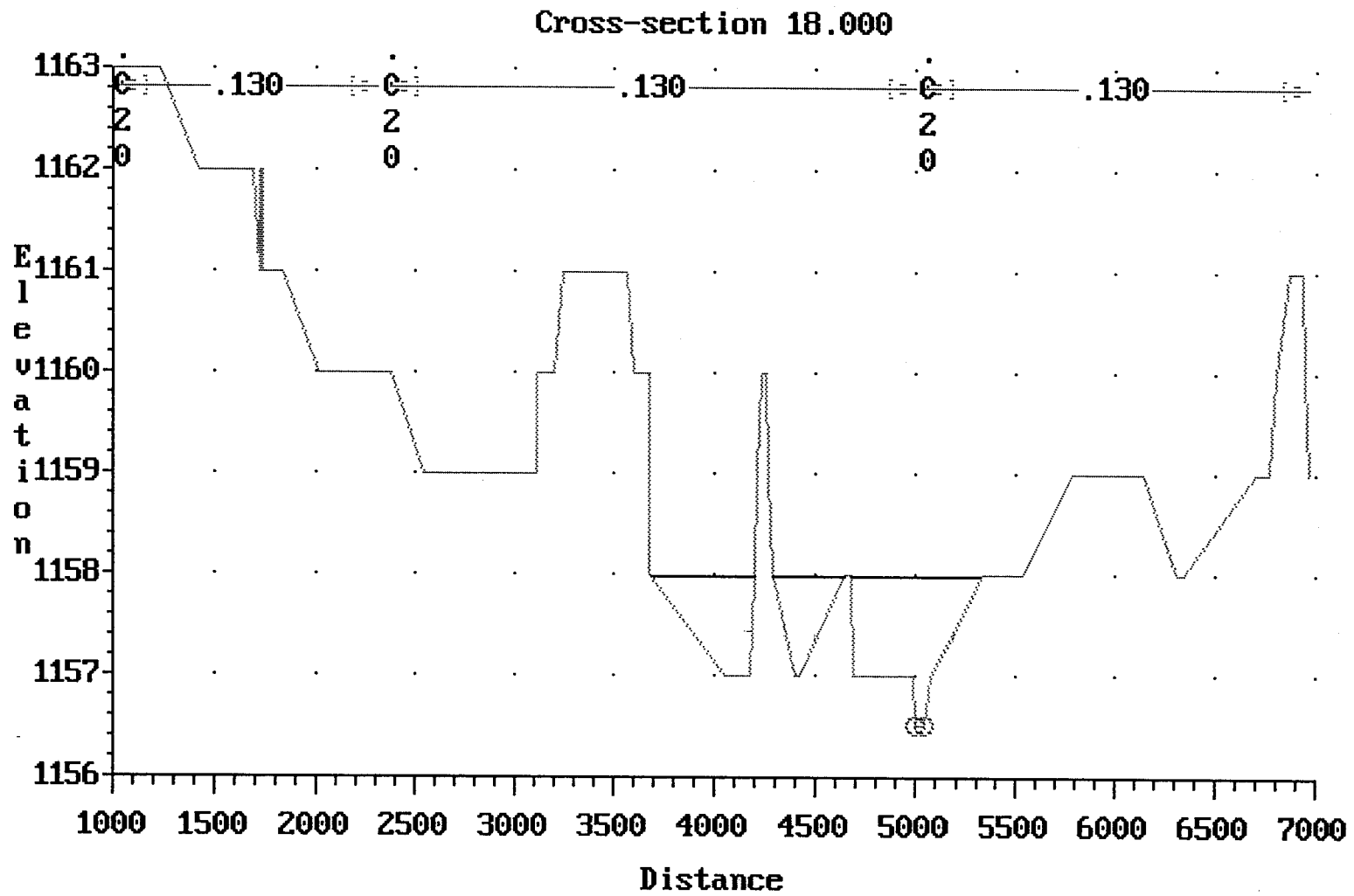


Figure 95 Main Channel HEC-2 Run
Cross-Section 18

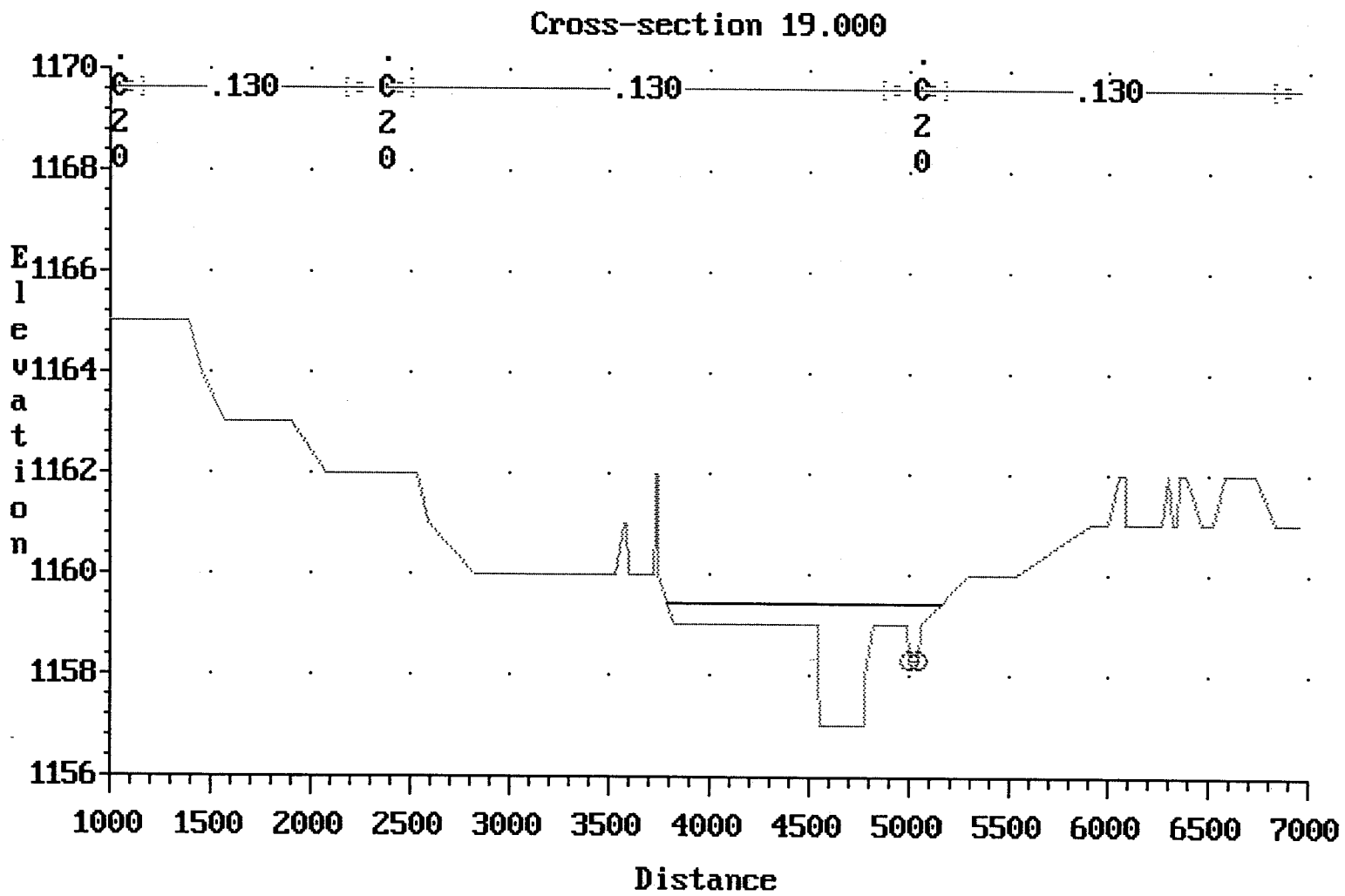


Figure 96 Main Channel HEC-2 Run Cross-Section 19

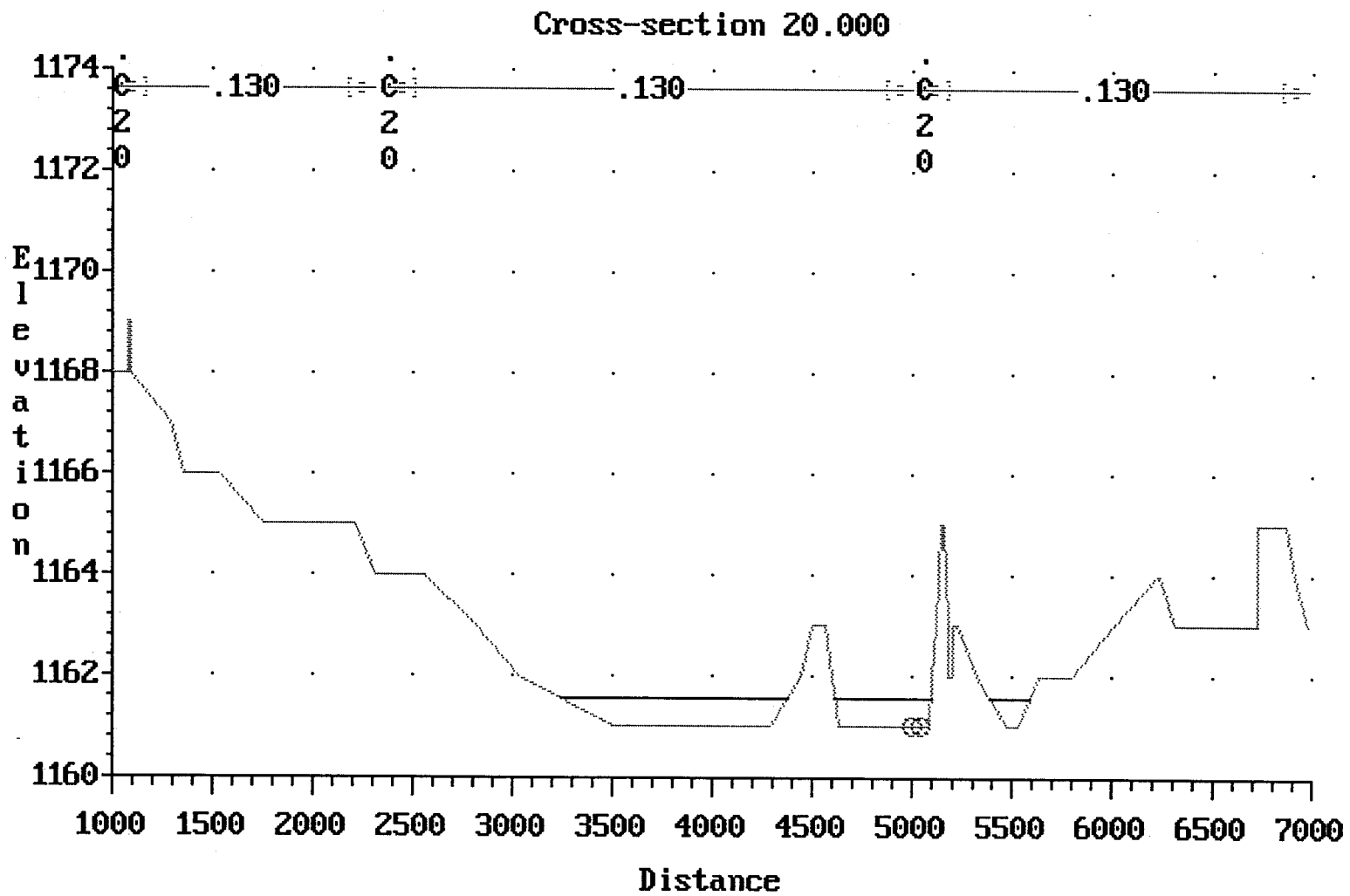


Figure 97 Main Channel HEC-2 Run
Cross-Section 20

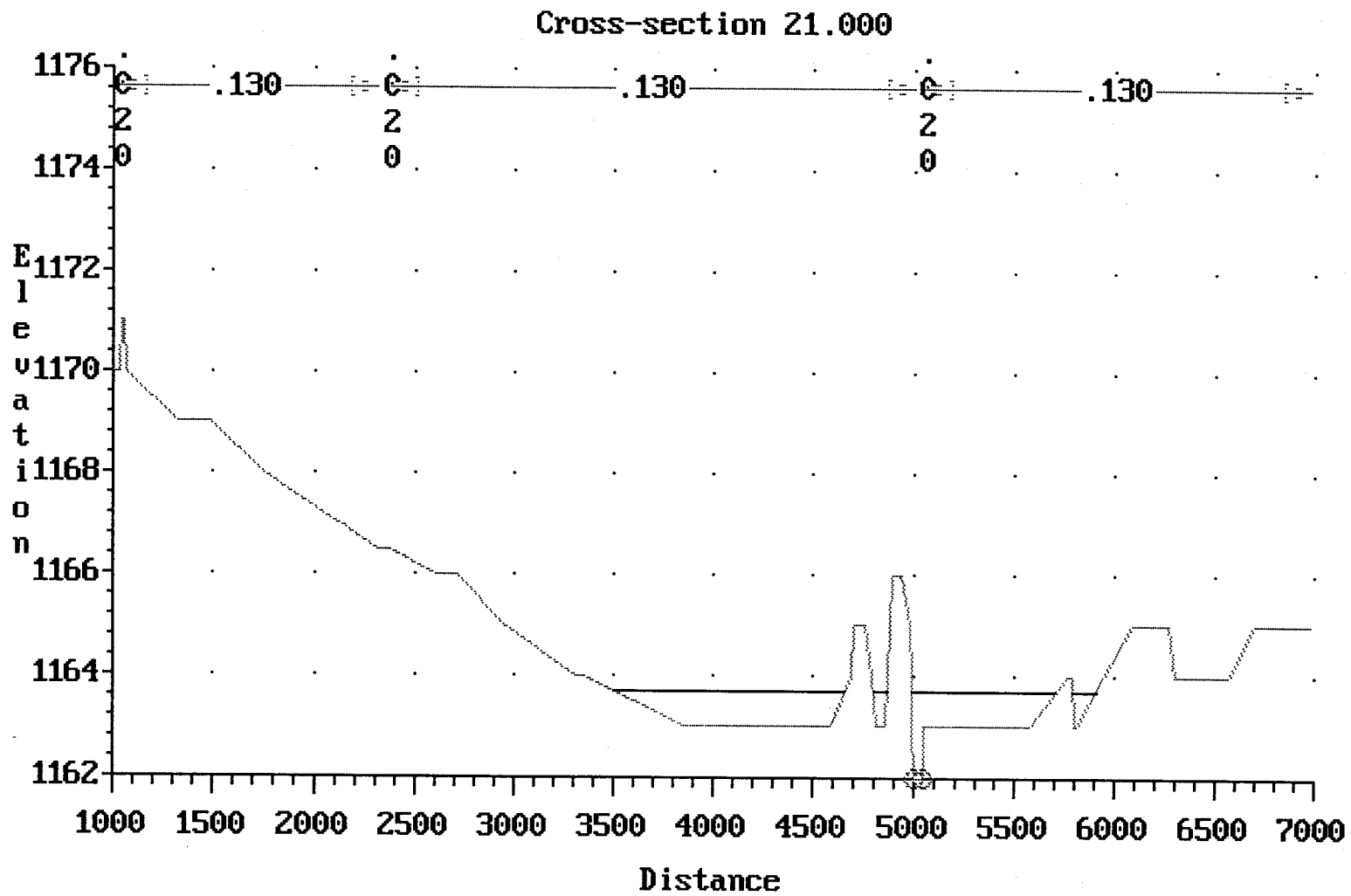


Figure 98 Main Channel HEC-2 Run
Cross-Section 21

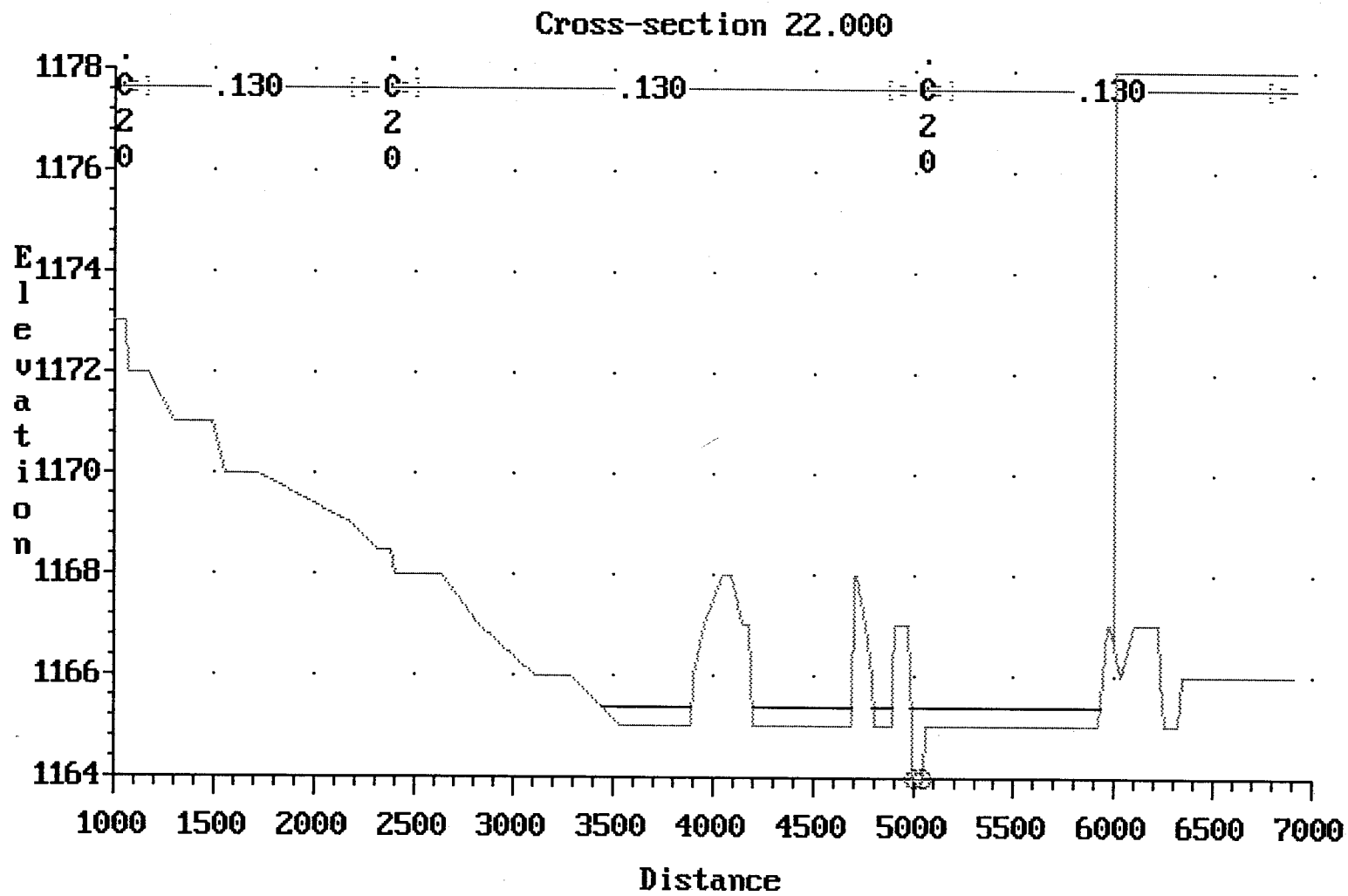


Figure 99 Main Channel HEC-2 Run
Cross-Section 22

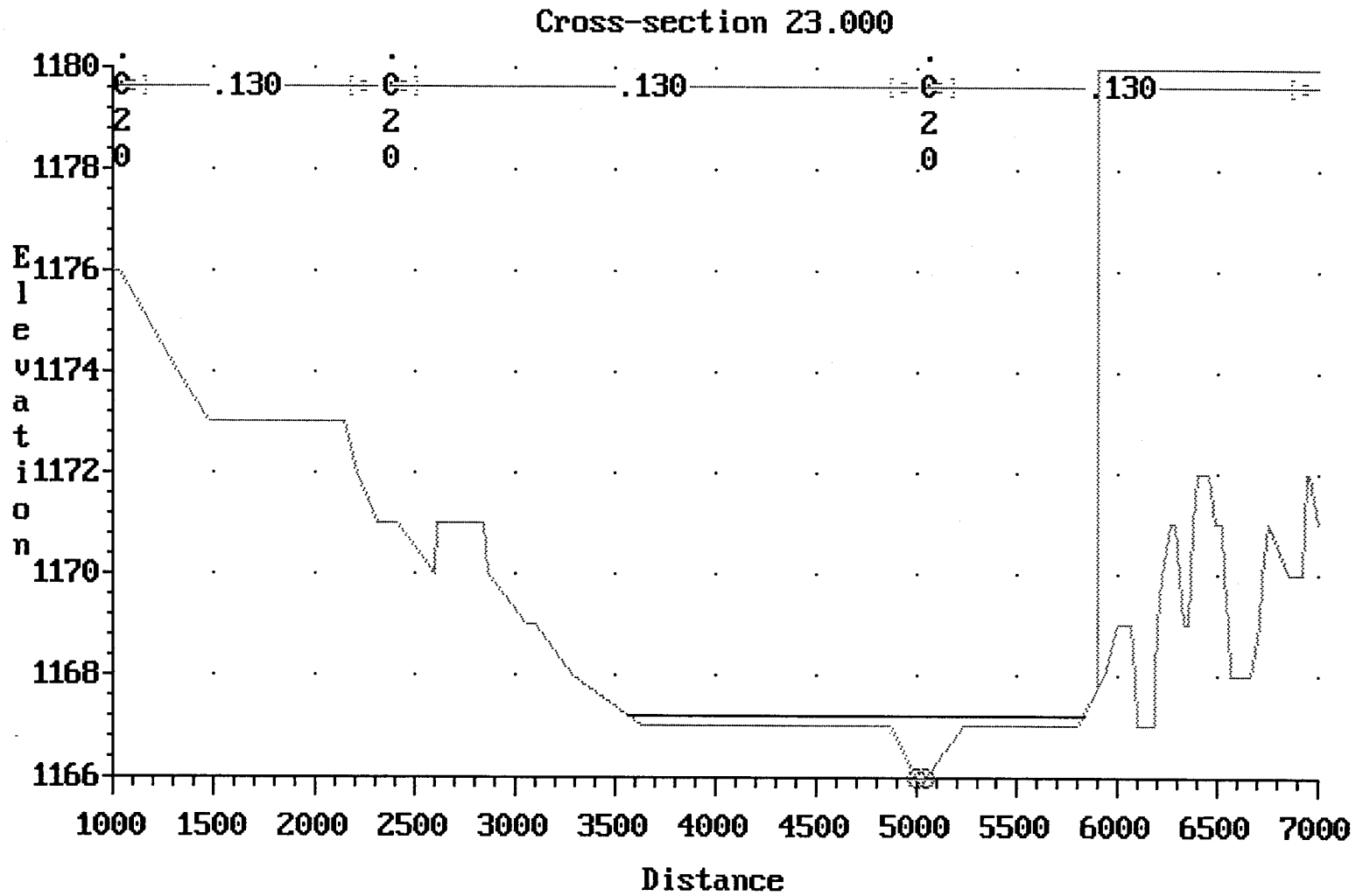


Figure 100 Main Channel HEC-2 Run
Cross-Section 23

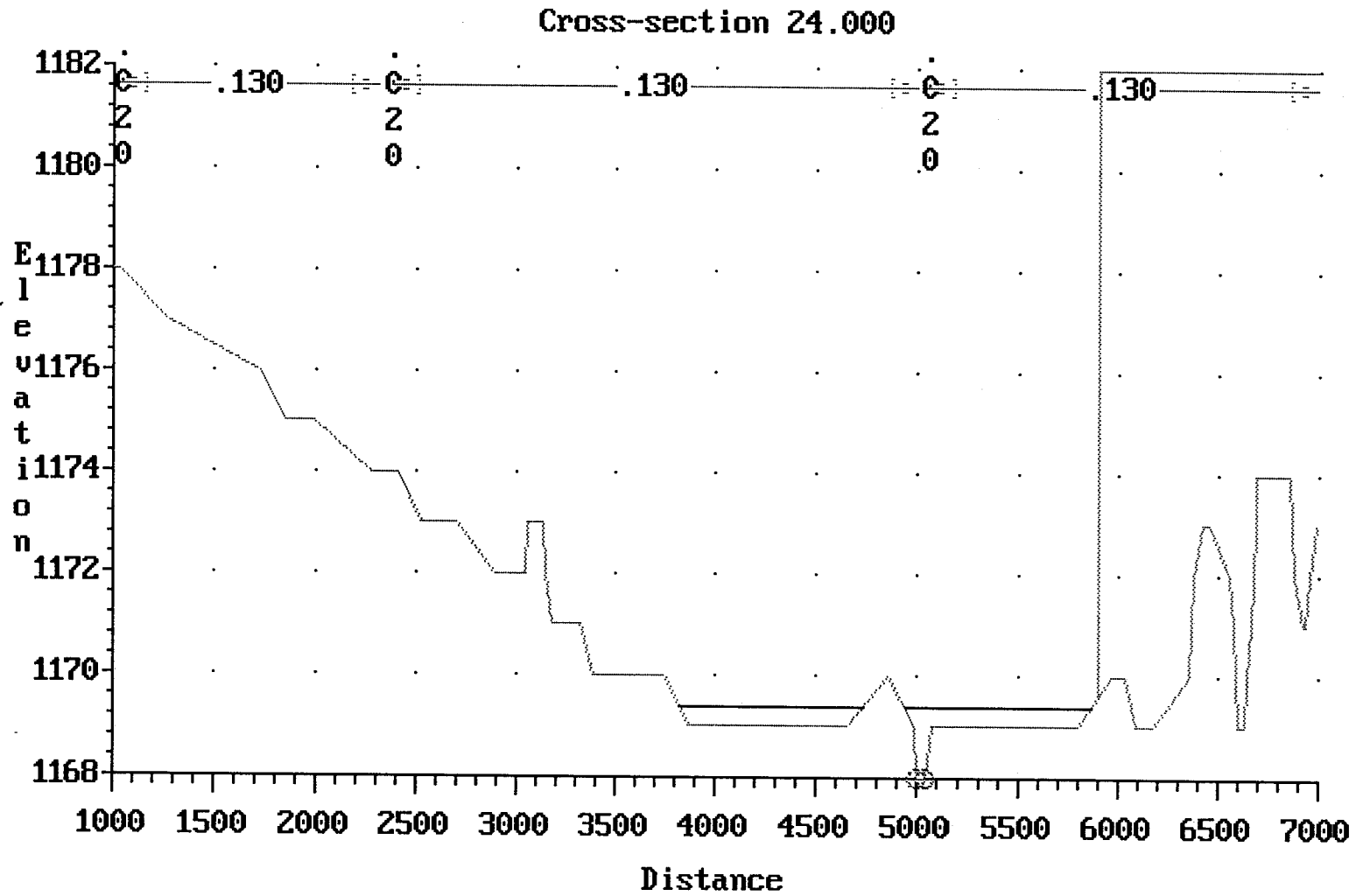


Figure 101 Main Channel HEC-2 Run
Cross-Section 24

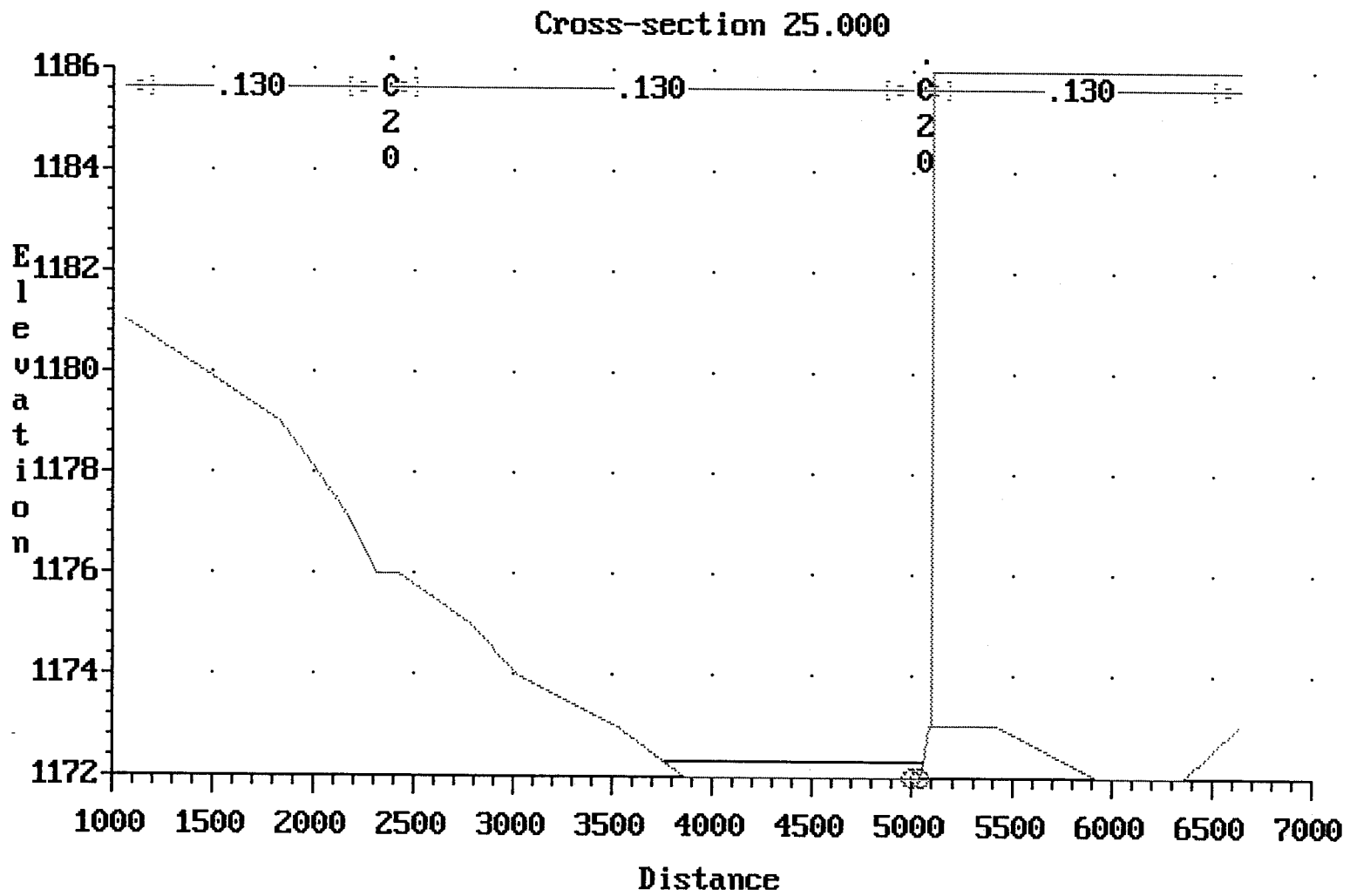


Figure 102 Main Channel HEC-2 Run
Cross-Section 25

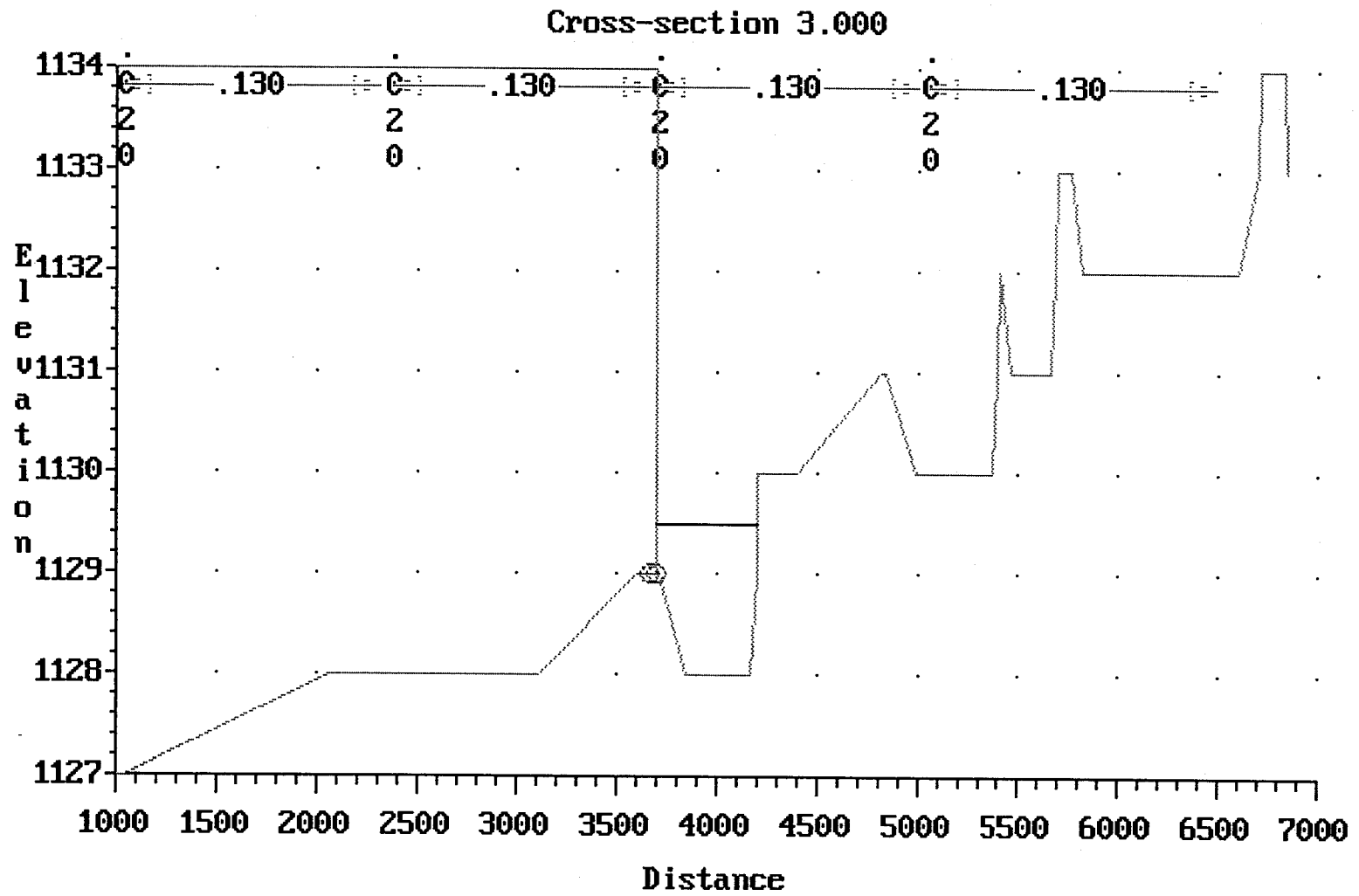


Figure 103 Lower 11th Ave HEC-2 Run
Cross-Section 3

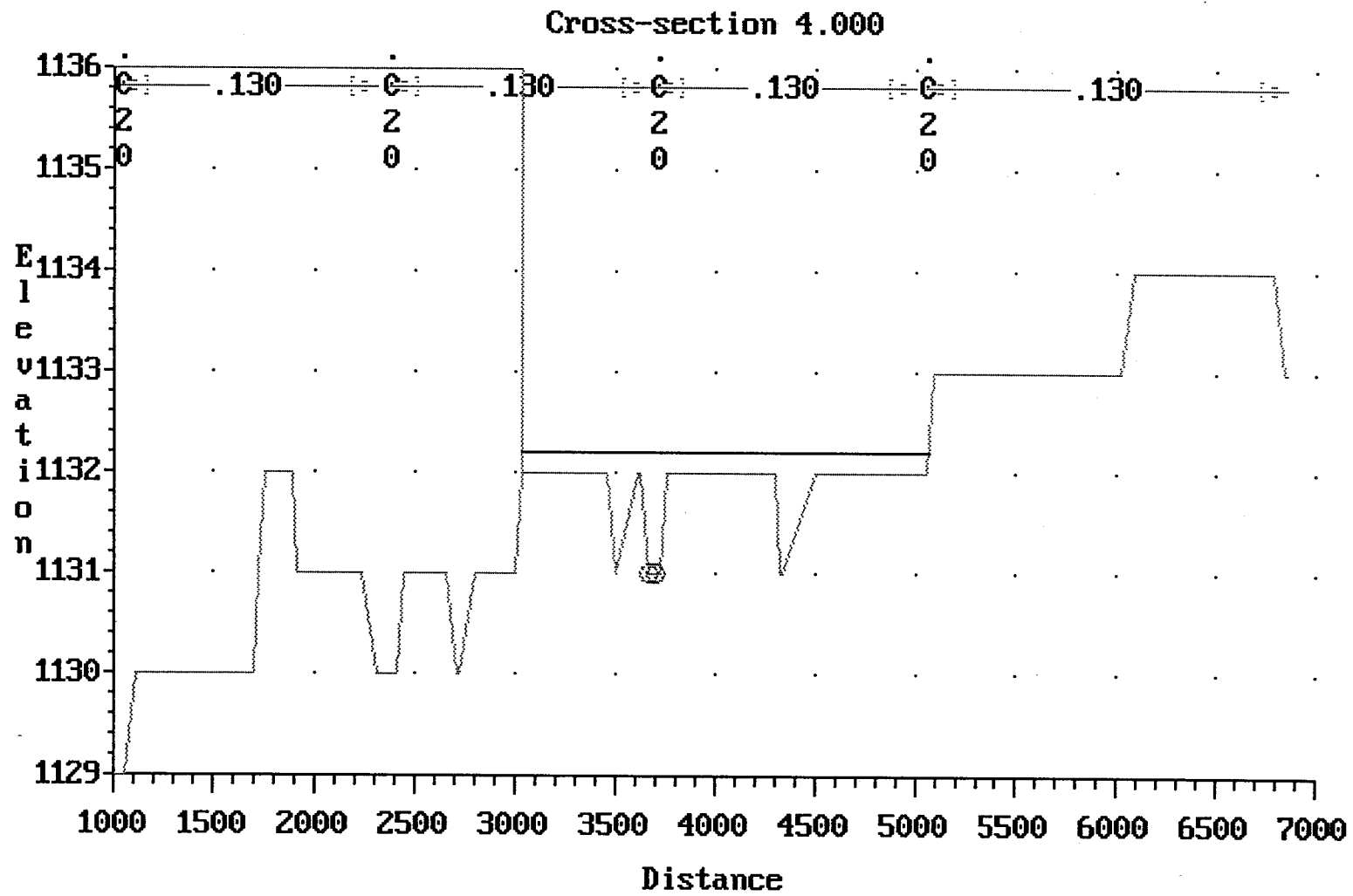


Figure 104 Lower 11th Ave HEC-2 Run
Cross-Section 4

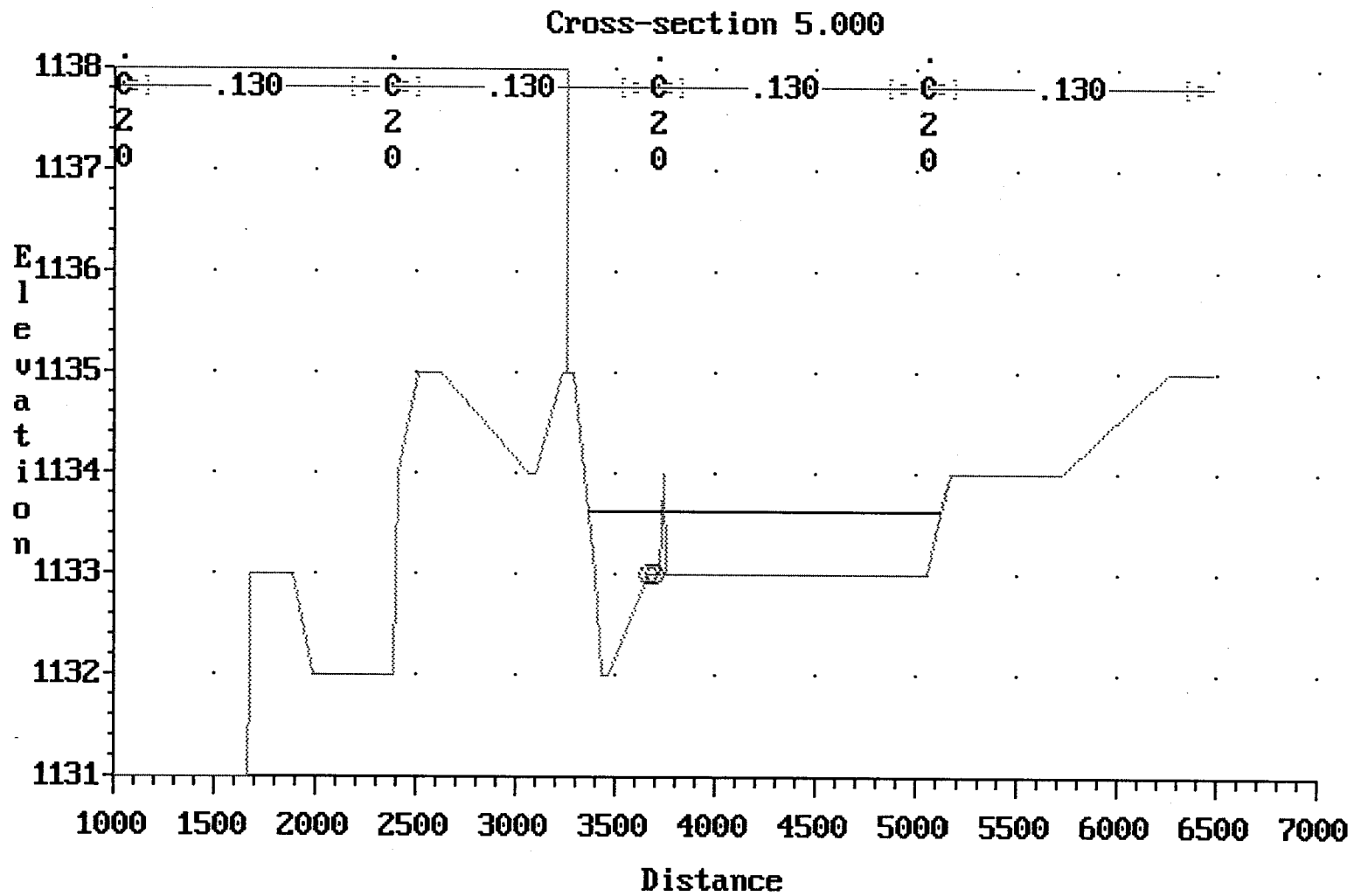


Figure 105 Lower 11th Ave HEC-2 Run
Cross-Section 5

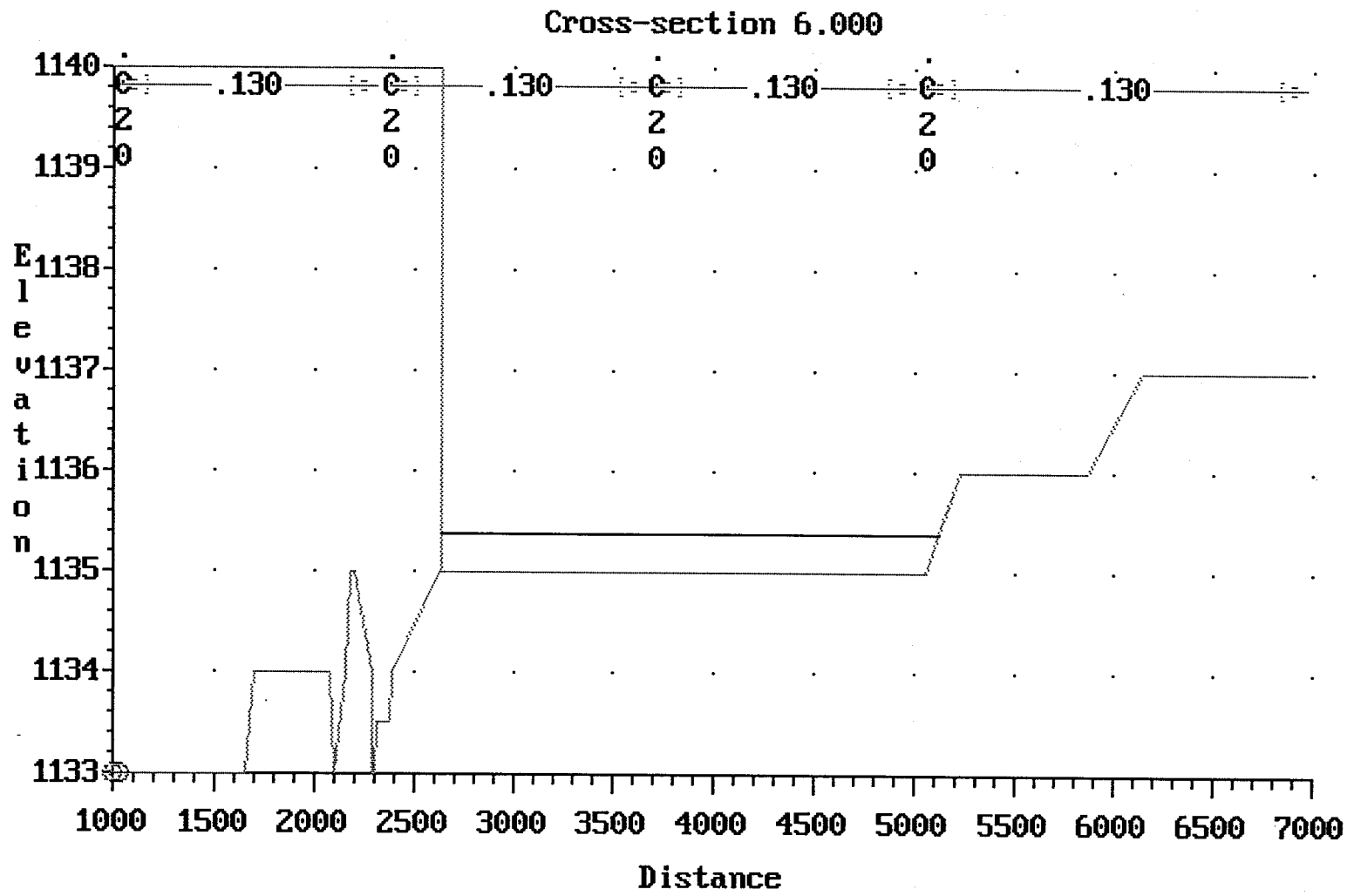


Figure 106 Lower 11th Ave HEC-2 Run
Cross-Section 6

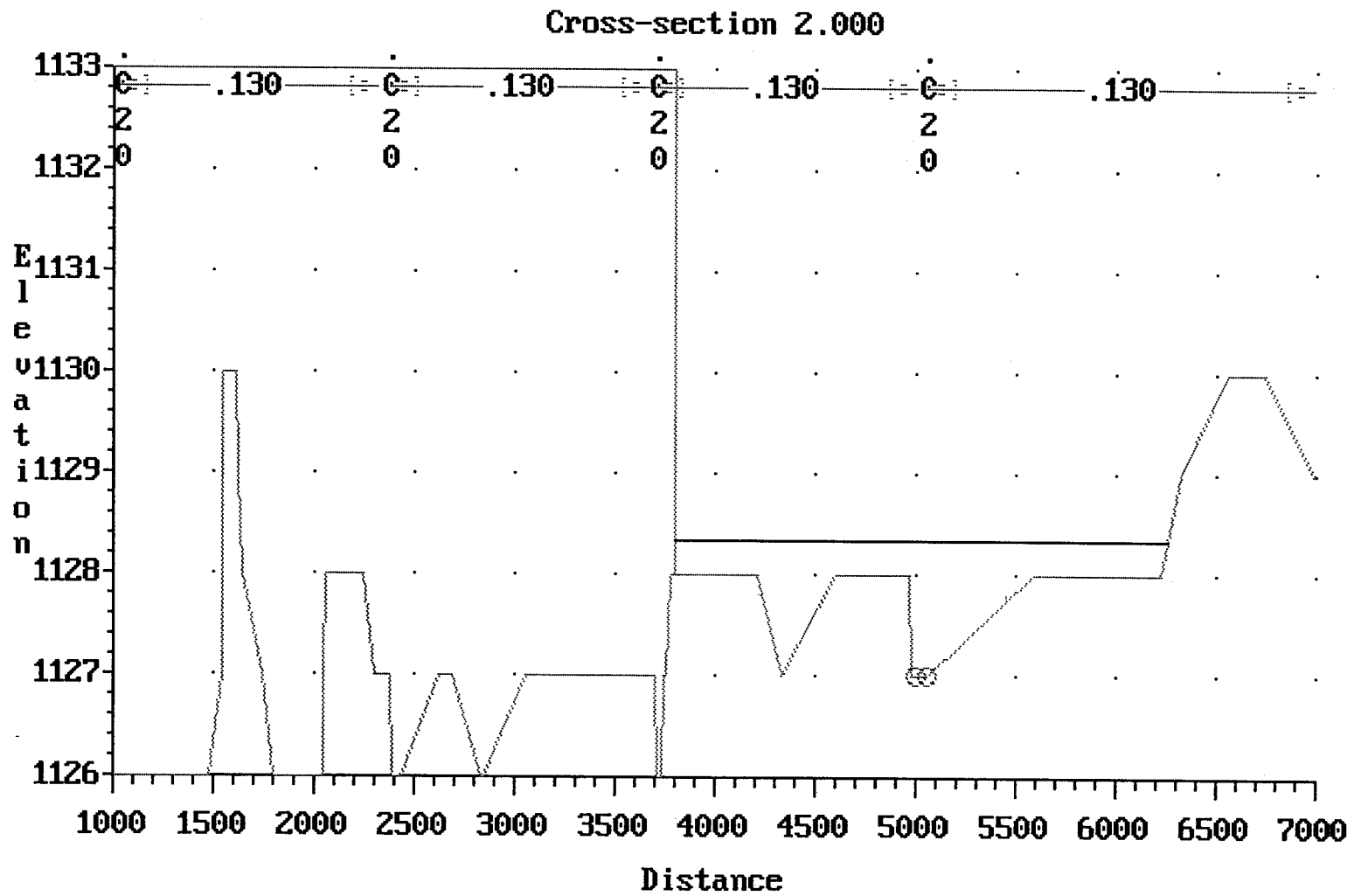


Figure 107 Lower 15th Ave HEC-2 Run
Cross-Section 2

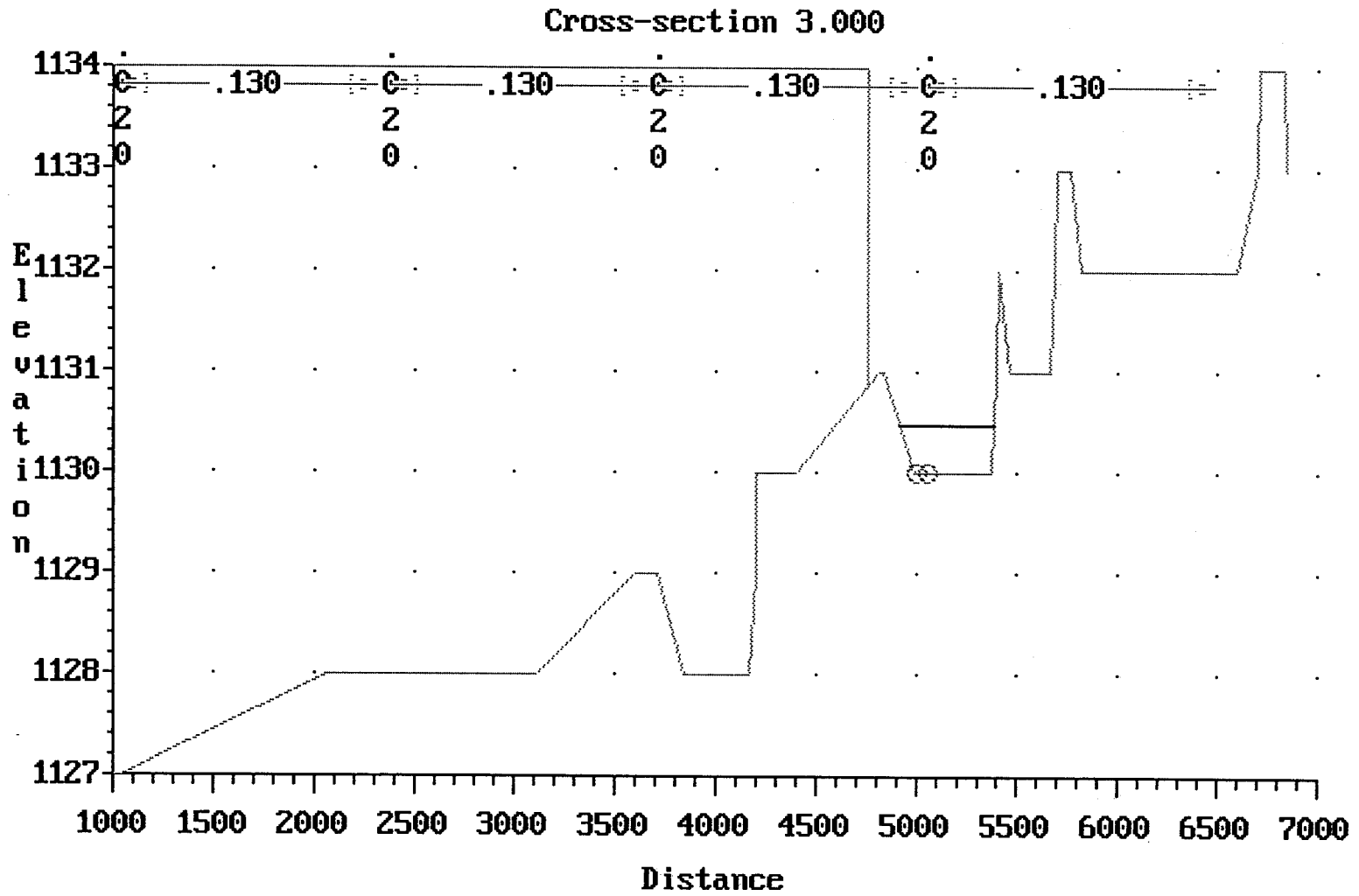


Figure 108 Lower 15th Ave HEC-2 Run
Cross-Section 3

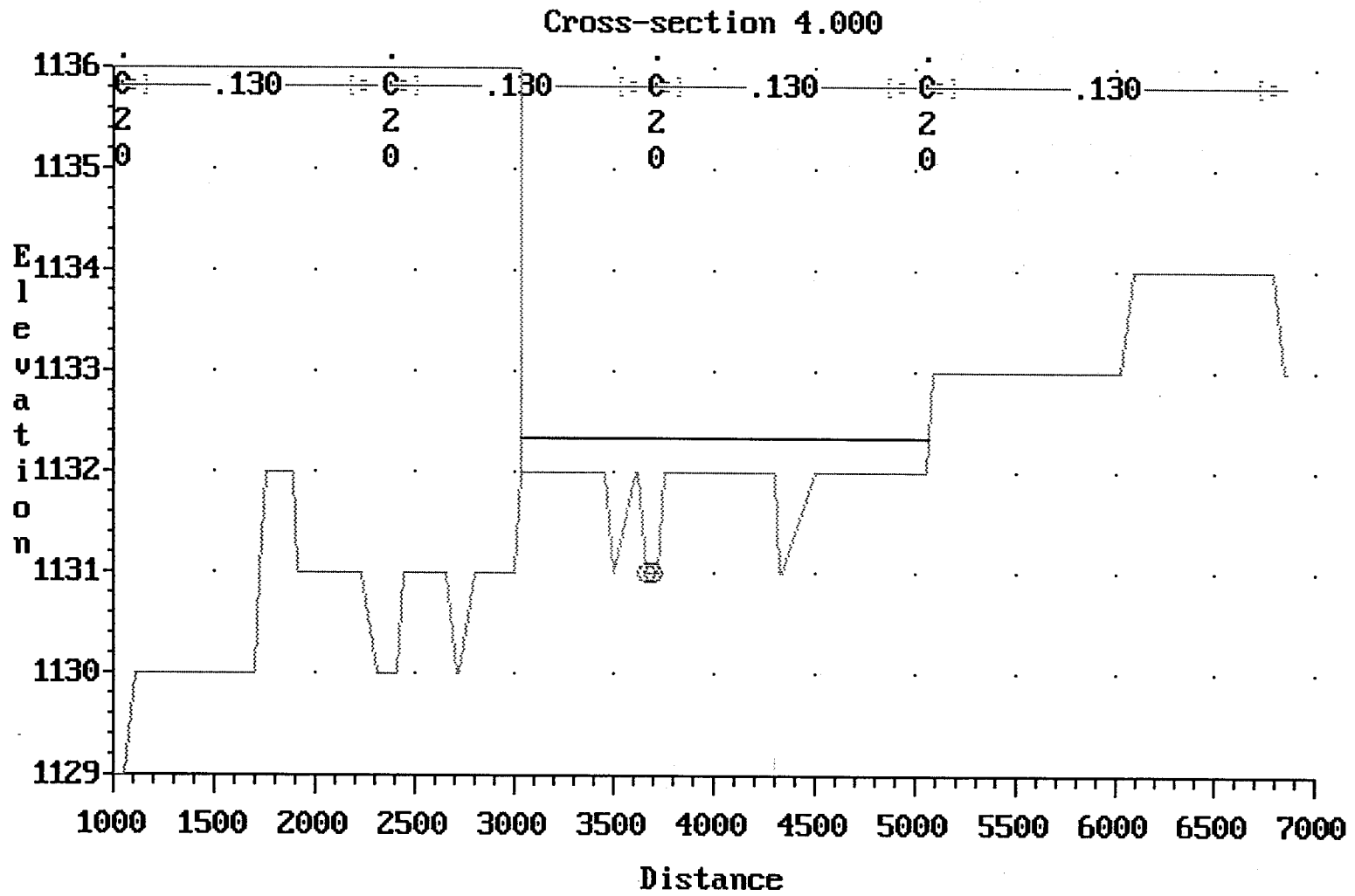


Figure 109 Lower 15th Ave HEC-2 Run
Cross-Section 4

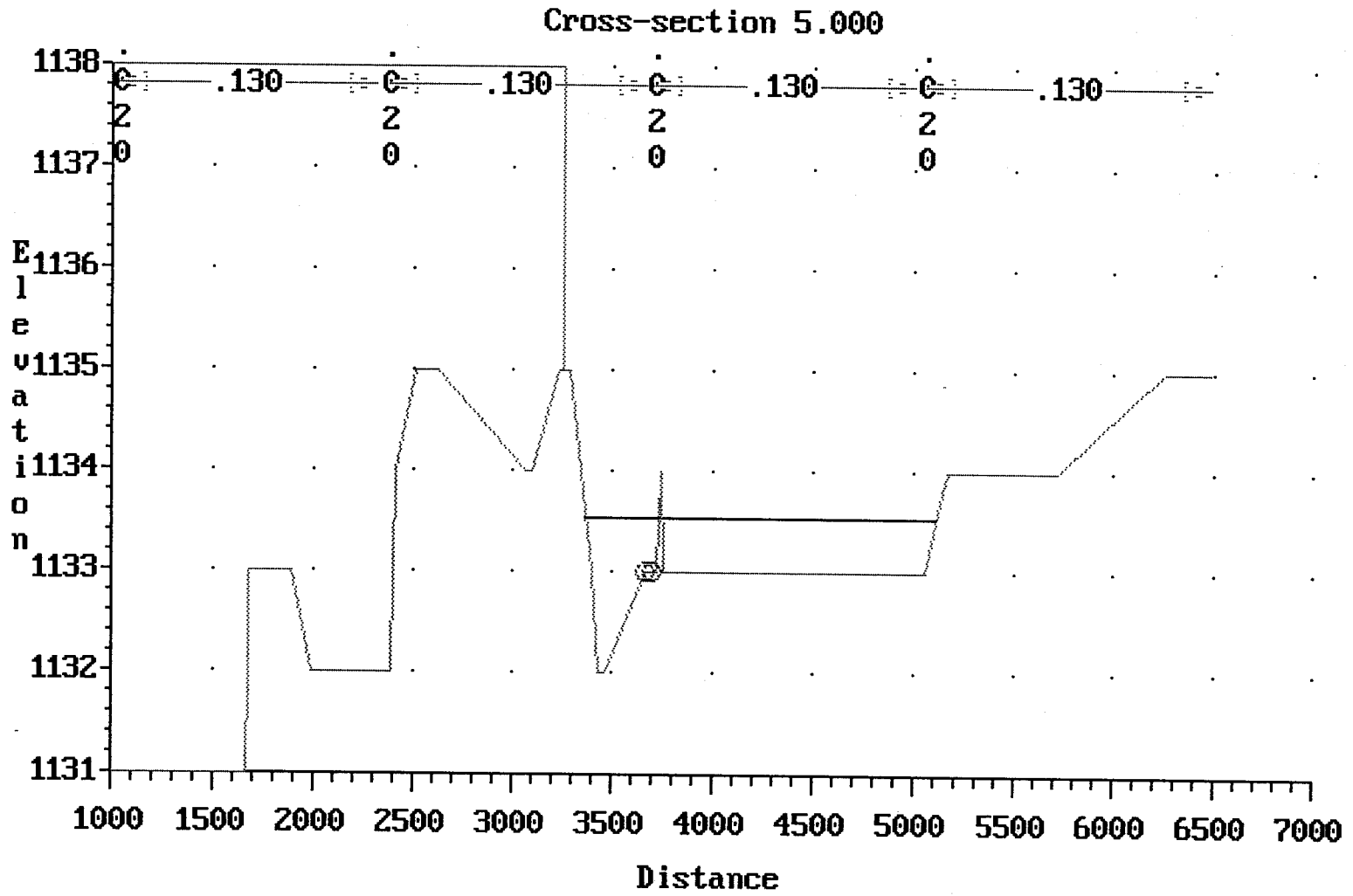


Figure 110 Lower 15th Ave HEC-2 Run
Cross-Section 5

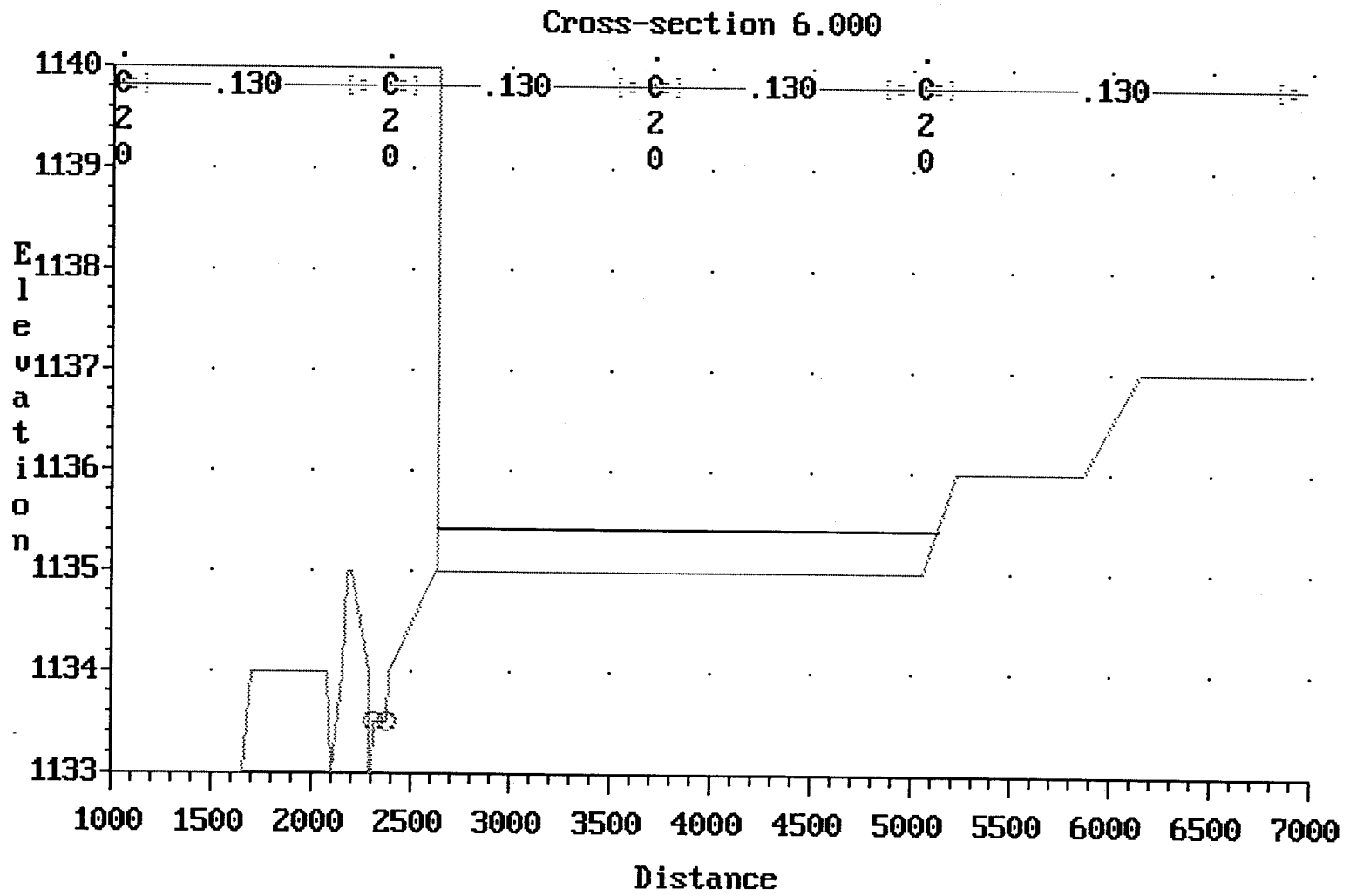


Figure 111 Lower 15th Ave HEC-2 Run
Cross-Section 6

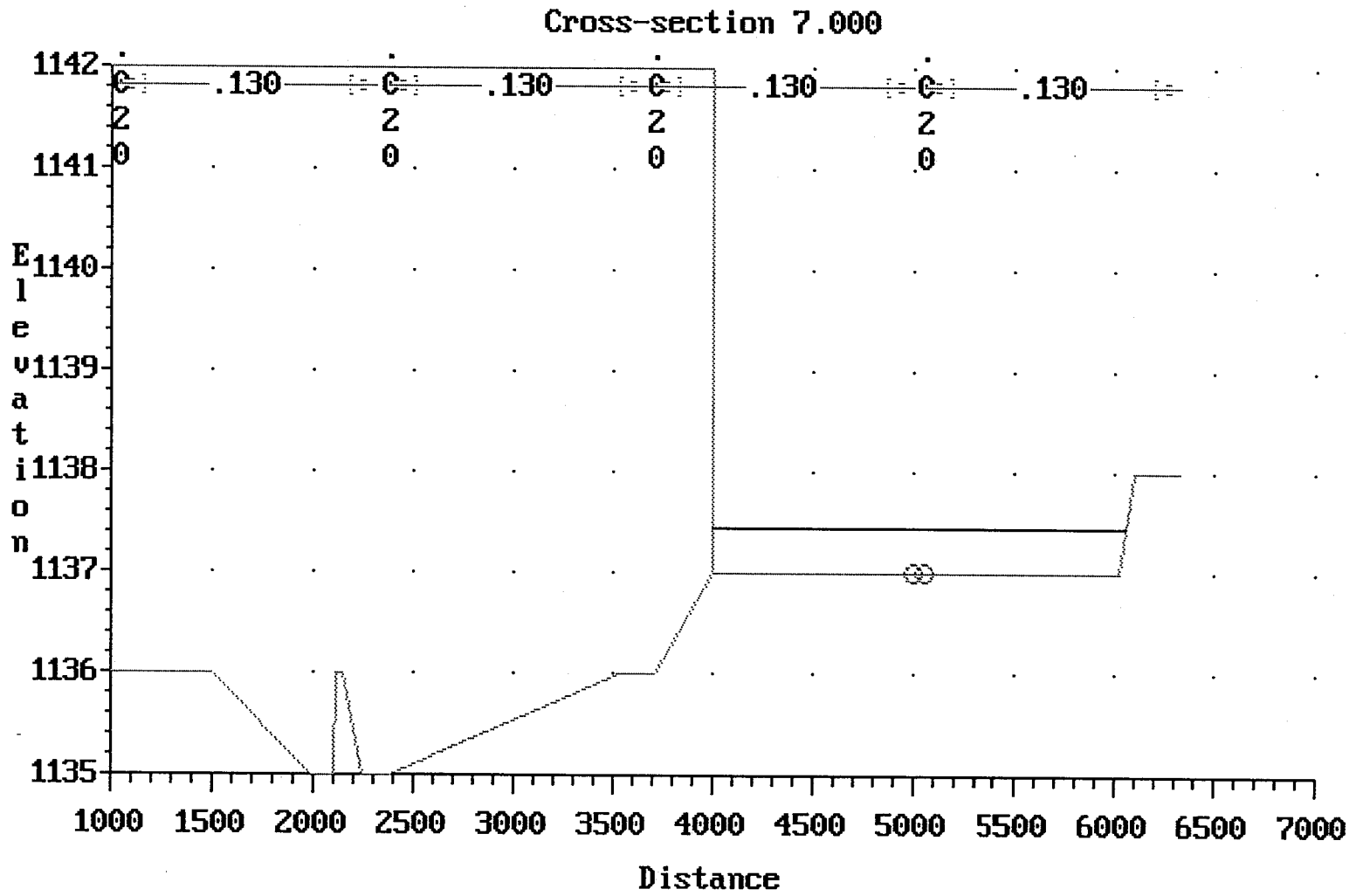


Figure 112 Lower 15th Ave HEC-2 Run
Cross-Section 7

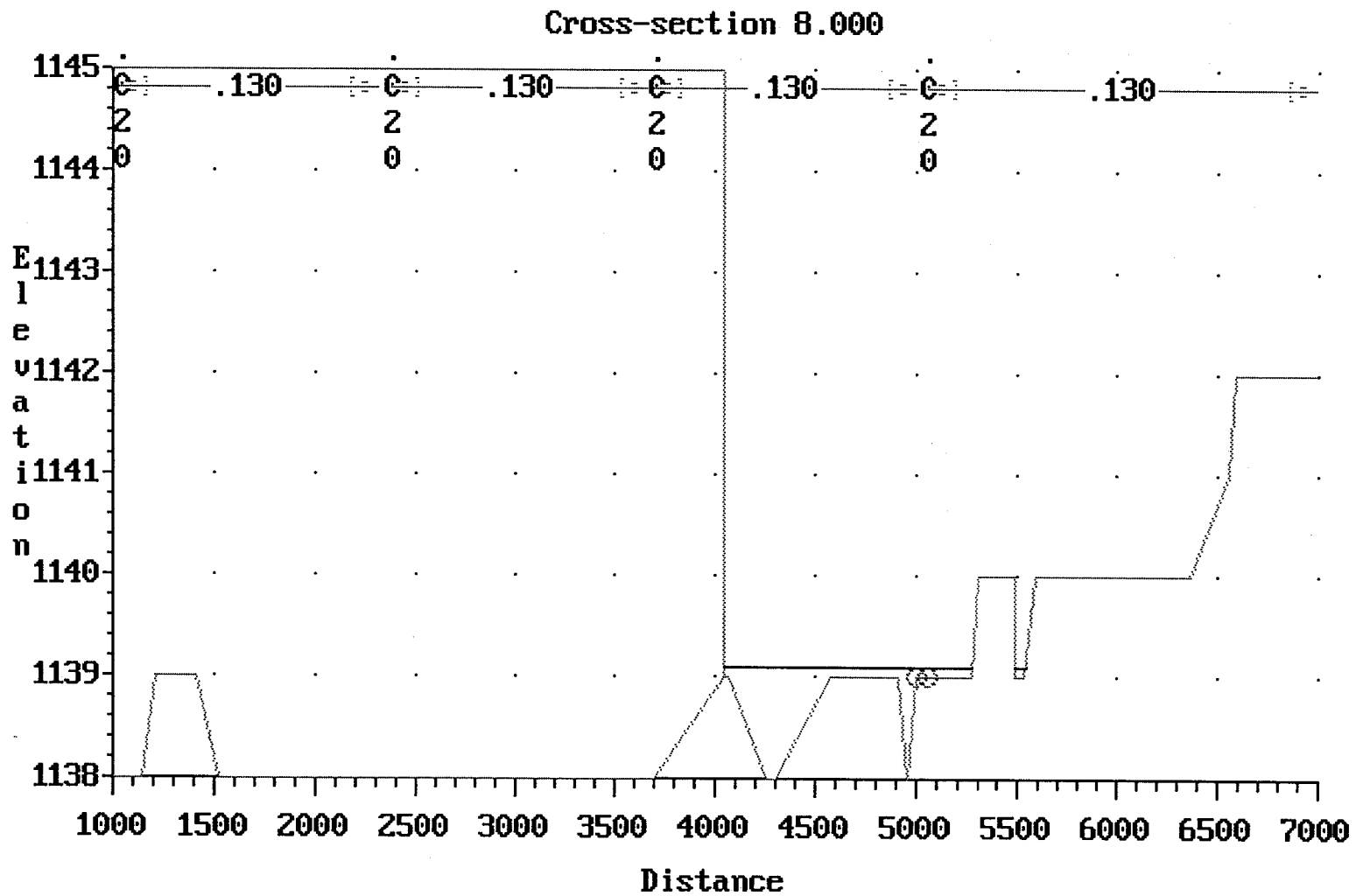


Figure 113 Lower 15th Ave HEC-2 Run
Cross-Section 8

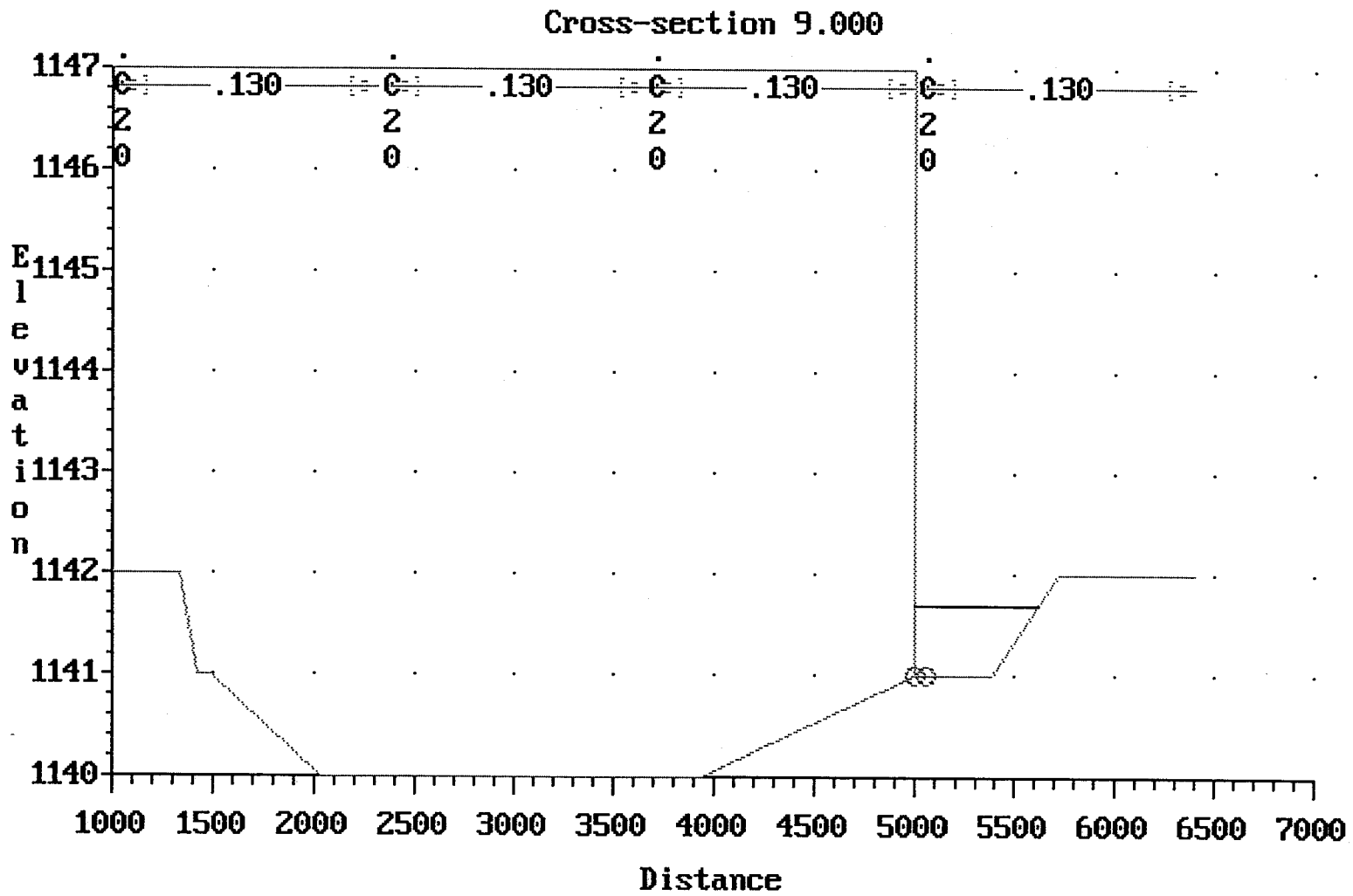


Figure 114 Lower 15th Ave HEC-2 Run
Cross-Section 9

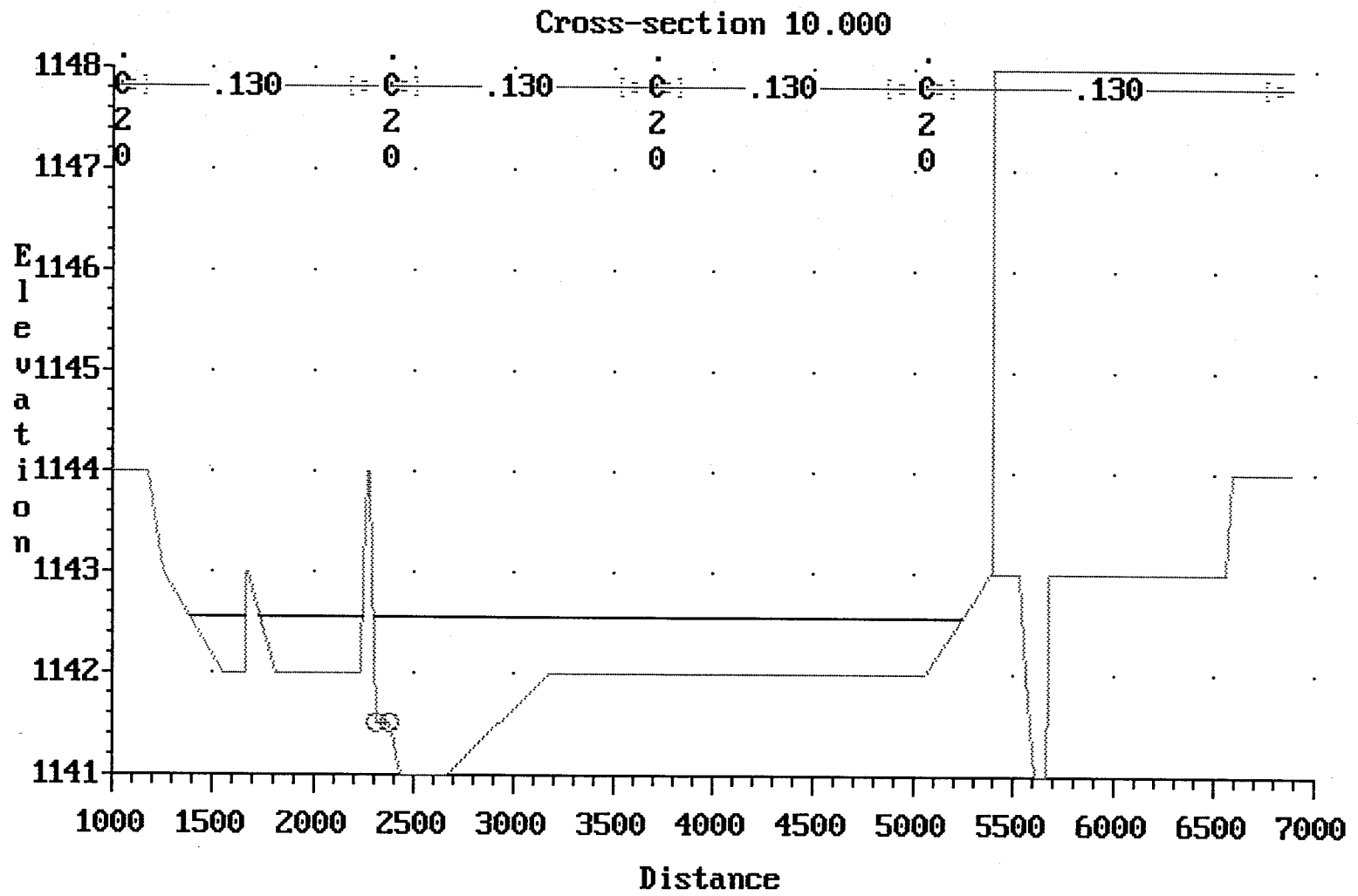


Figure 115 Lower 15th Ave HEC-2 Run
Cross-Section 10

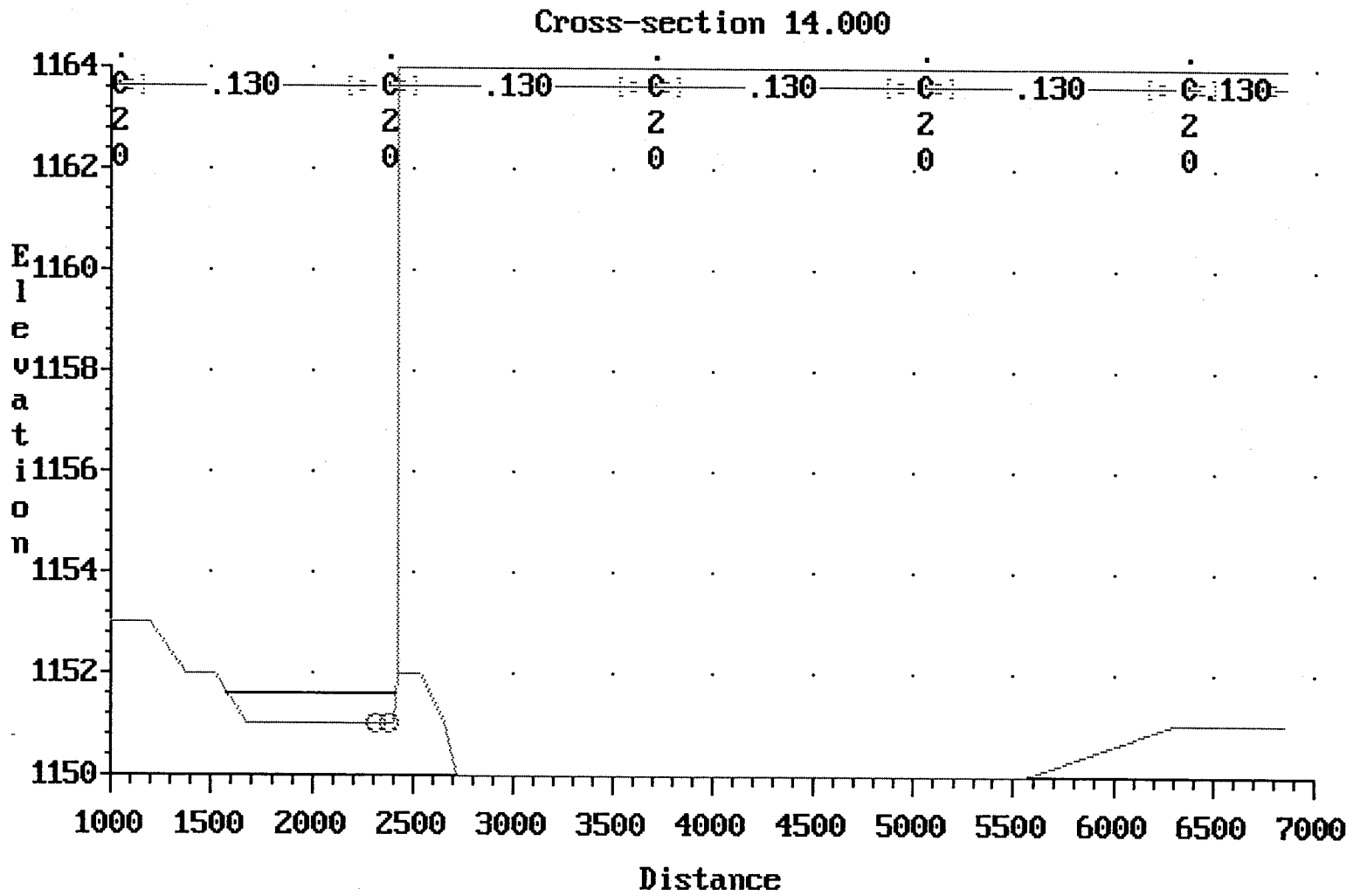


Figure 116 Upper 7th Ave HEC-2 Run
Cross-Section 14

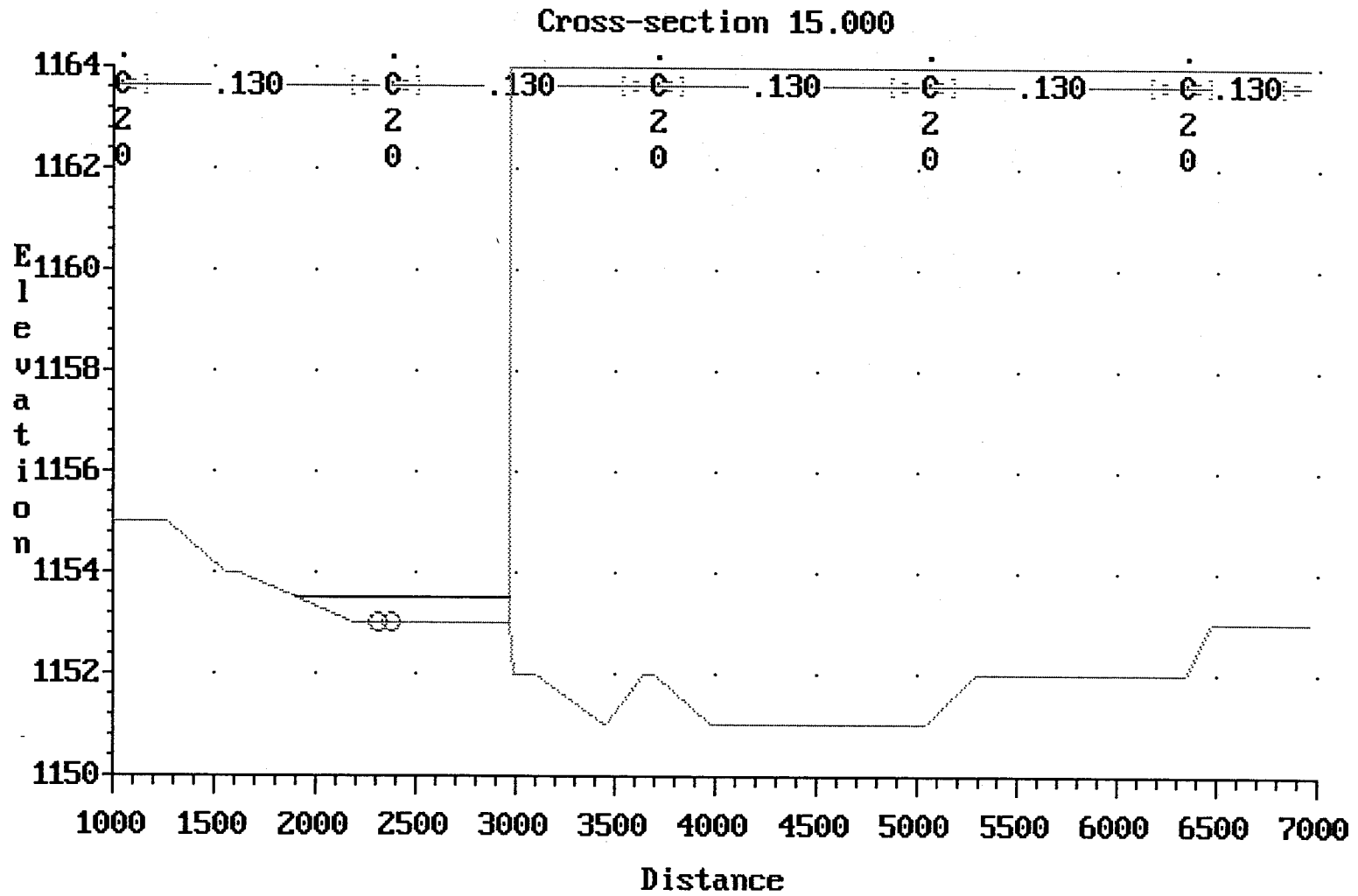


Figure 117 Upper 7th Ave HEC-2 Run
Cross-Section 15

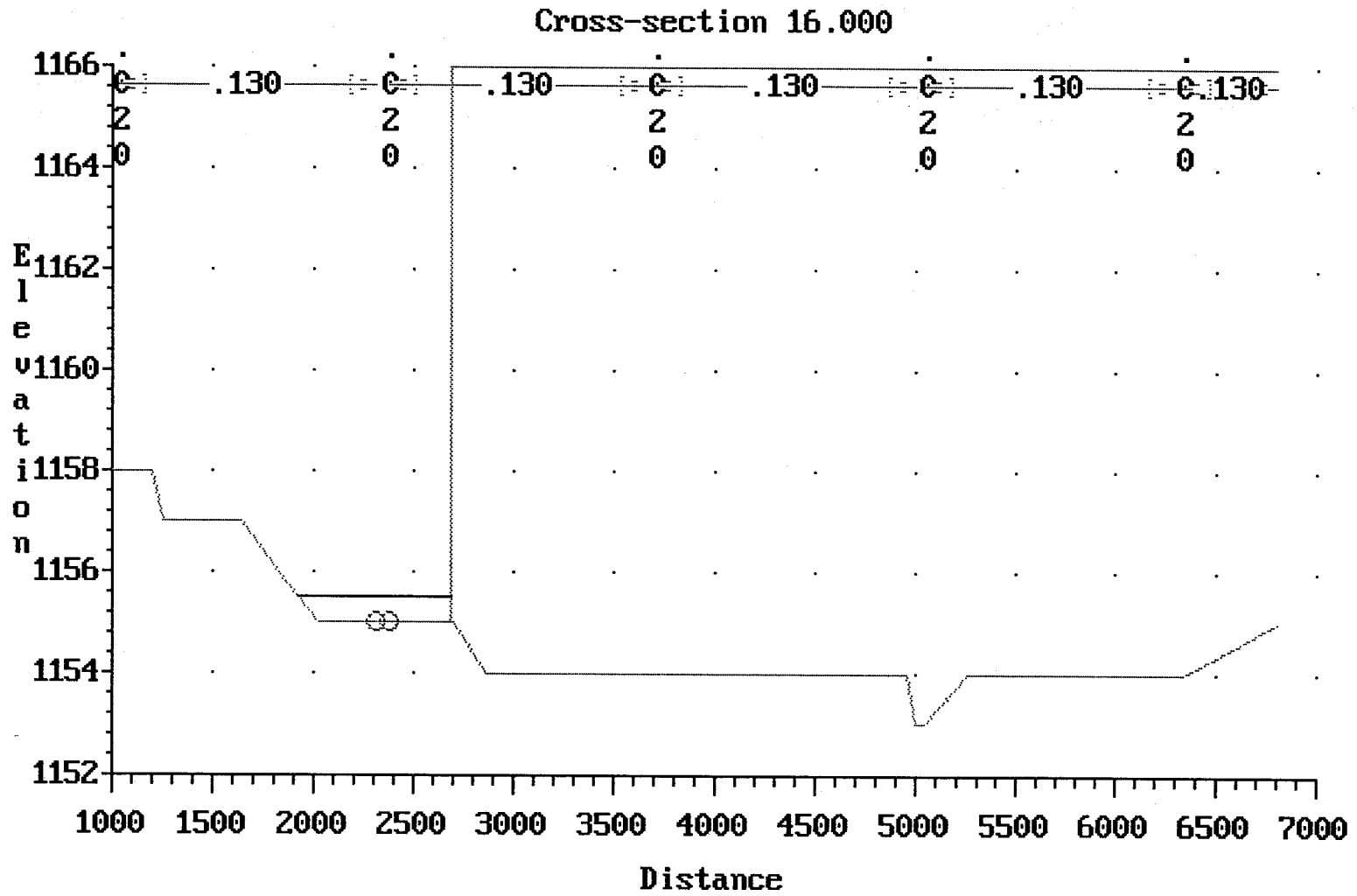


Figure 118 Upper 7th Ave HEC-2 Run
Cross-Section 16

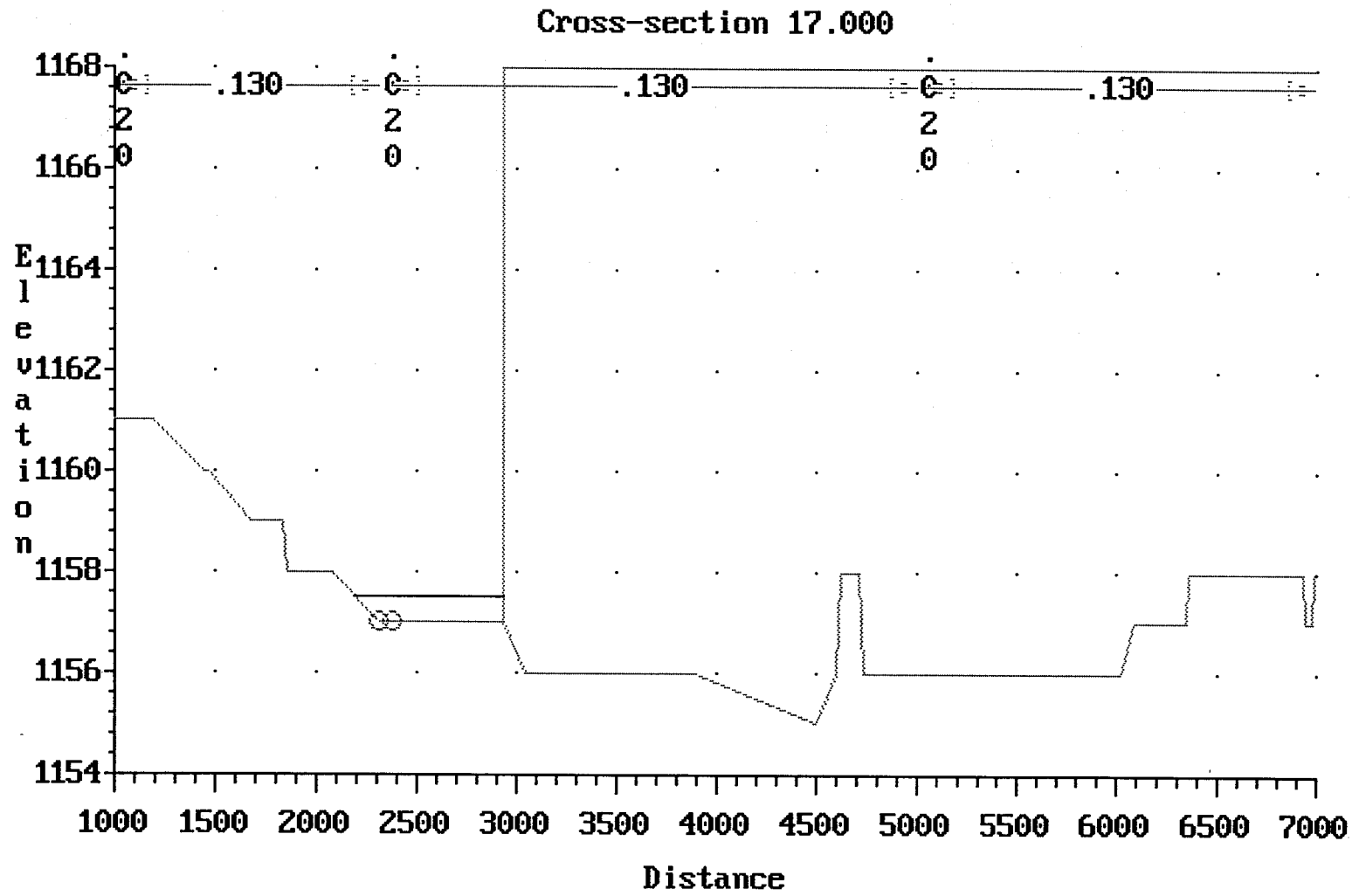


Figure 119 Upper 7th Ave HEC-2 Run
Cross-Section 17

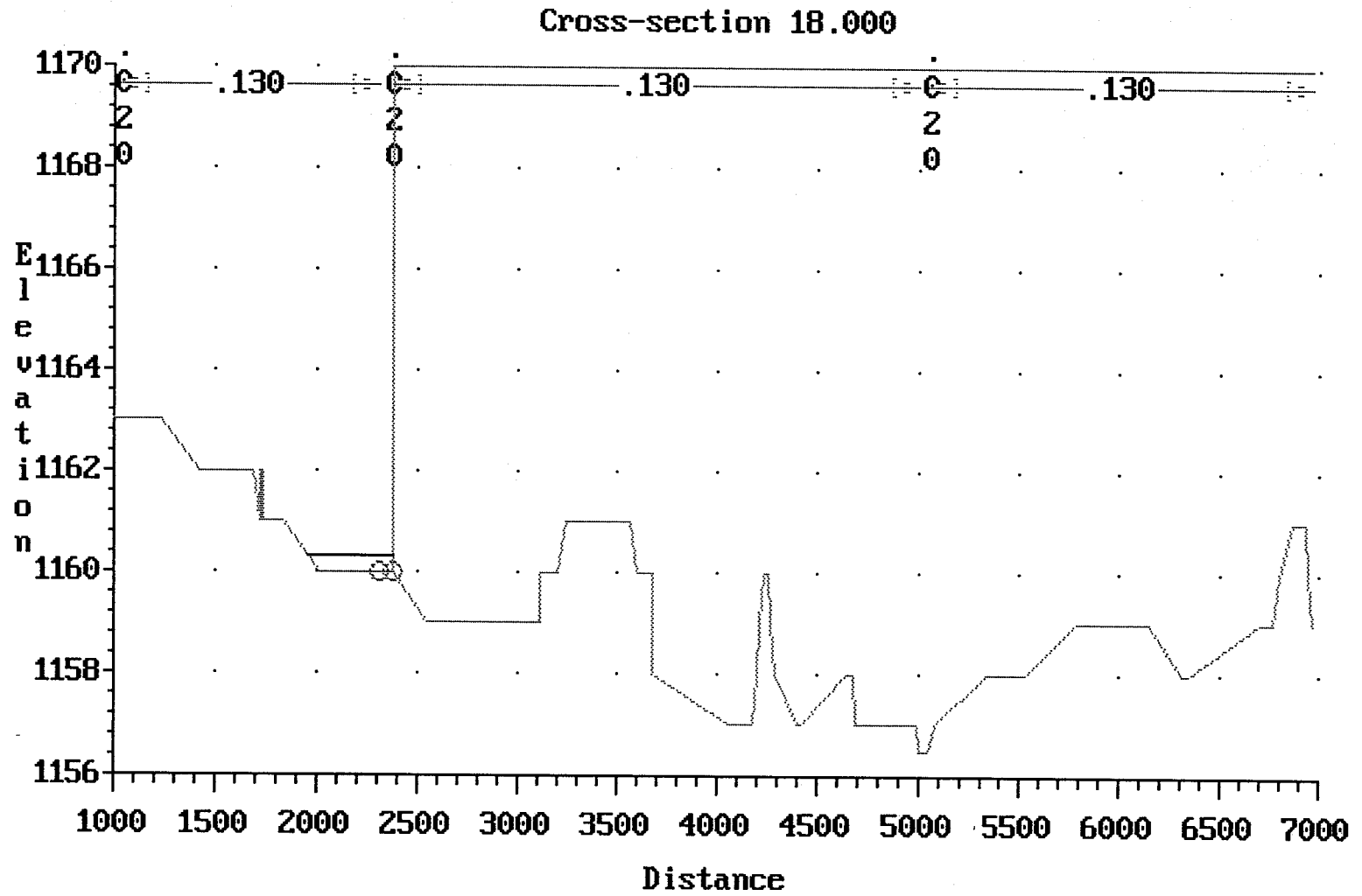


Figure 120 Upper 7th Ave HEC-2 Run
Cross-Section 18

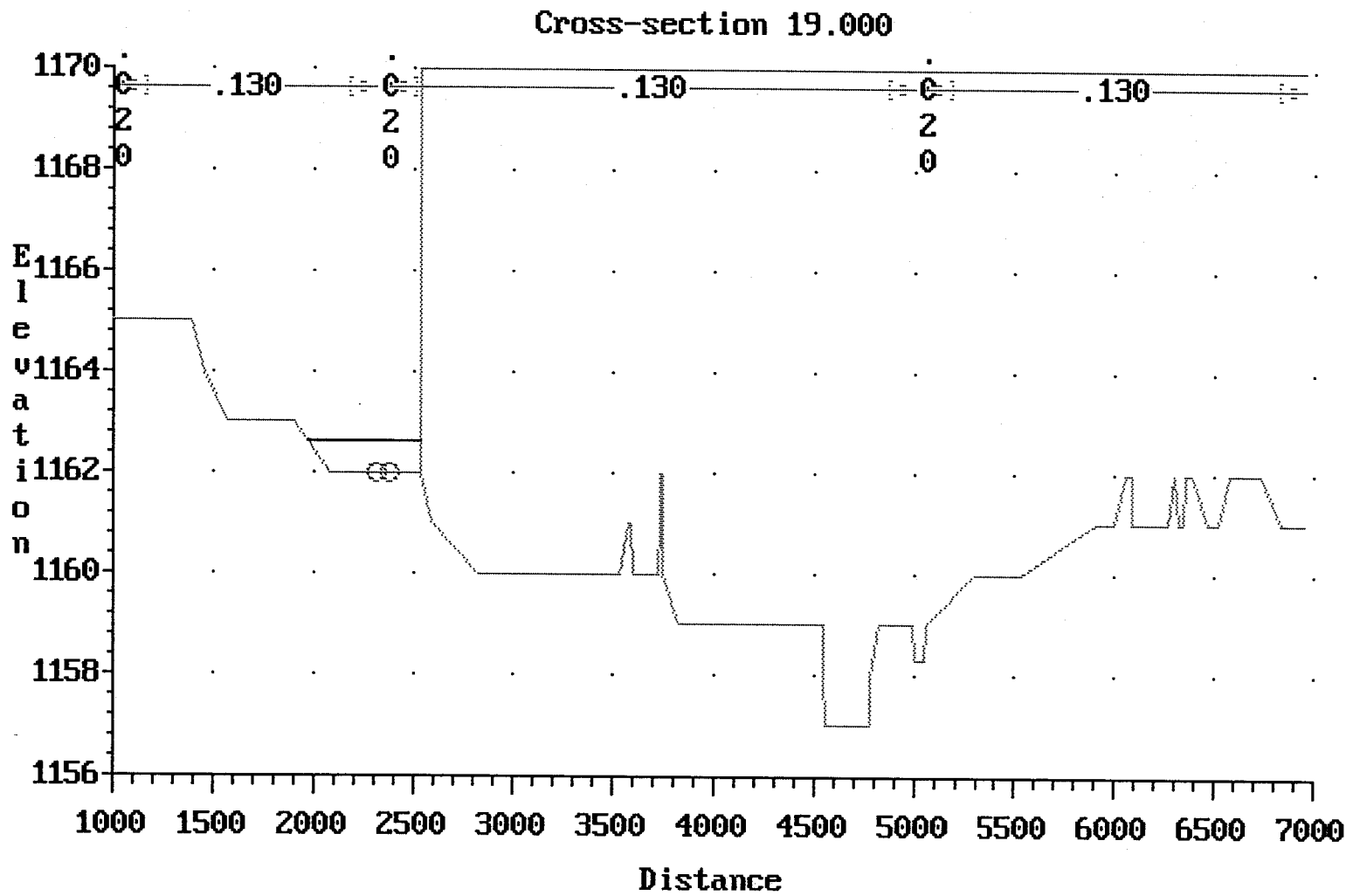


Figure 121 Upper 7th Ave HEC-2 Run
Cross-Section 19

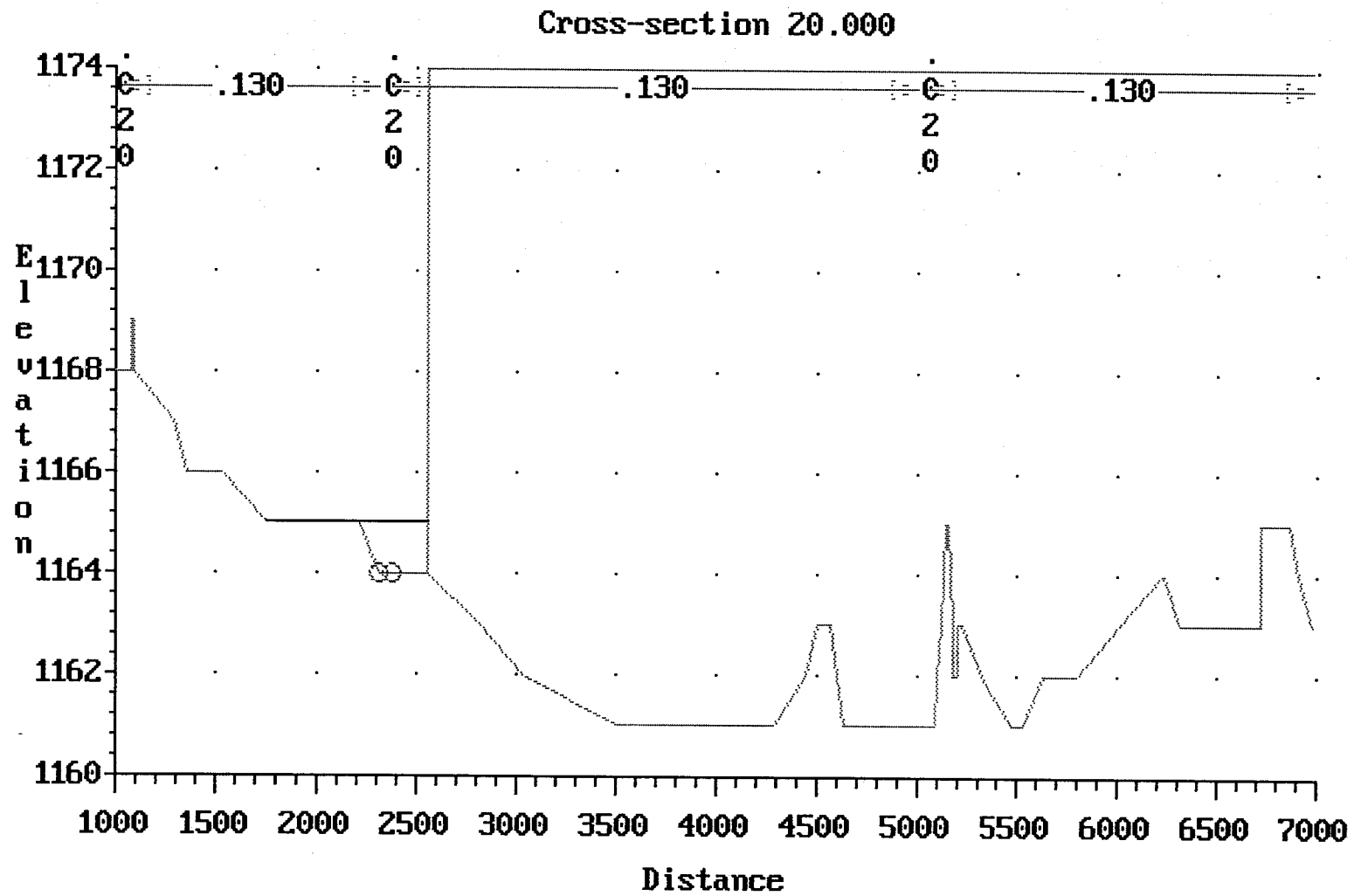


Figure 122 Upper 7th Ave HEC-2 Run
Cross-Section 20

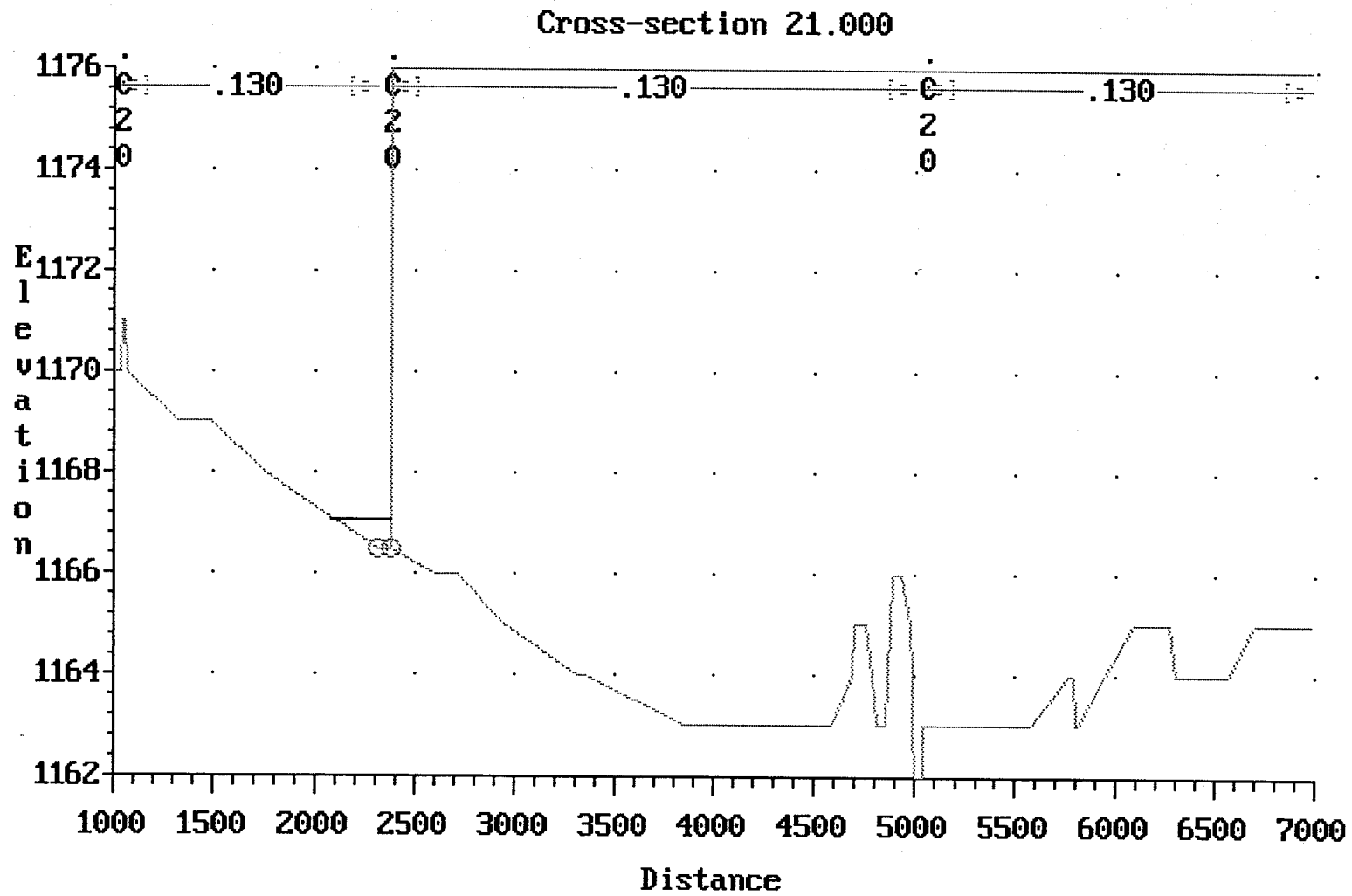


Figure 123 Upper 7th Ave HEC-2 Run
Cross-Section 21

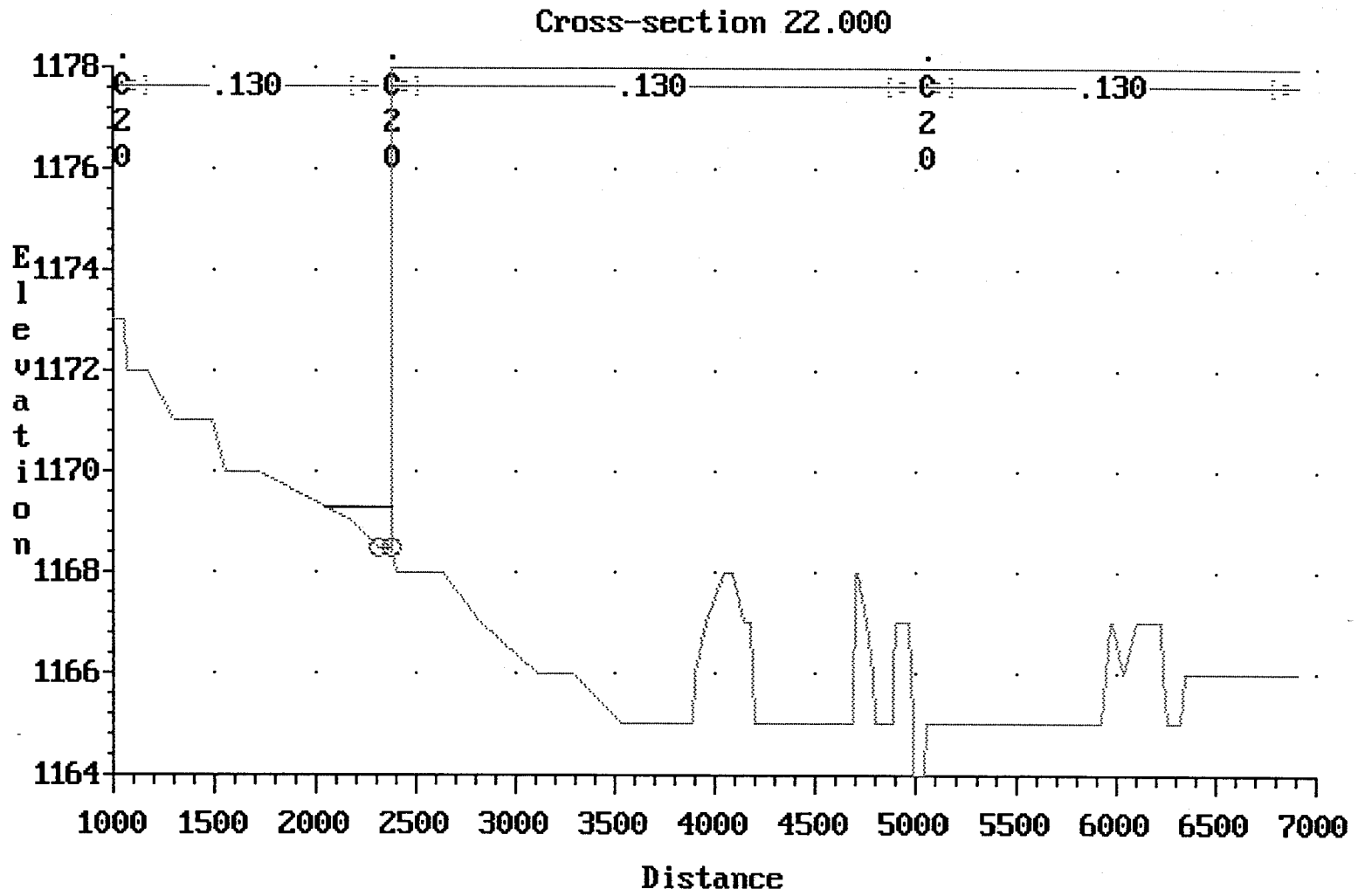


Figure 124 Upper 7th Ave HEC-2 Run
Cross-Section 22

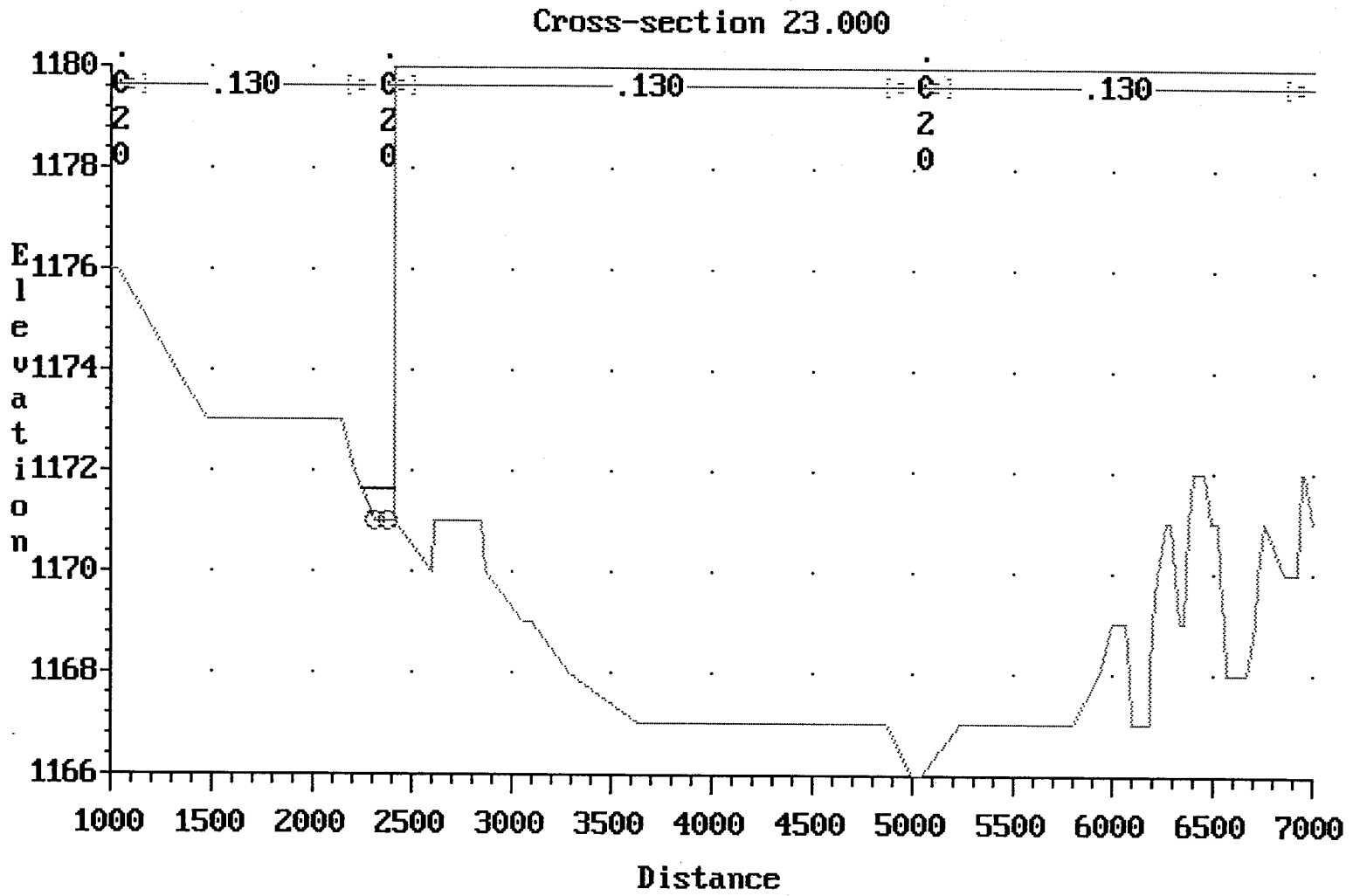


Figure 125 Upper 7th Ave HEC-2 Run
Cross-Section 23

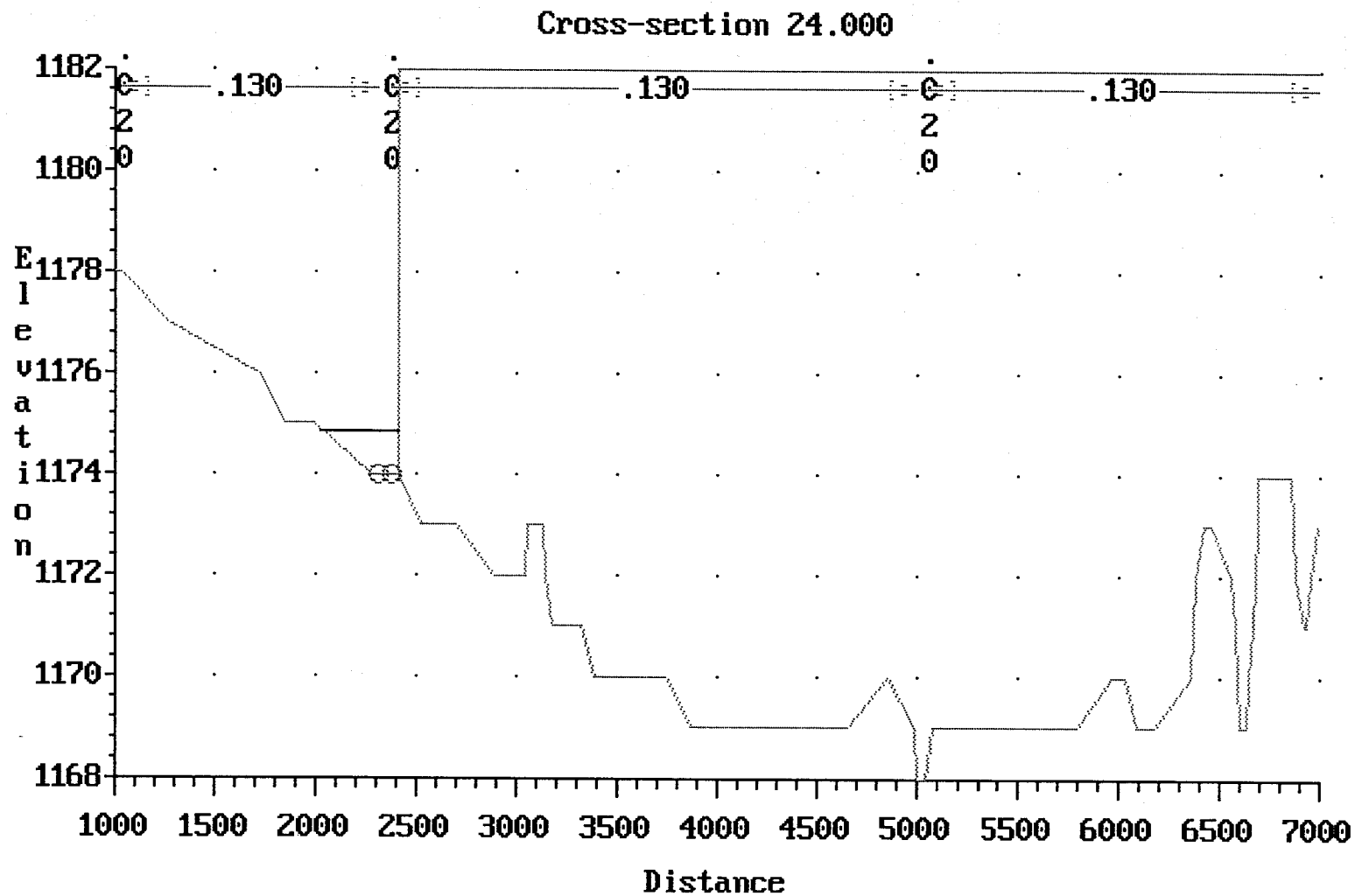


Figure 126 Upper 7th Ave HEC-2 Run
Cross-Section 24

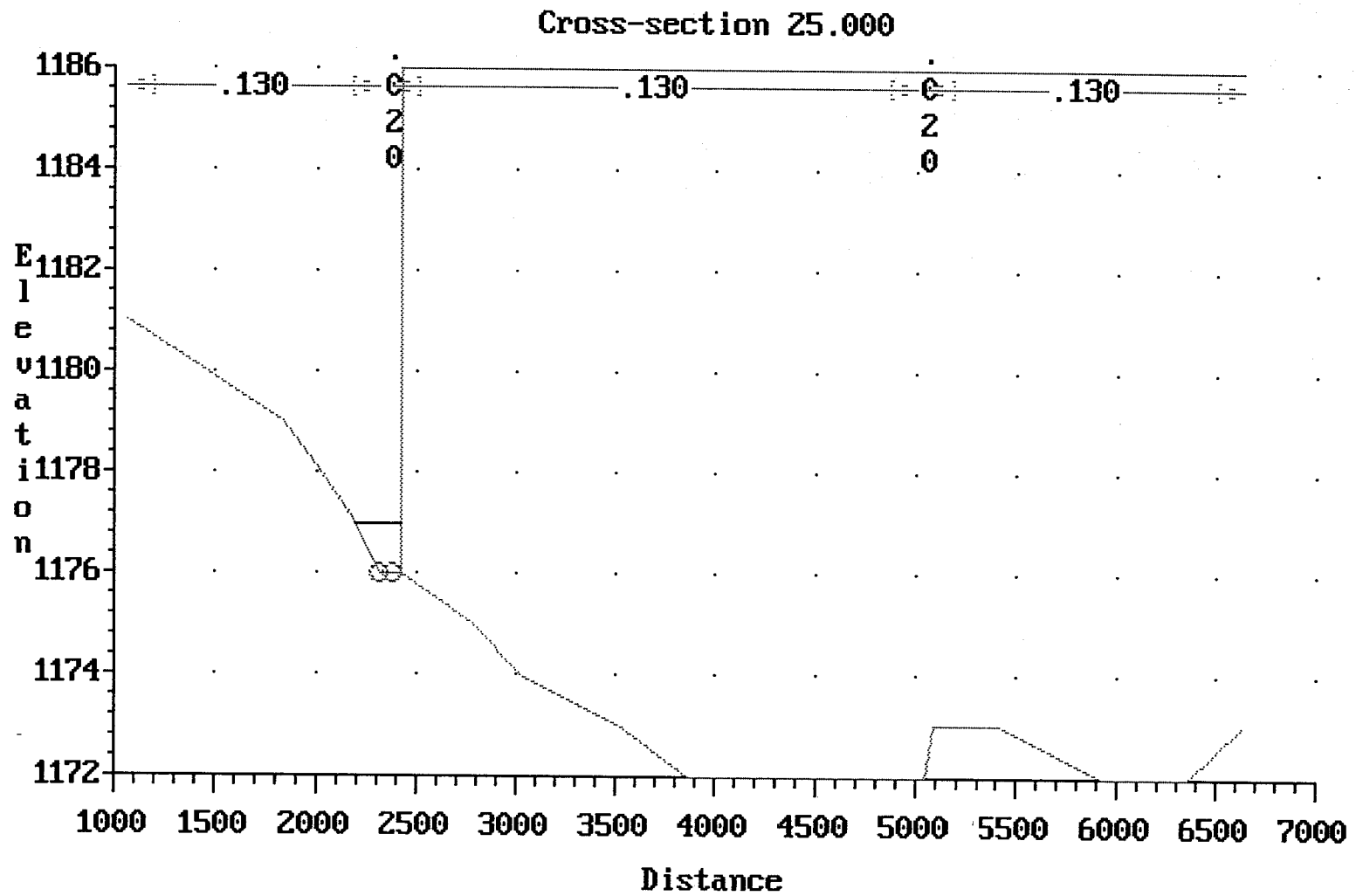


Figure 127 Upper 7th Ave HEC-2 Run
Cross-Section 25

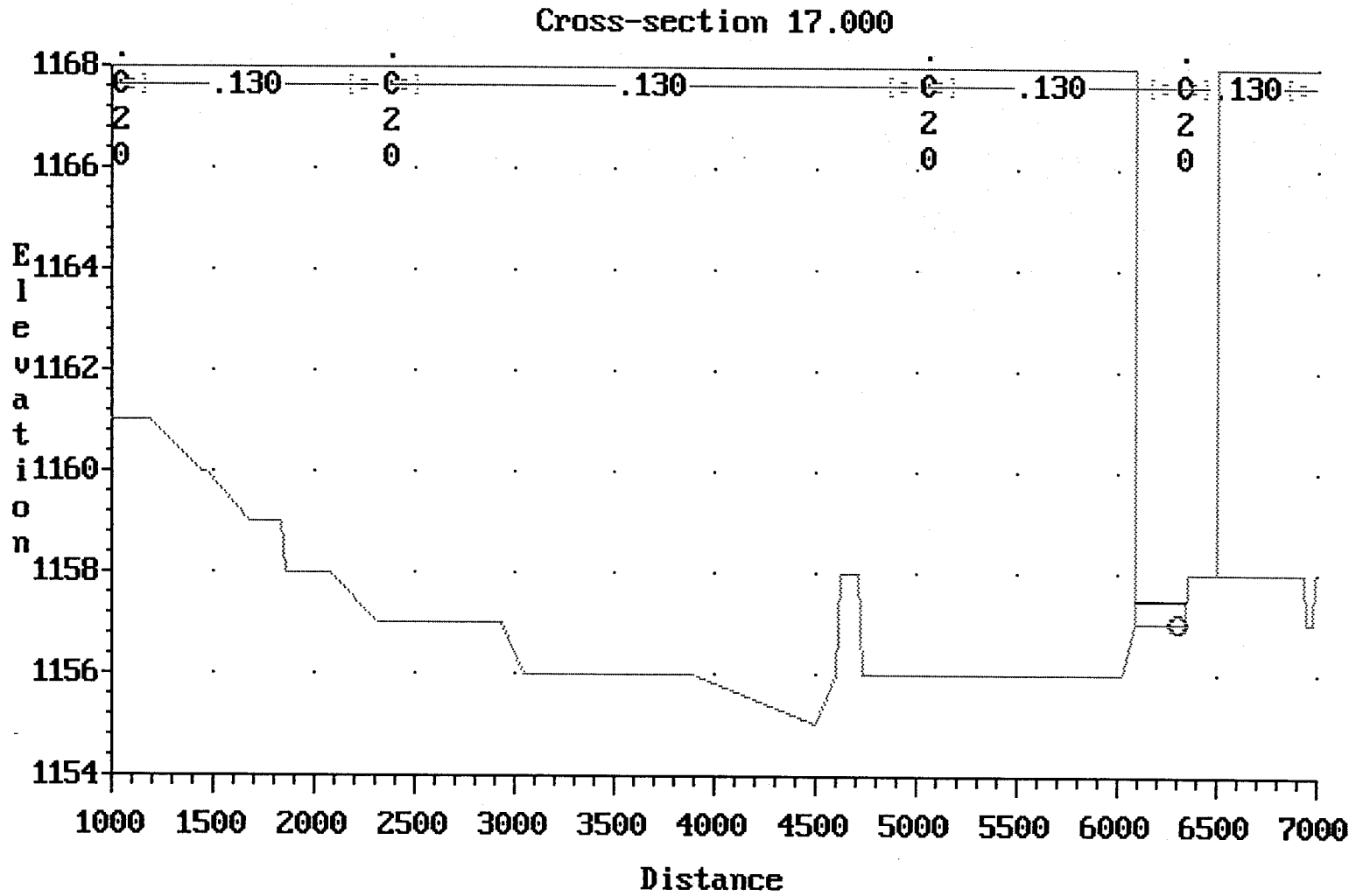


Figure 128 Upper 17th Ave HEC-2 Run
Cross-Section 17

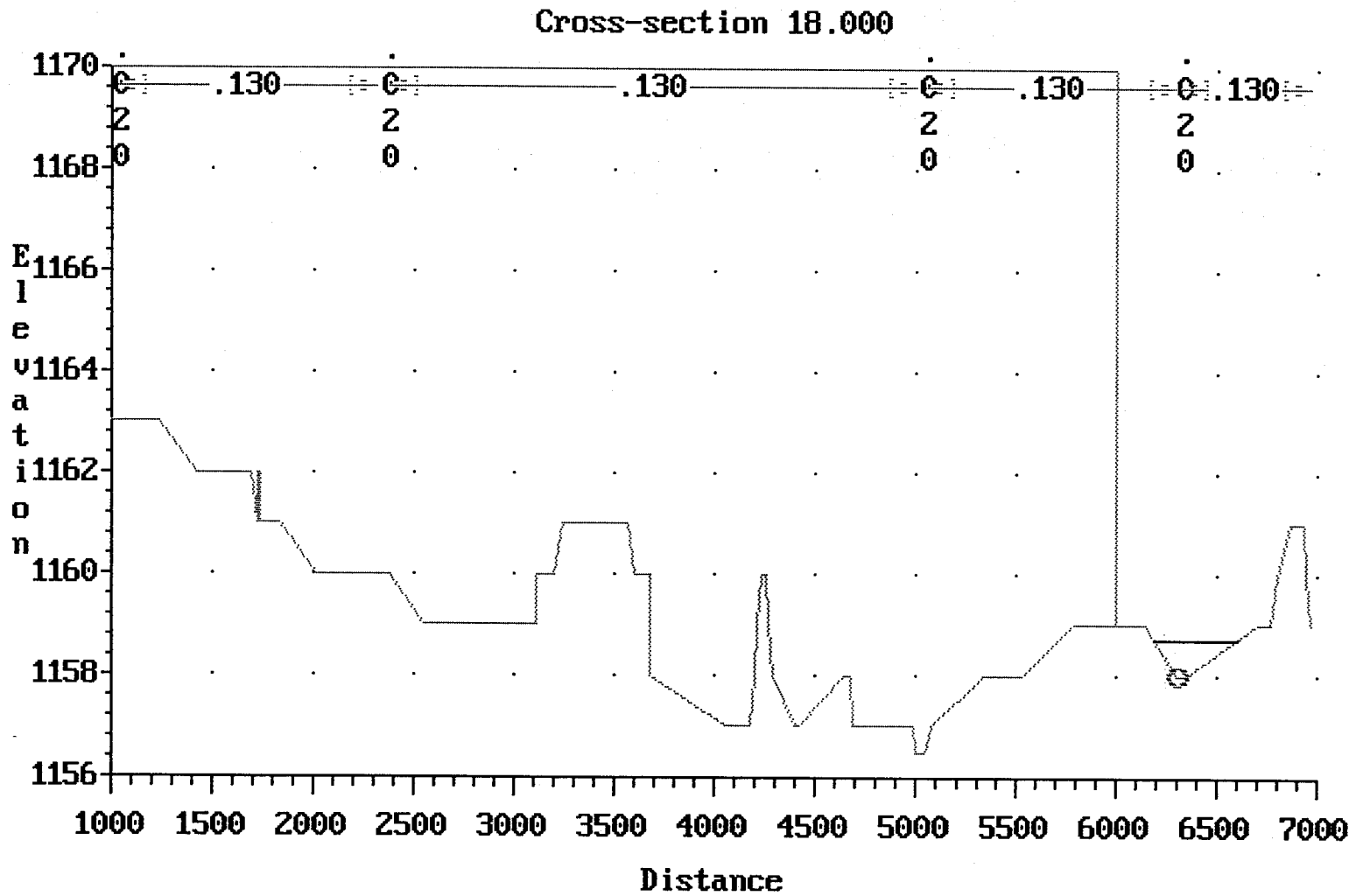


Figure 129 Upper 17th Ave HEC-2 Run
Cross-Section 18

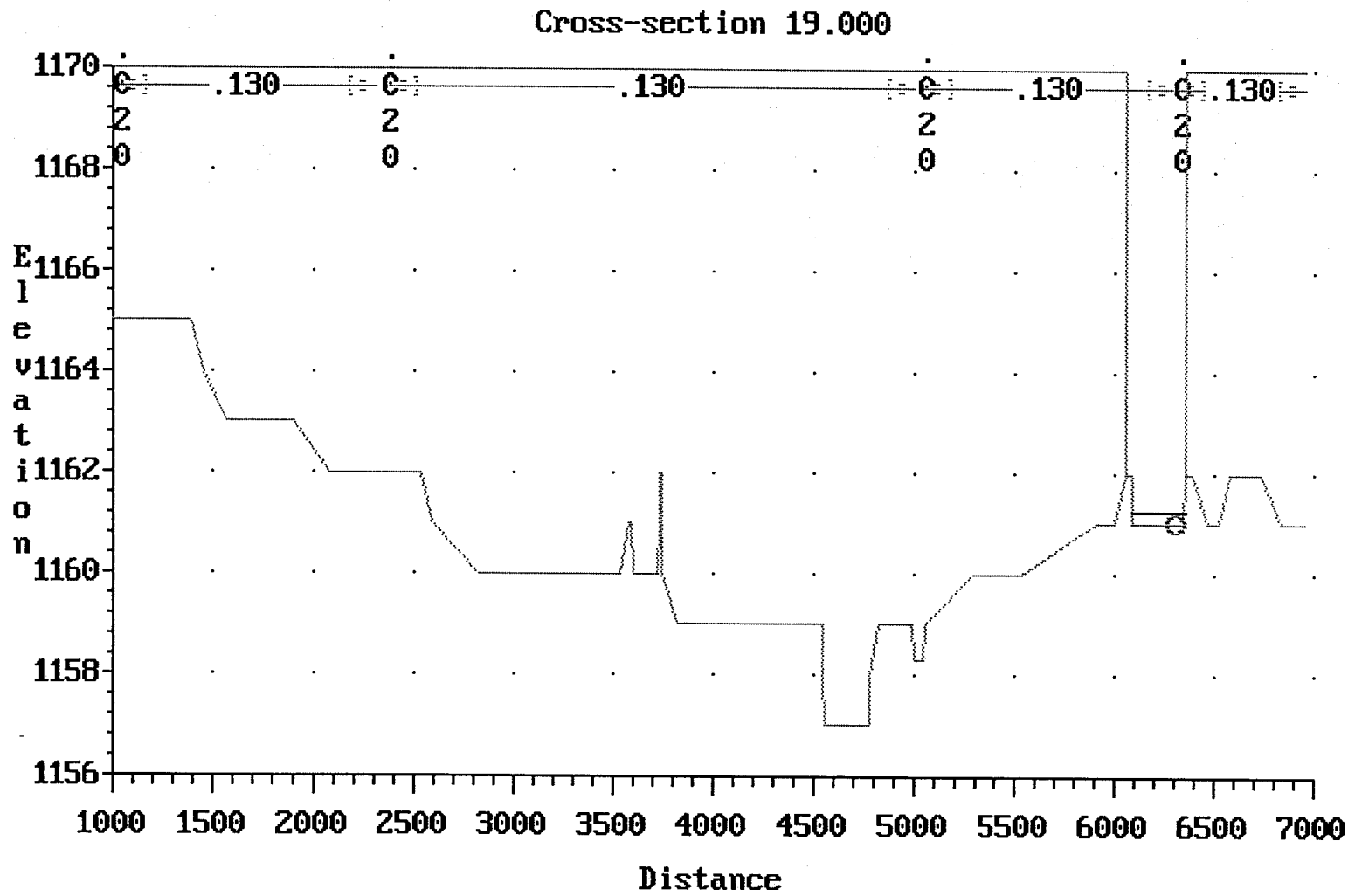


Figure 130 Upper 17th Ave HEC-2 Run
Cross-Section 19

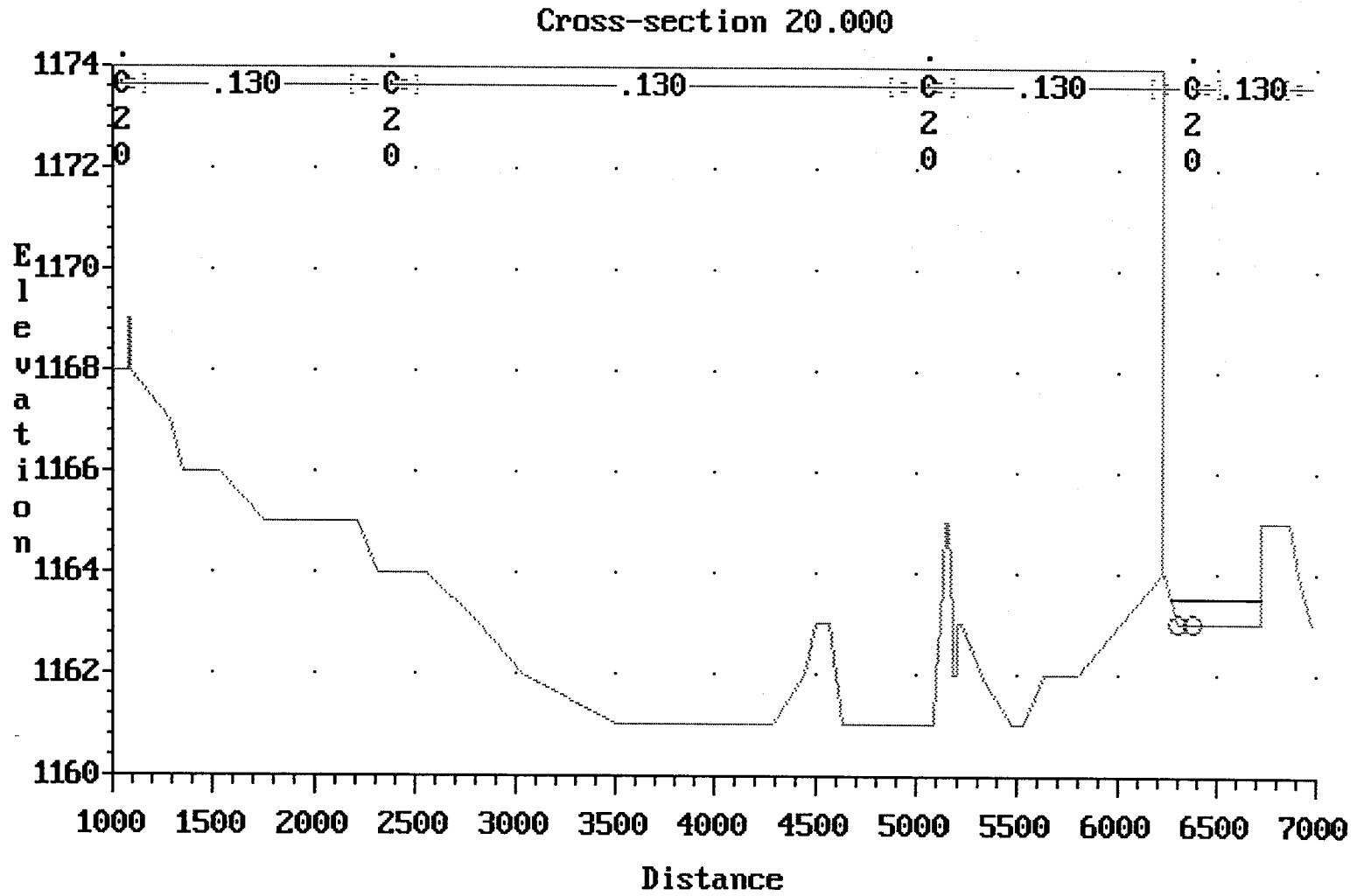


Figure 131 Upper 17th Ave HEC-2 Run
Cross-Section 20

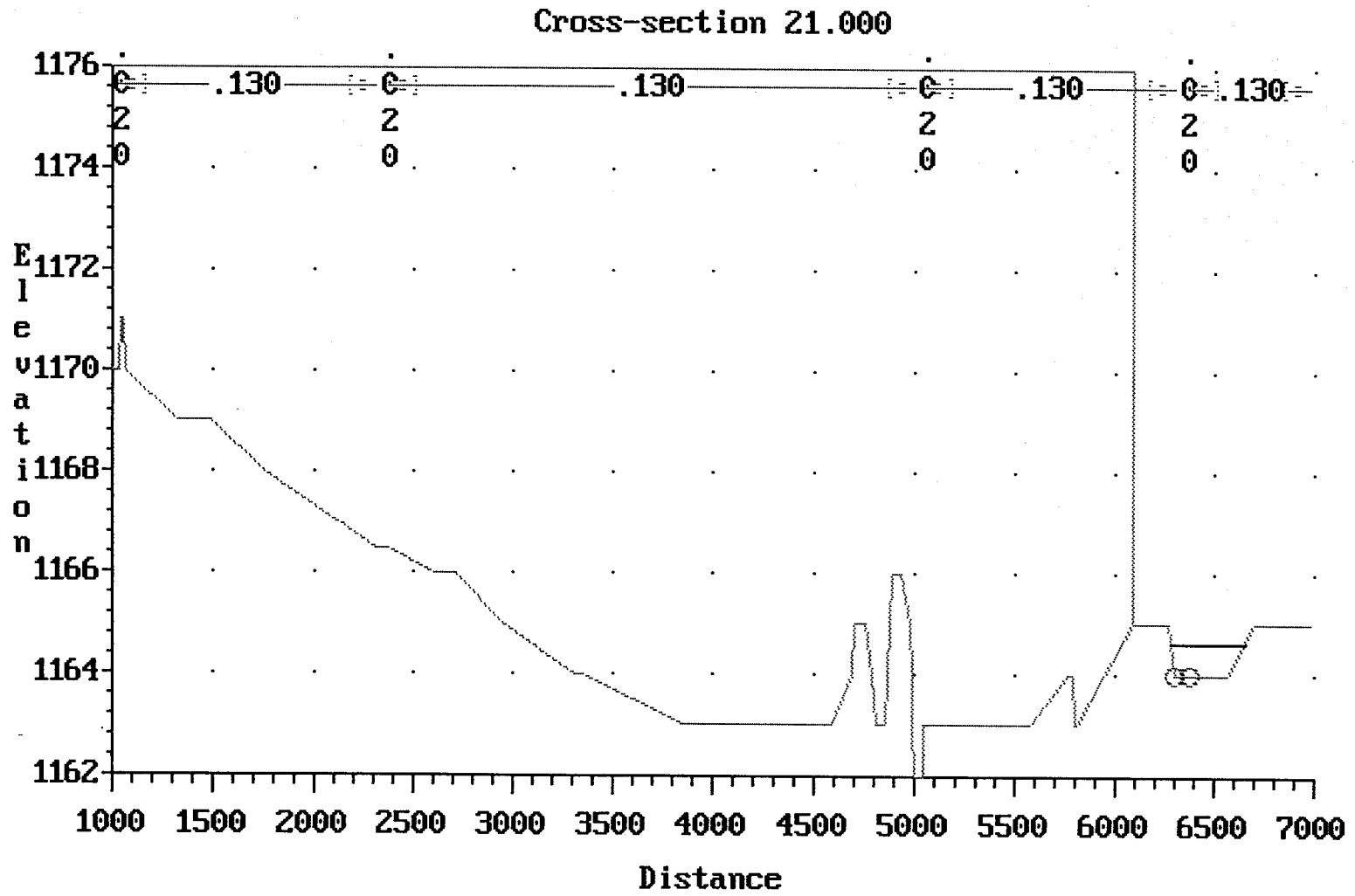


Figure 132 Upper 17th Ave HEC-2 Run
Cross-Section 21

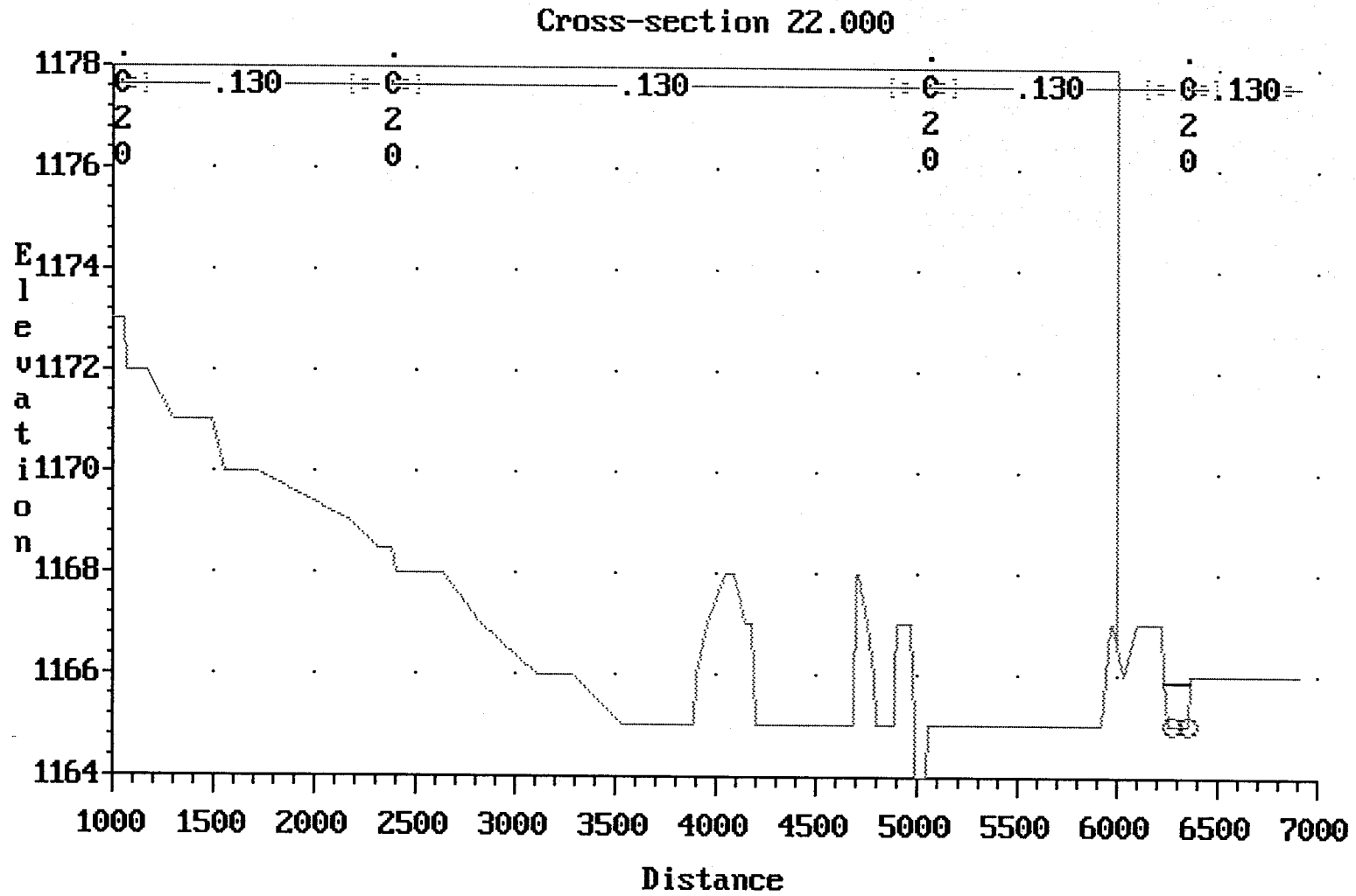


Figure 133 Upper 17th Ave HEC-2 Run
Cross-Section 22

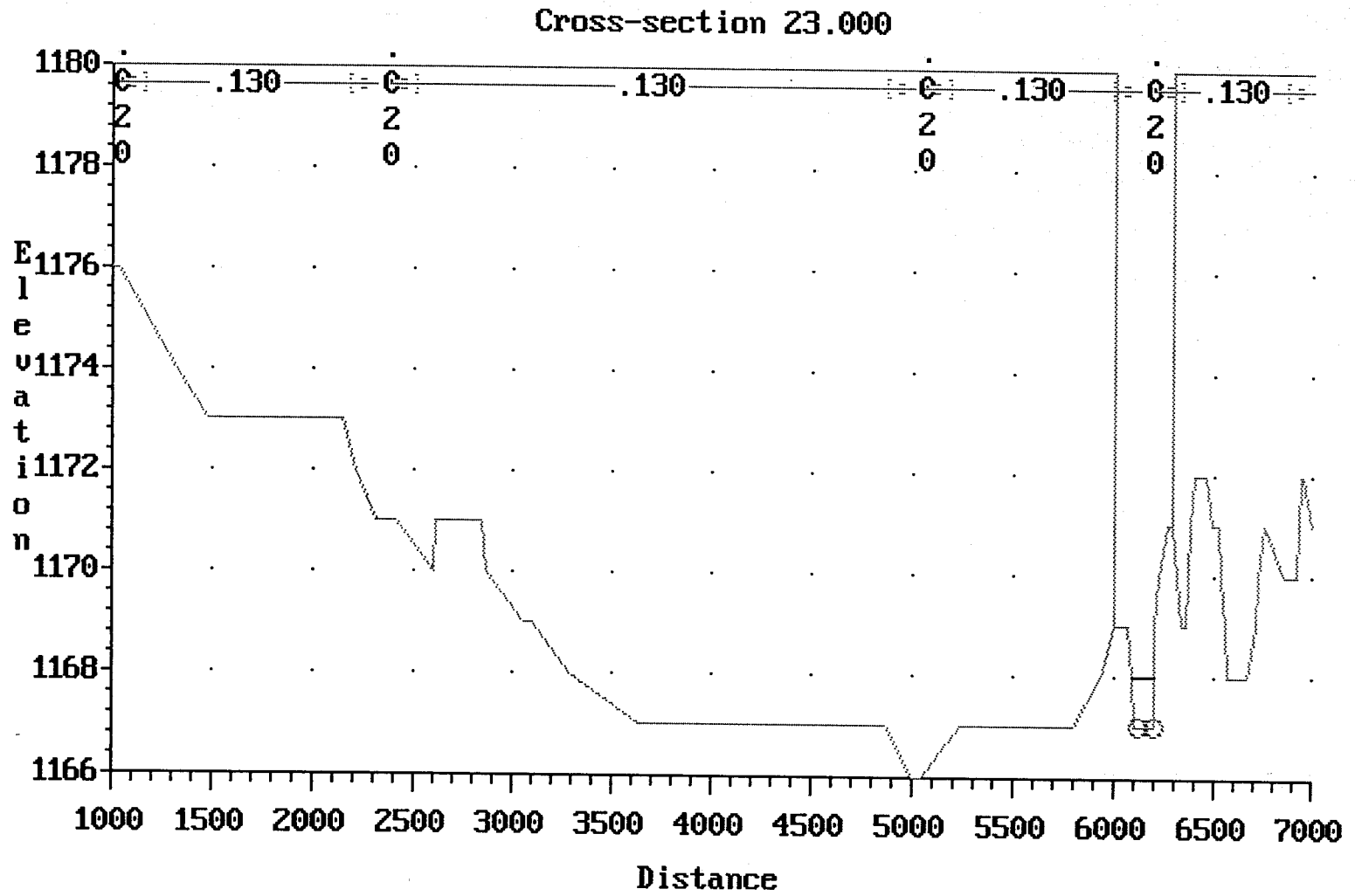


Figure 134 Upper 17th Ave HEC-2 Run
Cross-Section 23

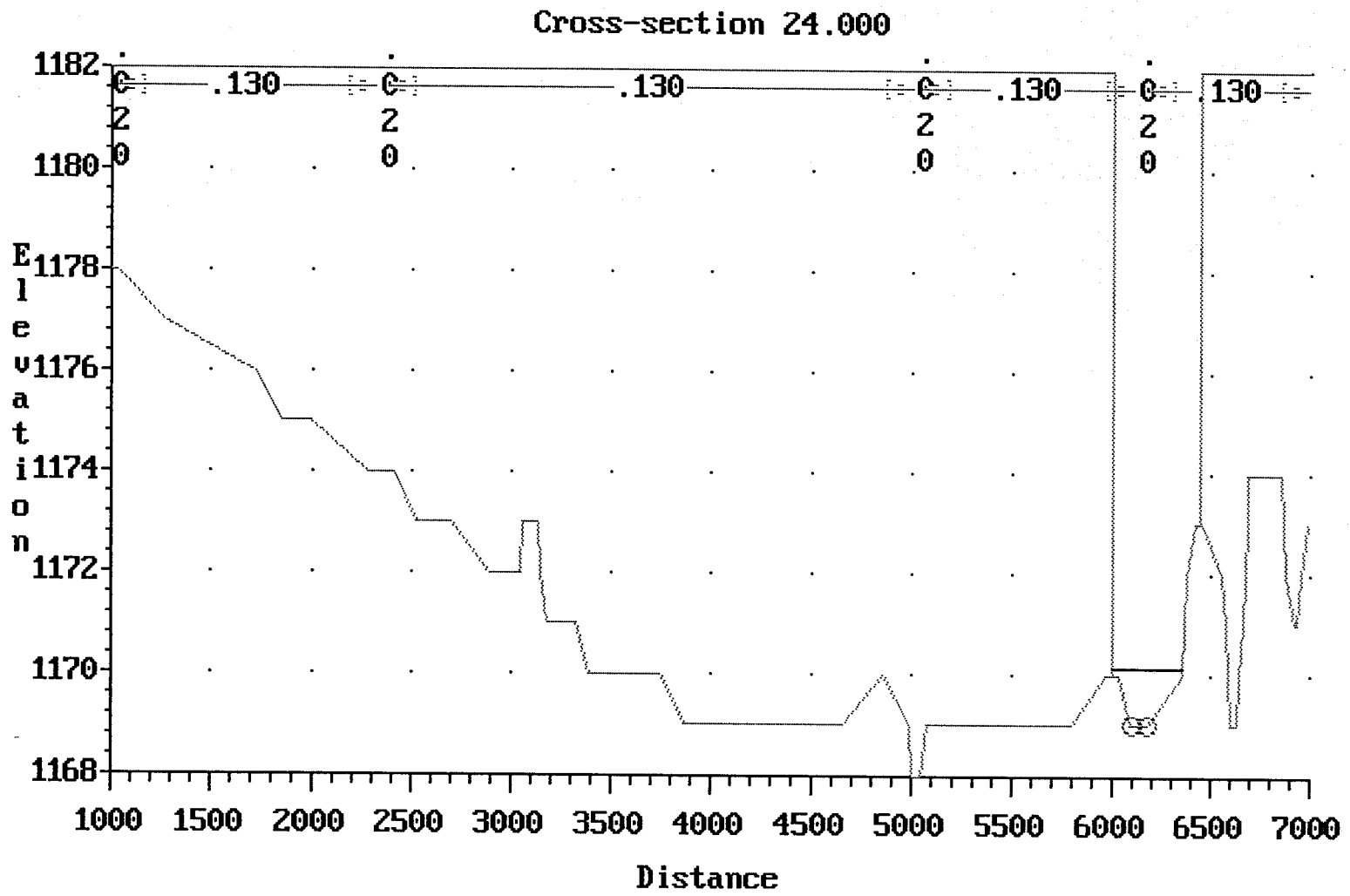


Figure 135 Upper 17th Ave HEC-2 Run
Cross-Section 24

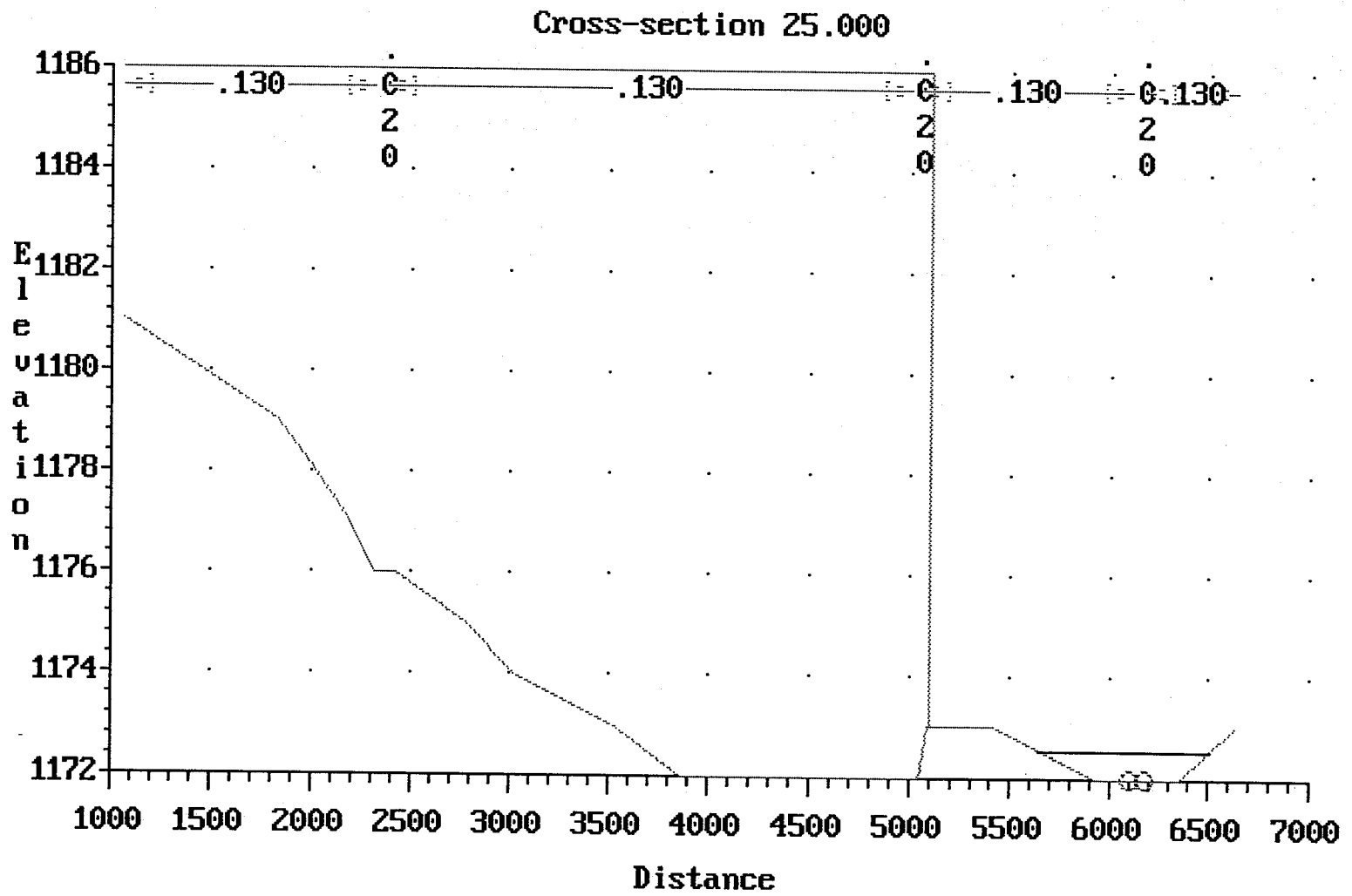


Figure 136 Upper 17th Ave HEC-2 Run
Cross-Section 25

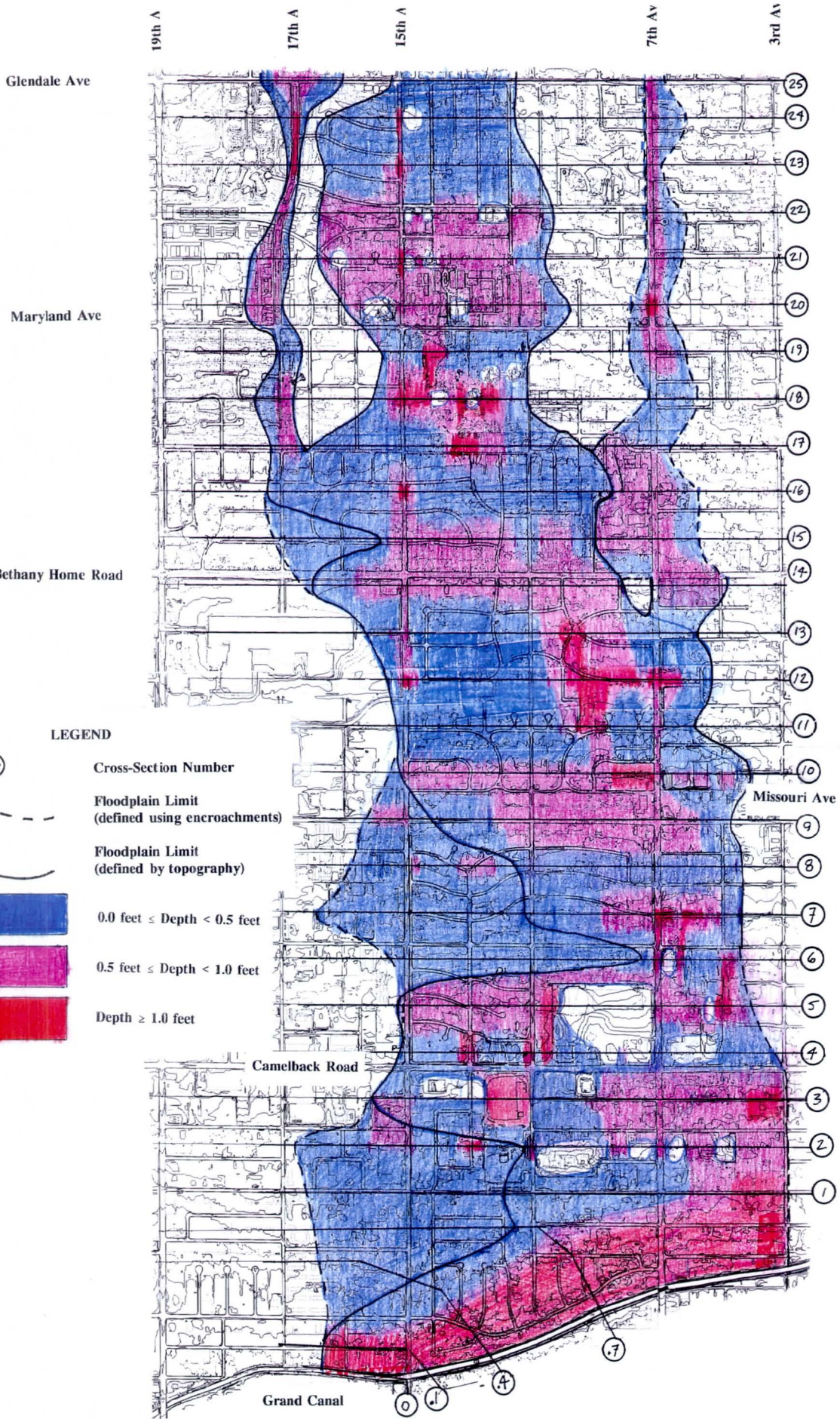


Figure 137 100-Year Floodplain and Depth Distribution
Current HEC-2 Analysis

Glendale Ave

Maryland Ave

Bethany Home Road

Missouri Ave

Camelback Road

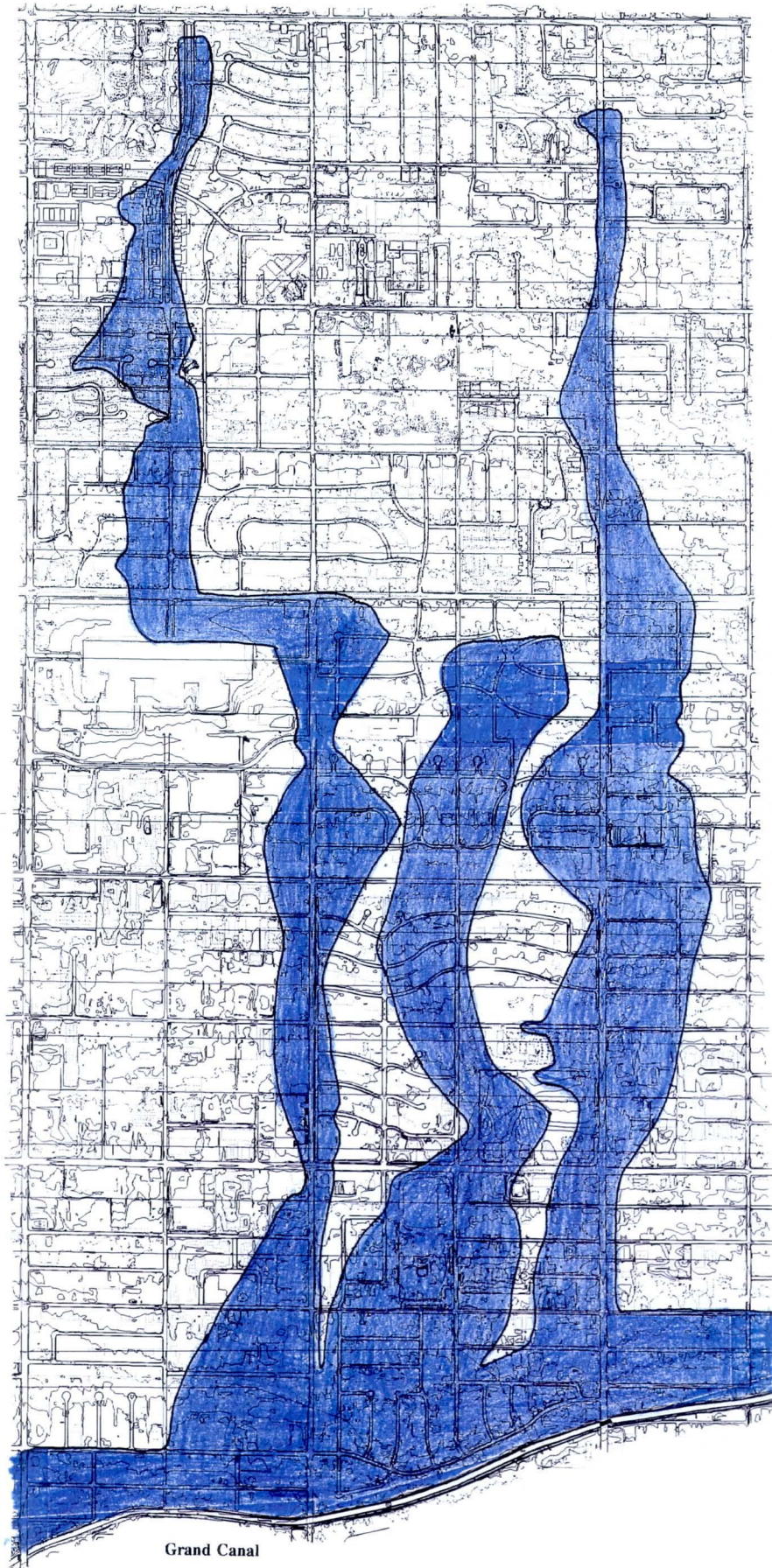
19th Ave

17th Ave

15th Ave

7th Ave

3rd Ave



Grand Canal

Figure 138 100-Year Floodplain
Previous Analysis